University of Kentucky

UKnowledge

Theses and Dissertations--Microbiology, Immunology, and Molecular Genetics

Microbiology, Immunology, and Molecular Genetics

2018

INSIGHTS INTO KEY GENE REGULATORY NETWORKS IN *BORRELIA BURGDORFERI*

William Kenneth Arnold
University of Kentucky, will43250@gmail.com
Author ORCID Identifier:
https://orcid.org/0000-0003-2447-3489
Digital Object Identifier: https://doi.org/10.13023/etd.2018.493

Right click to open a feedback form in a new tab to let us know how this document benefits you.

Recommended Citation

Arnold, William Kenneth, "INSIGHTS INTO KEY GENE REGULATORY NETWORKS IN *BORRELIA BURGDORFERI*" (2018). *Theses and Dissertations--Microbiology, Immunology, and Molecular Genetics*. 19.
https://uknowledge.uky.edu/microbio_etds/19

This Doctoral Dissertation is brought to you for free and open access by the Microbiology, Immunology, and Molecular Genetics at UKnowledge. It has been accepted for inclusion in Theses and Dissertations--Microbiology, Immunology, and Molecular Genetics by an authorized administrator of UKnowledge. For more information, please contact UKnowledge@lsv.uky.edu.

STUDENT AGREEMENT:

I represent that my thesis or dissertation and abstract are my original work. Proper attribution has been given to all outside sources. I understand that I am solely responsible for obtaining any needed copyright permissions. I have obtained needed written permission statement(s) from the owner(s) of each third-party copyrighted matter to be included in my work, allowing electronic distribution (if such use is not permitted by the fair use doctrine) which will be submitted to UKnowledge as Additional File.

I hereby grant to The University of Kentucky and its agents the irrevocable, non-exclusive, and royalty-free license to archive and make accessible my work in whole or in part in all forms of media, now or hereafter known. I agree that the document mentioned above may be made available immediately for worldwide access unless an embargo applies.

I retain all other ownership rights to the copyright of my work. I also retain the right to use in future works (such as articles or books) all or part of my work. I understand that I am free to register the copyright to my work.

REVIEW, APPROVAL AND ACCEPTANCE

The document mentioned above has been reviewed and accepted by the student's advisor, on behalf of the advisory committee, and by the Director of Graduate Studies (DGS), on behalf of the program; we verify that this is the final, approved version of the student's thesis including all changes required by the advisory committee. The undersigned agree to abide by the statements above.

William Kenneth Arnold, Student

Dr. Brian Stevenson, Major Professor

Dr. Ken Fields, Director of Graduate Studies

INSIGHTS INTO KEY GENE REGULATORY NETWORKS IN *BORRELIA BURGDORFERI*

DISSERTATION

A dissertation submitted in partial fulfillment of the requirements for the degree of Doctor of Philosophy in the College of Medicine at the University of Kentucky

By
William Kenneth Arnold

Director: Dr. Brian Stevenson, Professor of Microbiology, Immunology and Molecular Genetics and, and Professor of Entomology

Lexington Kentucky

2018

Copyright © William Kenneth Arnold 2018

ABSTRACT OF DISSERTATION

INSIGHTS INTO KEY GENE REGULATORY NETWORKS IN *BORRELIA BURGDORFERI*

Gene regulatory networks are composed of interconnected regulatory nodes created by regulatory factors of multiple types. All organisms finely tune gene expression in order to adapt to and survive within their current niche. Obligate parasitic bacteria are under extreme pressure to quickly and appropriately adapt their gene regulatory programs in order to survive within their given host. *Borrelia burgdorferi* is one such organism and persists in nature by alternating between two hosts; *Ixodes* spp. ticks and small vertebrate animals. These two hosts represent drastically different environments; requiring a unique gene regulatory program to survive and transmit between them. Microbiologists have long sought to better understand exactly what stimuli pathogens sense and how that information is relayed in to physiologic adaptation.

In this work I aimed to examine two parts of this interesting field. First, I sought to better understand the stimuli *B. burgdorferi* sense in order to adapt to their hosts by testing several hypotheses centered on the general notion that *B. burgdorferi* senses both internal and external metabolic cues as primary signals for adaptation. I demonstrated that a second messenger system immediately downstream of a critical metabolic pathway is important during vertebrate infection and that a key regulator of virulence is itself regulated by a factor involved in DNA replication.

Second, I sought to better define the topology of gene regulatory networks, known and unknown, that are important for the ability of the bacteria to adapt. The work in this section focus on the idea that *B. burgdorferi* gene regulatory networks are extremely complex and are not currently well defined in the literature. My studies revealed that *B. burgdorferi* possesses a large number of previously undefined regulatory targets, including extended 5' and 3' UTRs of known genes, and encodes several hundred-putative small non-coding RNAs. Furthermore, I demonstrate that two essential regulatory factors share substantial, independent, overlap in their regulons highlighting the still undefined complexity of regulatory networks at play in *B. burgdorferi*.

KEYWORDS: pathogen, gene regulatory networks, gene regulation, growth rate, bacteria

Will Arnold

Student's Signature

9/20/18

Date

INSIGHTS INTO KEY GENE REGULATORY NETWORKS IN *BORRELIA BURGDORFERI*

By

William Kenneth Arnold

Dr. Brian Stevenson

Director of Dissertation

Dr. Ken Fields

Director of Graduate Studies

9/20/18

Date

This work is a tribute to the family and friends who have supported my aspirations and education; specifically, Isabel, Woody, and my mother and father, Pam and Bill. Your support has been and continues to be invaluable.

Acknowledgements

I first have to thank my parents Bill and Pam for providing me every advantage possible to allow me to reach this stage. You made sure I understood early on that if I made a job out of what I love I wouldn't work a day in my life. Equally as important, you supported my higher education and development as a person. For that, I owe you my eternal gratitude.

I also thank the person who has been by my side from the literal start of this journey, Isabel. I could not have asked for a better friend and confidant. You have supported me during the depths of my prequalifying jitters, held down the fort during conference travel, and most importantly, unflinchingly supported me throughout these years. I cannot say where I would be had we not met, but without your support I know I would not be the man I am today.

I have to thank my mentor, Brian for guiding me throughout my graduate career with unwavering support. At the end of my first year I was planning on leaving this program; four rotations in and no good fitting lab tends toward that result. A week before finals as I contemplated the value of pursuing graduate training studying a topic I had minimal interest in, I received an email stating that the Stevenson lab was open for rotations and was looking for a student. Years later and I cannot emphasize enough how wonderful an opportunity that email would represent. Brian has, in every metric, been an extraordinary mentor. I have never come across a mentor who is more dedicated to the success of his students. Brian rarely grew frustrated with my pace or my mistakes, only offering technical and moral support when needed. Brian is well known to make sure his students

are well traveled and well connected. I attended ICLB in 2014 when I had been in the lab for two months, had no data, and realistically, could provide no contribution. Yet he insisted I went and introduced me to the field. Since then Brian has continued to give me every opportunity possible, even at significant personal expense. I doubt I will ever come across a mentor willing to take the steps Brian has taken to make me known. I will also struggle to meet a mentee who has summited an Austrian mountain and shared Beckerov in a dive bar in Prague with their mentor.

Finally, I have to thank all the wonderful friends and colleagues I have met over the years. I have had the opportunity to interact and work with some of the greatest people and scientists I have ever known. Fellow Stevenson lab members, both past and present, were invaluable in regard to both direct experimental support (Noted elsewhere) and stimulating conversation. The contributions of collaborators across the country from Dr. Jonathan Livny and Jessica Alexander at Broad Institute to Drs. Patricia Rosa's and Catherine Brissette's groups at Rocky Mountain Labs and The University of North Dakota were invaluable and are demonstrative of the positivity present in this community. In my opinion, an underappreciated aspect of the scientific pursuit is the kindness and support that can be present within the community. My colleagues in the Stevenson lab were invaluable in the completion of my work. Kathryn Lethbridge, Dr. Brandon Jutras, Alyssa Antonicello, Christina Savage, Leeza Khenner, and Allison Pecaro all provided substantial contributions to this work and my development. I have never met so many people, from students to established faculty, so willing to offer a kind

word, a letter of recommendation, a pat on the back, thoughtful advice, or an unending supply of starburst candy. I would not be where I am today through my own work, drive, or intelligence. Any success I have attained, or will ever attain, is a direct result of a fantastic network of colleagues and friends helping to stand me up. Science can be a lonely pursuit with long periods of failure punctuated by a moment of success but I don't believe it has to be or should be so lonely. The only thing that makes it all worth it are the people who pursue it together.

While potentially unusual, and unlikely to be read in its entirety, I would like to use this space to note those who are not mentioned elsewhere but have made this work possible through direct experimental, intellectual, or emotional support during my graduate career who are not named above; Dr. Maria and Will Dixon, Alex and Matt Nail, Joshua Ferrell, Dr. Sarah D'Orazio, Dr. Mike Fried, Dr. Jeramiah Smith, Dr. Anthony Sinai, Robert Hayman IV, Gabby Keb, Beth Oates, Tanya Myers-Morales, Dr. Beth Garvy, Dr. Carol Pickett, Melissa Keinath, Melissa Hollifield, Dr. Erin Garcia, Dr. Kate Wolf, Mrs. Linda, Phillip, Dr. Michelle Pitts, Dr. Animesh Dhara, Dr. Ken Fields, Dr. Jennifer Strange, Dr. Greg Bauman, Dr. Carrie Shaeffer, Tim Saylor, Dr. Don Cohen, Kate Fresca, Bridgette Szczapinski, Jennifer Kennedy, and Drs. Jeff and Carrie Boychuk. This list is presented in no particular order and is in no way an exhaustive listing of all those who have helped me during this time.

Table of Contents

Acknowledgements iii

Table of Contents vi

List of Tables viii

List of Figures ix

Chapter 1 Introduction 1
- ***Borrelia burgdorferi*** 1
- **Clinical Manifestations** 1
- **Epidemiology** 3
- **Ecology** 5
- **Critical aspects of each life stage** 6
- **Gene regulatory networks** 7
- **Mechanisms of regulation** 9
- **Summary** 14

Chapter 2 Materials and Methods 16
- **Strains and bacterial cultivation.** 16
- **Nucleic acid isolation (gDNA, plasmid, and RNA)** 17
- **Polymerase Chain Reaction (PCR, qPCR, and qRT-PCR)** 18
- **Animal Infections** 19
- **Cloning and plasmid analysis** 20
- **RNA-Seq Library preparation** 20
- **RNA-Seq Data Analysis** 21
- **Flow Cytometry** 22
- **Western Blotting** 22
- **2D-PAGE** 23
- **Electrophoretic Mobility Shift Assay** 24
- **DNA-Affinity Chromatography** 25
- **Liquid Chromatography Electrospray Ionization Tandem Mass Spectrometry (LC-ESI-MS/MS) Analysis** 25
- **MS/MS Protein Identification** 26
- **Recombinant protein expression and isolation** 27

Chapter 3 Metabolic linkages of signaling and gene regulation 31
- **Introduction** 31
- **Absence of *luxS* does not result in loss of fitness during single strain infection** 34
- **Loss of LuxS results in a quantitative loss of fitness during competitive infection** 34
- **Discussion** 35

Chapter 4 Mechanistic links between regulators of virulence and DNA replication 43
- **Introduction** 43
- **BpuR is highly expressed in unfed ticks but not vertebrates** 44
- **Perturbations of BpuR have a minimal impact on *in vitro* transcriptomes** 45
- **BpuR impacts the proteome of *B. burgdorferi*** 47
- **DnaA binds *bpuR* promoter DNA** 48
- **Discussion** 50

Chapter 5 Investigations into the *B. burgdorferi* transcriptome yield insight into transcriptomic dynamics and architecture 62
Introduction 62
***B. burgdorferi* differentially expresses numerous genes depending on growth phase** 67
Genome wide mapping of 5' transcript ends 69
Identification of intrinsic termination sequences 70
***B. burgdorferi* expresses hundreds of putative small non-coding RNAs** 72
Discussion 74

Chapter 6 Dissection of key gene regulatory networks in *B. burgdorferi* 84
Introduction 84
CsrA impacts the expression of a substantial number of genes involved in virulence and cell physiology 85
BadR regulates the expression of genes and involved in metabolism and virulence 87
The CsrA and BadR regulons share substantial overlap 89
Key virulence genes are expressed independently of RpoS and RpoN 91
Discussion 92

Chapter 7 Discussion 103
Summary 103
Growth control 104
Nutritional control of cell size 104
Nutritional control of DNA replication 105
Growth and virulence 106
***B. burgdorferi* metabolism in context** 108
Input and output of gene regulatory networks (GRNs) 113
Topology of critical gene regulatory networks 116
Closing thoughts 119

Appendix 120
Table 8-1 Differentially abundant transcripts when comparing early- to mid-exponential phase 121
Table 8-2 Differentially abundant transcripts when comparing mid-exponential to stationary phase 122
Table 8-3 Transcripts that were differentially abundant between early-exponential and stationary phase 125
Table 8-4 Identified Intrinsic Terminators 131
Table 8-5 Putative non-coding RNAs 136
Table 8-6 Differentially abundant transcripts comparing WT to Δ*rpoN* 145
Table 8-7 Differentially abundant transcripts comparing WT to Δ*rpoS* 146
Table 8-8 Differentially abundant transcripts comparing WT to Δ*badR* 147
Table 8-9 Differentially abundant transcripts comparing WT to Δ*csrA* 154

References 161

VITA 190

List of Tables

Table 2-1 Oligonucleotide primers used in these studies 29
Table 3-1 Results of the competitive infection study..... 38
Table 5-1 Metrics of RNA-Sequencing of wild-type *B. burgdorferi* 76
Table 5-2 Comparison of predicted transcriptional start sites with previously identified transcriptional start sites 77

List of Figures

Figure 1-1: Enzootic Cycle of *B. burgdorferi* 15
Figure 4-1: mRNA levels of *bpuR* throughout the enzootic cycle 53
Figure 4-2: Differentially expressed transcripts following *bpuR* induction 55
Figure 4-3: Validation of RNA-Seq 56
Figure 4-4: BpuR impacts SodA protein levels and binds *sodA* RNA and 57
Figure 4-5: *bpuR* is regulated at the level of transcription 58
Figure 4-6: Evidence that protein(s) specifically bind the *bpuR* upstream DNA 59
Figure 4-7: DnaA binds the *bpuR* promoter 60
Figure 4-8: Proposed mechanism of DnaA interaction with the *bpuR* promoter 61
Figure 5-1: Volcano plots of differentially expressed genes across growth phases 78
Figure 5-2: Histograms of distances of unambiguous 5' ends from start codon 79
Figure 6-1: Differentially expressed transcripts *B. burgdorferi* mutants examined in this study 95
Figure 6-2: Expression of select transcripts in Δ*csrA* mutant and wild-type *B. burgdorferi* 96
Figure 6-3: Expression of the *glpFKD* operon in a Δ*badR* mutant 97
Figure 6-4: Expression of select transcripts in Δ*badR* mutant and wild-type *B. burgdorferi* 98
Figure 6-5: Set analysis of differentially expressed gene sets 99
Figure 6-6: Expression of transcripts encoding proteins involved in chitobiose metabolism affected in Δ*badR* and Δ*csrA* mutants. 101
Figure 6-7: Promoter utilization of *rpoS* in an Δ*rpoN* mutant 102

Chapter 1 Introduction

Borrelia burgdorferi

Borrelia burgdorferi is the bacterial agent that causes Lyme borreliosis [40]. This bacterium traverses an enzootic cycle alternating between an *Ixodes* spp. tick vector and a vertebrate host, often a small mammal or bird [247] (Fig. 1-1). These two host organisms represent drastically different environmental niches for these bacteria, requiring significant alterations in behavior and physiology. All organisms maintain homeostasis by adapting their physiology through multiple mechanisms, including the regulation of gene and protein expression and functional modulation of enzymes. Bacteria, archaea, and single-celled eukaryotes are under significant evolutionary pressure to rapidly adapt to dynamic environments. Temperature, water content, nutrient availability, pH, and numerous other variables are often in constant flux, and single-celled organisms are more vulnerable to these fluctuations than multicellular organisms. In the studies described herein, I sought to better define the regulatory mechanisms, input, and topology of gene regulatory networks important for adaptation during the enzootic cycle of *B. burgdorfer*i.

Clinical Manifestations

Originally identified as an unusual outbreak of rheumatoid arthritis in children near Lyme, Connecticut, in 1976 [295], Lyme Borreliosis has become the leading tick-borne disease worldwide and represents a significant global disease burden [296]. These initial cases clustered near forested areas and were associated with tick bites, suggesting a potential tick-borne disease. In 1982, at the Rocky Mountain Laboratory, a spirochetal bacterium within *Ixodes scapularis* ticks was identified and eventually shown to be the etiologic agent of disease [40].

Following tick bite, acute infection is marked by the development of the distinctive *erythema migrans* (Latin, “chronic migrating redness”) or “bullseye” rash centered on the

site of the bite [291, 296]. This is often accompanied by general flu-like symptoms, which can last several days or weeks [291, 296]. The bullseye rash is common in the United states, but in Europe it is often less distinct and defined [296]. Lyme borreliosis manifests with diffuse symptomology, which can complicate accurate diagnosis [296].

Following acute infection, dissemination spreads primarily through skin, with a small subset of spirochetes transmitting via the blood stream, but not at high levels and or for extended periods of time [293]. The chronic phase of infection is characterized by arthritis, carditis, and neural complications [296]. The manifestation of these and other symptoms vary across the globe, with European disease manifesting with more frequent neural complications and the northeast American disease with more frequent arthritis [296]. The differences in these symptoms have variously been postulated to be dependent on genetic differences in the spirochetes or the patient population, but the exact cause remains unclear.

The diffuse and variable symptoms often make diagnosis difficult and are complicated by significant misinformation regarding diagnostic approaches [5]. Standard treatment is a 2-week course of doxycycline for adults, or amoxicillin for children or pregnant women [292]. A small fraction of patients (<10-20%) continue to report symptoms following treatment, including extended, >4-week treatment regimens [293]. Randomized trials aimed at testing the effect of extended antibiotic regimens have not found a significant difference in reported symptomology between treated and untreated groups [25]. The reason for this continued symptomology is not entirely clear, but persistent infection [94, 276], autoimmune dysfunction [31, 294], and psychological causes [287], amongst others, have been proposed. Histological and molecular examinations of synovial tissue before, during, and following antibiotic treatment demonstrate that chronic inflammation continues even in the absence of detectable spirochetes [280]. These

findings suggest that the persistent symptoms may be related to immune mediated damage at sites of previous infection.

Epidemiology

The range of both vectors and hosts of *B. burgdorferi* sensu lato is vast and encompasses significant swaths of North America, temperate Europe, and Asia. These include foci in the northeast and north-central United states, central Europe, Russia, China, and Japan [206]. Since the onset of surveillance in the U.S. in 1992, cases of Lyme have been on the rise, with an estimated 15,000 new cases each year in 2001 and 300,000/year by 2015 [291, 296]. This rise incidence is attributed to both higher rates of reporting and surveillance, as well as geographic expansion of the tick vector. The primary agent of Lyme borreliosis in the U.S. is *B. burgdorferi*, sometimes referred to *B. burgdorferi* sensu stricto. Recent work has indicated other related pathogenic *B*orrelia species, namely *Borrelia mayonii* [151, 245] and *Borrelia miyamotoi* [21, 218] are also present in certain areas of the U.S. and transmitted by the same species of ticks, though seemingly causing disease at much lower rates. In the U.S., the distribution of Lyme disease caused by *B. burgdorferi* is regional, but the incidence of disease appears to be rapidly expanding [205]. The locations with the highest incidence of disease are the northeast, mid-Atlantic coast, and north-central regions. A smaller range extends along the western U.S. coast from California to Washington. Interestingly, while both Canada and Mexico are colonized by competent vectors, the incidence of disease is much lower [206]. Less than a thousand cases were reported nationally in Canada from 2009 to 2013, and no evidence for human Lyme disease has been found in Mexico.

The incidence of Lyme borreliosis is wide-spread throughout western, central, and eastern Europe. In Europe, there are at least five recognized genospecies of *B. burgdorferi* sensu lato: *B. burgdorferi*, *B. afezlii*, *B. garinii*, *B. valaisiana*, and *B. lusitaniae*, which vary in relative abundance regionally, although only the first three have been demonstrated to

cause disease in humans [206]. This variation is proposed to be a result of regional differences in primary reservoir hosts. Incidence of disease is highest in central and northeastern European nations, with Austria, Estonia, Lithuania, and Slovenia leading, with annual reported cases sometimes ranging upwards of 100 cases per 100,000 individuals. Incidence generally decreases in all directions as one travels away from this central node [206].

The distribution of ticks capable of transmitting *B. burgdorferi* genospecies extends over large portions of Eurasia, including Russia, China, and Japan, and infected ticks are found across this range. Human incidence is variable, and in endemic areas is reported between 5-10 cases per 100,000 individuals annually. Infected ticks and animals have been found in at least 20 provinces of China, but information on human disease appears sparse. Incidence in Japan is very low (0.1 cases per 100,000 population) but is consistently reported, particularly on Hokkaido Island [205]. It is not entirely clear whether the lower rates of reported infection are due to differences in the enzootic cycle, genetics of the bacteria, or simply underreporting.

Populations particularly at risk across the globe are those that spend significant time outdoors in forested areas (i.e. the preferred environment for *Ixodes* spp. ticks) [205]. It is thought that the reforestation of the northeastern U.S., beginning in the mid-20th Century, following centuries of intensive development, partially explains the emergence of Lyme disease through the reestablishment of the vector and reservoir hosts' natural environments [20]. In the U.S., the highest rates of infection are in children aged between 5-15 years and adults older than 50 years of age. The incidence in males of all groups is higher, but this sex disparity is shrinking, and, in Europe, the distribution favors higher rates of infection in females [206]. These differences are thought to be explained by behavioral, rather than physiological, differences.

Ecology

Borrelia burgdorferi sensu lato is transmitted by a several species of hard-bodied *Ixodes* spp. ticks [20, 40, 206, 247]. *Ixodes* spp. ticks are from the family Ixodidae, which progress through three life stages before reaching maturity and mating [247]. At each stage of life, the ticks take a single blood meal, at which time bacteria can be acquired or, if already acquired, transmitted. The ixodid ticks that vector *B. burgdorferi* are slow feeders that remain attached to their hosts for several days. Well known vectors for *B. burgdorferi* sensu lato include *Ixodes scapularis* in the northeast and northcentral U.S., *Ixodes ricinus* in Europe, *Ixodes pacificus* in the western U.S., and *Ixodes persulcatus* in Eurasia [206]. The ranges of several of these species are overlapping and confound the identification of defined enzootic cycles in some locations [206].

The most well described enzootic cycle in the northeastern U.S. is thought to be maintained by cycling between *Ixodes scapularis* ticks and the field mouse *Peromyscus leucopus* [177] (Fig. 1-1). The larval and nymphal stages of tick feed on the same host and thereby propagate the cycle. Adult ticks feed on larger mammals, including white tailed deer and occasionally humans. Transovarial (mother to egg) transmission of *B. burgdorferi* does not occur, but ticks maintain infection during intervening molts [258].

Larval ticks emerge in the late summer and feed on their first host. They molt over the winter before emerging as nymphal ticks in the early spring of the following year. While nymphal ticks preferentially feed on small vertebrates, they occasionally do feed on larger mammals, such as humans. These nymphal ticks are thought to be the most common vector for human disease [247], due to their small size, approximately the size of a poppy seed, and the resultant difficulty of detection. Following a blood-meal, nymphs molt over the summer into adults, which are then active in the late summer and fall. Adults primarily prey on larger mammals and nymphs on smaller vertebrates, but as indicated above, nymphal ticks do also occasionally feed on humans. There is correlation between the burst

in nymphal activity in the early spring and outbreaks of Lyme disease in the summer due to this occasional feeding and the difficulty in the detection of nymphal ticks. Adult ticks are detectable by eye and frequently removed quickly, prior to bacterial transmission [241]. Nymphal ticks, on the other hand, often go unnoticed.

Critical aspects of each life stage

Colonization of each niche and transmission between them require extensive physiologic reprogramming, including drastic alterations to the cell surface and cellular metabolism. A significant difficulty has been, and remains, that many proteins encoded in the *B. burgdorferi* genome lack recognizable homologues outside the genus [58, 100] and, as a result, functional annotation is sparse. What has been reasonably inferred and demonstrated is that the physiology of the bacteria is significantly different when they occupy the tick vector or the vertebrate host [146, 242, 247]. The extracellular milieu which the bacteria occupy is vastly different between the vertebrate and tick. This difference impacts what surfaces the bacteria must adhere to, release from, and traverse through. In addition, the nutrient sources they rely on are quite different between niches [76, 237, 318]. Two critical environmental components for the enzootic cycle that have been investigated in some detail are host factor binding interactions and carbohydrate metabolism.

Many of the proteins that have been demonstrated to play a role in the survival and adaptation of the bacteria are lipoproteins involved in host or vector interaction. OspC, OspA, OspB, DbpA, DbpB, VlsE, and the Erp family of lipoproteins [349] are merely a small number of lipoproteins that have experimental support for a role in host interaction of the >120 lipoproteins thought to be encoded in the *B. burgdorferi* genome [83, 101]. Extensive research has been aimed at understanding how these factors are regulated, what stage of the cycle they are important for, and with what host/vector factors they interact. It is outside the scope of this work to detail what each lipoprotein interacts with.

It is sufficient to note that different factors are required to be expressed and repressed at different stages of the life cycle, and these lipoproteins and their functions are well reviewed elsewhere [247, 301].

Enzymes and transporters involved in carbohydrate metabolism have also been shown to play a key role in adapting *B. burgdorferi* to each particular niche. *B. burgdorferi* encodes a large number of validated and putative carbohydrate transporters [101], but appears to only survive on a relatively restricted number of sources [326]. Glucose is generally abundant in vertebrate hosts, is thought to be the carbohydrate of choice during infection, and defects in its uptake result in significant attenuation of ability to infect [76, 318]. In the tick vector, following the digestion of the blood meal, glycerol and chitobiose are thought to be the predominate carbon and energy sources [38, 76, 146, 237, 312, 313]. High-throughput transposon insertion sequencing has highlighted this difference in carbohydrate utilization both *in vitro* and *in vivo* [318]. As expected, the enzymes and proteins involved in carbohydrate utilization appear to be very tightly regulated and in tandem play a role in regulating other factors [169].

Gene regulatory networks

Homeostatic control of physiology is one of the defining characteristics of life. In all studied living organisms, a key mechanism of this homeostatic control is the regulated expression of genes and proteins. The mechanisms we today know as gene regulation were likely first identified during Barbara McClintock's seminal studies on transposable elements found in maize [204]. These studies were followed by the elucidation of the *lac* operon by Francois Jacob and Jacques Monod in *Escherichia coli* [148]. These findings sparked a revolution in the understanding of biology. From these works, and innumerable others, came the notion of the regulated operon: sets of genes of connected function that are produced and regulated in unison by one or more factors.

As data accumulated it became clear that some regulators impacted the expression of more than one operon. Maas and Clark coined the term regulon to describe this phenomenon [199]. Instead of a one regulator one operon system, it became clear that some regulators have more widespread effects and impact the expression of multiple operons. Some of these regulators span multiple biological processes and are now known as “global regulatory factors,” controlling expression from vast swaths of the genome. Specific cases of the induction of a “virulence program” are present in numerous pathogens [6, 41, 48, 60, 84, 86, 153, 184, 189, 192, 215, 217, 221, 256, 262, 334] along with more general responses such as the heat shock [225] stringent responses [61, 244]. These global and more narrowly acting regulatory factors are increasingly known to interact with one another. Some regulators converge on operons while individually regulating others [18, 79, 80, 198, 200, 201]. Thus, the concept of the gene regulatory network (GRN) was born.

Gene regulatory networks can be thought of as interconnected networks of regulatory proteins, both receiving and relaying signaling information. These networks allow for crosstalk and convergent regulation of genes and proteins at multiple levels, resulting in a rich physiologic response to dynamic environmental stimuli. The network architecture allows for a more robust and sensitive response, as well as creating redundancy in the system. From the perspective of *Homo sapiens* seeking to interrupt the ability of microorganisms to cause disease, these networks represent a key target. Some portions of the network have redundant mechanisms of activation and thus are resilient in the face of upstream interference (i.e immune responses or antimicrobial therapy), whereas other portions act as central nodes of information processing and take in many inputs and relay many outputs. It is these central nodes that possess the greatest potential for disruption. Defining the topology and logic of the networks allows scientists and physicians to not simply target the upstream signaling input or downstream enzymatic

activity of a process, but to target and interrupt these crucial information processing centers. Furthermore, understanding the topology of the network allows the informed development of multipronged approaches that target multiple, non-overlapping nodes. This is of key importance in combatting both microbial resistance as well as the *in situ* evolution of cancer during treatment [207]. By targeting multiple processes, we may ensure that microorganisms or cancerous cells do not develop a mechanism to circumvent a single node (i.e. the development of resistance).

Mechanisms of regulation

The expression of genes and proteins is regulated at numerous points along the central dogma of molecular biology [77]. The most well studied control point in many organisms is at the level of transcription initiation. Briefly, the RNA polymerase (RNAP) holoenzyme assembles at defined points along the genome called promoters. The RNAP core enzyme is composed of β, β', α, and ω subunits [90]. To bind to promoter DNA and become the RNAP holoenzyme, an additional subunit, called the σ subunit is required [145]. The σ subunit serves to define which promoter sequences a given RNAP holoenzyme will interact with and potentially transcribe. Upon binding to DNA, the RNAP holoenzyme can form an open complex, separating the strands of DNA, and begin transcribing RNA from the DNA template. A major point of control is the ability of RNAP to interact with a given promoter and form a productive transcriptional complex. This control can be accomplished, among other mechanisms, by altering which σ factor is present in the holoenzyme or by the binding of a protein near the promoter.

B. burgdorferi encodes three sigma factors: the housekeeping RpoD, and homologues to two alternative sigma factors called RpoS and RpoN [100]. The titles "RpoN" and "RpoS" in *B. burgdorferi* are entirely based upon homology to *E. coli* proteins and do not reflect their biological function [48]. The nomenclature can occasionally cause confusion as these sigma factors are not involved in nitrogen starvation or the stationary

phase, respectively, as are their *E. coli* homologues are. Both RpoN and RpoS are absolutely essential for vertebrate infection, and their absence results in the dysregulation of a large number of genes [48, 99]. The two alternative sigma factors have been proposed form a linear regulatory cascade that acts as the key gatekeeping mechanism regulating the induction of vertebrate-associated genes and the suppression of tick-specific genes [139]. The upstream signal for the activation of this proposed cascade is not well understood but is thought to involve the histidine kinase HK2 and the response regulator Rrp2 [28, 43, 230, 346]. Rrp2 is homologous to enhancer binding proteins (EBPs) [118] which are typically necessary for the RpoN-bound RNAP to recognize its unique -12/-24 promoter architecture. The stimuli which HK2 responds to has not been elucidated.

A small, but increasing, number of DNA-binding regulatory proteins in *B. burgdorferi* have been predicted or experimentally characterized [16, 34, 42, 100, 155, 173, 183, 210]. Some of these have been shown to be essential for the enzootic cycle, while others appear to be absolutely essential for viability. *B. burgdorferi* encodes at least four nucleoid associated factors proposed or demonstrated to play a role in the structure of the borrelial nucleoid: EbfC, Hbb, Dps, and Gac [153, 172, 173, 183]. BadR and BosR interact with the *rpoS* promoter at multiple sites, some of which are overlapping [140, 211, 231, 233, 234]. BadR is the only DNA binding protein studied in *B. burgdorferi* to date that is directly responsive to metabolites, namely phosphorylated sugars [210]. Additional DNA-binding proteins have been predicted based upon sequence homology [101] but have not yet been experimentally characterized, and additional yet unknown factors likely exist. There are other mechanisms which control the ability of an open complex to form, including local DNA structure and chemical microenvironment [172, 254].

The next major point of control is after transcription has begun and functions through transcriptional termination. There exist multiple mechanisms to control gene expression at this junction, but I will focus on those that have relevance to my studies: 5'

untranslated regions (UTRs) and intrinsic terminators. Most transcripts contain regions of DNA, both 5' and 3' of the coding sequence, which are transcribed but do not code for amino acids. In these UTRs, there can exist structural sequence motifs that cause RNAP to stall and potentially disassociate from the DNA template. A well-studied class of these structures are called intrinsic, or Rho-independent, terminators [121] which act to terminate transcription independently of additional protein cofactors. A G+C rich hair pin followed by a poly-uridine tract, as identified in *E. coli* and *Bacillus subtillis*, is an example of such [121]. The poly-uridine tract causes the RNAP to pause, and the hairpin both traps and causes extreme destabilization of the elongation complex [121, 347]. The exact sequence and free energy of the hairpin differs significantly across and between different organisms and has confounded the bioinformatic identification of such terminators.

The next point of regulatory control is post-transcriptional and often involves RNA structure, small RNAs, and RNA-binding proteins. As indicated above, most mRNAs are transcribed with a 5' UTR of variable length that can act as potential regulatory target. Some 5' UTRs can contain significant secondary structures that are responsive to a number of stimuli, including temperature and small molecules. This structural motif may overlap the ribosome binding site (RBS) and inhibit translation of the downstream protein. The binding of small RNAs, proteins, or both can induce or relax this inhibition depending on the particular system at hand [19, 95, 203, 228, 274]. Furthermore, proteins may bind directly over the RBS and impede productive translation [19, 158]. Five RNA binding proteins have been identified and experimentally characterized in *B. burgdorferi*: HrpA, CsrA, BpuR, SpoVG, and Hfq [155, 158, 163, 165, 195, 262, 266, 269, 307, 308]. All five have been shown to regulate the expression of varying numbers of proteins at the post-transcriptional level, though the exact mechanisms remain to be completely elucidated. HrpA is a helicase and significantly impacts the expression of several hundred proteins, though it remains unclear if these results are a pleotropic effect of perturbing RNA

biogenesis or the specific effect of a regulatory protein [262, 263]. CsrA [163, 165, 235, 266, 307, 308], BpuR [155, 158], and Hfq [195] have more well-defined mechanisms, with experimental evidence supporting direct interaction with mRNA and regulation of translation. BpuR is a major focus of this work and will be described in additional detail in Chapter Four.

Numerous mechanisms exist in other model systems which control protein function after translation: phosphorylation [255, 346], methylation [124, 178], acetylation [52, 135], targeted proteolysis [152], and sequestration [85], among others. *B. burgdorferi* encodes proteins either proposed or demonstrated to have a role in the post translational control of key proteins. These include two homologues to the Lon protease [67, 68] and a protein, BBD18, which regulates RpoS [86].

An additional mechanism of post-translational control is the production and sensing of signaling molecules called second messengers. The unifying theme of these factors is that they act by binding other proteins and impacting their function. These protein targets range in function from metabolic enzymes, polymerases, two component systems, and DNA/RNA binding proteins, and thus span all levels of gene regulatory control. Signaling molecules produced by *B. burgdorferi* include AI-2[13, 253, 297, 300, 325], cyclic-di-GMP [256], cyclic-di-AMP [268], cyclic-AMP [169], and (p)ppGpp [38, 61, 72, 84, 216, 244].

AI-2 is a molecule, sometimes interconverted to furosyl borate diester, produced by some bacteria as a quorum sensing molecule that can be sensed by different mechanisms in different bacteria. AI-2 and its involvement in *B. burgdorferi* gene regulation will be discussed in additional detail in Chapter 3. Cyclic di-GMP (c-di-GMP) and cyclic di-AMP (c-di-AMP) are generated by the cyclization of two tri-phosphate nucleotides, guanosine triphosphate or adenosine triphosphate, respectively. Single enzymes to produce both second messengers are encoded by *B. burgdorferi*. c-di-GMP

is produced by the diguanylate cyclase, Rrp1 and degraded by one of two phosphodiesterases, PdeA or PdeB. Rrp1 is proposed to be part of a two-component system that is essential for the tick stage of the enzootic cycle [126] and mutations in Rrp1 appear to have drastic transcriptomic effects [256]. c-di-GMP is proposed to exert much of its function through the only known c-di-GMP binding protein in *B. burgdorferi*, PlzA [104, 127]. The role of c-di-AMP in *B. burgdorferi* remains enigmatic. Enzymes to both generate and degrade the molecule, CdaA and DhhP respectively, are encoded in the genome [268, 348]. Intriguingly, while over expression of CdaA appears to have little to no effect on cultured *B. burgdorferi* [268], the phenotype of a conditional *dhhP* deletion mutant is significant and complete deletion mutants are not viable [348]. A role in the enzootic cycle for this second messenger remains to fully defined elucidated. Guanasine pentaphosphate (p)ppGpp represents the final known major second messenger produced by *B. burgdorferi* discussed in this work. In some systems, (p)ppGpp is produced during nutrient limitation in response to the accumulation of uncharged tRNAs [61]. In *E. coli*, this accumulation leads to the synthesis of (p)ppGpp by the enzyme RelA [244]. The hydrolytic enzyme, SpoT cleaves (p)ppGpp [244]. In other bacteria, including *B. burgdorferi*, synthesis and hydrolysis is accomplished by a compound enzyme that possesses both synthetase and hydrolase activities. One mechanism by which (p)ppGpp exerts its function is through binding of RNAP and destabilizing open complex formation, particularly at ribosomal RNA promoters [125] but the exact mechanism of varies across species. In *B. burgdorferi*, the enzyme Rel is important for survival during *in vitro* nutrient limitation, tick colonization, and mutations in the gene result in drastic differences in the transcriptome [38, 84]. An enzyme to generate cyclic-AMP also appears to be encoded by *B. burgdorferi* but its role is not well studied [169].

Summary

In this work described in the following chapters I studied two important aspects of *B. burgdorferi* biology; how these bacteria sense, and how they adapt to their dynamic and challenging enzootic lifecycle. *B. burgdorferi* has evolved to survive and transmit within a unique two-host life cycle with each niche representing a distinct environment with its own distinct set of challenges. I first sought to characterize how *B. burgdorferi* has evolved to sense key aspects of this life cycle and then I provide insight in to how the organism modulates gene regulatory networks to successfully adapt to these hosts.

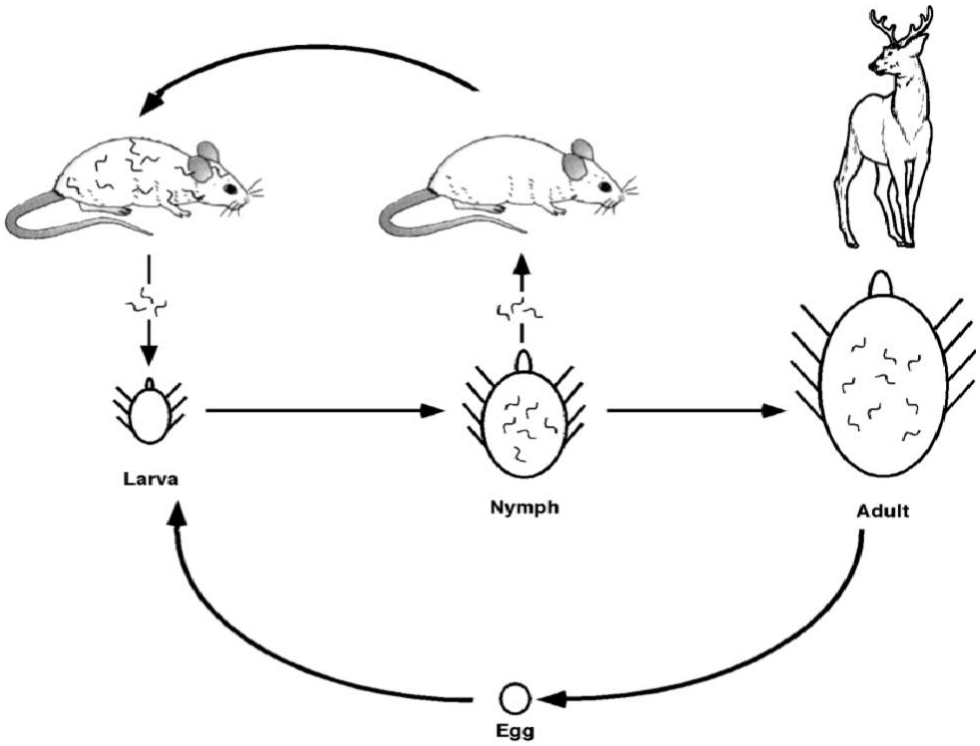

Figure 1-1: Enzootic Cycle of *B. burgdorferi*

The natural enzootic cycling of *B. burgdorferi* is depicted with its accompanying vector and reservoir hosts found in the northeast United States. Larval ticks are born free of the bacteria and both larval and nymphal ticks can only acquire it during a blood meal. The bacteria persist within the tick midgut during the molt and can then be transmitted to a naïve host during the nymphal blood meal. Adult ticks must feed on larger mammals and may also transmit the bacteria at this time. This figure was provided by Dr. Brian Stevenson.

Chapter 2 Materials and Methods

Strains and bacterial cultivation.

B. burgdorferi B31e2 is an easily transformable, noninfectious, laboratory-adapted clone of the B31 type strain. *B. burgdorferi* B31-A3 is a clonal fully infectious derivative of the species type strain [93]. It contains all of the naturally-occurring DNA elements of the sequenced culture of strain B31 except cp9. Absence of cp9 does not have any detectable effects on *B. burgdorferi* physiology either during infection or in culture [57, 101, 175, 246]. Immediately prior to all transcriptomic studies, the DNA content of B31-A3 cultures was assessed by multiplex PCR [39] to confirm the presence of all naturally-occurring plasmids.

Mutant strains of B31-A3 used for transcriptomic analyses, namely Δ*rpoS*, Δ*rpoN*, Δ*badR*, and Δ*csrA* were previously constructed by Dr. Patricia Rosa, Dr. Frank Gherardini, and Dr. Janakiram Seshu using allelic exchange [86, 99, 163, 210]. For studies investigating the role of *luxS* during vertebrate infection, an isolate of *B. burgdorferi* 297::ΔluxS (AH309) and its congenic parent was kindly provided by Dr. Michael Norgard. *B. burgdorferi* 297 is infectious isolate derived from human cerebrospinal fluid. This particular strain was constructed using allelic exchange targeting the *luxS* loci for insertion with an erythromycin resistance cassette. These mutants were then selected for by antibiotic treatment and passaged through a mouse. A significant caveat of this strain is that they have been strongly selected for suppressor mutations which mask the defect of Δ*luxS* during animal infection.

B. burgdorferi were cultured in Barbour-Stoenner-Kelly II (BSK-II) liquid medium, prepared in-house [350]. Culture conditions (condition variations temperature, serum percentage, and total dilution) depended upon the particular experiment but, in general, are identical to those conditions described by Jutras *et al* 2013 [157].

For all studies, bacteria were inoculated 1:100 from glycerol stocks into 5mL of fresh media and incubated at 35°C until cell density reached mid-late exponential phase (~1-5x10^7 cells/mL). For RNA-Sequencing these cells were diluted into 30mL of fresh BSK-II to a final density of 1x10^5 and incubated at 35°C. For the sequencing described in Chapter 5, aliquots of each culture were removed when bacterial densities reached the equivalents of early-exponential (~1x10^6), mid-exponential (~1x10^7), and stationary phases of growth (1 day after plateauing at 1x10^8). For the experiments described in Chapter 6, the total culture was harvested at ~1x10^7.

Nucleic acid isolation (gDNA, plasmid, and RNA)

Genomic DNA of *B. burgdorferi* for use in routine PCR was isolated using a DNeasy Blood and tissue kit (Qiagen, Germantown, MD) according to the manufacturer's instructions. For use in validation of primer specificity and as a reference for quantification studies of the *luxS* mutants, total bacterial DNAs were purified from mid-exponential-phase cultures (~10^7 bacteria/mL) of strains 297 and AH309 by use of DNeasy blood and tissue kits (Qiagen, Germantown, MD). For analyses of bacterial loads in mouse tissues, total DNAs were isolated from the indicated tissues using the Mo Bio Ultraclean tissue and cell DNA isolation kit (Mo Bio Laboratories, Carlsbad, CA) per the manufacturer's instructions. For rapid screening of *E. coli* colonies, standard colony PCR methods were used as described in Woodman *et al*. 2016 [339]. RNA for qRT-PCR and RNA-Sequencing was extracted using the Direct-zol purification kit (Zymo, Irvine, CA) with an on-column DNase I digestion or Turbo DNase (ThermoFisher, Waltham, MA) step according to manufacturer's instructions. RNA integrity and quantity was assayed using the RNA Nano 6000 Kit on an Agilent Bioanalyzer (Agilent, Santa Clara, CA) if the sample was to be used in RNA-Seq studies. If RNA was to be used for qRT-PCR, quantities were assessed by UV-Vis measuring absorbance A260 on a Nanodrop 2000 (ThermoFisher, Waltham, MA).

Polymerase Chain Reaction (PCR, qPCR, and qRT-PCR)

For routine detection and amplification of DNA sequences, rTaq (Bulldog Bio, Portsmouth, NH) was used according to the manufacturer's instructions. For routine PCR screening, primers were used at a final concentration of 300nM and depending on template, between .5ng and 50ng of isolated nucleic acid material or a small picking of a *E. coli* colony was used. Optimal annealing temperatures were determined for each for each primer pair and extension times were determined based upon the size each fragment to be amplified (in general, 30 seconds per kilobase). For all cloning steps and EMSA probe generation, the following proof reading polymerases were used according to their manufacturers protocols: Long Expand High Fidelity (Roche, Basel, Switzerland), Q5 Polymerase (NEB, Ipswitch, MA), or DeepVent Polymerase (NEB, Ipswitch, MA). Selection of enzyme alternated between particular applications (long template versus short template) and based on optimizing for the enzyme providing the highest yield. Concentrations of primers, template, annealing temperatures, and extension times were all determined for each particular primer pair, the nature of the template, and the length of the product, according to the respective manufacturers instructions.

Bacterial burdens in mouse tissues were assessed using Idaho Technologies/BioFire buffers (BioFire Diagnostics, Salt Lake City, UT) and Platinum *Taq* polymerase (Life Technologies, Grand Island, NY) with a CFX96 Touch real-time PCR detection platform (Bio-Rad, Hercules, CA). Cycling was performed as follows: 94°C for 3 min and 40 cycles of 94°C for 10 s followed by 30 s at 60°C. Standard curves for each oligonucleotide pair were generated by diluting a known quantity of genomic DNA in a series of 10-fold serial dilutions. Threshold cycle (C_T) values obtained for experimental samples were then plotted against this curve to determine quantities of each target. Melting curve analyses were performed to validate the presence of single products.

Results were analyzed using CFX Manager software (Bio-Rad, Hercules, CA). Data comparisons were analyzed by unpaired two-tailed *t* tests.

Isolated gDNA depleted RNA was converted to cDNA using the iScript cDNA synthesis kit (Bio-Rad, Hercules, CA). qRT-PCR was performed essentially as previously described [212], using a Bio-Rad CFX96. Comparisons were made using the $\Delta\Delta C_T$ method [271] normalizing against *ftsK* or the geometric mean of *ftsK* and *flaB* as reference genes [14]. Samples lacking reverse transcriptase enzyme mixture were prepared and assayed in tandem to ensure efficient depletion of gDNA.

Animal Infections

BALB/cJ mice were used for both the ΔluxS individual and competitive infection studies. Mid-exponential cultures (~10^7 cells/mL) were adjusted to a density of 10^5 cells/mL using phosphate buffered saline (PBS). For individual infection studies, 8 BALB/cJ mice per group were subcutaneously inoculated with 10^4 of either 297 or 297::ΔluxS bacteria. For competitive infection studies, 8 BALB/cJ mice were inoculated subcutaneously with 10^4 of each 297 and 297::ΔluxS (AH309) at a 1:1 ratio. *B. burgdorferi* for use in routine PCR was isolated using a DNeasy Blood and Tissue Kit (Qiagen, Germantown, MD), according to the manufacturer's instructions. For use in validation of primer specificity and as a reference for quantification studies of the *luxS* studies, total bacterial DNAs were purified from mid-exponential-phase cultures (approximately 10^7 bacteria/mL) of strains 297 and AH309 by use of DNeasy Blood and Tissue Kits (Qiagen, Germantown, MD). For analyses of bacterial loads in mouse tissues, total DNAs were isolated from the indicated tissues using the Mo Bio Ultraclean Tissue and Cells DNA Isolation Kit (Mo Bio Laboratories, Carlsbad, CA) per the manufacturer's instructions. 2016 [339]. RNA for qRT-PCR and RNA-Sequencing was extracted using the Direct-zol Purification Kit (Zymo, Irvine, CA) with an on-column DNase I digestion or Turbo DNase

(ThermoFisher, Waltham, MA). RNA integrity and quantity was assayed using the RNA Nano 6000 Kit on an Agilent Bioanalyzer (Agilent, Santa Clara, CA) if the sample was to be used in RNA-Seq studies.

Cloning and plasmid analysis

pGJ1 was previously constructed by Grant Jones [158]. pWA11 was constructed using the Gibson Assembly method implemented in the Gibson Assembly Kit (NEB, Ipswich, MA). Briefly, the plasmid pJSB268 was linearized by PCR removing the *luc* gene and adding 15nt overhangs complimentary to the *bpuR* locus. The *bpuR* locus was PCR amplified and 15nt overhangs complimentary to either side of the insertion site in pJSB268. Gibson assembly was performed per the manufacturer's instructions and cloned into TOP10 *E. coli* (Invitrogen, Carlsbad, CA). All clones were screened by colony PCR [339] and clones containing an insert of the correct size were selected, subcultured, miniprepped, and sequenced to ensure no mutations were introduced. *B. burgdorferi dnaA* was cloned in to the pET200 vector per the manufacturer's instructions. All clones generated in these studies that appeared to have a correctly sized insertion by colony PCR were subcultured, plasmid DNA isolated, and sequenced to ensure no mutations had been introduced.

RNA-Seq Library preparation

Cells harboring pWA10 were inoculated 1:100 from -80°C stocks and grown at 34°C until reaching mid-exponential phase (~$1x10^7$ cells/mL). An aliquot of these cells was passaged to 2 sets of triplicate cultures of fresh BSK-II to a final density of $1x10^5$ cells/mL in 20mL of BSK-II and placed at 34˚C. Upon reaching ~$1X10^6$ cells/mL IPTG was added to a concentration of 0.5mM to three of the cultures and cultures were returned to 34°C. These cultures were harvested upon reaching $1x10^7$ cells/mL (~24 hours) by centrifugation at 8200XG for 30 minutes at 4°C. One of the un-induced cultures could not

be harvested due to contamination. Pellets were suspended in pre-warmed (60˚C) Trizol (ThermoFisher, Waltham, MA) and stored at -80°C.

Cell-TRIzol suspensions were thawed at room temperature. RNA was isolated from 500mL of cell suspension using the Zymo RNA Direct-Zol Miniprep Kit (Zymo, Irvine, CA) and eluted in in 35µl RNase-free water. Isolated RNA was stored at -80°C. RNA integrity was assayed by microfluidic analysis using an Agilent 2100 Bioanalyzer and with the Agilent RNA 6000 Nano chip kit (Agilent, Santa Clara, CA) and all samples assayed were of high quality, with a RIN score > 9. RNA quantity was also assayed using a Nanodrop 2000 (ThermoFisher, Waltham, MA)

Illumina cDNA libraries were generated using the RNAtag-seq protocol essentially as described, with minor modifications [14, 281], by Jonathan Livny and Jessica Alexander at the Broad Institute. Briefly, 840ng of total RNA was fragmented, depleted of genomic DNA, dephosphorylated, then ligated to DNA adapter barcodes. Barcoded RNAs were pooled and depleted of rRNA using the RiboZero rRNA Depletion Kit (Illumina, San Diego, CA). Pooled barcoded RNAs were converted to Illumina cDNA libraries in 3 main steps: (i) reverse transcription of template by priming a constant region of the barcoded adaptor; (ii) degradation of the RNA followed by template switching addition of a second poly G priming site; (iii) PCR amplification using primers that target the constant regions of the 3' and 5' ligated adaptors and contain the full sequence of the Illumina sequencing adaptors. cDNA libraries were sequenced an Illumina Nextseq 500 (Illumina, San Diego, CA) in the paired end configuration for 75 cycles.

RNA-Seq Data Analysis

For the analyses of RNAtag-Seq data, reads from each sample in the pool were identified and deconvoluted based on their associated barcode using custom scripts [191]. Up to 1 mismatch in the barcode was allowed, with the caveat that it did not enable assignment to more than one barcode. Quality of reads was assessed prior to quality

trimming using FastQC (v0.11.5) [10]. Paired FastQ files were trimmed of low quality sequences and reads before being filtered to remove reads which contained less than 25 bases using Trimmomatic (v0.36) [30]. A custom transcriptome file described previously was indexed using the Salmon –index function set for quasi mapping with default settings and auto library detection (v0.8.2) [238]. Mapping and counting was conducted using Salmon (v.0.8.2) in quasi mode with seqBias and GCbias flags activated. All code, QC metrics, read mapping statistics, and intermediary data files for data generated in Chapter 6 are available on Figshare (https://doi.org/10.6084/m9.figshare.5502175). Raw reads have been deposited to the NCBI SRA database under Bioprojects (PRJNA408156 and PRJNA339291).

Flow Cytometry

B. burgdorferi B31e2 harboring pGJ1 were inoculated from glycerol stocks and first passaged as described above. Mid-exponential-phase cultures of each transformed *B. burgdorferi* strain were passaged in to BSK-II supplemented with 6% rabbit serum (complete media), BSK-II supplemented with 1.2% rabbit serum, or complete media diluted to 25% strength supplemented with 6% rabbit serum with PBS. Upon reaching mid-exponential phase cultures were pelleted, washed and resuspended in PBS and were assayed for GFP expression using a FACSCalibur flow cytometer (BD Biosciences, San Jose, CA), with excitation at 488 nm and detection at 530 nm. KS20 cultures harboring the promoter-less GFP plasmid (pBLS590) were used as negative controls to subtract for autofluorescence. Each experiment involved measuring a minimum of 75,000 events.

Western Blotting

BpuR, SodA, and FlaB western blots of BpuR overexpressing strains were performed essentially as described previously [158]. Cells were grown and induced identically to those used for RNA-Seq and qRT-PCR with the modification of an increase

to 50mL of total culture volume. Cells were pelleted at 4˚C at 27,000XG for 15 minutes following a 24hr induction with .5mM IPTG and resuspended in 10mL ice cold, filter-sterilized PBS. Cells were pelleted at the same centrifugation conditions as noted above with the modification of being spun for 10 minutes. Cells were washed twice more in equal volumes of PBS before being resuspended in 250ul ddH_2O. An equal amount of 2X SDS Loading dye was added and samples were boiled for 10 minutes. Aliquots of 20ul were loaded on 12.5% resolving SDS-PAGE gels and electrophoresed at 100V through the stacking layer before being electrophoresed at 200V for 60-80 minutes. Proteins were electroblotted on to nitrocellulose membranes. Membranes were stained with Ponceau S to confirm approximately equal loading. Ponceau S was removed by repeated, short washes in room temperature ddH_2O before being blocked in 5% milk in TBS-T overnight at 4˚C or for 1 hour at room temperature. Primary rabbit anti-BpuR (1:100) and Mouse anti-SodA (1:2000) antibodies were incubated overnight at 4˚C. The production of Polyclonal BpuR and monoclonal FlaB antibodies has been described previously [158], and SodA antibodies were generously provided by Dr. Janakiram Seshu [96]. Anti-FlaB monoclonal antibody was incubated with agitation for 1 hour at RT. Membranes were washed 3 times with agitation in 10-15mL of TBS-T for 10 minutes each at RT. Horse radish peroxidase (HRP) conjugated secondary antibodies (protein A-HRP and goat anti-rabbit IgM-HRP) (GE Life Sciences, Marlborough, MA), were diluted 1:10,000 in TBS-T and incubated with agitation on membranes for 1 hour at RT. Membranes were developed using the Super Signal West Pico substrate (ThermoFisher, Waltham, MA) and imaged by autoradiography.

2D-PAGE

2D gel electrophoresis was performed essentially as described previously [324] using the BioRad 2D-PAGE Starter Kit (BioRad, Hercules, CA). Briefly total cell pellets of *B. burgdorferi* that constitutively express high levels of BpuR or those transformed with an

empty vector control and express wild-type levels of BpuR were resuspended in equilibration buffer and loaded on to precast IPG strips (BioRad, Hercules, CA) (pH 4-7). Strips were subject to isoelectric focusing at 3000 Volt-hours (V-hrs). Following focusing strips were equilibrated and loaded into the tops of conventional 12.5% SDS-PAGE gels and electrophoresed for 100 min. Gels were stained with Sypro Ruby (ThermoFisher, Waltham, MA) and imaged using a conventional UV box imaging system.

Electrophoretic Mobility Shift Assay

Nucleic acids utilized as probes in this study are described in Table 2-1. Double-stranded DNA probes were generated either by PCR or by annealing complimentary oligonucleotides as essentially as previously described [16, 158]. RNA probes were synthesized by a third party (IDT, Coralville, IA). Longer probes were prepared by PCR using Q5 polymerase with a biotinylated 5' primer and an unlabeled 3' primer (IDT, Coralville, IA) using genomic DNA isolated from B31 MI-16. These amplified probes were gel purified by gel extraction using the PCR Clean-Up Kit (Promega, Madison, WI) and re-amplified. Competitors were generated by proofreading PCR or by annealing of oligonucleotides (IDT, Coralville, IA). Oligonucleotide competitors used in EMSA were annealed by mixing equimolar quantities, heating to 98C, and then allowing to cool to room temperature.

EMSAs were performed as described previously [16, 42, 158]. Binding reactions took place in EMSA binding buffer (50mM Tris, 1mM EDTA, 1mM DTT, 10% Glycerol v/v, 2.4% Protease inhibitor cocktail v/v, and .6% phosphatase inhibitor cocktail v/v) with 1nM biotin labeled nucleic acid, various amounts of recombinant protein, and 100nM of various competitors where appropriate. After incubation at room temperature for 20 minutes, 2.5µl of loading dye (15% w/v Ficol, .04% w/v Orange G) was mixed with the reaction, and 5.5µl of this was electrophoresed on 6% TBE acrylamide gels (ThermoFisher, Waltham, MA) for 60 minutes at 100V. Labeled DNA was then electroblotted to nylon Biodyne B

membranes (ThermoFisher, Waltham, MA) for 45 minutes at 100V on ice. Nucleic acids were crosslinked to the membrane using a Stratagene UV Crosslinker (Stratagene, San Diego, CA) on the automatic setting. Labeled nucleic acid was visualized using the Chemiluminescent Nucleic Acid Detection Module Kit (ThermoFisher, Waltham, MA).

DNA-Affinity Chromatography

DNA affinity chromatography was performed essentially as described previously [161]. Primers BiobpuRP-1 and bpuRP-2 (Table 2-1) were used to PCR amplify the *bpuR* promoter coding sequence from B31-A3 genomic DNA. This DNA fragment was purified by gel extraction and re-amplified to obtain sufficient amounts. Cleaned, isolated probe was mixed with 200µl of streptavidin coated magnetic beads. Magnetic beads were mixed with crude cytoplasmic extracts of mid-log ($1x10^7$ cells/mL) *B. burgdorferi* B31-A3 in the presence of 10µg/mL Poly (dI-dC) to compete for nonspecific binding of DNA. These bead:DNA:protein complexes were then washed repeatedly in buffer BS/THES supplemented with 10µg/mL Poly (dI-dC). Proteins were eluted from DNA by washing in the presence of increasing amounts of NaCl to disrupt protein:DNA interactions. Total fractions were run on 12.5% SDS-PAGE and stained with Sypro Ruby. Lanes which contained distinct bands were excised using clean fresh razors and submitted to the University of Kentucky Mass Spectrometry Core for identification.

Liquid Chromatography Electrospray Ionization Tandem Mass Spectrometry (LC-ESI-MS/MS) Analysis

All mass spectra reported in this study were acquired by the University of Kentucky Proteomics Core Facility. The protein gel slice was subjected to dithiothreitol reduction, iodoacetamide alkylation, and in-gel trypsin digestion using standard protocols and the tryptic peptides were subjected to shotgun proteomics analysis as previously described in

Yang et al. [344]. The resulting tryptic peptides were extracted, concentrated, and injected for nano-LC-MS/MS analysis.

LC-MS/MS analysis was performed using an LTQ-Orbitrap mass spectrometer (ThermoFisher Scientific, Waltham, MA) coupled with an Eksigent Nanoflex cHiPLC™ system (Eksigent, Dublin, CA) through a nano-electrospray ionization source. The peptide samples were separated in? a reversed phase cHiPLC column (75 µm x 150 mm) at a flow rate of 300 nL/min. Mobile phase A was water with 0.1% (v/v) formic acid, while B was acetonitrile with 0.1% (v/v) formic acid. A 50-minute gradient condition was applied: initial 3% mobile phase B was increased linearly to 40% in 24 min and further to 85% and 95% for 5 min each before it was decreased to 3% and re-equilibrated. The mass analysis method consisted of one segment with eight scan events. The 1st scan event was an Orbitrap MS scan (300-1800 m/z) with 60,000 resolution (FWHM) or parent ions followed by data dependent MS/MS for fragmentation of the 7 most intense multiple charged ions with collision induced dissociation (CID) method.

MS/MS Protein Identification

The LC-MS/MS data were submitted to a local mascot server for MS/MS protein identification via Proteome Discoverer (version 1.3, ThermoFisher Scientific, Waltham, MA) against a custom database containing 990 reviewed proteins of *Borrelia burgdorferi* (downloaded 08/19/2015). Typical parameters used in the MASCOT MS/MS ion search were: trypsin digest with maximum of two miscleavages, cysteine carbamidomethylation, methionine oxidation, a maximum of 10 ppm MS error tolerance, and a maximum of 0.8 Da MS/MS error tolerance. A decoy database was built and searched. Filter settings that determine false discovery rates (FDR) are used to distribute the confidence indicators for the peptide matches. Peptide matches that pass the filter associated with the FDR rate of 1% and 5% are assigned as high and medium confident peptides, respectively. An

extracted ~58kD band was positively and unambiguously identified as the *B. burgdorferi* DnaA homologue.

Recombinant protein expression and isolation

For recombinant protein expression and purification, the *B. burgdorferi dnaA* gene was PCR amplified (Table 2-1) using Q5 polymerase, cloned in to the pET200 vector (ThermoFisher, Waltham, MA) and transformed in to *E. coli* Top10 cells (ThermoFisher, Waltham, MA). Transformants were screened by colony PCR [339] for insertion size and positive colonies were isolated, miniprepped (Zymo, Irvine, CA), and sequenced using flanking T7 promoter and terminator primers (Eurofins Genomics, Louisville, KY) to validate that no mutations had been introduced. Error-free plasmids were transformed into Rosetta 2 DE3 pLysS (Millipore, Billerica, MA) cells. An isolated colony was picked and grown over night in LB media containing 50µg/mL of kanamycin and 34µg/mL of chloramphenicol. These overnight cultures were passaged 1:100 in to 2L of super broth and cultures were induced with 0.5mM IPTG once the culture reached an OD ~0.8. Cultures were allowed to continue for 2 hours before harvesting by centrifugation at 8200XG at 4˚C for 10 minutes. Pellets were stored at -80°C until further processed.

Pellets were thawed and resuspended in 20mL of ice cold washing/binding buffer (100mM HEPES, 10mM Imidazole, pH 7.5). An appropriate number of EDTA-free protease inhibitor mini tablets (1 tablet/10mL suspension) were added for the volume used (ThermoFisher, Waltham, MA). Cell suspensions were lysed by sonication with a Branson 102C sonicator (Emerson, St. Louis, MO) at amplitude of 20% for 15 seconds. This was repeated for a total of 5 cycles. Cellular debris was pelleted by centrifugation at 4°C for 30 minutes at 27,000XG. Soluble fractions were mixed with 1mL MagneHis beads (Promega, Madison, WI) at 4°C for 1 hour. Beads were pulled down by magnet, decanted, and washed with fresh washing/binding buffer. This was repeated 5 times. Remaining bound proteins were eluted in a three-step series of 500µl fractions using Elution buffer (100mM

HEPES, 500mM Imidazole, final pH 7.5). Fractions positive for protein by A280 measurement were pooled and dialyzed overnight in 10K MWCO cassettes (ThermoFisher, Waltham, MA) against EMSA Dialysis buffer (10% v/v Glycerol, .5mM EDTA, 50mM Tris pH 8.0, .1% PMSF, .01% Tween-20, 50uM KCl, 1mM DTT). Dialyzed samples were concentrated using Amicon 50K Ultra Centrifugal Units (Millipore, Billerica, MA). Concentrated protein was aliquoted and frozen at -80C.

Table 2-1 Oligonucleotide primers used in these studies

Oligonucleotide Name	Sequence	Purpose
NidoF	CCAGCCACAGAATACCATCC	Specific detection of mouse chromosomes
NidoR	GGACATACTCTGCTGCCATC	Specific detection of mouse chromosomes
flaBF	GGAGCAAACCAAGATGAAGC	Specific detection of bacterial DNA
flaBR	TCCTGTTGAACACCCTCTTG	Specific detection of bacterial DNA
LuxSF	GAGCACATAGGAGCTACTTTACTT	Specific detection of uninterupted *luxS* allele
LuxSR	TTCCTTAAAACATGCAGGAATTGAC G	Specific detection of uninterupted *luxS* allele
ErmCF	AAACGCTCATTGGCATTACTTT	Specific detection of erythromycin cassette
ErmCR	TGAGCTATTCACTTTAGGTTTAGGA	Specific detection of erythromycin cassette
BioBpurProbe1	BIO/CCTTCTTTTTAAATCGCCCGCC	Generation of *bpuR* promoter pulldown probe
Bpur Probe2	GATTTATTGTAATGTTATTTTTAGCTA GC	Generation of *bpuR* promoter pulldown probe
BpurP-1	CAATTTCCTCCACACAAGTTTTTG	*bpuR* promoter competitor 1 F
BpurP-2	GTACAATTAATTTAGCTTAAATGTAG TCAAGT	*bpuR* promoter competitor 1 R
BpurP-3	GACTACATTTAAGCTAAATTAATTGT AC	*bpuR* promoter competitor 2 F
BpurP-4	GATTTATTGTAATGTTATTTTTAGCTA GC	*bpuR* promoter competitor 2 R
BpurP-5	GCTAGCTAAAAATAACATTACAATAA ATC	*bpuR* promoter competitor 3 F
BpurP-6	GGACGCAATACAATAATTTACTTATA T	*bpuR* promoter competitor 3 R
BiobpuRp-11	BIO/CAATAATTTACTTATATAAAAA	*bpuR* promoter EMSA probe F
bpuR-14	CCACACAAGTTTTTGTACTTGAC	*bpuR* promoter EMSA probe R
sodA 5' (RNA)	AUCAUAACCAAGUUCUGGCAGCUU AAACAUAAAAACCUCCUGUUUUAAC UUUUGCCAUGA	*sodA* RNA for BpuR binding
BioRNAbpuRp-F (RNA)	CUUAAAUGUAGUCAAGUACAAAAAC UUGUGUGGAGGAAAUUGAUGGGAG AGAGAGGGGAAGUAUACUCU	Positive control for BpuR binding
BioRNAbpuRORF (RNA)	AAACUAUUUACAGAGUCUGAGAGAA CUUAUUUUUUUAAUGUCAAGGAAAA UAGAAAAGGAGAUUAUUUU	Negative control for BpuR binding

Table 2-1 Cont

Bio oriC F	BIO/GAAGAATCAAAAATTATTTTAAAC	Labeled *oriC* probe F
oriC R	GAAGAATCAAAAATTATTTTAAAC	Unlabeled *oriC* probe R
oriC F	CATGATGCCTCCTTATATATTCTATTAC	Unlabeled *oriC* probe F
ospC F	CTTGCTGTGAAAGAGGTTGAAG	qPCR
ospC R	CTCCCGCTAACAATGATCCA	qPCR
rpoN F	GGCCAATGAACTTGAGCATTT	qPCR
rpoN R	GCTCCACCAACAGAGCTAAA	qPCR
sodA F	TGTCCTGAGAGTGGCCTTA	qPCR
sodA R	GCATGCTCCCAAACATCAATAC	qPCR
dbpA F	GCTGCTCTTAAGGGCGTAAA	qPCR
dbpA R	CTACTGTAGTAGCTCGCACTTT	qPCR
ftsK F	GACCTTCTGATGAGCCAATGT	qPCR
ftsK R	GCTGCTCTGTTGTAACCTATCT	qPCR
qlp28-4 F	GCGTATAGTTCGTTGGCTGTA	qPCR
qlp28-4 R	GCAGTGGGTCTAGGCATATTAC	qPCR
qDnaA F	CCAAFTCCAACTCCACCATAAA	qPCR
qDnaA R	GGGCCAAATAATAAACTTGCTTACA	qPCR
bpuR F	GGCTCTTCTGCAAGGCATAAT	qPCR
bpuR F	GCCCGCCTGATAAATGAGATT	qPCR
hslU F	CAAACCGCCAATTCCCATATC	qPCR
hslU R	GCAGGTGAGCTTGATGATACTA	qPCR
hslV F	ATGATGCTTGTTGCTGATTCTAAC	qPCR
hslV R	CACCACTGCCAATCGAAATAAC	qPCR
flaB F	CCTTCTCAAGGCGGAGTTAAT	qPCR
flaB R	AGCACCTAAATTTGCCCTTTG	qPCR
rpoS F	TTTGGGACTATTGTCCAGGTTAT	qPCR
rpoS R	CCCTTGAACAAGATTCAACTCTAAA	qPCR

This table contains the sequences of all primers used in these studies and their purpose.

Chapter 3 Metabolic linkages of signaling and gene regulation

This work described in this chapter has been published: Arnold WK, Savage CR, Antonicello AD, Stevenson B. 2015. "Apparent role for *Borrelia burgdorferi* LuxS during mammalian infection." Infect Immun 83:1347-1353.

Introduction

Many bacteria occupy complex multicellular communities composed of both kin and non-kin species of bacteria [213]. Members of these communities often exhibit communicative behavior through either direct contact [108] or the secretion of signaling molecules [24, 74, 213]. One of the better studied examples of the signaling molecule secretion system is that of *Vibrio harveyi* and *Vibrio fischeri*, marine organisms which luminesce in response to high cell density [213]. This behavior and the mechanisms defining it are termed "quorum sensing." Different organisms utilize different types of systems and, even within the same species, there can be multiple types of quorum sensing, involving different signals, receptors, and pathways. The studies described in this chapter focus will on the role of the small molecule 4,5-dihydroxy-2,3-pentanedione (DPD) and its various equilibrium products, collectively known as autoinducer 2 (AI-2) during *B. burgdorferi* pathogenesis.

DPD and homocysteine are produced by the enzyme LuxS. Numerous pathogenic bacteria, including *Salmonella enterica* serovar Typhimurium [305], *Vibrio cholera* [214], and *Borrelia burgdorferi* [253, 297, 300], possess homologues of the LuxS enzyme and in several cases, the enzyme has been shown to play an important role in virulence [259]. LuxS is a component of the activated methyl cycle, which detoxifies and recycles the toxic byproducts of methylation reactions utilized for physiological processes. Briefly, S-adenosylmethionine (SAM) is used to methylate various substrates, including DNA [29]

and proteins [124, 178], through the activity of methyl transferases. This reaction generates the toxic byproduct S-adenosylhomocysteine (SAH). In some organisms, SAH can be directly converted to homocysteine and adenosine through the activity of SAH hydrolases, which *B. burgdorferi* does not encode [253]. SAH can also be detoxified by the activity of Pfs, which converts SAH to S-ribosylhomocysteine (SRH) and adenine. SRH is nontoxic, and the related spirochete, *Treponema pallidum*, appears terminate the pathway at this step [336]. Most other bacteria use a complete version of one of these cycles to regenerate homocysteine for reuse in the activated methyl cycle. The case of *B. burgdorferi* is an interesting one in that it encodes an incomplete cycle but continues to the LuxS step (Fig. 3-2). If SRH is non-toxic and other organisms with highly reduced genomes seem to have successfully dispensed with their LuxS homologue [325], why then is it retained in *B. burgdorferi*?

Our lab has previously shown that wild-type *B. burgdorferi luxS* can complement an *E. coli* Δ*luxS* mutation, and *B. burgdorferi* secretes a molecule into media which induces luminescence in *V. harveyi* reporter assay [297, 300, 325]. These results indicate that *B. burgdorferi* produces an AI-2-like molecule that elicits signaling responses in other bacteria. Furthermore, adding exogenous AI-2 to cultures of either Δ*luxS* mutant or wild-type *B. burgdorferi* results in differences in expression of multiple proteins, including several involved in vertebrate infection: VlsE, ErpA, and LA7. The expression of ErpA and VlsE was examined specifically upon the addition of exogenous AI-2 in wild type *B. burgdorferi* and while both were expressed in absence of exogenous AI-2, their expression was notably increased upon its addition [17]. The expression of *luxS* was measured during both *in vitro* and *in vivo* cultivation and is most highly expressed during exponential growth [253] and during tick feeding [223], both of which are periods of relatively rapid growth rates [242].

It came as quite a surprise, when the ability of *luxS* mutant bacteria to traverse the full enzootic cycle was tested, there were not significant differences between the mutant and wild-type strains. In two studies, a mutant strain of *B. burgdorferi* unable to produce LuxS, and thus AI-2, was able infect mice by needle inoculation, be acquired by feeding ticks, survive tick molting, and then transmit to naïve mice. In addition, development of disease, as measured by histopathology scoring, was not significantly different between strains [27, 137]. However, these studies unfortunately suffer from several key shortcomings.

First, no quantitative information regarding bacterial burdens was measured. While there were no significant differences in the number of mice or ticks that became infected following the experiment, it remains unclear if the relative numbers of bacteria differed between wild type and mutant during any stage of the infection. Second, and more importantly, the mutant was selected for in an unusual way that is likely to have generated suppressor mutants. Possible mutants were initially identified by erythromycin sensitivity screening and, following electroporation and selection, were immediately inoculated into sterile dialysis chambers and implanted into rat peritoneal cavities. These bacteria were allowed to grow for an additional 15 days in the dialysis chamber before being removed and syringe inoculated intraperitoneally in to wild-type mice. After two weeks, ear punch biopsies were performed and viable, erythromycin resistant spirochetes were plated and isolated as single colonies. While this method certainly enriches for Δ*luxS* mutants who retain the full required compliment of plasmids for infection, it also strongly selects for mutants that have suppressed the effect of any deleterious effects on vertebrate infection of the mutation. As the Stevenson lab has already demonstrated, the effects of AI-2 on *B. burgdorferi* gene regulation does not appear to act as an ON-OFF switch, but as a tunable response [325]. This led me to hypothesize that *B. burgdorferi* unable to sense or produce AI-2 would be at a competitive disadvantage to those that could. As the mechanism of

sensing AI-2 in *B. burgdorferi* is not well understood, I chose to examine the effects of altering production of the molecule.

In this chapter I performed studies aimed at testing this hypothesis while addressing the first above mentioned concern, namely that there may exist quantitative differences in bacterial burden between wild type *B. burgdorferi* and those that are mutated in *luxS*.

Absence of *luxS* does not result in loss of fitness during single strain infection

I tested if wild type or *luxS* mutant bacteria grew to different densities in the context of a vertebrate infection. To test this in the context of the previously described studies [27, 137], I chose to perform the below-described studies using the same mutants derived in those studies. Eight BALB/cJ mice were infected by needle inoculation with $1x10^4$ wild type (297) or Δ*luxS* mutant (AH309) bacteria from mid-exponential phase cultures. Mice were euthanized the mice after 28 days, allowing sufficient time for the establishment of disseminated infection, and sterilely harvested hearts and ears. Total DNA was isolated from these samples.

To examine bacterial burden, I measured the abundance of the single copy *B. burgdorferi* gene, *flaB*, compared to the single copy *M. musculus* gene, *nido* by qPCR as proxies for genome equivalents. Mice infected with AH309 contained slightly higher numbers of bacteria in their hearts than did mice inoculated with 297 ($P = 0.049$), but there were no statistically significant differences in the bacterial loads of ears from mice infected with 297 or AH309 (Fig. 3-3). These data further demonstrate that the Δ*luxS* mutant does not have any significant metabolic deficiencies that inhibit mammalian infection.

Loss of LuxS results in a quantitative loss of fitness during competitive infection

Many mutations result in subtle phenotypes when examined in isolation [15, 26, 193, 322]. To test for subtle effects and to more closely model natural environments where

subtle negative genotypes present in a multi-strain infection are selected against by evolution, competitive models have been increasingly utilized. To test the effect of a Δ*luxS* mutation in a more sensitive manner, I examined relative bacterial burdens of *B. burgdorferi* strains 297 (WT) and AH309 (Δ*luxS*) in a competitive infection model. Alyssa Antonicello and I simultaneously inoculated with equal numbers ($1x10^4$ cells) of both 297 and AH309. After 28 days Alyssa and I harvested sterilely hearts, ears, and urinary bladders and isolated total DNA from the tissues.

To discriminate between the wild-type and Δ*luxS* mutant strains in the mixed infection samples, PCR primers were designed which specifically amplify only the wild-type or mutant Δ*luxS* locus (Fig. 3-4). Control PCRs with purified DNA from each strain confirmed that the oligonucleotide pairs were equally efficient at priming PCR from their respective templates and could be compared. I performed qPCR analyses of heart, ear, and urinary bladder tissues of eight dually-infected mice. The analyzed tissues were all distant from the site of inoculation and therefore measured the bacteria's ability to disseminate through mice and colonize, rather than simply survive at the site of injection. Comparisons of resultant data indicated that all tissues of all mice contained statistically significantly larger numbers of wild-type than mutant bacteria (Fig. 3-5). Variations in wild-type/mutant ratios occurred between mice and between tissues of the same animals. The greatest degree of variation was found in the most distal tissue, the ears, with 3-fold to 18-fold more wild-type borreliae. Less variability was seen in the internal organs, i.e., the hearts and urinary bladders.

Discussion

These data highlight several salient aspects that have been widely underappreciated in the field of microbial pathogenesis. First, perturbations (either deletions or overexpression) of many genes result in subtle effects on the ability of microbial pathogens to infect and cause disease in their hosts, especially when examined

outside of their natural context. Quantitative measurements, particularly in a competitive or community setting, are critical to delineating these subtler effects.

Second, AI-2 based signaling is intimately tied to microbial growth and physiology. As noted above not all LuxS enzymes are necessarily involved in what is typically known as quorum sensing behavior. LuxS plays an essential role in recycling of homocysteine and perpetuation of the activated methyl cycle in many bacteria. On the other hand, this intimate linkage offers a unique mechanism with which to tie metabolic activity to bacterial communication. It would seem a reasonable hypothesis that some organisms make dual use of this pathway. The *B. burgdorferi* LuxS produces both AI-2 and homocysteine, but current evidence suggests that *B. burgdorferi* is unable to recycle homocysteine [325].

A significant question remains regarding how *B. burgdorferi* senses the AI-2 molecule and affects the previously observed gene regulatory changes. Sensing of AI-2 is most often associated with a two-component type LuxPQ or an ABC-transporter type Lsr system [128]. *B. burgdorferi* encodes two two-component regulatory systems, Hk2/Rrp2 and Hk1/Rrp1, neither of which share significant homology to the LuxPQ system [101]. The signals for either system remain unknown, but they are essential for the vertebrate adaptation stage of the infectious cycle or for cellular viability, respectively. In the light of the above findings, namely that LuxS is not absolutely essential for vertebrate infection, I find it less likely that AI-2 is the cognate signal for either system.

S. typhimurium also lacks a recognizable LuxPQ system and instead imports AI-2 via an ABC transporter with homology to those that import ribose [310], termed the Lsr system. *B. burgdorferi* encodes numerous transporters to support its extreme auxotrophy and harvest required nutrients from the extracellular milieu, including a large repertoire of ABC transporters with homology to carbohydrate transport systems. One of these systems is annotated as having homology to a ribose ABC transporter, but *B. burgdorferi* does not utilize ribose as a nutrient source [326]. AI-2 molecules bear significant similarity to ribose

molecules, and, in *Actinobacillus actinomycetemcomitans*, the ribose binding protein, RbsB, also binds AI-2 at the same active site as it does ribose [149]. A reasonable hypothesis is that the annotated ribose transporter in *B. burgdorferi* may, in fact, act to import AI-2 into the cell. A potential link from this import to the observed changes in gene expression is through the carbohydrate responsive DNA-binding protein BadR. BadR regulates several hundred genes (described in further detail in Chapter 6), though the number of directly regulated targets remains relatively unknown, and DNA binding activity is regulated by carbohydrate binding. Namely, the addition of phosphorylated sugars, including ribose-5P to DNA binding assays inhibits the ability of BadR to bind at least one of its targets, *rpoS* [210]. Potential mechanisms thus exist to generate, import, and sense extracellular and intracellular production of AI-2.

Examining the response to exogenous AI-2 on mutants in BadR or the other putative carbohydrate responsive DNA binding protein XylR-1 could prove interesting. If, in fact, either of these proteins were responsive to AI-2, I would expect that response to be ablated in their absence. Furthermore, transposon mutants exist for many of the carbohydrate transporter subunits. Tracking the import of labeled AI-2 in these mutants could shed light on whether AI-2 is transported back into the cell and if any of these transporters are required, or if AI-2 is sensed extracellularly.

In summary, AI-2 and quorum sensing in *B. burgdorferi* remains an interesting and relatively unexplored area of study. A focus on “all or none” pathogenesis and a relatively unusual set of studies have unfortunately reduced enthusiasm for the field. The relatively straightforward studies described above could reignite interest in the study of the system.

Table 3-1 Results of the competitive infection study

	Heart				Bladder				Ear			
	297		AH309		297		AH309		297		AH309	
Animal	Mean	SD	Mean	SD	Mean	SD	Mean	SD	Mean	SD	Mean	SD
1	31.068	0.729	32.86	0.281	30.863	1.422	33.555	0.208	30.55	0.811	32.775	0.661
2	30.265	0.296	32.763	0.272	30.673	0.534	33.893	0.419	31.62	0.44	32.798	0.511
3	31.173	1.667	33.18	0.913	30.293	0.571	32.17	0.612	30.493	0.456	33.683	1.429
4	30.37	0.921	33.143	0.452	30.728	2.049	31.733	1.112	30.865	0.389	33.325	0.106
5	30.703	1.517	33.13	1.3	30.138	0.676	32.763	1.055	30.81	0.819	34.763	2.401
6	31.395	1.759	33.015	0.843	30.68	1.953	30.738	0.787	30.17	0.561	32.355	0.324
7	29.795	1.186	33.035	1.138	30.638	0.296	31.88	1.612	30.578	0.096	32.883	1
8	30.295	1.193	31.79	0.707	30.375	0.423	33.003	0.604	33.083	2.005	34.08	0.042
P value	< 0.0001				0.0015				0.0003			

C_T values were measured by qPCR for each target gene in each tissue in eight individual mice. Values represent the means for two separate trials, with two measurements per trial. Student's t test was performed on the C_T values obtained for target loci of strains 297 and AH309.

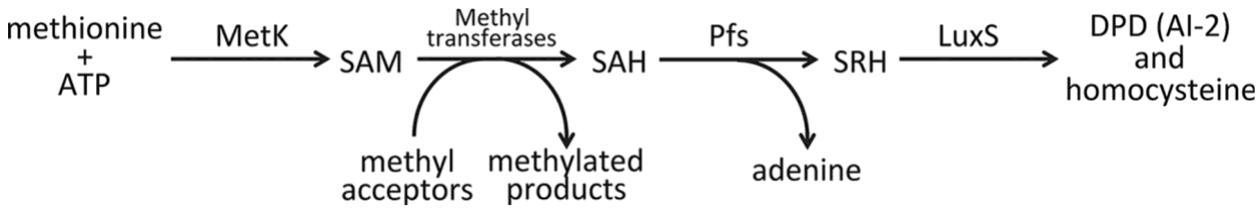

Figure 3-1: Production of AI-2 in *B. burgdorferi*

The activated methyl reaction as it exists in *B. burgdorferi*. Compared to the complete cycle depicted, *B. burgdorferi* lacks either SAH hydrolase or mechanisms to recycle homocysteine.

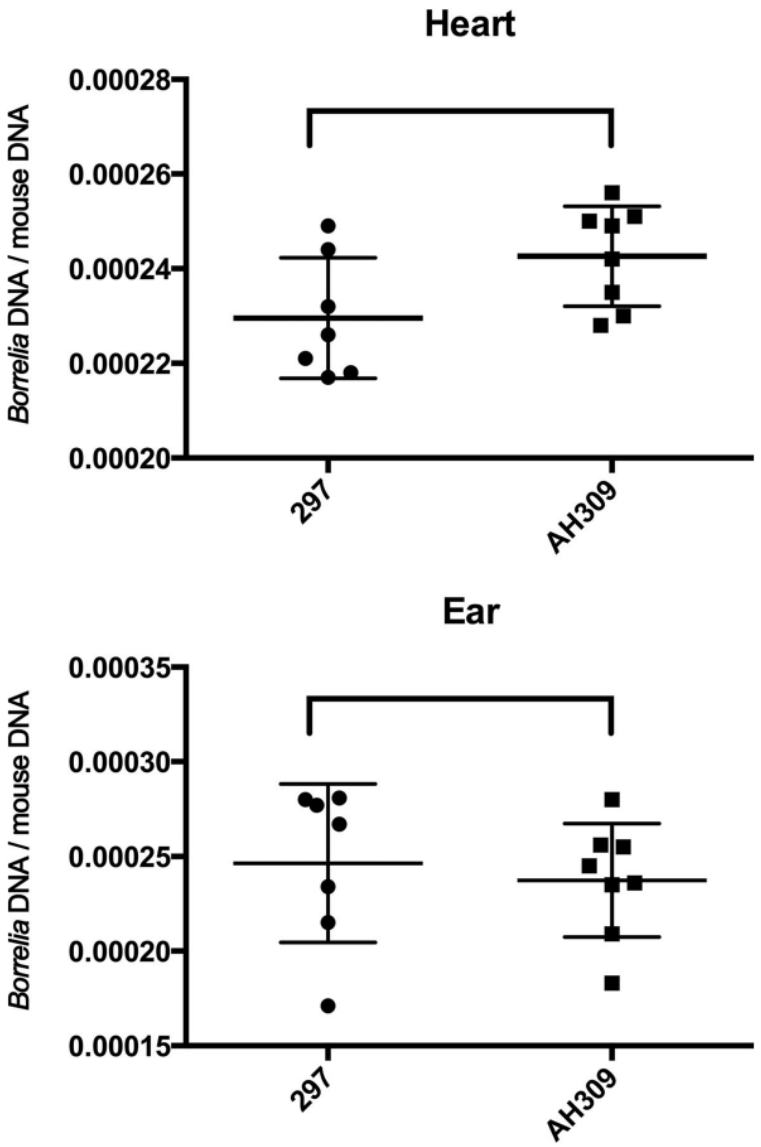

Figure 3-2: Bacterial burdens during individual infection

Burdens of *B. burgdorferi* were measured in mouse tissues 28 days after needle inoculation. Equal amounts of WT or ΔluxS mutant bacteria were inoculated in to separate groups of 8 mice by intraperitoneal injection. Quantitative PCR targeting the single copy *B. burgdorferi* gene *flaB* and the single copy mouse gene *nido* as proxies for genome equivalents in the samples.

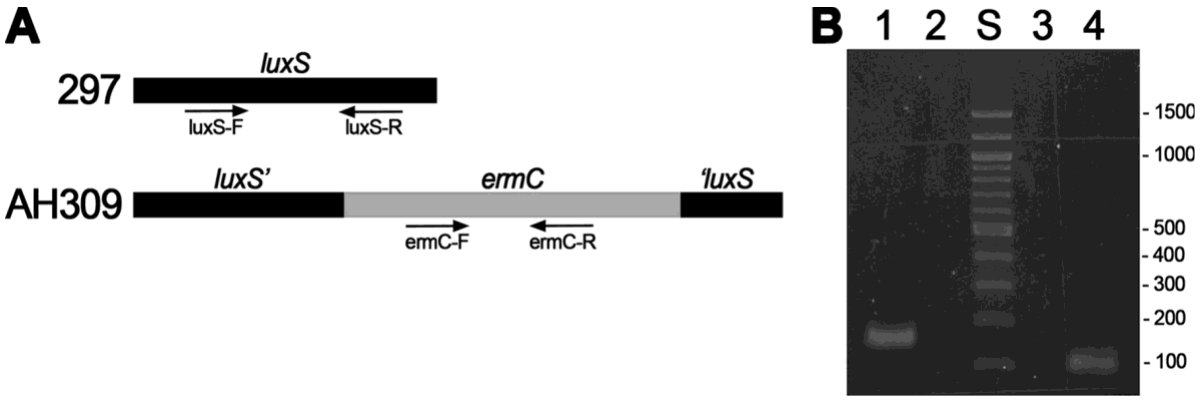

Figure 3-3: Validation of primers for discrimination between strains

(A) The structure of the luxS locus in WT (297) and mutant (AH309) bacteria is given along with the locations of primers used for qPCR. The *ermC* erythromycin resistance marker was inserted in to the native locus by allelic exchange [27].

(B) Agarose gel demonstrating the specificity of amplification for each set of primers on each strain. Lane 1 and 2 use primers luxS-F and luxS-R and lanes 3 and 4 utilize primers ermC-F and ermC-R. Lanes 1 and 3 were performed on DNA from strain 297 and lanes 2 and 4 were performed on DNA from AH309.

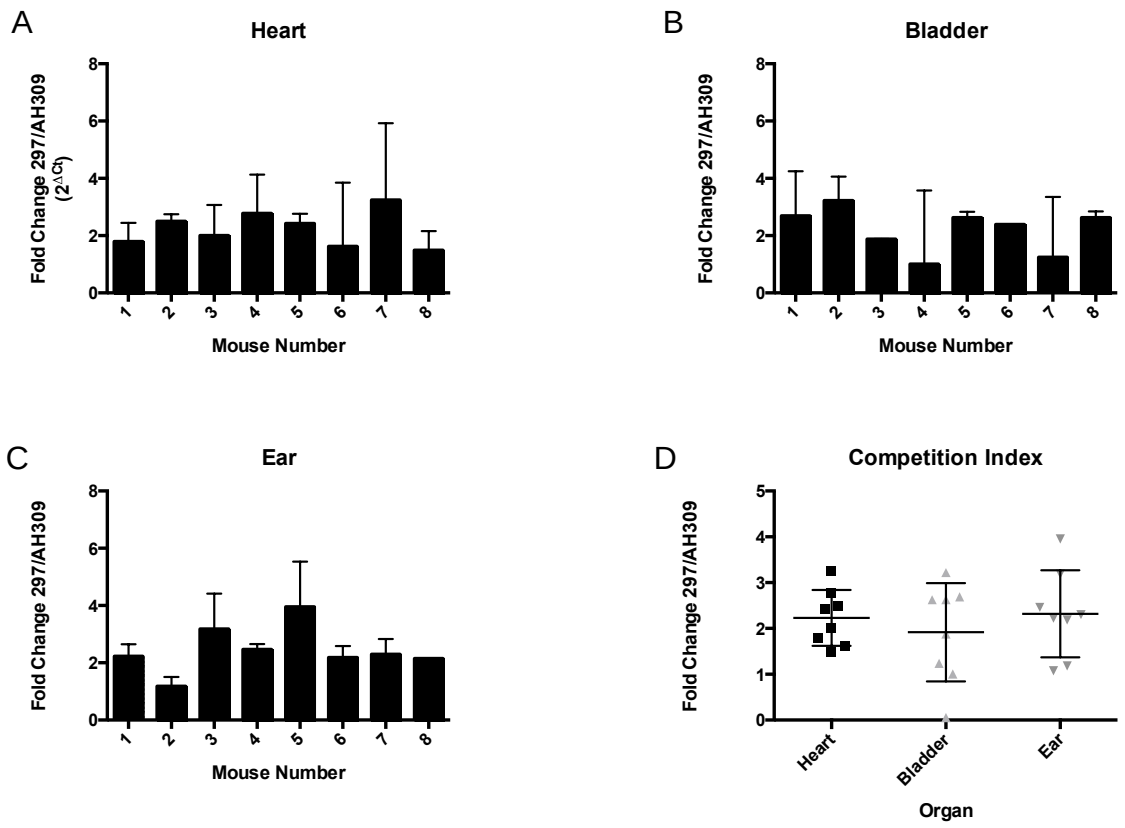

Figure 3-4: Relative bacterial burden between WT and Δ*luxS* mutant

One set of 8 mice was infected with equal numbers ($1x10^4$) of each strain, 297 and AH309. After 28 days, (A) hearts, (B) bladders, and (C) ears were harvested and genomic DNA was isolated. Relative burden was assayed by qPCR with primers specific for either the mutant or wildtype locus and is reported as fold difference of WT/Mutant. (D) The data are summarized as a mean competitive index across all animals and strains.

Chapter 4 Mechanistic links between regulators of virulence and DNA replication

This work is being prepared for submission to Molecular Microbiology under the working title: The expression of BpuR, a key regulator of virulence determinants, is controlled by the master regulator of DNA replication. This was a highly collaborative work, spanning several years across multiple labs. Data and strains were generated and analyzed by myself (IPTG-inducible BpuR construct, RNA-Seq, flow cytometry, SDS-PAGE, EMSA, DNA affinity chromatography), Dr. Brandon Jutras (2D-PAGE, RIP-PCR, Tet-inducible BpuR construct), Dr. Grant Jones (GFP reporter plasmid and strain construction), Kathryn Lethbridge (qRT-PCR validation), Jonathan Livny and Jessica Alexander (RNAtag-Seq library construction and sequencing), and was supported by the University of Kentucky Flow Cytometry and Proteomic Core facilities. Quantitative measurements of *bpuR* expression in ticks was performed at Rocky Mountain Labs by Dr. Patricia Rosa, Aaron Bestor, Dr. Phil Stewart, and Dr. Kit Tilly. Measurements of *bpuR* expression in vertebrates was performed at the University of North Dakota by Dr. Catherine Brissette and Dr. Robert Gaultney. Junior trainees Allison Pecaro, Leeza Kenner, and Walt Finch all assisted with various assays over the course of several years.

Introduction

All cells must eventually relay the information they sense about either external or internal processes (nutrient availability, signaling molecules, etc.) into action, including changes in gene and protein expression or activity, or fail to adapt and die. In the previous chapter, I described a specific metabolite, AI-2, that plays a role in signaling gene and protein expression changes important for infection. A key limitation of that work was a lack of understanding regarding the mechanism

by which the bacteria relayed that information sensed. In this chapter, the focus is on a key regulator of virulence proteins, titled BpuR, and how it is controlled.

BpuR is PUR domain containing protein originally identified by the Stevenson lab as a binding protein that interacted with the *erp* operator DNA [155]. BpuR binds RNA, dsDNA, and ssDNA, in that order of affinity. *In vitro* assays indicated that BpuR acts as a corepressor of the *erp* loci, having no effect on expression unless the primary repressor, BpaB, was also present. Finally, expression of BpuR was examined during *in vitro* differential growth conditions known to partially mimic aspects of the enzootic cycle and was found to be negatively correlated with growth rate (i.e. BpuR expression was high when growth rate was low and vice versa) [155]. In a follow-up study, it was demonstrated that BpuR not only regulated the transcription of the *erp* loci, but that it also bound its own mRNA and negatively regulated its translation [158]. This previous work set the stage for the following questions posed in this chapter: specifically, how is BpuR regulated, and what are the more global consequences of differential expression of this nucleic acid binding regulatory protein?

BpuR is highly expressed in unfed ticks but not vertebrates

Considering the regulated expression of BpuR *in vitro* and the role of PUR domain proteins as pre- and post-transcriptional regulators in *B. burgdorferi* and other model organisms [116, 132, 158], I hypothesized that BpuR levels would be regulated during different stages of the enzootic cycle. In order to test this hypothesis, our lab collaborated with Dr. Patricia Rosa's group at the Rocky Mountain Laboratory and Dr. Catherine Brissette's laboratory at the University of North Dakota. Levels of *bpuR* mRNA at several stages of the life cycle of *B. burgdorferi* were assessed: within unfed ticks, at two time-

points during tick feeding, after tick drop off, and during an established murine infection. Naïve, laboratory-reared *I. scapularis* larvae were fed to repletion on mice infected with wild type B31 MI-16 *B. burgdorferi*. These ticks were allowed to molt to nymphs. In replete larvae and post-molt, unfed nymphs, we found that *B. burgdorferi* produce high levels of *bpuR* mRNA (Fig. 4-1A). During tick feeding, *B. burgdorferi* enter a replicative burst [242] and begin expressing genes and proteins important for transmission and vertebrate infection [146, 264, 272, 298]. At the same time, they begin repressing genes important for tick colonization [146, 220, 272]. When we examined *bpuR* mRNA levels at 24 and 48 hours after the onset of tick feeding, we found that *bpuR* mRNA levels significantly decreased when compared to levels within an unfed tick (Fig. 4-1A). Levels of *bpuR* mRNA in untransmitted bacteria rebounded following tick drop off after feeding. It is unclear if this relative increase in *bpuR* levels compared to those during feeding occurs because all remaining bacteria upregulate *bpuR* levels to pre-feeding levels or that the population of bacteria which fail to transmit are those which persistently express high levels of *bpuR* and thus are enriched following the completion of feeding).

We then examined *bpuR* levels in the context of a disseminated vertebrate infection. Expression of *flaB* and *bpuR* mRNA was assayed in the joints and hearts of mice 28 days after needle inoculation. We found that while *flaB* was readily detected, *bpuR* mRNA was undetectable, even after 40 cycles of amplification (Figure 4-1B). These data suggest that *bpuR* expression is important for the adaptation *B. burgdorferi* to the tick vector but not for the vertebrate host, or that *bpuR* expression is deleterious within the vertebrate host.

Perturbations of BpuR have a minimal impact on *in vitro* transcriptomes

Considering the wider role of the other *erp* regulatory proteins EbfC and BpaB [63, 153] and BpuR's regulated expression *in vivo* and *in vitro* [158]; I hypothesized that BpuR may regulate additional targets. Since *bpuR* is most highly expressed within a tick, is

undetectable within a vertebrate, and co-represses the *erp* genes, I hypothesized that BpuR may act to induce “tick-like” physiology by repressing vertebrate factors, inducing tick specific factors, or a combination of both. Repeated attempts to delete the *bpuR* locus by allelic exchange have been unsuccessful and, to my knowledge, the *bpuR* locus has not been successfully targeted during transposon mutagenesis screens [185, 186, 317]. For this reason, I chose to perturb *bpuR* levels by overexpression. This methodology has been used to successfully study other essential regulatory factors in *B. burgdorferi* [158].

To test the hypothesis that BpuR affects the transcription of other genes outside the *erp* loci, we performed RNA sequencing in collaboration with Jonathan Livny and Jessica Alexander at the Broad Institute on strains that produce either wild-type levels of *bpuR* or those induced to produce higher levels *in vitro*. I transformed a wild-type infectious *B. burgdorferi* strain B31-A3 with the plasmid pWA10, generating a strain (WA11) that expresses high levels of BpuR following the addition of IPTG. I induced high level BpuR expression with the addition of 0.5mM IPTG for 24 hours before harvesting cells. These were compared to uninduced controls. Only two transcripts were statistically and biologically significantly impacted (Fig. 4-2) as defined by FDR corrected $p<.05$ and a greater than two times change in expression in either direction. As expected, the transcript for *bpuR* was increased 4.28 times. The only other transcript affected was *hslU* (*BB_0295*), which was increased 2.58 times. *hslU* encodes the ATPase subunit of the proteasome-like complex HslUV. No other genes in the operon containing this gene were impacted, including the other component of this complex, *hslV* (*Bb_0296*). Kathryn Lethbridge and I examined the expression of *bpuR*, *hslU*, and a number of other transcripts by qRT-PCR from independently grown and induced cultures (Fig. 4-3). As was observed by RNA-Seq, *bpuR* abundance was significantly increased, but no other transcripts assayed in this experiment were significantly differentially expressed. Notably, *hslU* was not significantly impacted by the over expression of *bpuR* when examined by

qRT-PCR of independently grown cultures, suggesting the impact on *hslU* transcript is not reproducible.

BpuR impacts the proteome of *B. burgdorferi*

In work aimed at testing if BpuR was a global regulator of *B. burgdorferi* gene expression Dr. Brandon Jutras performed a number of global expression studies. After demonstrating that BpuR was a dual RNA/DNA binding protein, Dr. Jutras undertook studies to test the effect of elevated levels of BpuR production on the *B. burgdorferi* proteome. *B. burgdorferi* that were engineered to express higher than normal levels of BpuR were assayed by 2D-PAGE and compared to those that did not. A large number of protein spots were identified as differentially abundant between samples. Several of these protein spots were extracted from the 2-D PAGE gels and identified by LC-MS/MS [158]. One protein that was less abundant in induced compared to uninduced cultures was identified as SodA.

SodA is a superoxide dismutase that is essential for vertebrate infection and its deletion results in complete attenuation of *B. burgdorferi* during vertebrate infection. Dr. Jutras further demonstrated that *sodA* mRNA coprecipitated with BpuR protein in live cells assayed by RNA-Immunoprecipitation (Unpublished). To test if BpuR bound a similar region in *sodA* as it does its own mRNA, I designed a biotinylated RNA probe spanning 60bp encompassing the start of the *sodA* coding sequence and tested for BpuR binding by EMSA (Figure 4-4A). Labeled *sodA* RNA probe was incubated with several increasing concentrations of BpuR protein and I found that BpuR specifically bound this region. Control RNAs composed of the *bpuR* 5' UTR and start of translation or downstream coding sequence that BpuR has been previously demonstrated to bind and not bind respectively described in Jutras 2013 [158], were used to confirm that this batch of recombinant BpuR's activity was sequence specific.

Unlike previously observed BpuR-RNA binding sites, I found that increasing amounts of BpuR protein resulted in the formation of one and then two shifted complexes. BpuR is thought to bind its nucleic acid targets in a dimeric form [154]. These results may suggest that this *sodA* RNA probe may either possess multiple BpuR binding sites or that monomeric BpuR can bind this specific site and increasing concentrations of BpuR result in the previously described dimeric binding. The use of variant BpuR mutants deficient in dimerization could provide support for the latter hypothesis. The location of this BpuR binding site is consistent with a model, similar to the previously described BpuR:*bpuR* mRNA interaction, in which BpuR binds *sodA* transcript near the ribosome binding site and potentially interferes with productive translation. Supporting this model is the existence of a perfect Shine-Dalgarno sequence in the middle of the probe.

The transcript encoding *sodA* was not impacted by BpuR overexpression as assayed by RNAtag-Seq. Considering the result of my RNA-Sequencing study, which utilized a newly constructed inducible BpuR construct, I confirmed that the newly derived strain produced similar changes in protein abundance across multiple protein spots when comparing induced and uninduced cells by 2D-PAGE. These data suggest that, during *in vitro* propagation 34˚C, BpuR exerts its regulatory effects primarily at the post-transcriptional level.

DnaA binds *bpuR* promoter DNA

The next set of questions I addressed are centered around how and by what mechanism BpuR is regulated. Transcript levels of *bpuR* are altered over the course of the enzootic cycle. For this reason, I chose to examine *bpuR* promoter activity using green fluorescent protein (GFP) fusion assays, in which the *bpuR* promoter was fused to the GFP protein coding sequence. I grew the previously-generated *B. burgdorferi* strain harboring this construct [158] in established [157] fast and slow growth conditions (34˚C/Full media, 34˚C/1.2% Serum Media, 34˚C/25% BSKII Media) and assayed the

expression of GFP by flow cytometry (Fig 4-5). I found that bacteria cultured at slow growth conditions produce substantially more GFP than those cultured in fast growth conditions. This suggests that the *bpuR* promoter driving GFP expression is more active during periods of slow growth in *B. burgdorferi*.

To begin investigating potential mechanisms for this difference in activity, I tested if any protein(s) produced by *B. burgdorferi* would bind the *bpuR* promoter DNA. I performed electrophoretic mobility shifts assays (EMSAs) using total cytoplasmic extract and a fragment of DNA which spanned the *bpuR* promoter. I found that at least one protein bound this probe (Fig 4-6). To ascertain the identity of this protein or proteins, I used DNA-Affinity Chromatography as an unbiased assay to pull down proteins which specifically interact with the *bpuR* promoter. I generated a biotinylated dsDNA probe that spanned the *bpuR* promoter and several hundred nucleotides of the coding sequence (CDS). The 3', CDS proximal end of this was biotinylated to ensure the actual binding site was accessible when the DNA probe was bound to streptavidin coated magnetic beads. Beads were coated in the DNA bait and the procedure was performed as previously described [161]. Specifically-bound proteins were eluted by serial washes of high salt buffer and eluents were separated by SDS-PAGE. Three different sized bands were excised across all eluents and submitted for mass spectroscopy identification. Two of these three were found to be OspC and OspA protein, and I hypothesize that these represent membrane contamination, as they are two of the most abundant lipoproteins that *B. burgdorferi* expresses at 34°C. The *B. burgdorferi* homologue of DnaA was unambiguously identified in a ~58kD band extracted. One other protein, Ef-Tu, was also identified at low abundance. I chose not to pursue OspC, OspA, and Ef-Tu during these studies, as they had no previously recognized DNA binding activity and are more likely to represent non-specific contaminants.

I cloned and purified recombinant DnaA, with the assistance of Allison Pecaro and Leeza Khenner, and tested its ability to specifically interact with the *bpuR* promoter by EMSA. I first tested the ability of recombinant DnaA to interact with a known target, the origin of replication [239, 240], by incubating increasing amounts of recombinant protein with a labeled DNA fragment containing the *B. burgdorferi oriC*. I found that DnaA specifically interacts with the origin of replication, but not an unrelated DNA fragment (Fig. 4-7A). DnaA bound this DNA in the presence of 100X molar excess of unrelated DNA, but binding was competed away in the presence of unlabeled probe.

I then tested if and at what location DnaA bound the *bpuR* promoter. To identify where the DnaA binding site was located, I utilized a competitive EMSA approach. I generated a labeled DNA probe by PCR that spanned 147bp of the upstream *bpuR* DNA, including the 5' UTR, promoter, and ~70bp upstream of the promoter. Three unlabeled fragments of DNA that span the entire probe sequence, in overlapping segments of approximately the same length, were generated by PCR for use as competitors (Fig 4-7C). EMSAs were performed that included each of these sub-fragments individually (Fig 4-7B). Competition for binding was only observed for a single fragment, Fragment 2. This fragment is centered over the core promoter of *bpuR*, and the only unique sequences not covered by the other probes is the sequence located between the -10 and -35 sites.

Discussion

When I began these studies, current data suggested that BpuR was a global transcriptional regulator that also possessed post-transcriptional, autoregulatory activity. My current studies do not support the hypothesis that BpuR is a global transcriptional regulator in these specific culture conditions. Rather, my data support the hypothesis that BpuR's primary role in these conditions is that of a post-transcriptional regulator. Specifically, the transcriptomes of bacteria which express higher levels of BpuR are not significantly different than those that express normal levels. On the other hand, when

examining the proteomes of these bacteria, both Dr. Brandon Jutras and I found significant differences in the abundance of multiple proteins. BpuR was the third RNA binding protein identified in *B. burgdorferi* [195, 262, 263, 308]. These data also suggest that the effects of BpuRs activity on the proteome are primarily mediated by through modulation of translation, rather than by impacting transcript stability. While significant effort was dedicated to ensuring that BpuR levels truly were elevated at the transcript and protein levels and that the *bpuR* gene on the overexpression plasmid remained free of mutation following induction, there remains a possibility that unknown suppressor mutation(s) developed elsewhere in the genome, blunting the expected transcriptomic differences. Full genome sequencing of generated mutants or generation of independent mutant strains could shed light on this. These experiments served to set the stage for the following section focused on examining the mechanisms by which BpuR is regulated.

Previous studies demonstrated that BpuR controlled its own translation, but not its transcription. This led to the question, is BpuR only regulated post-transcriptionally, or do other factors affect its transcription? Importantly, BpuR has never been identified in the differentially expressed gene set of any regulatory factor yet examined in *B. burgdorferi* [38, 99, 126, 146, 147, 230, 251, 256, 262, 329]. That suggests that if it is regulated by any of these factors, that regulation is context dependent, and that context has also not yet been identified. Alternatively, it could be that a novel regulatory factor is at play. This work provides the first conclusive evidence that *bpuR* is regulated at the level of transcription, both in culture and during the enzootic cycle. I then showed that some protein(s) bound the DNA containing the *bpuR* promoter in a DNA-Pulldown system. I was able to identify at least one of these proteins as DnaA, marking the first time, to my knowledge, that DnaA has been implicated in the control of virulence in a pathogenic bacterium. While DnaA has been long known to play a role in the control of transcription in several species of bacteria [70, 133, 134, 162, 209, 285, 332], much remains to be

learned regarding the mechanism of control. My competitive EMSA data suggest that the mechanism in this case may be that of a repressor. By binding DNA containing regions of the core promoter, it seems likely that DnaA would compete with RNAP, inhibiting its ability to bind and form a productive transcriptional complex.

Many questions remain regarding this potential regulatory function remain. Does DnaA truly repress transcription? What are the binding kinetics of the interaction? Does ATP/ADP bound status impact the binding as it does in other systems [290]? While many questions remain, it seems clear that DnaA has an underappreciated role in the control of physiology in bacteria outside of its role in the initiation of DNA replication. I present a potential model in Figure 4-9 that includes preliminary information from our own work as well as inferences from other bacteria. It is presented not as fact, but merely, to this author, as a reasonable model to frame and test future hypotheses.

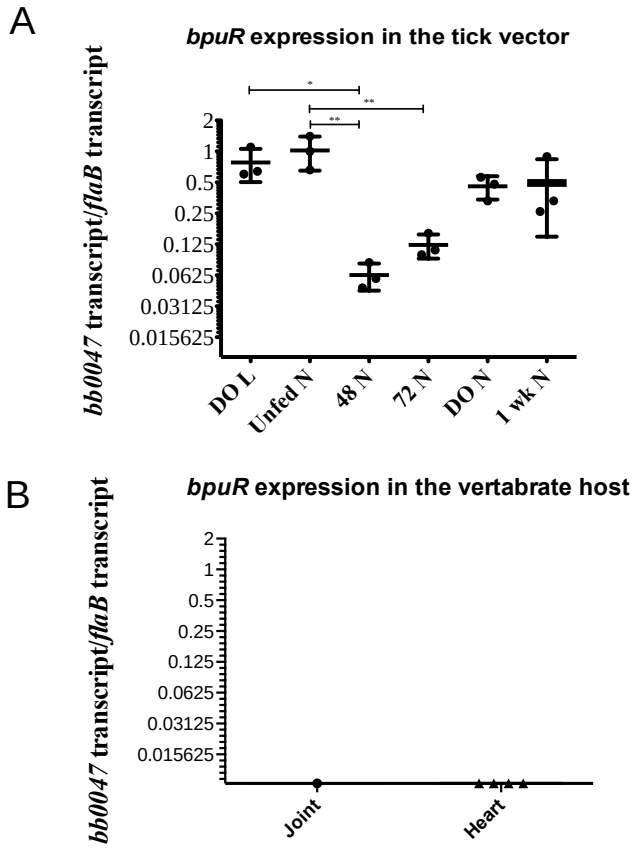

Figure 4-1: mRNA levels of *bpuR* throughout the enzootic cycle

(A) Total RNA was isolated from *Ixodes scapularis* larvae ticks that were fully engorged and dropped off naturally (DO L). Those ticks molted and RNA was isolated from unfed nymphs (Unfed N). During nymphal tick feeding on naive mice, ticks were removed at 48 and 72 hours post attachment, and *B. burgdorferi* RNA isolated (48N and 72N, respectively). RNA was also isolated from ticks that had dropped off naturally following repletion (DO N), and 1-week post drop off (1 Wk N). All RNA samples were reverse transcribed into cDNA, and qRT-PCR was used to determine copies of *bpuR (bb0047)* mRNA relative to house-keeping *flaB* copies [32]. Statistical significance was determined using Turkey's Multiple comparison test ($p<0.5$). * and ** Indicate statistical significance in *bpuR* mRNA between bracketed samples. Data was generated and analyzed by Dr.

Patricia Rosa, Dr. Kit Tilly, Aaron Bestor, and Dr. Phil Stewart at Rocky Mountain Labs. Adapted with permission from Jutras *et al.* 2013.

(B) Total RNA was isolated from infected mouse tissues after one month of infection. RNA was reverse transcribed into cDNA, and qRT-PCR was used to determine *flaB* and *bpuR* (*bb0047*) in each tissue. Data was generated and analyzed by Dr. Catherine Brissette, Dr. Robert Gaultney, and Brandee Stone at The University of North Dakota.

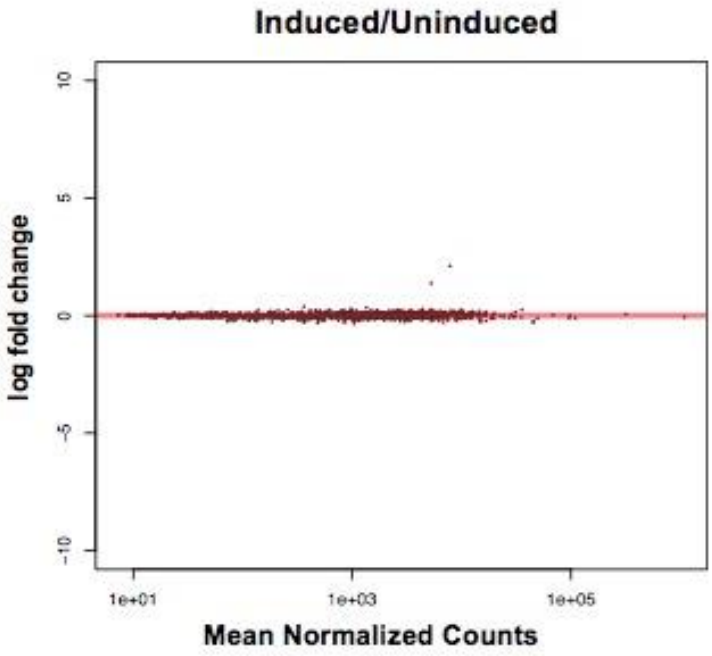

Figure 4-2: Differentially expressed transcripts following *bpuR* induction

MA (log ratio between samples vs. mean abundance of transcripts) of *B. burgdorferi* expressing elevated levels of *bpuR* compared to those which produce wild-type levels. *B. burgdorferi* that harbored an IPTG inducible copy of *bpuR* on a plasmid (WA11) were grown at 34˚C in BSK-II. Bacteria were inoculated at $1x10^5$ cells/mL and induced when cultures reached $1x10^6$ cells/mL. Induced and un-induced cultures were harvested after 24 hours (Approximately $1x10^7$ cells/mL). RNA was isolated, Illumina cDNA libraries were prepared, and sequenced [14] as described previously. Reads were mapped to the *B. burgdorferi* genome and counted using Salmon [238], and tested for differential expression using DESeq2 [194] in R [1].

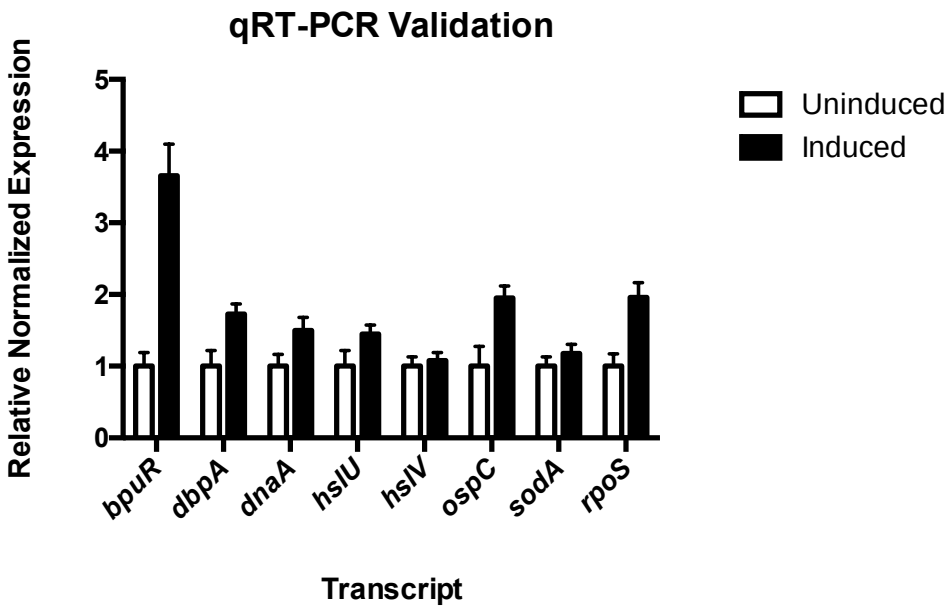

Figure 4-3: Validation of RNA-Seq

qRT-PCR measurements of select impacted and non-impacted transcripts. All measurements were normalized to the mean expression of the house-keeping genes *flaB* and *ftsK* and are relative to the uninduced samples.

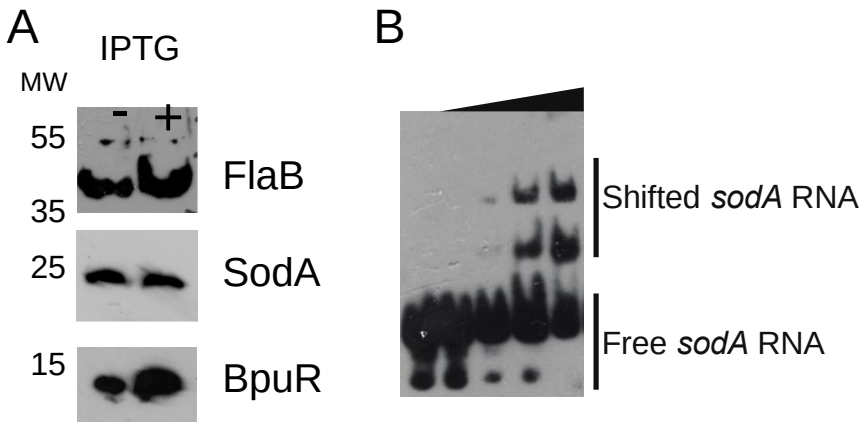

Figure 4-4: BpuR impacts SodA protein levels and binds *sodA* RNA and

(A) Expression of BpuR, SodA, and FlaB was assayed in uninduced and induced *B. burgdorferi* WA11 by western blot using antisera against BpuR and SodA and monospecific antibodies against FlaB. Band intensity was quantified using the ImageJ densitometry plug-in.

(B) BpuR was tested for binding of a 60bp biotinylated RNA probe centered on the *sodA* start codon by electrophoretic mobility shift assay. Lane 1 contains no protein and Lanes 2-5 contain increasing amounts of recombinant BpuR.

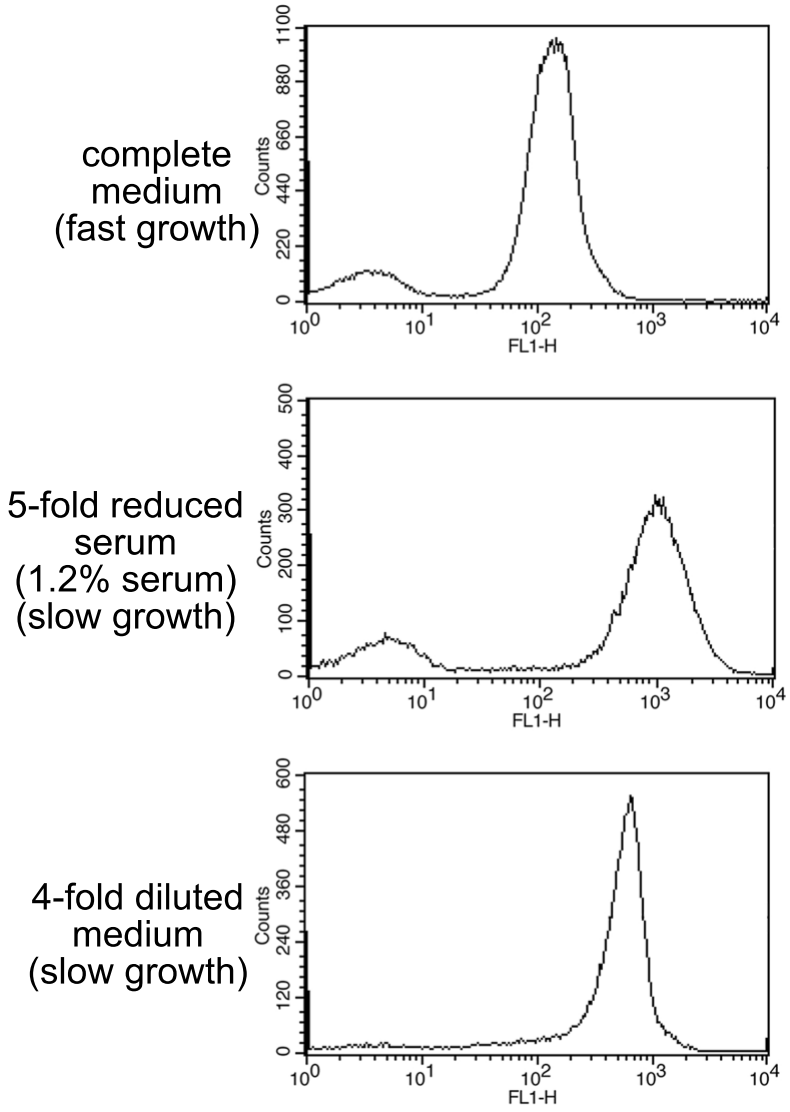

Figure 4-5: *bpuR* is regulated at the level of transcription

The previously constructed *bpuR* promoter : GFP reporter fusion [158] was introduced into the readily transformable *B. burgdorferi* strain B31e2. Transformed bacteria were grown in fast growth or slow growth conditions. Cells were pelleted, washed with and resuspended in PBS and assayed by flow cytometry for GFP expression.

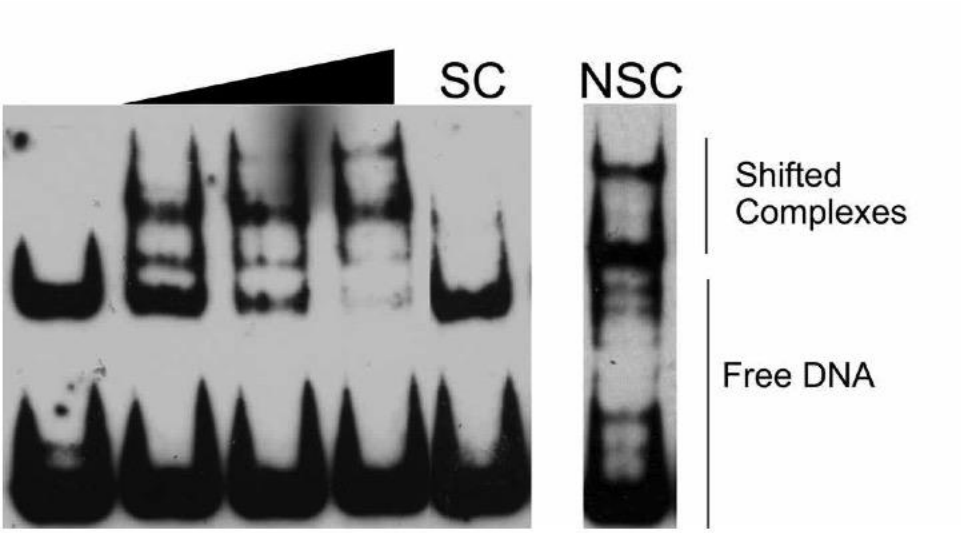

Figure 4-6: **Evidence that protein(s) specifically bind the *bpuR* upstream DNA**

Whole cytoplasmic lysates were incubated with biotinylated *bpuR* upstream DNA in increasing amounts (Lane 2-3). SC indicates the lane contains 100X molar excess of specific competitor (unlabeled probe) and NSC indicates the lane contains 100X molar excess of a non-specific competitor (unlabeled, unrelated DNA). Lane 1 contains labeled DNA alone.

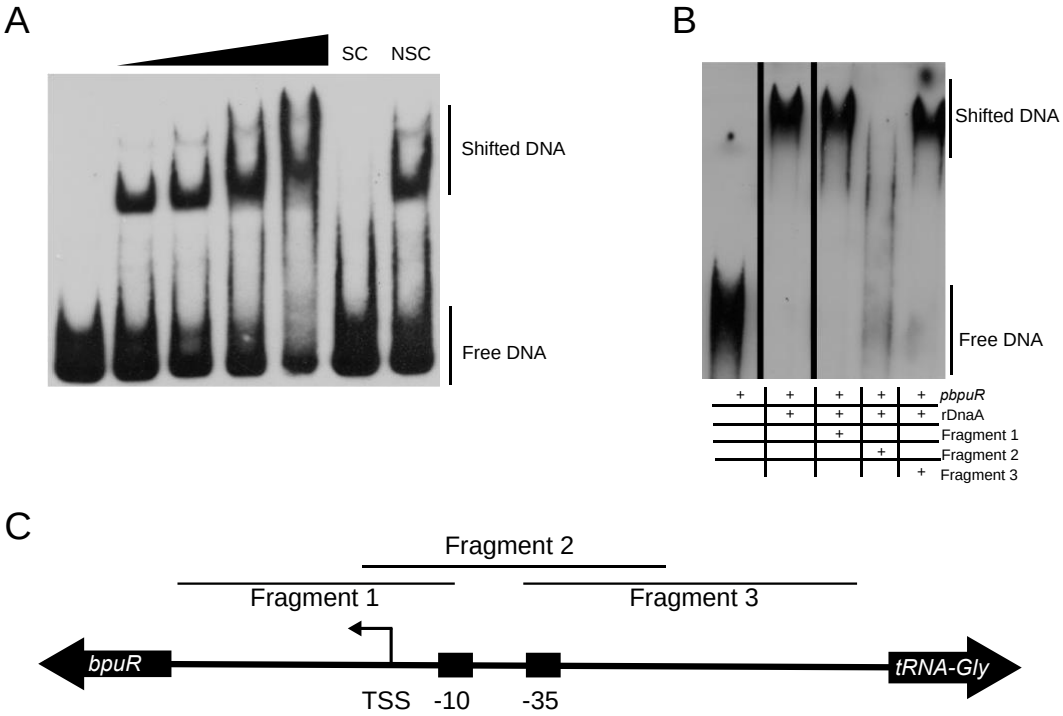

Figure 4-7: DnaA binds the *bpuR* promoter

(A) Increasing amounts of rDnaA (Lanes 2-4) incubated with 1nM labeled B. burgdorferi *oriC*. Lane 1 contains labeled DNA alone. SC and NSC contain 100X molar excess of specific and non-specific competitors respectively. (B) Testing for binding of DnaA to the *bpuR* promoter using three overlapping competitors. Specificity was tested in additional EMSAs, but is also confirmed here by Fragments 1 and 3 failing to compete, and only Fragment 2 competing. (C) Diagram of *bpuR* promoter and three competitors used to define DnaA binding region.

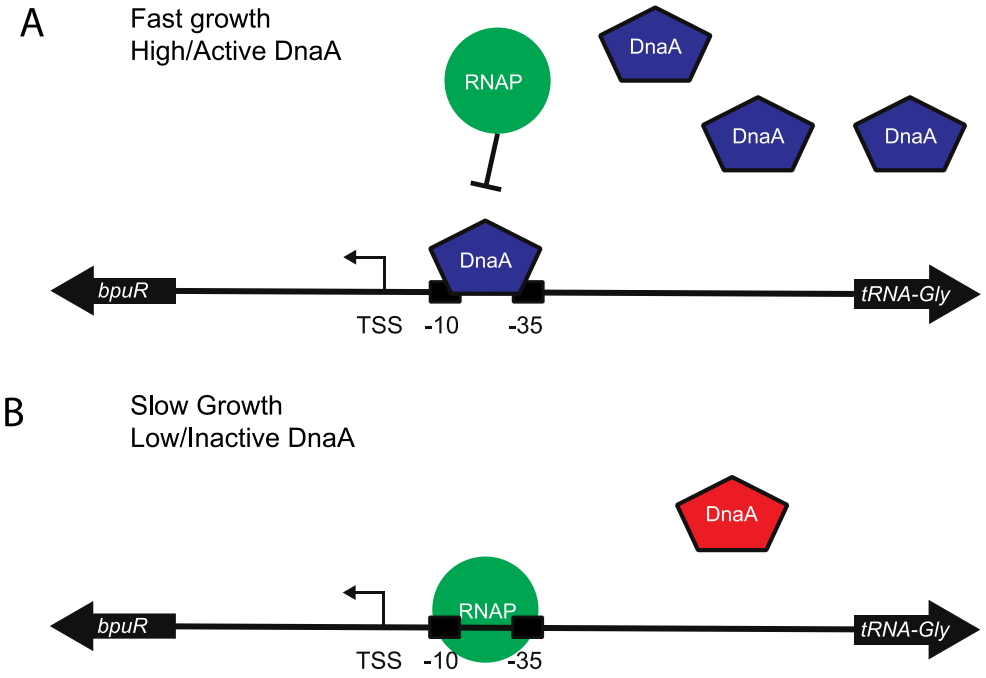

Figure 4-8: Proposed mechanism of DnaA interaction with the *bpuR* promoter

(A) During fast growth or high nutrient conditions and (B) during slow growth or nutrient limited conditions where I predict active DnaA levels are lower.

Chapter 5 Investigations into the *B. burgdorferi* transcriptome yield insight into transcriptomic dynamics and architecture

This work described in this chapter has been published: Arnold WK, Savage CR, Brissette CA, Seshu J, Livny J, Stevenson B. 2016. "RNA-Seq of *Borrelia burgdorferi* in multiple phases of growth reveals insights into the dynamics of gene expression, transcriptome architecture, and noncoding RNAs." PloS One 11:e0164165.

I generated the source RNA for total RNA-sequencing of the wild-type strain B31-A3 and performed the downstream filtering analysis of 5' ends, putative non-coding RNAs, and investigation of intrinsic termination sites. Library construction, read filtering and mapping, and prediction of transcriptional units was performed in collaboration with Dr. Jonathan Livny at the Broad institute. qRT-PCR validation was performed with the assistance of Kathryn Lethbridge and Christina Savage. The B31-A3 strain was acquired from Dr. Patricia Rosa. Multiplex PCR validation of plasmid content was performed by Drs. Bobby Gaultney and Catherine Brissette.

Introduction

A major interest of this work and of the Stevenson laboratory as a whole is to better understand both the input (Chapters 3 and 4) and the topology (Chapters 5 and 6) of the gene regulatory networks (GRNs) important for *B. burgdorferi*'s challenging life cycle. To this end, I specifically sought to identify novel regulatory mechanisms encoded in the genome of *B. burgdorferi* (this chapter) and to better define the topology of the known GRNs important for allowing this bacterium to adapt to and survive within its unique, two-host lifecycle (Chapter 6).

As described in previous chapters, numerous genes and proteins are differentially expressed over the course of the enzootic cycle. A handful of factors, including nucleic acid (DNA and RNA) binding proteins,[16, 42, 62, 153, 156, 160, 163, 173, 195, 210, 231, 254, 262, 269, 283, 308], alternative sigma factors [284], two-component systems [28, 256], and second messengers [227, 268, 348] have emerged as key players in the regulation of many of differentially expressed genes and proteins. The most extensively studied of these are 2 two-component regulatory systems (HK1/Rrp1 and HK2/Rrp2) and alternative sigma factors (RpoS and RpoN). In addition to these two-component systems and alternative sigma factors, an increasing number of nucleic acid binding and second messenger signaling proteins have studied in varying degrees of detail. Some of these nucleic acid binding proteins are essential for completion of the enzootic cycle [46-48, 127, 211] while others appear to be essential for cellular viability [153, 158, 185, 348]. Numerous transcriptomic studies have sought to identify the regulons of these factors in order to better understand the regulatory architecture important for vector or vertebrate adaptation. Generally, these studies have been confounded or limited by variances in choice of experimental condition, strain, and technology [14, 38, 84, 99, 126, 147, 251, 255].

The studies described in this chapter sought to provide additional insight into the dynamics and structure of the *B. burgdorferi* transcriptome using the novel method of RNAtag-Seq. Nearly all previous transcriptomic studies of *B. burgdorferi* were performed using microarrays that solely examined the expression of protein coding ORFs [147]. In the last several years, a handful of RNA-sequencing studies were performed, but they also only investigated the expression of protein coding genes and were not strand specific [46, 84, 153, 169]. As a result of this technological limitation, no comprehensive characterization of transcriptome architecture (5' transcript ends and termination sites) or putative non-coding RNAs had been attempted.

RNA Sequencing approaches have the significant benefit when compared to other expression profiling technologies in that they lend themselves to both discovery and hypothesis testing within the same experiment. Though numerous bacteria, including *B. burgdorferi*, are known to differentially express genes during batch cultivation [87, 103, 136, 143, 174, 250], no comprehensive evaluation had taken place to examine the effect of culture phase on *B. burgdorferi* transcriptomes over time in the same culture. Different researchers often harvest cells at different growth phases or even refer to different culture densities as the same growth phase. To test if, and to what extent transcripts are differentially expressed across different growth phases, we performed RNAtag-Sequencing and differential expression analysis of *B. burgdorferi* at multiple points during batch cultivation. This work provides a resource for other researchers to understand the transcriptomic context of their own experiments.

The second component of this study sought to identify novel targets or mechanisms of regulation that had not been explored in a comprehensive, global, manner. Low throughput analyses using 5' RACE and primer extension have been performed on select genes [67, 91, 123, 226, 232, 253] but, prior to this work, nothing was known regarding the length, content, and/or structure of 5' transcript ends (and potential 5' UTRs) on a genome wide scale. Additionally, while a small number of intrinsic terminators [347] had been identified [82, 249], manual identification of more than a handful had proven difficult due to *B*. *burgdorferi*'s very low G+C content. My more global analysis provides greater insight in to both how transcripts begin and how they end. Of interest to our lab and others within the field is the identification of extended 5' UTRs preceding important genes and the presence of terminators between genes or within transcripts. 5' UTRs can adopt secondary structures that are responsive to small molecules, temperature, and other stimuli [22], or act as targets for RNA binding regulatory proteins [228]. Intrinsic terminators are structural sequence elements that can cause robust and immediate

termination of transcription, and, while more widely known as signals to terminate transcription at the end of a gene, numerous regulated terminators exist that are responsive to temperature, small molecules, proteins, and RNAs at the end, middle, and beginning of genes [267].

Finally, a bioinformatic analysis aimed at identifying potential small RNAs in *B. burgdorferi* was performed in 2004 [229], but only a small number of targets were identified (eleven transcripts total). These primarily consisted of highly conserved stable RNAs (*6S*, *tmRNA*, *srp*, *rRNA*) and a single, small regulatory RNA, *dsrA*, which is now known to post-transcriptionally regulate the production of RpoS. Those authors concluded that *B. burgdorferi* encoded relatively few small RNAs. However, that study suffered from several significant limitations. First, it was performed very early on in the days of prokaryotic small RNA biology, and, therefore, the data sets queried for homology were relatively limited. Second, small RNAs are notoriously difficult to identify based upon homology or sequence identity alone. In the case of small regulatory RNAs, they often target small portions of coding genes by binding complementarity and thus can be less conserved than protein coding homologues at the nucleotide sequence level. Finally, this approach solely examined intergenic regions and was not able to successfully detect any antisense transcripts. Global measurements of transcript abundance across the genome at a single nucleotide resolution provide a direct route to the identification of these difficult to predict transcripts.

In this study, I generated insight into the dynamics and architecture of the *B. burgdorferi* transcriptome, serving as a future resource for both the Stevenson lab and the field at large. We first identified the transcriptomic changes that *B. burgdorferi* undergo during batch cultivation, providing a deep understanding of the background physiology of the organisms when performing future studies of cultured organisms. We then used this total RNAtag-Seq data set to globally identify 5' transcript ends and providing experimental

support for the bioinformatic prediction of intrinsic terminators. Finally, we identified nearly 350 novel, putative, small, non-coding RNAs transcribed from across the genome.

RNA-Sequencing of cultured *Borrelia burgdorferi*

Across all nine samples (3 time points in triplicate), between 2.57 and 46.5 million reads were sequenced, with a mean of 17.9 million reads per sample (Table 5-1). As ribosomal RNAs were depleted prior to library construction, the majority of reads aligned to coding sequences, with a smaller fraction aligning to intergenic or antisense regions (discussed in more detail below). Between 0.97% - 8.27% of reads aligned to ribosomal RNA regions. Presumably due to their highly processed and modified nature, tRNAs were underrepresented in our sequencing data. Some samples had lower numbers of reads successfully mapping to the genome for an as of yet undetermined reason. Even in the low mapping sample, nearly 1 million reads successfully aligned to the genome. A depth of one million aligned reads has been empirically demonstrated to detect the majority of ORFs in a bacterium with a genome twice the size of *B. burgdorferi* [122]. Furthermore, a more deeply sampled RNA-Seq data set was subsampled down to 600,000 reads and was still able to detect 60-90% of differentially expressed genes identified in the full set, depending on fold change cut off.

The sequenced isolate of *B. burgdorferi* B31 genome encodes 1386 annotated genes across the main chromosome and small replicons. Expression was detected in at least one replicate from 92% of these genes as determined by counting >10 FPKMO (fragments per kilobase per million reads aligning to annotated ORFS). Individual samples had detectable expression of 81.8% - 87.8% of annotated genes with a mean of 84.9%. Expression measurements of biological replicates were highly correlated, with a Pearson correlation exceeding $r = 0.96$.

B. burgdorferi differentially expresses numerous genes depending on growth phase

It is well known that bacteria alter their transcriptional profiles during *in vitro* cultivation as they transition through growth phases (lag phase, exponential, stationary phase, and death phase) [174]. We chose to assay the transcriptomes of bacteria at the first three stages of growth, as they are the most commonly examined by other groups and serve as the best resource for future comparisons. A total of 243 (17.6%) annotated ORFs were found to be differentially expressed when comparing any of the three growth phases. A key finding of these differential expression testing results was that previously presumed invariant housekeeping genes, such as *flaB* and *recA*, are in fact differentially expressed depending on growth phase (discussed in further detail below).

I found relatively small numbers of transcripts are differentially expressed during the transition from early to mid-exponential phase (Figure 5-1A and Appendix Table 8-1), with only 9 transcripts of annotated genes being differentially expressed between early-exponential and mid-exponential cultures. Four transcripts increased and 5 decreased during the transition to mid-exponential stage. Of the four transcripts that increased, three are of unknown function, and the fourth is a putative bacteriophage integrase on the small replicon lp56. Of the five genes that were statistically and biologically significantly reduced, four are *bpaB* genes encoded on the cp32 prophages. Previous studies found that *bpaB* transcript levels decreased as *B. burgdorferi* growth rate increased [157] consistent with BpaB's role in repressing *erp* gene transcription [160].

Significantly greater numbers of transcripts were altered during the transition in to stationary phase (2 days following the attainment of 10^8 cells/ml). These differences were most accentuated when comparing early-exponential phase to stationary phase with 129 genes expressed at higher levels and 98 genes expressed at lower levels (Figure 5-1B and Appendix Table 8-3). When comparing mid-exponential phase with stationary phase,

66 genes were increased and 7 genes decreased in transcript abundance (Figure 5-1C and Appendix Table 8-2).

Transcripts of several genes important for infection and host surface adhesion were elevated during stationary phase, including *dbpA*, *dbpB*, and *sodA* (2.4, 4.5, and 2.25 times respectively). The most highly elevated when comparing early-exponential to stationary phase transcript encodes the RNA component of the signal recognition particle (11.5 times). Among the genes that decreased in abundance during the exponential-stationary transition were factors involved in DNA repair and replication (*dnaA*, *polA*, *recD*, and *recB*), genes involved in central metabolism (*pfs* and *metK*), and those involved in sperimidine uptake and metabolism. The transcript encoding the alternative sigma factor *rpoN*, which is important for vertebrate infection, was also expressed at significantly lower levels during stationary phase. Those observations are consistent with an overall slowdown of cellular metabolism and cessation of DNA replication and are consistent with the hypothesis that genes important for host adaptation are responsive to changes in growth rate [157].

Relative expression levels of select genes were assessed by qRT-PCR, permitting comparisons of transcript level determination by the RNA-Seq and qRT-PCR methods. Transcripts that RNA-Seq indicated were increased, decreased, or remained stable across all three culture stages were assayed. When comparing early-exponential to stationary phase of growth an increase in *dbpA* transcript and a decrease in *rpoN* transcript was detected by both DEseq [9] analysis of RNA-Seq and by qRT-PCR. When assayed by qRT-PCR and DESeq, *sodA* levels did not significantly change during cultivation. DESeq analysis of *ospC* indicated a dip in transcript abundance in mid-exponential phase, which was not detected by qRT-PCR. This last measurement, of *ospC*, highlights the exquisitely sensitive tuning of expression of this particular transcript that will be discussed in additional detail in Chapter 6.

The *flaB* transcript is frequently used as a reference transcript qRT-PCR [164, 212]. The *recA* mRNA has also been used on occasion as a reference, under the same assumption of invariance [164, 348]. However, our RNA-Seq analyses consistently revealed differences in both *flaB* and *recA* transcript levels when comparing early or mid-exponential to stationary phases. For this reason, we mined our data for a more stably-expressed mRNA. The *ftsK* message was identified as being nearly unchanged across growth phases, varying at most by 0.98 times. Therefore, all qRT-PCR results in this particular study were analyzed using *ftsK* as the internal, constant standard.

Genome wide mapping of 5' transcript ends

Methods have been developed that can enrich for RNAs that carry a 5' triphosphate and therefore may represent primary transcripts [277]. These approaches allow for the differential examination of RNA-Seq (dRNA-Seq) libraries, which are enriched in primary transcripts. While such methods facilitate identification of transcript start sites, data from RNAtag-Seq can also be analyzed to identify probable transcription starts. Newly-developed methods for analysis of total RNA-Seq data have mapped start sites that agree well with both dRNA-Seq and low throughput methods such as 5' RACE [330] further supporting the power of this approach. RNA-Seq was also recently used by another group to identify the putative transcriptional promoters of the *B. burgdorferi tamB* and *bamA* genes [144].

To this end, we mined our RNAtag-Seq data for increases in read coverage within a narrow window upstream of coding sequences. Between 591–793 (591 in early exponential, 599 in mid-exponential, and 793 in stationary phase) putative transcript 5' ends were identified as functions of growth phase. Though this number and location varied slightly, dependent on growth phase, the highest density of these putative 5' ends mapped between 20 and 40 base pairs upstream of the nearest annotated start codon (Figure 5-2) for all examined conditions.

While many transcripts appeared to begin relatively near the beginning of their start codon, some key operons known to be important for the enzootic cycle were transcribed along with extended 5' UTRs. The glycerol utilization (*glpFKD*) operon is required for maximal survival within an unfed tick and encodes proteins for the uptake and utilization of glycerol in glycolysis and membrane synthesis [237]. The *glpFKD* operon transcript's 5' end was detected at the -190 position in both early and mid-exponential phase, which is consistent with data from a separate study placing the transcriptional start site at position -196 [4]. Furthermore, a recent study identified sequences that appear to be important for transcriptional control of the operon within this region [120].

The transcriptional start sites of several *B. burgdorferi* operons have previously been mapped by methods such as primer extension, 5' RACE, or, more recently, RNA-Seq. The majority of previously-determined 5' ends were also identified in our data set and matched either exactly or within a few bases of our identified 5' ends, adding to confidence that these newly-identified 5' ends are likely to represent accurate transcriptional start sites (Table 5-3).

Identification of intrinsic termination sequences

Rho-independent, or intrinsic, terminators can abruptly end extension of a transcript, or serve as regulatory sequences. Prior to performing RNA-Seq, the *B. burgdorferi* B31 genome sequence was analyzed by combined use of three separate intrinsic terminator prediction programs implemented in the sRNA detection pipeline SIPHT [190]. Those in silico analyses predicted the existence of 201 Rho-independent termination sites across the *B. burgdorferi* genome (Appendix Table 8-4).

I manually inspected RNA-Seq data for abrupt drops in mapped reads surrounding those sites, as expected from active Rho-independent termination. Many of the predicted terminators were followed by distinct reductions of reads mapped (Figure 5-3 and Figure 5-4), although some exceptions were found. Some of these discrepancies may reflect the

fact that the Rho-independent terminator prediction algorithm with the largest number of predicted terminators, Transterm, was trained and vetted on *B. subtillis*, whose nucleic acid composition is substantially different from that of *B. burgdorferi* (43.5% versus 29% G+C, respectively). Visual examination of read mapping across the genome supports this notion, as many transcripts appeared to terminate abruptly, similar to those near predicted Rho-independent terminators, but were not predicted by sequence analysis. Without additional study, it is difficult to say if these were the result of Rho-independent termination or if these represent processed transcripts.

Of the 201 in silico predicted Rho-independent terminators that were supported by RNA-Seq data, 99 (49%) resided within 100bp 3' of a stop codon or had transcriptomic support for an extended 3' UTR that ended at the predicted terminator. Examples include *flaB* and the *bmpDCAB* operon (Figure 5-3). The flagellin-encoding *flaB* gene is expressed at relatively high levels so a strong terminator that prevents read-through into the unrelated downstream gene is likely quite important. The *bmpDCAB* locus constitutes a complex operon. Two intrinsic terminators have previously been identified previously, residing between *bmpD* and *bmpC*, and between *bmpA* and *B* [82, 249]. The algorithms used in this study predicted the *bmpD–bmpC* terminator, which was supported by RNA-Seq read mapping (Figure 5-3). The *bmpA–bmpB* terminator was neither predicted algorithmically nor apparent from experimental data.

Intrinsic terminators residing within the 5' UTR or inside the coding region of an mRNA can have regulatory effects on transcriptional elongation and, therefore, protein expression. Nineteen percent of the predicted terminators are located within 150bp of a start codon of an annotated gene. Two representative examples are shown in Figure 5-4 and include apparent early termination in *holA* and *Bb_0709*. *holA* encodes the delta subunit of DNA polymerase and has been shown to be repressed during the stringent response in *E. coli*, though the mechanism was unclear [89]. The remaining percentage

of identified intrinsic terminators resided either well within genes or were located intergenically and not within 100bp of any annotated gene or putative ncRNA.

Other transcripts were associated with distinct decreases in coverage at their 3' ends that did not overlap a predicted Rho-independent terminator, suggesting that these 3' boundaries may be due to RNA processing of longer transcripts or highlight that the sequence requirements for Rho-independent termination in *B. burgdorferi* vary significantly from those in other model organisms.

The 3' ends of the majority of genes lacked any predicted intrinsic terminator and lacked discrete ends. These transcripts generally ended with regions of gradually declining transcript abundance after the stop codon. This gradual trailing off of transcript coverage could be a result of a number of reasons, including Rho-dependent termination or degradation. Because of these uncertainties and the variability in length of decline, I chose not comprehensively analyze 3' ends of transcripts that did not contain apparent Rho-independent terminators.

***B. burgdorferi* expresses hundreds of putative small non-coding RNAs**

Modern approaches to/. the preparation of RNA-Seq libraries have the ability to investigate transcriptional activity from both strands of DNA. This allows the unbiased discovery of both intergenic noncoding RNAs (ncRNAs) and RNAs that are transcribed antisense to protein-coding ORFs (asRNA). To identify candidate *B. burgdorferi* ncRNAs, we mined our RNA-Seq data for relatively short (<425nt) putative transcriptional units located in non-coding regions of the genome or antisense to annotated protein encoding genes. This analysis yielded 351 putative ncRNAs (Appendix Table 8-5), of which 129 were transcribed from the main linear chromosome, 82 from the resident cp32 prophages, and 140 from the remaining linear and circular plasmids. Slightly more than half (186) of the ncRNAs were transcribed antisense to annotated coding sequences. Sixty-two putative ncRNAs were encoded in intergenic regions without any overlap of known ORFs.

One hundred and three contained both antisense and intergenic sequences, of which 39 included sequences that are antisense to or overlap with pseudogenes.

Among the most highly expressed ncRNAs were homologs of stable regulatory and catalytic RNAs, including 6S rRNA [333], tmRNA [167], and the RNA subunits of RNase P [171] and SRP [8] (Figure 5-5ABCD). Levels of the *srp* RNA were significantly increased upon entry into stationary phase. The other stable RNAs were not differentially expressed over the course of the experiment. The last remaining previously identified small RNA, *dsrA,* an ncRNA that regulates translation of the RpoS alternative sigma factor, was also readily detected (Figure 5-5E). One of the most highly-expressed transcripts under all culture conditions was a previously unannotated transcript of 401 nucleotides. This novel RNA was designated *bsrW* (borrelial small RNA W). It is encoded by a chromosomal locus that is between the genes *fusA* and *Bb_0542* (Figure 5-6A). Although unannotated in the NCBI genome entry for *B. burgdorferi B31*, the nucleotide sequence is conserved across much of the genus. Upon manual inspection, *bsrW* was found to contain a small ORF predicted to encode a 76 residue polypeptide. BLAST-P analyses (http://blast.ncbi.nlm.nih.gov/Blast.cgi) revealed homology with other bacterial proteins that contain KTSC (**L**ysine **t**RNA **s**ynthetase **C**-terminal domain) domains. Although such proteins are found in other bacterial species, their functions are not known. If *bsrW* does in fact encode a small protein, it would have unusually long 5' and 3' untranslated regions (102 and 82 nucleotides, respectively). Those lengths are on the upper bound of the previously described distribution of lengths identified in my data set, and suggest the potential protein is tightly regulated.

I was also able to identify 186 transcripts that are transcribed antisense to coding sequences. I chose a relatively conservative expression cutoff in order to minimize false positives. Many of these putative ncRNAs overlap genes important for infection and tick colonization, including *rpoN*, *glpF*, and *Bb_0347* (Figure 5-6BCD). Antisense RNAs can

have myriad effects on their cognate genes, including influencing transcriptional initiation and read through efficiency via polymerase competition or base pairing with complementary transcripts to alter transcript stability [303].

Discussion

All organisms regulate the expression of their genes and proteins in order to adapt to and survive in dynamic environments. In this study, I sought to identify novel regulatory mechanisms by characterizing the dynamics and architecture of the *B. burgdorferi* transcriptome. I hypothesized that additional regulatory complexity existed in the *B. burgdorferi* genome and would be identifiable using transcriptomics.

Decades of work prior to this study demonstrated unequivocally that *B. burgdorferi* alters gene and protein expression during *in vitro* cultivation in response to various stimuli [33, 54, 273, 298, 299, 316], including, but not limited to, changes in growth phase [250]. Yet with that knowledge in hand, no comprehensive analysis of gene expression during *in vitro* batch cultivation had been performed. This factor is confounding for gene expression studies within the field, as different groups often classify early, mid, late-exponential and stationary phases differently, raising the possibility that studied differences. While one group may harvest cells at $1X10^7$ cells/mL as mid-exponential, another may refer to mid-exponential as $9X10^7$ (A difference of nearly a logarithm and 36 hours!). While these represent the extremes, many points in between these two are commonly referred to as mid-exponential.

Prior to this work, little to no information existed regarding 5' transcript ends (and, by extension, 5' UTRs), intrinsic termination sites (thus, terminator anti-terminator systems), or non-coding RNAs (thus, antisense and sRNA regulatory systems). These three transcriptional features have the potential to exert significant regulatory control, as is known in other model systems, but most stuides regarding *B. burgdorferi* biology have thus far focused on only a handful regulatory factors that generally control transcriptional

initiation. The work described in this chapter as well as the two additional studies described below set the stage for a new era of *B. burgdorferi* biology.

Immediately following the publication of the work described in the chapter, two additional groups published studies using specific approaches aimed at defining either transcriptional start sites or small RNAs [4, 243]. While I have not completed a comprehensive comparison between the 5' ends and putative non-coding RNAs identified in our data sets, examining several examples of special interest suggested general agreement. Not surprisingly both studies, due to their tailored approaches, identified significantly greater numbers of each feature (Over 1000 putative small RNAs and over 2000 5' transcript ends respectively).

Rho-independent terminators in *E. coli* and *B. subtillis* are composed of G+C rich stems followed by poly-U tracts, and their composition may not be strongly conserved in *B. burgdorferi*. For this reason, this method may have substantially underestimated the true number of Rho-independent terminations in *B. burgdorferi*.

These studies, in total, represent a quantum leap in the study of *B. burgdorferi* biology and gene regulation. They offer a comprehensive resource for those interested in where transcripts begin, end, and where previously unknown transcriptional activity exists. Future work to integrate these resources would be of tremendous benefit. As these resources were all built using effectively the same technology (RNA-Seq), the raw data could be combined and a well-defined transcriptome could be constructed using newer transcriptome assembly tools [102, 115]. It would be intriguing to investigate operon structure more closely and perform a more comprehensive analysis of the 3' ends of transcripts without predicted intrinsic terminators. This work has already served as a resource in our lab, and all putative ncRNAs identified have been added to a custom index used for transcript quantification in Chapter 6.

Table 5-1 Metrics of RNA-Sequencing of wild-type *B. burgdorferi*

Sample	Total Reads	Total Reads Aligned	Percent Reads Aligned	Percent Ribosomal
A3 E1	6.07E+06	2.41E+06	72.81	4.78
A3 E2	1.17E+07	5.09E+06	78.89	2.76
A3 E3	1.53E+07	6.79E+06	82.42	3.52
A3 M1	2.57E+06	8.65E+05	56.60	1.44
A3 M2	4.65E+07	1.31E+07	47.56	0.97
A3 M3	3.56E+07	1.10E+07	53.62	2.41
A3 S1	1.72E+07	2.62E+06	24.47	6.41
A3 S2	1.57E+07	3.31E+06	35.05	8.27
A3 S3	1.05E+07	2.91E+06	47.32	2.59

Sequencing metrics for each sample including sample name, total reads, total reads aligned to the B31-MI genome, percentage of reads aligned to the B31-MI genome, and the percentage of reads mapping to ribosomal RNA loci.

Table 5-2 Comparison of predicted transcriptional start sites with previously identified transcriptional start sites

Gene	5' End Mapped	Citation	RNA-Seq Early-exponential	RNA-Seq Mid-exponential	RNA-Seq Stationary
ospC	-20	[86]	-21/-21/-19	-21	-16
secA-sod	-100	[87]	-100	-100	-100/-27
bpuR	-42	[18]	-44	-44	-44
chbC	-42	[88]	-24/-25/-28	-29/-41/-46/	-26/-24
lon-1	-19	[75]	Not detected	-17	-17
Bb_0794	-13	[71]	Not Detected	-13	-13
bamA	-343	[71]	Not Detected	-348	-348

Comparison of genes with previously identified transcriptional start sites that were also identified by RNA-Seq. Columns list the gene, the previously identified location, citation for that determination, and RNA-Seq determined sites during early-exponential, mid-exponential, and stationary phases of growth. For some operons, transcriptional unit identifying algorithms identified different start sites from different cultures; in which case, all called start sites are listed.

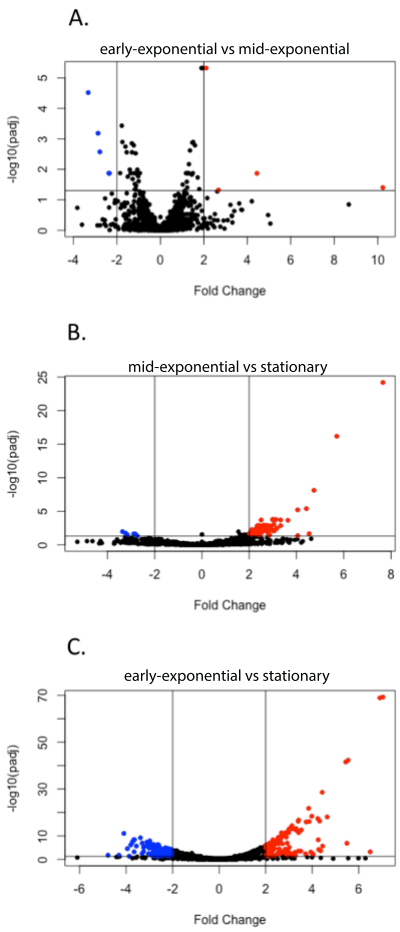

Figure 5-1: Volcano plots of differentially expressed genes across growth phases

Fold changes between genes were plotted compared to adjusted p-value when comparing (A) early-exponential against mid-exponential, (B) mid-exponential against stationary, and (C) early-exponential against stationary. Criteria of >2X change in expression and <0.05 adjusted p-value were used to define significantly changed genes, and are shown on the plot with the appropriate limiting lines. Genes which met the criteria and were expressed at higher levels in a particular comparison are shown in red and those which were expressed at lower levels are shown in blue.

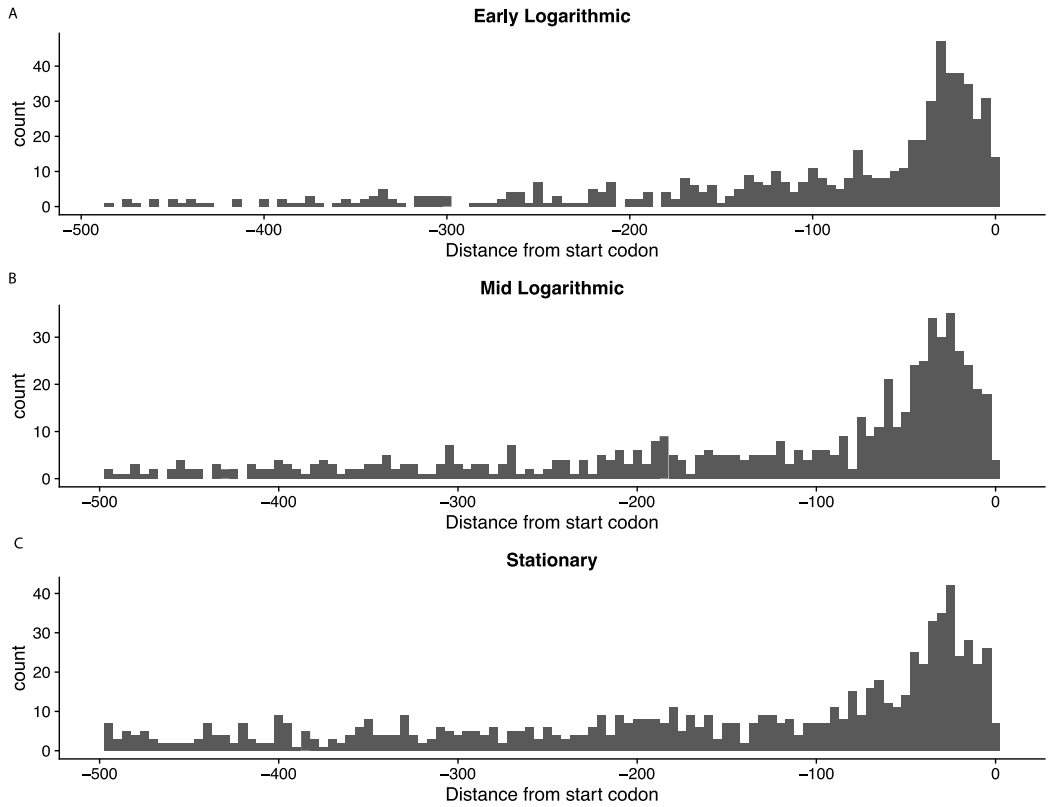

Figure 5-2: Histograms of distances of unambiguous 5' ends from start codon

Distributions of unambiguously identified 5' ends compared to their closest start codon in (A) Early-exponential, (B) Mid-exponential, and (C) Stationary phases of growth. Consistent with other studied bacteria, the largest proportion of 5' ends cluster within 30-50bp of the start codon [277].

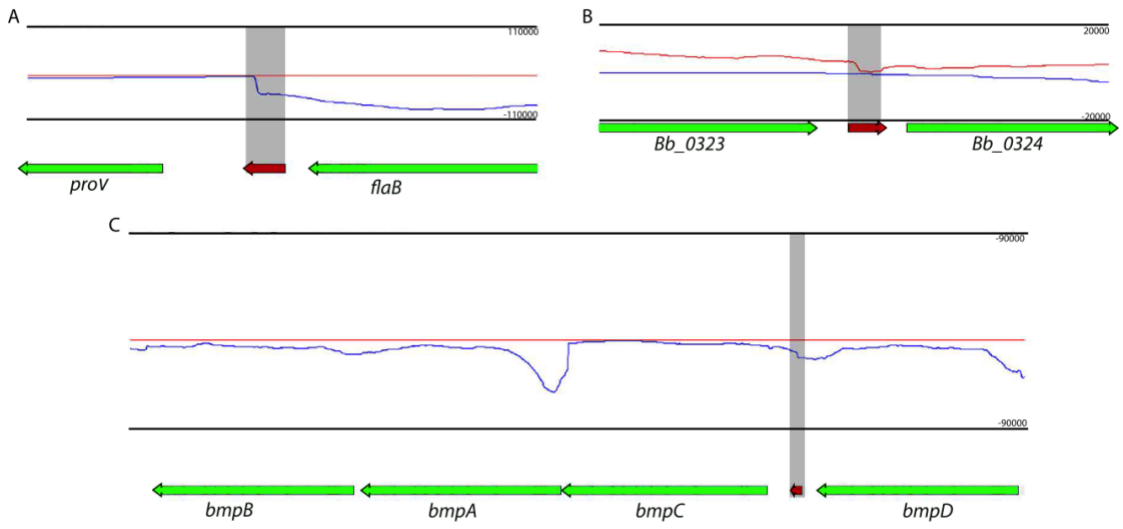

Figure 5-3: Predicted intrinsic termination sites with transcriptomic support.

(A) *flaB*; **(B)** *Bb_0323*; and **(C)** *bmpDCAB*. Thin red lines indicate transcript abundance from the + strand (left to right) and thin blue indicate transcript abundance from the – strand (right to left), and are shown above (+) and below (-) the central axis. Genes are noted below coverage plots and directionality is indicated by arrows at the ends of genes. Relative orientation of genes on the X axis is consistent with RefSeq annotations. Coverage per base is given on the Y axis to the left of the plot. Predicted Rho-independent terminators are indicated by red boxes on the same plane as the gene annotations and directionality is indicated by arrows. Terminators and the associated coverage at their location are highlighted by grey boxes.

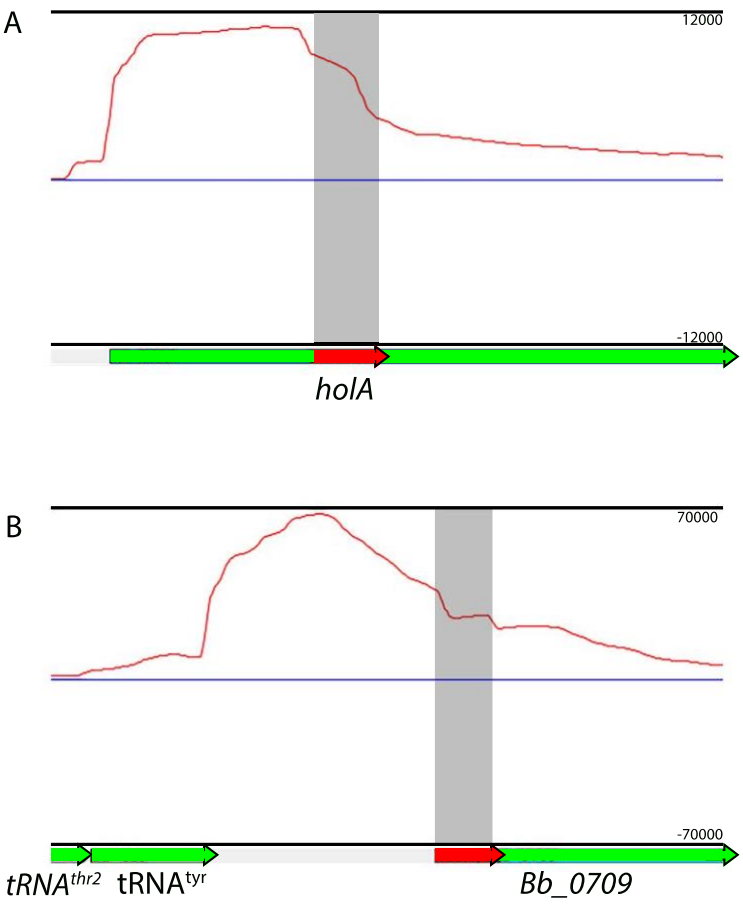

Figure 5-4: Examples of termination events within or upstream of genes

(A) *holA* and (B) *Bb_0709*. Thin red lines indicate transcript abundance from the + strand (left to right) and thin blue indicate transcript abundance from the – strand (right to left), and are shown above (+) and below (-) the central axis. Genes are noted below coverage plots and directionality is indicated by arrows at the ends of genes. Relative orientation of genes on the X axis is consistent with RefSeq annotations. Coverage per base is given on the Y axis to the left of the plot. Predicted Rho-independent terminators are indicated by red boxes on the same plane as the gene annotations and directionality is indicated by arrows. Terminators and the associated coverage at their location are highlighted by grey boxes.

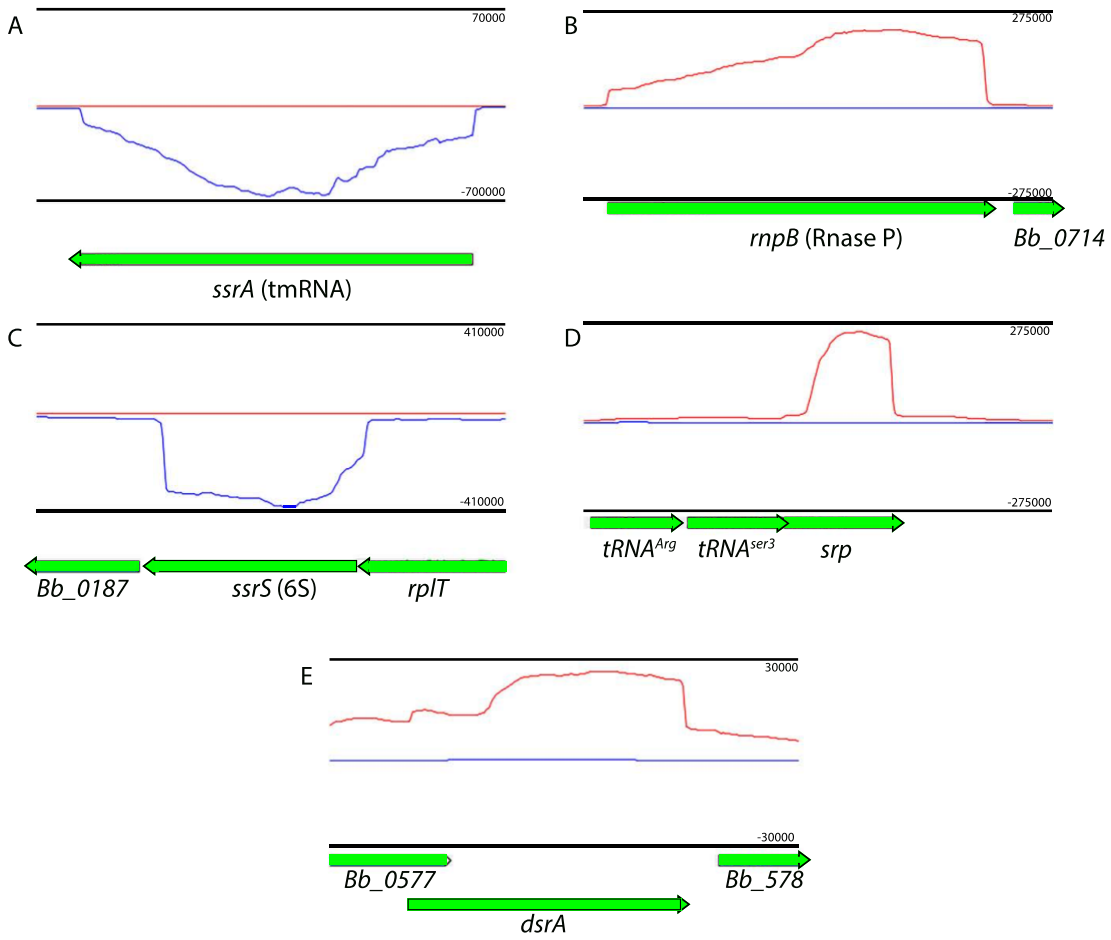

Figure 5-5: Examples of stable non-coding RNAs

Red lines indicate transcript abundance from the + strand (left to right) and blue indicate transcript abundance from the – strand (right to left), and are shown above (+) and below (-) the central axis. Genes are noted below coverage plots and directionality is given by arrows at the ends of genes. Relative orientation of genes on the X axis is consistent with RefSeq annotations. Coverage per base is given on the Y axis to the left of the plot. Neither *dsrA* (E) nor *6S* (C) are currently annotated in either GenBank or RFAM. *dsrA* is shown as the longest possible transcript described in [196].

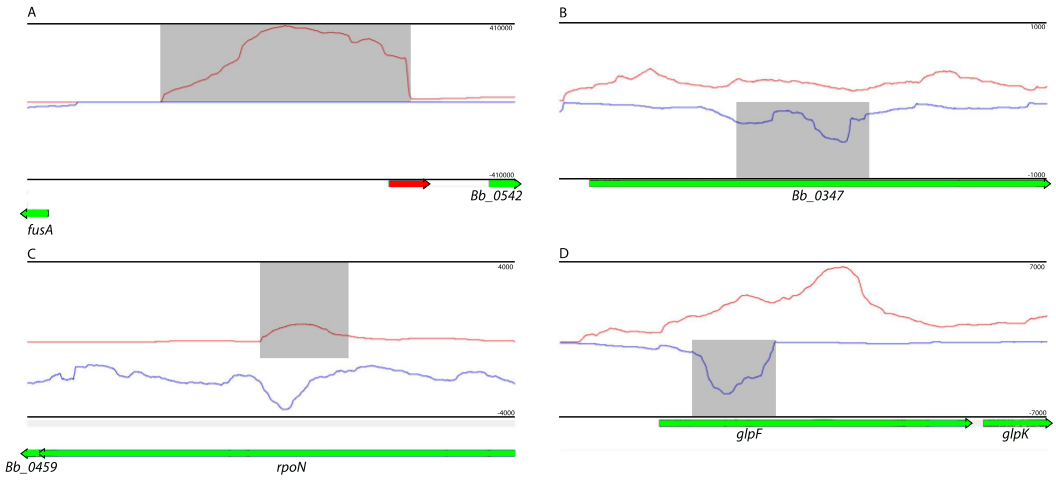

Figure 5-6: Example of newly identified putative noncoding RNAs

Read coverage histograms newly identified ncRNAs that are intergenic or overlap; *rpoN, glpF*, and ORF *Bb_0347*. Red lines indicate transcript abundance from the + strand (left to right) and blue indicate transcript abundance from the – strand (right to left), and are shown above (+) and below (-) the central axis. Genes are noted below coverage plots and directionality is given by arrows at the ends of genes. Relative orientation of genes on the X axis is consistent with RefSeq annotations. Grey boxes highlight the coordinates called for each newly identified transcript. Coverage per base is given on the Y axis to the left of the plot. Terminators are indicated by red boxes, and directionality is shown by arrows at their ends**.**

Chapter 6 Dissection of key gene regulatory networks in *B. burgdorferi*

This work has been published: Arnold, W. K., Savage, C. R., Lethbridge, K. G., Smith, T. C., 2nd, Brissette, C. A., Seshu, J., & Stevenson, B. (2018). Transcriptomic insights on the virulence-controlling CsrA, BadR, RpoN, and RpoS regulatory networks in the Lyme disease spirochete. PLOS ONE, 13(8), e0203286. doi:10.1371/journal.pone.0203286

The Δ*badR* and Δ*csrA* deletion strains were acquired from Dr. Janakiram Seshu and Dr. Trever Smith [165, 210]. Dr. Patricia Rosa and Dr. Frank Gherardini provided the Δ*rpoS* and Δ*rpoN* [98] strains respectively [98]. Dr. Catherine Brissette and Dr. Robert Gaultney performed plasmid content analysis on A3, Δ*rpoN*, Δ*rpoS*, Δ*csrA*, and Δ*badR* strains. Dr. Jonathan Livny and Jessica Alexander prepared and sequenced RNAtag-Seq libraries. Christina Savage performed qRT-PCR validation of the sequencing results.

Introduction

The comparison of experimental findings related to gene regulation in *B. burgdorferi* from disparate groups, or even the same group over time, has been confounded by variations in experimental design, including choice of strain background or media composition. Strain background appears to significantly affect gene expression and response to a stimulus, including the basal and induced expression of key virulence factors, such as OspC [202, 340, 342]. Similarly, culture media composition is also known to strongly affect cultured *B. burgdorferi*'s response to environmental stimuli, specifically temperature and pH shifts [315, 327, 345]. It comes as no surprise then, that different groups, using different strains, in different culture conditions, using different technologies, would come to contradictory or uncorrelated results [46, 49, 99, 127, 147, 230, 255, 256].

In the decades following the discovery of *B. burgdorferi*, a number of regulatory factors essential for vertebrate infection, including alternative sigma factors and nucleic acid binding proteins, have been discovered. CsrA is an RNA binding protein, well studied in other bacteria, and is essential for *B. burgdorferi* pathogenesis and also seems to directly regulate genes involved in motility. BadR is a carbohydrate and DNA binding protein that has been shown to regulate >200 genes [210]. Two alternative sigma factors, RpoN and RpoS, have been previously proposed to form a linear cascade, in which RpoN allows the transcription of *rpoS*, which allows recognition of select promoters by RNAP to transcribe a regulon important for transmission and infection.

In the previous chapter, I utilized RNA-Seq to provide deeper insight into the *B. burgdorferi* transcriptome and to shed light on novel potential regulatory mechanisms. In this chapter, I use the same technology to examine how the regulons of four essential regulatory factors; CsrA, RpoS, RpoN, and BadR interact with and overlap one another to better understand the structure of regulatory networks that allow vertebrate adaptation. I made a number of important observations in that regard. I supported the hypothesis that the CsrA and BadR regulons share substantial overlap in their identity and direction of impacted transcripts but do not appear regulate one another. Further, I provide evidence refuting several hypotheses regarding sigma factor selectivity. Importantly, and in the same vein of study as the previously described *flaB* variability (Chapter 5), I provide evidence that plasmid maintenance in *B. burgdorferi* is also a dynamic process. Gene regulatory studies that examine population-level statistics should consider the described data in the future.

CsrA impacts the expression of a substantial number of genes involved in virulence and cell physiology

CsrA (Carbon storage regulator A) is well known in other systems to regulate diverse cellular processes including virulence through its RNA binding activity. While not

as extensively studied in *B. burgdorferi*, previous studies have provided significant evidence that CsrA is important for the life cycle of the organism [163, 266, 307]. In *B. burgdorferi*, CsrA appears to regulate a number of important virulence-associated lipoproteins, binds RNAs of motility-associated genes, and is essential for the vertebrate stage of infection [165, 266, 307, 308]. To further delineate the role of CsrA in the biology of *B. burgdorferi*, we examined the transcriptomes of bacteria that harbored deletions of the *csrA* locus.

The deletion of csrA caused dysregulation in 239 transcripts, with 153 expressed at lower levels and 86 expressed at higher abundance (Fig. 6-1A and Appendix Table 8-9). The majority of these DE transcripts were composed of mRNAs encoding ORFs and were plasmid encoded. Of key note, the deletion of *csrA* had no impact on the expression of the three other regulatory factors under examination in this chapter (ie *rpoN*, *rpoS*, or *badR*). The known or proposed functions for the differentially expressed (DE) ORFs include those involved in both infection and housekeeping functions. The deletion of *csrA* negatively affected the expression of several genes encoding proteins associated with transmission from ticks and survival within the vertebrate host; including *ospC*, *dbpB* (Fig 6-2), *vlsE*, and *arp* [142, 202, 257, 279, 314]. This downregulation could be a direct result of CsrA inducing their expression when present, or through an effect on a secondary regulator.

Metabolic adaptation of pathogens to their particular hosts is becoming increasingly well known to play a major role in virulence [95, 192, 236, 288]. The expression of transcripts encoding several key nutrient scavenging enzymes, including those known to be important for vertebrate colonization, were positively affected by the deletion of *csrA*. Specifically, those genes involved in purine scavenging (*guaA* and *BB_B23*) and glucose transport (*BB_B29*) were all expressed at higher levels in the *csrA* mutant when compared to wildtype. It is interesting to note that, while surface factors that

are known to play a role in vertebrate colonization are expressed at lower levels in the mutant, transcripts encoding proteins important for metabolic adaptation are expressed at higher levels.

While I have not performed a comprehensive GO-Term or pathway enrichment analysis for the affected ORFs, the data generally support the hypothesis that CsrA acts to regulate vertebrate adaptation by regulating, directly or indirectly, surface lipoproteins and metabolic genes. Of key importance is that the deletion did not affect the expression of either *rpoS* or *rpoN*, the hypothesized gatekeepers of vertebrate adaptation (Fig. 6-2). This suggests that there are alternative mechanisms beyond these two alternative sigma factors that help adapt *B. burgdorferi* to its respective niche.

BadR regulates the expression of genes and involved in metabolism and virulence

Previous work has demonstrated that the deletion of *badR* results in large changes in several hundred transcripts as measured by microarray [210]. A number of these transcripts encode proteins involved in the uptake of metabolites from extracellular milieu. Under the growth conditions I examined, a total of 235 transcripts that were differentially expressed (DE) by the deletion of *badR* (Fig 6-1B and Appendix Table 8-8). Of these 135 transcripts were decreased in expression and 100 were increased in expression. Similar to the findings from the Δ*csrA* strain, a significant fraction of the affected transcripts was composed of newly identified small ncRNAs identified in Chapter 5. As noted for the *csrA* mutant, the *badR* mutant did not affect the expression of *csrA*, nor any of the other examined regulatory factors. Transcripts that were affect by both *badR* or *csrA* will be discussed in further detail in a later section; the remainder of this section will focus on transcripts affected only by *badR*.

Several transcripts encoding genes associated with second messenger signaling were also affected by the deletion. A single cyclic-di-AMP synthase, CdaA [268], has been identified in *B. burgdorferi*, and the expression of its transcript was significantly reduced

(2.15 times) in the *badR* mutant. Furthermore, the gene encoding one of the few potential cyclic-di-AMP binding proteins, *cabP* [268], was also reduced in expression. Intriguingly, the phosphodiesterase responsible for the degradation of c-di-AMP was unaffected. These findings are consistent previous work highlighting the complexity of synthesis, signaling, and degradation of the c-di-AMP regulatory network [268, 348] in *B. burgdorferi*. c-di-AMP is essential for viability for *B. burgdorferi*, but little else of its role in the physiology of the organism is understood [348].

Glycerol is a key carbohydrate essential for maximum fitness during tick colonization [237]. The operon encoding the genes important for this function, *glpFKD*, is regulated by a number of proteins and signaling molecules including SpoVG, RpoS, (p)ppGpp, and cyclic-di-GMP [38, 46, 120, 269]. This operon also appears to be regulated by BadR. In the mutant *badR* strain, all four genes, *glpFKD* and an ORF of unknown function, were significantly upregulated. An antisense RNA to *glpF*, *ncRNA0042*, was down regulated (-3.6 times). A reasonable hypothesis is that BadR or a BadR-regulated *trans*-acting factor regulates the transcription of *ncRNA0042* (the anti-*glpF* sRNA), which then negatively regulates transcription from the *glpFKD* operon. This asRNA could also have effects on the translation or stability of existing *glpFKD* transcripts in the cell, but significant additional study outside the scope of this work is required to support this hypothesis.

Of substantial note, while a previous study had demonstrated a role for BadR in the regulation of *rpoS* using transcriptional profiling of this same *badR* mutant and DNA binding assays of recombinant BadR [211], I found no such impact. Neither *rpoS*, nor any of its known regulators (*dsrA*, *hfq*, *bosR*, or *rpoN*) [11, 98, 141, 195, 231, 283], were affected by the deletion in *badR* in this study. I will elaborate on possible explanations for this inconsistency in this chapters' discussion.

The CsrA and BadR regulons share substantial overlap

As described above, the primary focus of this study was to better define how the regulons of four important regulatory factors (CsrA, BadR, RpoS, and RpoN) intersect and diverge with one another. None of the factors described in this work appeared to regulate one another in our conditions. Transcriptomic studies of Δ*rpoN* and Δ*rpoS* strains previously indicated that both factors affected the expression of several hundred genes. I was not able to recapitulate those findings in my current study. The transcription of several genes (*ospC* and *dbpBA*) has been described as absolutely dependent on the activity of RpoS or RpoN [92]. This work, and the work of others [59], unequivocally demonstrates that such assumptions are unsubstantiated. I will further describe these findings in the following section and for the moment focus exclusively on the substantial overlaps between the BadR and CsrA regulons.

Overlap analysis indicated that the BadR and CsrA regulons dually regulate 150 transcripts under the examined conditions. Of these, 81 transcripts were expressed in lower amounts in both mutants and 66 were expressed more highly in both. The remaining 3 transcripts were affected in opposite directions. In total, 98% of transcripts that were DE in both mutants were DE in the same direction. When combined with the fact that neither factor affected one another, these data suggest that, when the BadR and CsrA regulons overlap, they generate a nearly identical transcriptomic program. It is impossible to discern how much of this similarity is due to each factor acting independently on the same targets or by converging on a single, other, trans-acting factor without additional study. One trans-acting factor in particular, however, emerges as a potential candidate.

Both BadR and CsrA mutants affected the abundance of a transcript encoding a nucleic acid binding global regulatory factor titled SpoVG [41, 156, 269]. The transcript encoding SpoVG was increased 3 times in the *badR* mutant and 2.3 times in the *csrA* mutant. SpoVG binds both DNA and RNA and affects the expression of multiple house-keeping

and virulence associated proteins in *B. burgdorferi*. Studies are still ongoing in the Stevenson lab to critically evaluate the scope of SpoVG's role in the life cycle of *B. burgdorferi*, but early indications suggest it plays a critical role in regulating the physiology of the cell [269].

Cell wall synthesis appears to be a significant point of dual regulation. Mutations in *badR* were previously shown to have a significant effect on the expression of genes involved in chitobiose uptake and utilization [210]. That observation was mirrored in this study. In fact, the genes composing the chitobiose operon represented three of the most highly upregulated transcripts in this experiment (*chbCAB* was upregulated between 35-65 times). Deletion of *csrA* had a similar, though less profound, effect, with an 2.8-5.2 times induction. Chitobiose is a dimer of N-acetylglucosomine, which can be used as an energy source but is also required for the synthesis of peptidoglycan utilized in newly synthesized cell walls [111]. Chitobiose has been proposed to be the other major nutrient, glycerol being the predominant nutrient, during utilized during tick colonization as chitin and chitobiose derived from tick cuticle are present in substantial amounts in the midgut [252, 309, 312, 313]. NanE is an epimerase that converts N-acetylglucosamine-6-phoshpate into GlcNAc-6P, and its transcript was increased in both mutants. Finally, MurG is a key enzyme involved in the formation the cell wall, transferring GlcNAc moieties from lipid intermediate I to lipid intermediate II. The transcript encoding this enzyme was biologically and statistically increased by 3 times and 2.6 times in *badR* and *csrA* mutants, respectively.

Carbohydrate-utilization pathways and other host associated metabolic pathways were also impacted by both mutations. These included increased levels of transcripts encoding the putative sugar transporter IIABC component (*BB_408*) (2.5X and 2.8X, respectively) and a subunit of another putative carbohydrate ABC transporter (*BB_0678*) (2.2 foldand 2.9 times, respectively). Polyamines are cationic, organic bases that are

present at significant levels within vertebrate hosts and can affect a wide variety of biological processes, including those involved in stress and osmotic responses [275]. In *B. burgdorferi*, the polyamines spermine and sperimidine are important for bacterial growth control and expression of vertebrate associated proteins. Polyamines can be transported by the PotABCD transporter or produced de novo from arginine. *B. burgdorferi* seems to encode part of the arginine deaminase pathway, consisting of the enzymes ArcA, which converts arginine to citrulline, and ArcB, which converts citrulline to ornithine and carbamoyl-phosphate [101, 187]. Both *badR* and *csrA* mutants exhibited increased expression of *arcA* (9.2 times and 2 times, respectively), *arcB* (6.7 times and 2.2 times, respectively), and *potD* (2.1 times and 2.3 times, respectively).

Key virulence genes are expressed independently of RpoS and RpoN

I did not detect significant changes in the transcriptomes of bacteria mutated in either of the genes encoding the alternative sigma factors *rpoN* or *rpoS* (Fig. 6-1CD). While this certainly hindered any ability to make inferences regarding the structure of these two regulons in the context of mutations in *csrA* and *badR*, it did provide substantial evidence arguing against the long-standing hypothesis that RpoN and RpoS constitute a regulatory cascade in which RpoN directs the transcription of *rpoS*, which goes on to transcribe a vast regulon, suggested to include >400 genes [48, 147, 284]! It has been previously reported that RpoS is absolutely essential for the transcription of several essential transmission and vertebrate specific factors, namely *ospC* and *dbpBA*. I found, in these specific conditions, that the deletion of *rpoS* or *rpoN* had no impact on the expression of these genes (Appendix Table 8-7 and Appendix Table 8-6). Additionally, I found that the expression of *rpoS* was not impacted by the loss of RpoN in these conditions, suggesting that, in this particular case, *rpoS* is transcribed via a previously-described, housekeeping, RpoD-dependent promoter [197]. When I examined read mapping near the 5' portion of the *rpoS* locus, I found additional support for this hypothesis (Figure 6-7). I found no

obvious difference between reads mapped spanning the *rpoS* promoter in the Δ*rpoN* strain compared to wild-type, suggesting that, in both strains, *rpoS* is transcribed from the RpoD-type promoter.

Discussion

This work represents the first comprehensive transcriptomic examination of more than two of *B. burgdorferi*'s essential regulatory factors ever undertaken in the same study and is also the first to examine the role of these essential factors in the regulation of small ncRNAs in *B. burgdorferi*. I provide evidence in support of, and against, several important hypotheses: first that the essential regulatory factors in *B. burgdorferi* regulate some genes together and some genes separately; second, that genes essential for vertebrate infection are regulated independently of the alternative sigma factors RpoN and RpoS. I find it likely that the uniform effect is mediated, at least in part, by SpoVG. If this hypothesis were true, absent any other confounding variables and in the simplest case, I would expect the DE changes to be more apparent in the BadR mutant, as it had a larger fold increase in *spoVG*. While some transcripts follow this pattern (*chbABC* and *murG*), others do not. These findings suggest a more complicated scenario in which some of the effects of SpoVG are moderated or enhanced these two factors acting directly or indirectly, by other regulators acting at each specific locus.

In general, these data are consistent with an increase in cellular growth necessitating an enhanced internalization of nutrients and flux through carbon metabolism and an increase in production of peptidoglycan and its precursor metabolites. These findings are consistent with the previously described patterns of expression for CsrA and BadR as well as the well characterized defects in infectivity [165, 210, 233, 266, 307].

A significant limitation of this work is that the studies were performed on cultured bacteria at a single culture condition. As discussed in significant detail in previous chapters, *B. burgdorferi* is exquisitely sensitive to changes in environmental conditions

and alters gene regulatory networks in response to numerous, sometimes relatively innocuous, conditions. Additional conditions, be they growing bacteria at elevated temperatures, decreased pH, elevated or decreased osmolarity, or real-world environmental cues experienced during the enzootic cycle would all be informative. Currently, transcriptomics of *in vivo* derived spirochetes remains a challenge due to the extremely low burdens present in both tick and vertebrate hosts. Previous work has used a variety of approaches including whole transcriptome amplification [146] and the examination of spirochetes concentrated in dialysis membrane chambers (DMC's) implanted in rat peritoneal cavities [50]. While both of these approaches have provided additional insight into the transcriptomes of bacteria during *in vivo* or *in vivo*-like conditions, they come with significant limitations. Whole transcriptome amplification can introduce biases in transcript abundance, particularly in poorly expressed transcripts [97]. While the only study describing such a procedure found generally good agreement between amplified and unamplified control samples, only 70% of transcripts encoding ORFs were measured as expressed above background in both condition [146]. DMCs allow the free exchange of small metabolites and signaling molecules (<5 KDa), but do not allow for the spirochetes to physically interact with their surroundings [7, 45]. Considering the large number of lipoproteins encoded in the *B. burgdorferi* genome and its well-established propensity to interact with host factors [35-37, 51, 53, 224, 323, 349], this condition does not fully replicate the true in vivo state within a vertebrate host.

Considering all these limitations, I chose an approach that would provide insight in a method which could be quickly and reproducibly accomplished in standard conditions. While these conditions may not be fully representative of the enzootic cycle, gene regulatory networks can be dissected independently of the natural stimuli. My hope is that this work, along with other recent transcriptomic studies of *B. burgdorferi* [59] will provide the early foundational data for establishment of *B. burgdorferi* specific databases in the

same tradition as RegulonDB for *E. coli*, FlyBase for *Drosophila melongaster*, and WormBase for *Caenorhabditis elegans*.

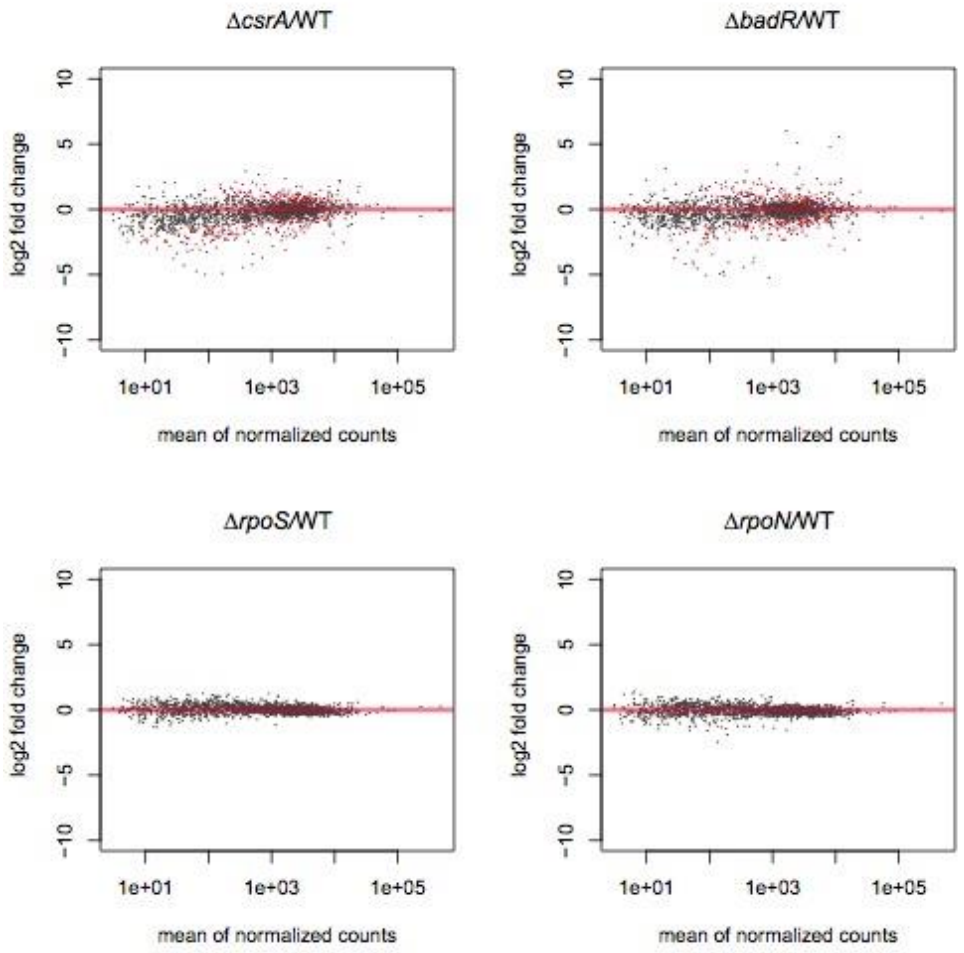

Figure 6-1: Differentially expressed transcripts *B. burgdorferi* mutants examined in this study

(A) *csrA*, (B) *badR*, (C) *rpoS*, and (D) *rpoN* mutants compared to the cognate wild-type strain. RNA was isolated, Illumina cDNA libraries were prepared, and sequenced [14] as described previously. Reads were mapped to the *B. burgdorferi* genome, counted using Salmon and tested for differential expression using DESeq2 [194] in R [1].

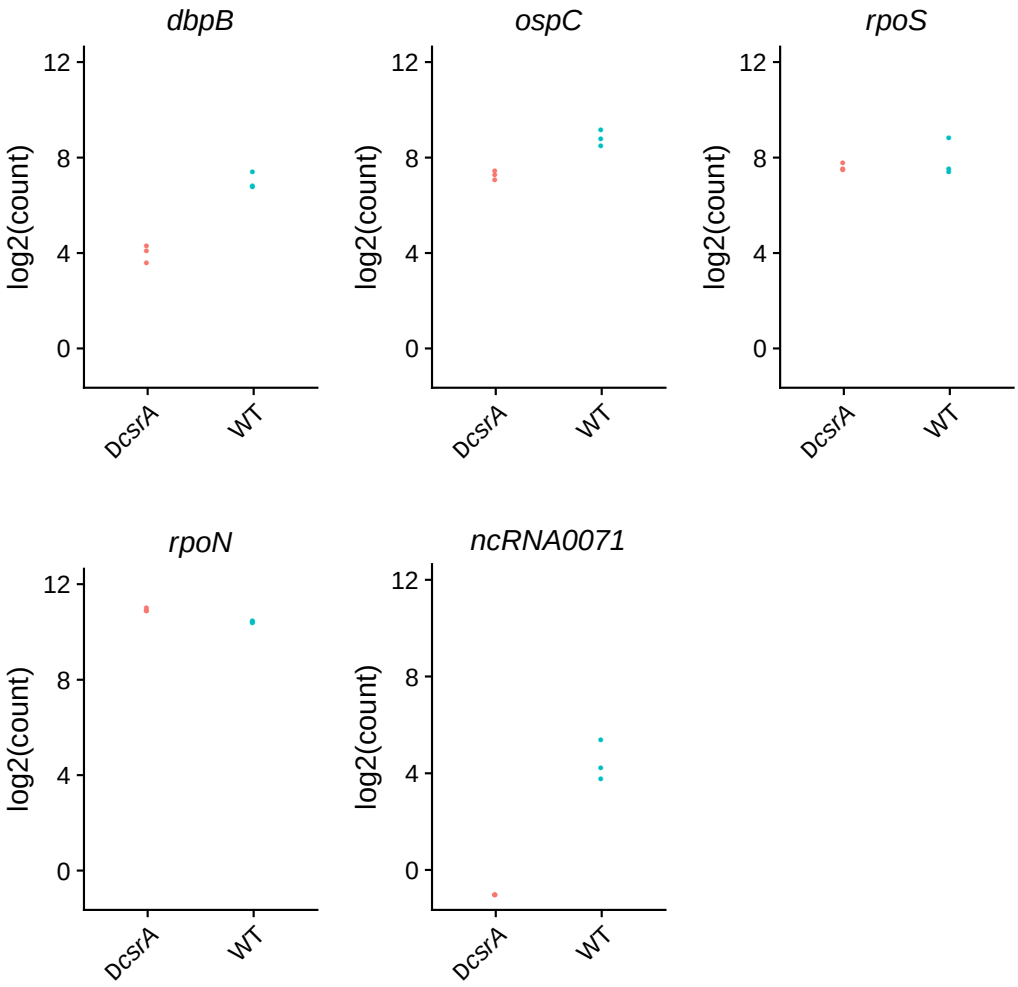

Figure 6-2: Expression of select transcripts in Δ*csrA* mutant and wild-type *B. burgdorferi*

Read counts for select transcripts were extracted from the library size normalized data set, $\log_2$ transformed, and plotted from wild-type and Δ*csrA B. burgdorferi* samples. Replicate samples are plotted together.

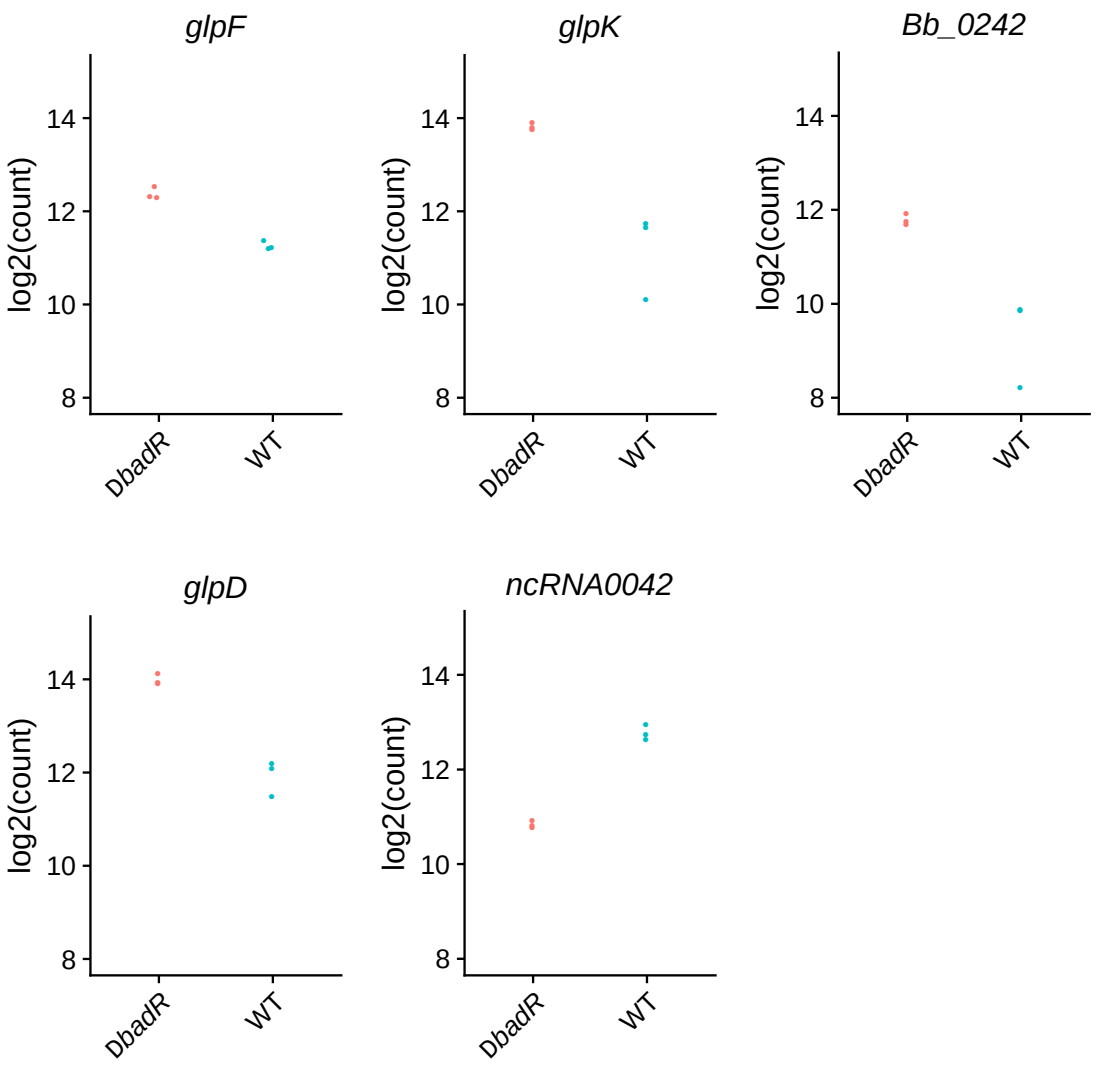

Figure 6-3: Expression of the *glpFKD* operon in a Δ*badR* mutant

Read counts from the *glpFKD* operon and the anti-*glpF* small ncRNA (*ncRNA0042*) were extracted from the library size normalized data set, $\log_2$ transformed, and plotted in Δ*badR* mutant and wild-type *B. burgdorferi*.

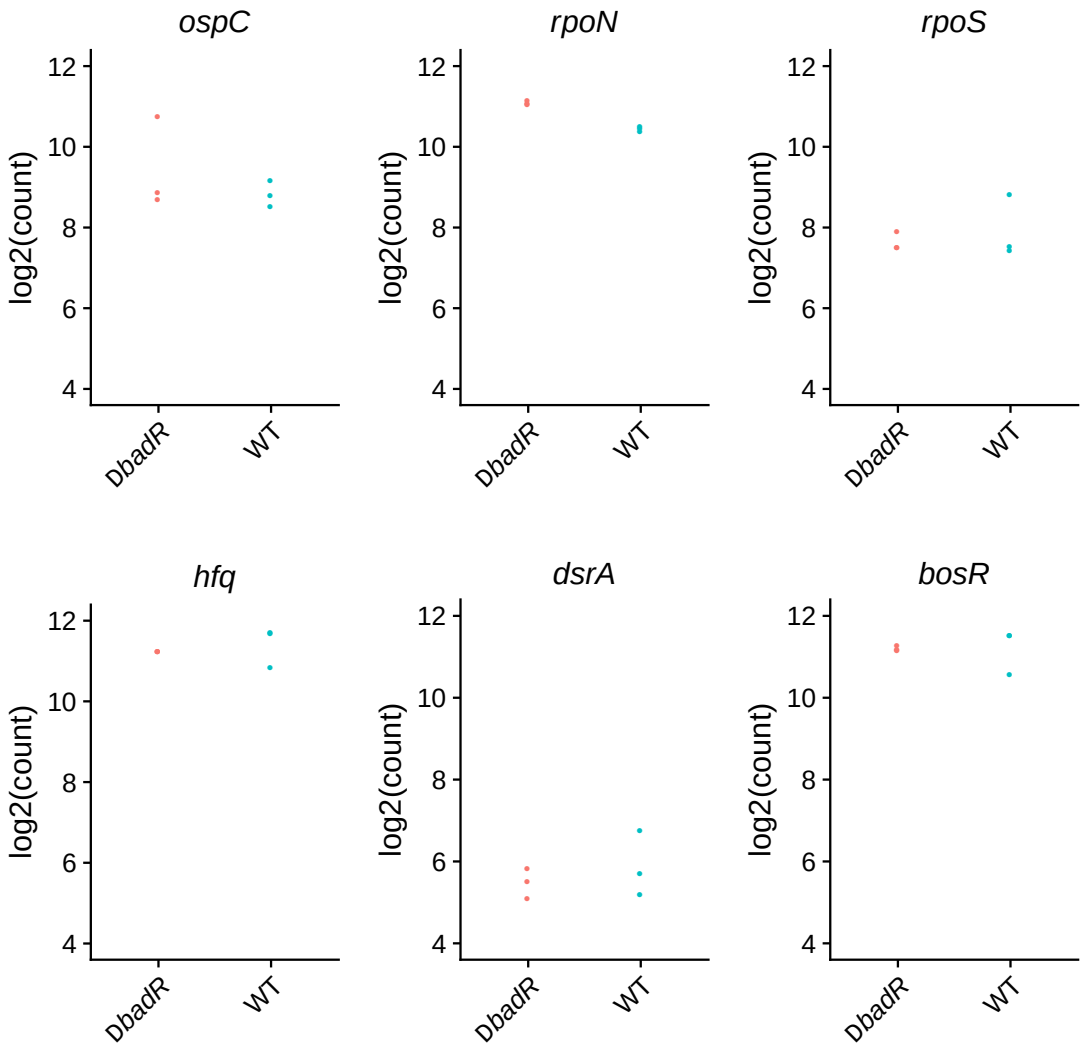

Figure 6-4: Expression of select transcripts in Δ*badR* mutant and wild-type *B. burgdorferi*

Read counts for select transcripts were extracted from the library size normalized data set, $\log_2$ transformed, and plotted from wild-type and Δ*csrA B. burgdorferi* samples. Replicate samples are plotted together.

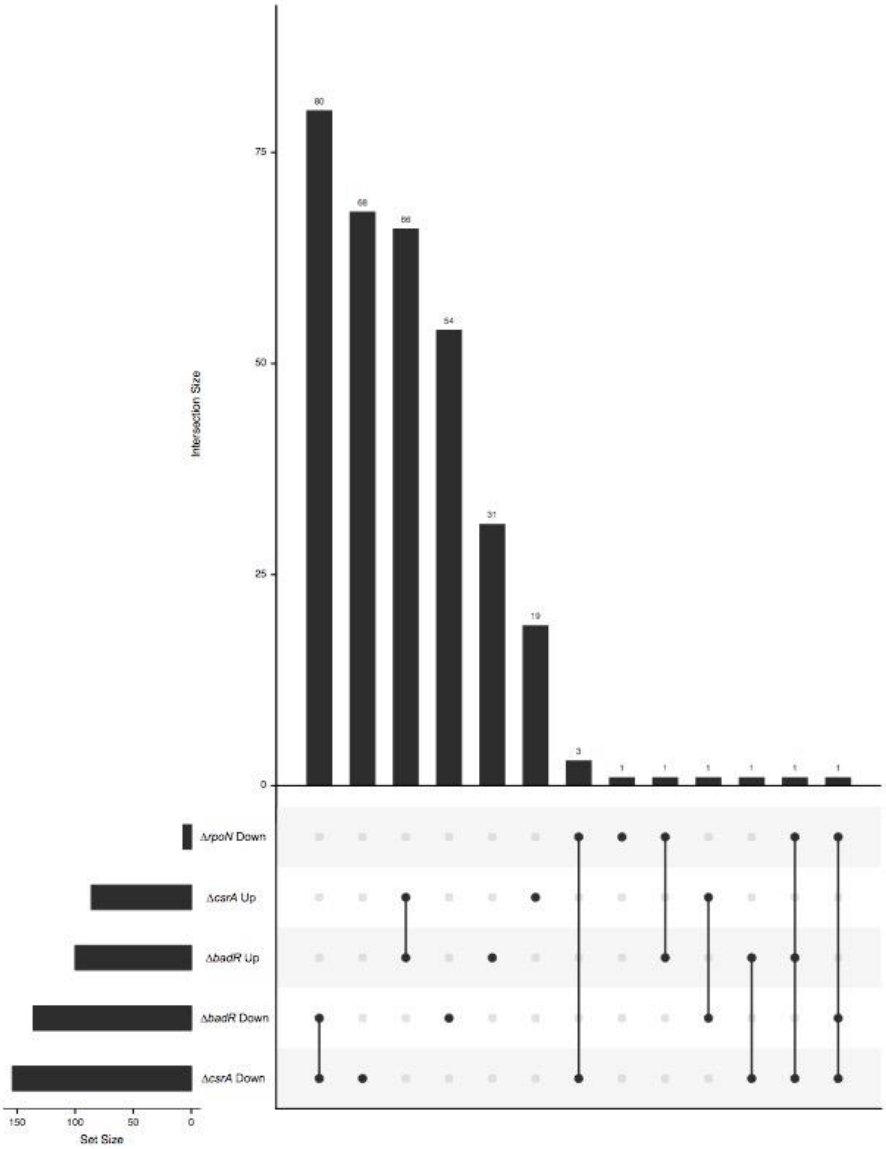

Figure 6-5: Set analysis of differentially expressed gene sets

The differentially expressed transcripts from each of the mutant to wild-type were compared for any overlap in identity using the UpsetR package [73]. Affected transcript sets were first filtered by higher or lower abundance to create 8 possible sets (four regulators, at higher or lower abundance). The lower left horizontal bars indicate the total size of a given set. The central, main bar plot indicates the size of the overlapping set, and the identity of the intersecting sets is indicated by the variously connected or separate dots

below. A line connecting darkened dots indicates the two sets of differentially expressed transcripts contain shared transcripts. Empty sets are not shown.

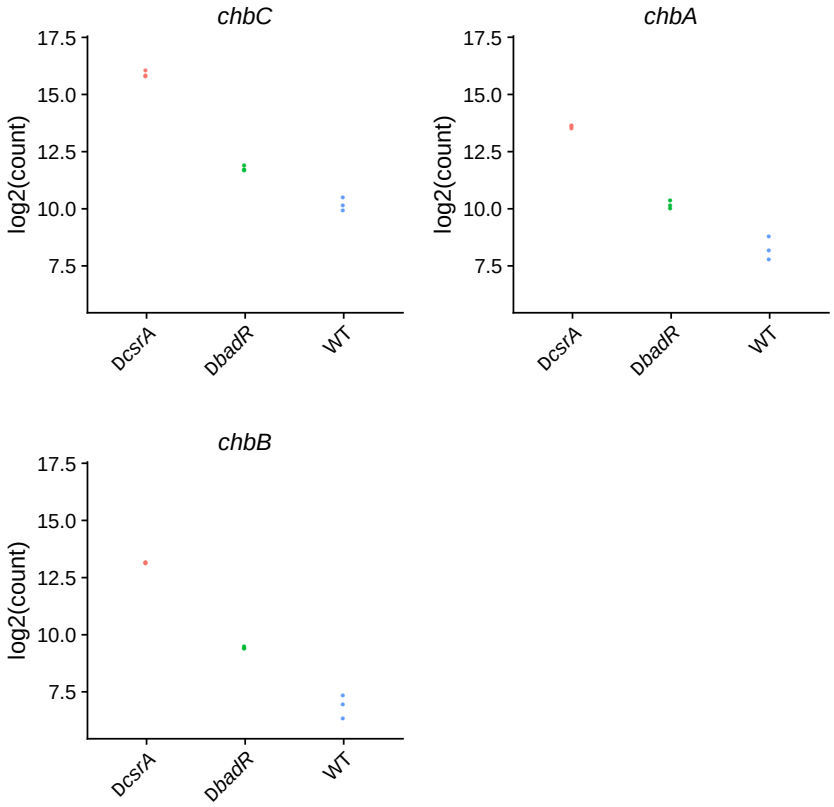

Figure 6-6: Expression of transcripts encoding proteins involved in chitobiose metabolism affected in Δ*badR* and Δ*csrA* mutants.

Read counts for transcripts derived from the chitobiose operon were extracted from the library size normalized data sets, $\log_2$ transformed, and plotted from Δ*csrA,* Δ*badR,* and wild-type *B. burgdorferi* samples. Replicate samples are plotted together.

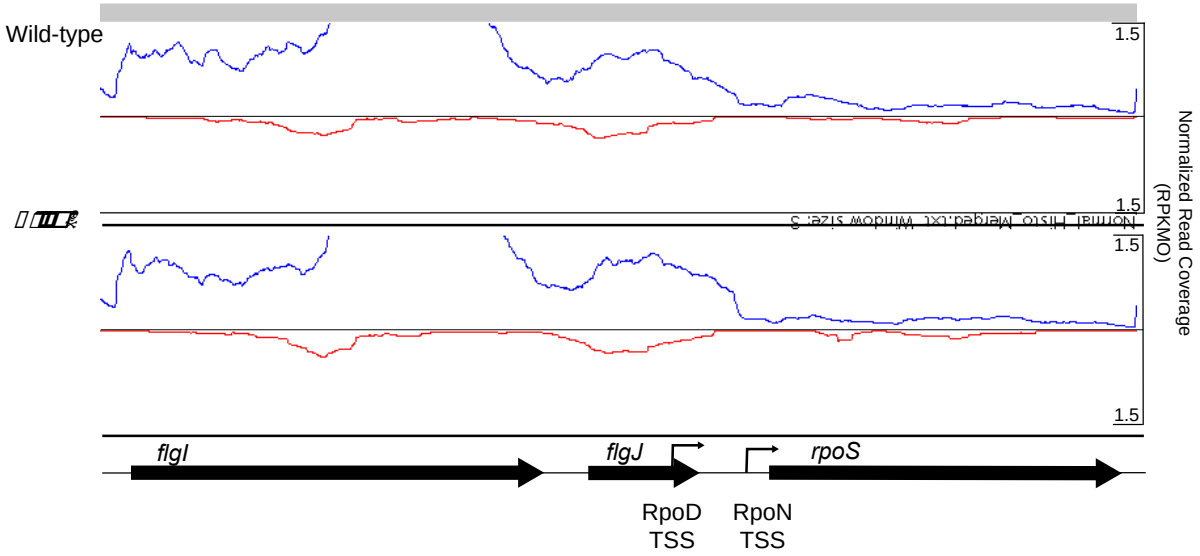

Figure 6-7: Promoter utilization of *rpoS* in an Δ*rpoN* mutant

Read coverage histograms of *rpoS* locus and upstream genomic region in wild-type and Δ*rpoN* strains. Abundance plots represent the merged normalized expression from three, independent biological replicates. Blue lines indicate relative transcript abundance from left to right (the coding strand of *flgI, flgJ* and *rpoS*) and red lines indicate relative transcript abundance from the opposite strand (right to left), and reside above (+) and below (-) the central axis. Open reading frames are indicated below coverage plots, and the direction of transcription is given by arrows at the ends of genes. Normalized read coverage of each strand is given as RPKMO (reads per kb of gene per million reads aligning to annotated ORFs) is given on Y-axis on the left. The RpoN- and RpoD-dependent transcriptional start sites were previously identified [3, 196, 265].

Chapter 7 Discussion

Summary

B. burgdorferi is the most common vector-borne pathogen in large swaths of the world and causes disease in both humans and animals of human concern [296]. The global distribution of disease is widespread and incidence continues to rise year over year [206]. *B. burgdorferi* was established early on as a model of vector borne disease, offering insight into other arthropod transmitted pathogens. Since then, it has also served well as a model of other pathogens and microbial physiology more generally [16, 75, 156, 254]. It has become evident that pathogenic bacteria, including *B. burgdorferi*, alter gene regulatory patterns during different stages of their life cycles. The Stevenson lab demonstrated in 2013 that some of these gene regulatory changes in *B. burgdorferi* are, in part, mediated by sensing changes in rates of cellular growth [157].

Combined with this new perspective on previous data in the field, members of the Stevenson lab have become interested in investigating if *B. burgdorferi* directly senses its own growth rate and if so, defining the gene regulatory mechanisms that allow the cell to adapt to its changing environments. My studies investigate two general themes in this line of study. In Chapters 3 and 4, I better define the role of a metabolically entangled signaling molecule in vertebrate infection and test the hypothesis that a conserved nucleic-acid binding protein, BpuR, is directly controlled by cellular growth rates. In Chapter 5 and 6, I focused on a broader understanding of *B. burgdorferi* gene regulation as it relates to niche adaptation. I accomplish this by defining new potential gene regulatory mechanisms (sRNAs, extended 5' UTRs, and intrinsic terminators) and testing hypotheses related to the complexity and connectivity of gene regulatory networks important for vertebrate adaptation.

Growth control

All living things are defined by a drive to replicate and transmit their genetic information. At their very core, all living things do this through the increase in number and size of living units, i.e. individual cells. Bacterial cells have served to better understand basic cellular processes related to these drives. To quote the late Stanley Falkow, "'the goal of a bacterium is to become bacteria" [219]. This goal is complicated by the fact that nutrients, and thus energy, available to a given cell are a finite resource, and so a cell must actively control how much energy it expends in order to survive. These decisions are at the very core of my studies in that I sought to better understand how *B. burgdorferi* makes the decision to grow or not grow, and how that decision is relayed into physiologic adaptation to environments it occupies.

Nutritional control of cell size

Sixty years ago, Schaechter, Maaløe and Kjeldgaard first observed a linear relationship between growth rate and cell size in *Salmonella enterica* Typhimirium [270] demonstrating that growth rate, rather than culture media composition, was responsible for differences in cell size. Since then, the study of cell size control and the so called "Growth Law" has remained active [65, 311, 319, 320, 328, 335, 337], yet conserved molecular mechanisms underlying this phenomenon are still not well understood. Furthermore, while some themes appear to be conserved across the bacterial kingdom, significant differences exist. In the case of *E. coli* and *B. subtillis*, two unique proteins, OpgH [131] and UgtP [66, 335], respectively, sense UDP-Glucose and tie it to the ability of the division ring protein FtsZ to oligomerize and function in cell division.

To the best of my knowledge, no comprehensive study of *B. burgdorferi*'s adherence to the "growth law" has been undertaken, but anecdotal evidence in my own studies suggest that it does: rapidly growing cells in rich media are generally short, while those in in slow growth conditions, nutrient or temperature induced, are more extended in

physical length. Without quantitative, single-celled, phenotypic data from well-controlled studies, it is impossible to say at this time if the “growth law” is truly observed by *B. burgdorferi*. With that said, there is preliminary evidence that *B. burgdorferi* does coordinate cell size with division, with longer cells containing greater numbers division sites than shorter cells [159]. As noted above regarding glucose metabolism, while many bacteria appear to have a mechanism tying nutritional status to cell size, the exact molecular mechanisms appear to be more divergent. For example, *B. burgdorferi* does not encode recognizable homologues to either OpgH or UgtP; thus, if it ties cell size control to nutrient status, it does so in some other way.

Nutritional control of DNA replication

A key criterion for increases in cell size or increases in rates of division is the control of the rate of DNA synthesis. Any cell that divides without a complete complement of the genome is unlikely to survive to divide again. It should come as no surprise then, that the master regulator of DNA replication in most bacteria, DnaA, is often intimately tied to cell division and nutritional status of diverse bacterial species [114, 117, 181, 222]. Control of all aspects of growth and division must be intimately tied to available levels of nutrients. In conditions where nutrients are limiting, cells must actively adapt, often by slowing or ceasing growth in order to survive. In conditions where nutrients are abundant, it behooves the cell to grow and divide as rapidly as possible so as to best spread its genetic material. This is of critical importance in relation to the regulation of DNA synthesis. In most bacteria, initiation of chromosomal replication is a once per cell cycle event, and cells that commit to the initiation of DNA replication must complete synthesis and division or they may not survive. Cells have thus evolved elaborate mechanisms to ensure the process can actually be completed prior to initiation.

DnaA is a DNA binding protein with a AAA+ ATPase domain and is the master regulator of DNA replication [162]. The function of DnaA is regulated at numerous steps,

including transcription and translation, and its activity is tightly coupled to cellular ATP/ADP ratios [64, 69, 71, 106, 113, 134, 152, 166, 168, 170, 179-181, 208, 248, 260, 261, 282, 289]. DnaA levels are also controlled by proteolysis during adverse conditions. In *Caulobacter crescentus*, DnaA is a substrate for Lon protease, and, during periods of carbohydrate starvation, translation of DnaA is slowed while proteolysis remains steady. This results in an overall decrease in DnaA levels during adverse conditions and facilitates growth arrest during carbohydrate limitation. Recent work suggests that Lon does not target DnaA through the unfolded protein response, but instead recognizes native DnaA; this degradation is thought to potentially be dependent on the nucleotide bound state [188].

Growth and virulence

The key difference between pathogenic and commensal microbes is the causation of damage, which we call disease [55]. Commensal or mutualistic microorganisms have established a balance with their host, which allows them to grow, divide, and colonize new hosts without causing disease. Pathogenic bacteria, on the other hand, are those that occupy a host, or inappropriate part of an otherwise normal host, with which they have not evolved to appropriately coexist, or they may be an obligate parasite of that host organism. If a microbe is unable to grow, divide, and spread, generally, it cannot cause disease. Much work has focused on the regulation, mechanism, and effects of so called “virulence factors” without placing them in to the larger context of bacterial physiology. It should be clear by the end of this work that I feel a new paradigm is emerging. If bacteria intend to expand their numbers, and some bacteria do this through mechanisms which cause harm to other organisms, it would seem eminently reasonable that they may tie growth and division to the regulation of these virulence factors.

Many bacteria have evolved mechanisms to persist when challenged with stressful conditions, such as starvation or host immune pressures [110, 130]. Most study in this

regard has focused on host factors or antimicrobial therapies as the cause of such conditions. There exist numerous examples of pathogenic bacteria which have evolved elaborate mechanisms to survive within their respective hosts. *Mycobacterium tuberculosis* [110] and *S. enterica* survive for extended periods within host macrophages [109]. Spore-forming pathogens, such as *Bacillus anthracis* and several species in the genus *Clostridium*, have evolved elaborate life stages that produce environmentally stable, metabolically inactive structures called endospores, which allow them to persist in extended, nutrient poor conditions [105, 130, 150]. When these spores enter a more favorable environment, they interconvert back into vegetative cells capable of division and growth. Similar processes are apparent in pathogenic Chlamydia, which survive through developmental interconversion between reticulate and elementary bodies, which are metabolically active and inactive forms, respectively [2].

B. burgdorferi has also evolved mechanisms to survive extended periods of stress through apparent decreases in replicative or metabolic activity [38, 76, 242]. *B. burgdorferi's* lifestyle has required the evolution of slow growth states outside of the vertebrate/tick host. I specifically choose to not refer to this adaptation as "persistence,"" as the term is closely associated with specific adaptations of certain bacterial species to stochastically enter a physiologic state resistant to antibiotic therapy [182]. To date, there exists no convincing data that *B. burgdorferi* enters such a state. During colonization of the tick midgut, *B. burgdorferi* transitions into a quiescent-like state, in which it does not undergo significant expansions in number and exhibits reduced motility [88, 242]. This is not surprising, given what is known regarding the nutrient content of *Ixodes* spp. tick midguts. Specifically, following digestion of the blood meal, the midgut is dominated by high levels of glycerol, an energy poor carbohydrate [111, 237]. As described in earlier chapters, concomitant with ticks' ingestion of a blood meal, *B. burgdorferi* cells undergo a burst of replication, facilitating their transmission to and colonization of the vertebrate host.

Exact molecular mechanisms underlying this rapid and drastic alteration in behavior are not yet clear, but they are likely related to a combined increase in temperature, nutrient availability, and the presence or absence of specific vertebrate or tick factors. The mechanisms by which *B. burgdorferi* ties this enhancement of growth rate to the induction of vertebrate specific factors [157] and repression of tick-specific ones is still unclear, but the studies contained herein begin to shed some light on these processes.

***B. burgdorferi* metabolism in context**

In these studies, with the support of my colleagues, I begin to elucidate how these processes are interconnected. I demonstrated that the metabolically intertwined signaling molecule AI-2 is essential for maximal fitness within the vertebrate host, and that the master regulator of DNA replication, DnaA, is associated with the expression of the nucleic acid binding protein BpuR. While they may appear disparate, these processes are intimately intertwined. During DNA replication, the newly synthesized strand of DNA must be methylated to ensure it is not cleaved by bacterial restriction systems [282, 338]. During periods of rapid DNA replication, flux through the LuxS enzyme would likely be increased due to this presumed elevated number of methylation reactions, and thus AI-2 abundance should be elevated. As previous work from the Stevenson lab has demonstrated, addition of AI-2 to *B. burgdorferi* cells results in enhanced production of several key vertebrate-associated factors, and AI-2 reaches peak production during exponential growth [17, 253]. During these same periods of rapid DNA replication, I likewise expect there to be an increase in levels of cellular DnaA. These high levels of DnaA could result in a higher occupancy of the protein at its binding sites, including the *bpuR* promoter. While I have not provided evidence that the occupancy of DnaA at this location has an effect on transcription or gene expression, significant precedent exists for this hypothesis [133, 134, 209, 285, 289, 306, 332].

As with any academic work, much remains to be done to better understand these systems. As described in Chapter 3, AI-2 has significant impacts on the *B. burgdorferi* proteome and the expression of some important proteins (ErpA/I/N and VlsE) [17, 297]. No obvious homologues for the first discovered AI-2 sensing networks, such as those found in *V. cholerae* and *Pseudomonas aeruginosa* [259], are encoded by the *B. burgdorferi* genome. In Chapter 3, I elaborated upon some potential candidates for AI-2 sensors. These included both a ribose ABC-type transporter system and a carbohydrate-responsive DNA-binding protein. Ribose-importing ABC-type transporters have been previously shown to play a role in AI-2 intake in *S. enterica Typhimurium* and *E. coli* [310, 341]. The ribose transporter RbsB has been experimentally demonstrated to bind AI-2 in *Actinobacillus actinomycetemocomitans* and has a role in the uptake of AI-2 and biofilm phenotypes of *Haemophilus influenzae* [12, 149]. *B. burgdorferi* encodes some components of a putative ribose ABC-transporter system (Rbs), but no identifiable homologues of the actual ribose binding protein, RbsB, are obvious. It is possible that this represents an orphan system that is in the process of being lost during evolution, or the ribose binding component of the system may be significantly divergent from established homologues. Studies using labeled ribose or AI-2 in the context of the deletion of components of these systems would provide insight into the activity of the Rbs system in *B. burgdorferi*. Follow-up experiments in the same vein as those described in Babb *et al*. [17] and Stevenson and Babb [297] in these newly constructed Rbs mutants would further test if the system is both active for AI-2 uptake and/or mediates the sensing of that AI-2.

Even if an AI-2 binding or importing protein were to be identified, how AI-2 is then sensed is also an open question. One potential mechanism to explain the signal transduction is through the carbohydrate responsive DNA binding protein BadR. *B. burgdorferi* possess two proteins annotated as xylose responsive repressor type proteins, XylR-1 and XylR-2 [101]. Upon closer study it became apparent that *B. burgdorferi* cannot

metabolize xylose [326] raising questions about its true function. XylR-1 was eventually retitled BadR and found to play a significant role in *B. burgdorferi* gene regulation, including repressing the transcription of the alternative sigma factor *rpoS*. Intriguingly, coincubation of BadR with Ribose-5P blocked its ability to interact with *rpoS* DNA in EMSAs. In some model organisms, AI-2, once internalized, is phosphorylated [341]. Ribose-5-phosphate and AI-2 are structurally similar molecules, and detailed X-ray crystallographic studies show that one protein encoded in the LuxR-responsive *l*sr operon, LsrF, bind can bind ribose-5-phosphate in the same pocket as phospho-AI-2 [81]. Therefore, there exists precedent that proteins that can bind Ribose-5-phosphate can also bind phospho-AI-2 molecules.

This model would be consistent with the observed data in *B. burgdorferi*: specifically, that AI-2 is produced most highly during periods of rapid growth. In this potential model, when AI-2 is produced at higher levels, it would increasingly bind BadR and inhibit its ability to bind target DNA sites to repress their transcription. In this scenario, the ability of BadR to repress *rpoS* transcription would be inhibited. *rpoS* is most highly transcribed during periods of transition to rapid growth. This coincides with the high-level production of AI-2 and the induction of the gene regulatory program utilized to transmit and colonize the vertebrate host, which is controlled partly by RpoS. Similarly, to the above described future experiments, one could test if labeled AI-2 is bound by BadR and if AI-2 or phospho-AI-2 interferes with the ability of BadR to bind target DNA. A significant caveat to this model is that no obvious homologues to the LsrK kinase known to phosphorylate AI-2 are encoded in the *B. burgdorferi* genome.

As I hope I have made clear, physiologic processes are regulated by numerous inputs, and, while AI-2 signaling appears to play a significant role in adapting *B. burgdorferi* to its vertebrate host, it is only one component of this process. DNA replication is one of the points of signal integration in which bacteria make major physiologic decisions. As

described above, DnaA is the master regulator of DNA replication initiation in almost all bacteria [282]. DnaA is a multi-domain enzyme with and is composed of a DNA-binding domain, an oligomerization domain, a Walker-type ATPase domain, and a domain with a yet unknown role [107]. Prior to this work, the *B. burgdorferi* homologue of DnaA had not been directly studied beyond bioinformatic attempts to identify its potential binding sites within the origin of replication [239, 240].

While the work described in the Chapter 4 provides substantial new data regarding DnaA's potential role in *B. burgdorferi* gene regulation, the larger questions surrounding its biogenesis and activity during the course of the enzootic cycle remain completely unanswered. Intriguing questions exist regarding how DnaA is made, in what quantities, and in what form over the course of this bacterium's life. As indicated earlier, the *B. burgdorferi oriC* had been previously investigated with the primary goal of understanding the location at which DNA begins replication. This location was identified experimentally for the main linear chromosome and computationally for the other genetic elements. At the location of initiation of the main linear chromosome no canonical DnaA binding sites (DnaA boxes, TTAT(C/A)CA(C/A)A)) were identified by sequence analysis but several degenerate repeated sequences ((A/T)A(A/C)(A/C)TACAA) were present [239, 240].

While this degenerate site is present in numerous copies throughout the genome, it is not conserved at the DnaA binding region I identified in the *bpuR* promoter. I identified one additional binding site for DnaA in the *B. burgdorferi* genome by EMSA that includes the promoter elements for the *dnaX* gene. DnaX encodes the gamma and tau subunits of DNA polymerase [153]. Motif analysis of the sequences known validated *B. burgdorferi* DnaA binding sites (*oriC*, *bpuRp*, and *dnaXp*) do not share any obvious significant shared motifs. There are a number of potential explanations for this observation. As has been described previously, the binding site for DnaA differs depending upon its ATP versus ADP bound state [290]. Thus, DnaA can vary its DNA binding targets depending on both

cellular ATP/ADP ratios as well as the rate of replication, as DnaA-ATP is converted to DnaA-ADP following initiation of replication (regulatory inactivation of DnaA or RIDA) [166]. Considering our data demonstrating that *bpuR* expression is high during slow growth and very low during vertebrate infection, and previous data demonstrating the *dnaX* is most highly expressed during periods of rapid growth [153], it is possible that the DnaA binding site, and any outcome on gene expression, is different in these two locations. This biphasic model does not fully explain why neither of these sites share a motif with *oriC*. It is possible that difficulty in identifying these sites is compounded by the small sample size of known sites. It is worth noting that the previously mentioned sequence identified in the *oriC* is not present in potential replication origins on non-chromosomal elements [239, 240].

In Chapter 4, I proposed a model wherein DnaA-ATP binds the *bpuR* promoter and interferes with productive transcription (Figure 4-8). This is premised on the idea that, during periods of rapid growth, DnaA-ATP levels are high, and, during slow growth, DnaA-ATP levels are low. Data described in Chapter 5 provide some support for the above model, although with significant caveats. As *B. burgdorferi* transitions in to stationary phase, *dnaA* transcript abundance decreases and *bpuR* transcript becomes more abundant. The significant caveats are that both *dnaA* and *bpuR* are subject to multiple post-transcriptional controls, and thus their transcript levels may not reflect protein abundance or activity levels of either protein.

DnaA is becoming increasingly known as a major regulator of transcription, in some cases acting through other DNA-binding proteins [285, 332]. EMSAs performed as described in Chapter 4 with alternative conditions or mutagenized DnaA could begin testing this model. Unfortunately, due to its key role in life of the cell, deletion, overexpression, or mutagenesis of the ATP- or DNA-binding domains of DnaA is either impossible or fraught with confounding variables. The use of uniformly ADP or ATP bound

DnaA in EMSAs could provide similar insight. If ATP/ADP binding does impact the results of the EMSAs, mutagenesis of the key residues of the nucleotide binding region could further test if ATP/ADP bound status impacts DNA binding specificity. Not only do we know little about the DNA-binding activity of DnaA, we know nothing regarding the expression and nucleotide bound state of DnaA during the natural enzootic cycle. Further complicating this model, we know very little about cellular levels of ATP at any stage of *B. burgdorferi*'s life cycle. Presumably, during tick colonization, when resources are less abundant, cellular ATP levels are lower than those during vertebrate colonization when glucose is abundant, but this remains unknown.

If further experiments in *B. burgdorferi* can test whether DnaA does regulate the expression of *bpuR*, it would be the first such example in a pathogen utilizing DnaA in the regulation of genes involved in infection of the vertebrate host. ChIP-seq and *in vitro* transcription have both been used to test hypotheses regarding DnaA activity at specific loci [306, 332] and could provide insight in to this specific case. I hope that with additional study, we may be able to understand how *B. burgdorferi* uses the same information to make replication initiation decisions as it does host adaptation decisions.

Input and output of gene regulatory networks (GRNs)

As described in Chapter 1, many biological processes are commonly thought to be organized into tidy pathways, with a limited number of forks or alternative routes. Reality has proven to be far more complex. Regulatory factors are no exception to this, and when studied in detail, apparently linear pathways often emerge as highly interconnected networks with abundant crosstalk, feedback, feedforward, and control centers [23]. A large amount of work in the field of *B. burgdorferi* biology and gene regulation has focused on two separate regulatory cascades, HK2-Rrp2-RpoN-RpoS and HK-1-Rrp1-PlzA, thought to be important for vertebrate or tick colonization, respectively.

Testing specific hypotheses regarding function of gene regulatory networks requires knowledge of the network. Inference of existing networks based upon homology has significant limitations, and, in evolutionarily divergent organisms, the limitations are even more significant. This limitation is apparent in the field of *B. burgdorferi* biology, where only a small handful of canonical transcription factors and even fewer post-transcriptional regulators were identified by genomic sequence similarity. Yet, additional factors have been discovered nearly every year since the original genomic annotation. Some of these are based upon the addition of new data to reference databases [155, 268, 348], some following detailed experimentation on their regulatory targets [42, 156, 161, 254], and others through the study of related processes or screens [169, 286]. These discoveries are often based upon the generation of new information or the implementation of new technologies.

One such revolutionary technology is high-throughput RNA-Sequencing, which has provided the unprecedented ability to investigate transcript abundance at the single nucleotide level [281, 331]. Not only can RNA-Seq be used as the measurement for a variety of expression screens, it can also be used to interrogate transcriptome structure. Control of gene expression is well known to extend beyond simply proteins that induce or repress transcription, but includes RNA structure [119, 129], small non-coding RNAs [112, 176, 228, 243, 302, 303, 321, 333], and the expression of alternative transcripts [4, 11, 195], to name a few.

With these possibilities in mind, and the dearth of literature regarding these mechanisms, in *B. burgdorferi* or any spirochete, I sought to test if any of these non-proteinaceous mechanisms were at play. In performing whole transcriptome analysis, I was able to generate insight into transcriptome dynamics by examining these data in time-series. I found that, similar to nearly every studied prokaryotic organism, *B. burgdorferi* expresses a large set of small RNAs, with both intergenic and antisense transcripts found

in abundance. I found small RNAs encoded across all seventeen replicons contained within the B31-A3 isolate sequenced. The only well studied sRNA known prior in *B. burgdorferi*, *dsrA*, plays a key role in the post-transcriptional regulation of RpoS [197], highlighting that sRNAs likely play an important role in gene regulation in this organism. *dsrA* works in concert with the RNA-binding protein, Hfq, to affect its function [195]. Hfq-sRNA mediated control of expression is a well-known process in other bacteria [236], and likely mediates the effects of other sRNAs in *B. burgdorferi*. An additional study by Popitsch and colleagues further supported my findings using a sRNA-enriched sequencing strategy that identified many hundreds of small RNAs [243]. Newly identified antisense-RNAs are contained within genes encoding proteins of diverse biological function, including DNA replication, metabolism, and virulence. Small RNA's often act as tuning switches for gene regulatory processes, similar to the role of AI-2 described earlier in my studies.

Computational sequence analysis revolutionized the ability predict gene function in diverse organisms. Sequence analysis is not without limitations, and evolution introduces difficulty in making correct inferences on sequence alone. Identification of promoter elements controlling gene expression is also notoriously difficult based on solely on sequence. While well-defined promoters have been elucidated in several model organisms, the sequence of any individual promoter varies within and across organisms. Therefore, while the identification of putative protein coding genes is generally thought to be straightforward and relatively accurate, the prediction of non-coding portions of transcripts is significantly more challenging. RNA-sequencing allows for direct measurement of such features.

My studies described in Chapter 5 present just such an experimental data set. I was able to unambiguously identify 5' ends for up to ~700 transcripts, depending on time point, during *in vitro* growth. While I have not mined this data to identify the number of

unique operons represented, at minimum, it constitutes identification of 5' ends for greater than 1/3 of all predicted protein coding genes. At this time, I have not extracted sequence information for the genomic regions immediately preceding these sites, and thus can provide no comprehensive statements regarding potential promoter sequences or alternative promoter utilization. I did compare previously identified transcriptional start sites to my data and found generally good agreement. I was also able to examine specific transcripts of known importance for *B. burgdorferi*'s enzootic cycle, including *rpoS* and *glpFKD*. Findings at both of these loci provided substantial insight in to their regulation, supporting previous and recently published hypotheses [120, 269]. A study by Adams *et al.* [4] recently undertook a comprehensive characterization of transcriptional start sites and, while, I have not completed a full comparison between our datasets, select transcripts were in good agreement. Riboswitches, which are important, non-coding, transcribed elements that may be responsive to diverse inputs including temperature, metabolites, and secondary messengers [22, 129, 278, 304], are not well studied in any spirochete, and none have been experimentally defined in *B. burgdorferi*. If riboswitches exist in the *B. burgdorferi* genome, and I suspect they do, then these 5' UTR data could be readily mined for candidate identification. Non-coding elements are becoming increasingly well known to be major regulators of biological processes and my hope is that these datasets will serve as foundational resources for the field of *B. burgdorferi* biology.

Topology of critical gene regulatory networks

Finally, to begin providing insight in to critical protein-based gene regulatory networks in *B. burgdorferi* biology, I examined the transcriptomes of deletion mutants of four regulatory factors essential for completion of the enzootic cycle (CsrA, BadR, RpoS, and RpoN). While several of these factors have been examined in isolation previously, culture conditions, strain background, and technology have confounded the dissection of how these factors interact to generate the complex phenotype of vertebrate adaptation. I

found that none of the four regulatory factors examined regulate one another in the specific conditions examined. This means that all the transcripts that have been found to be regulated by two or more factors are likely the result of convergent regulation. This is in stark contrast to much of the current thought in the field that vertebrate adaptation is mediated largely through the HK2-Rrp2-RpoN-RpoS cascade. That being said, my data do not preclude a situation in which any of these given factors convergently regulate a third, which then goes on to regulate all the shared targets. As I said in Chapter 6, I consider a combination of both possibilities the most likely scenario.

I found that of these factors, while RpoS and RpoN appear to not be activated in the examined conditions, CsrA and BadR regulate large numbers of genes. Not surprisingly, given their essentiality for vertebrate infection, the direction of differentially expressed transcripts, supported these observations. In general, the deletion of either factor lowered the expression of known vertebrate specific genes and enhanced the expression of known tick specific ones. The fact that these factors may coregulate an additional, third factor presents a potential opportunity, in that targeting the inputs of a single, key regulator may allow for interruption of the ability of pathogens to properly adapt.

In the cases of the RpoN and RpoS deletion mutants, it may seem quite a surprise, given the current literature [47-49, 118, 127, 138, 230, 232, 343], that almost no transcripts were differentially expressed in my study. Upon careful consideration, the limitations of existing literature in that they often used specific *rpoN* and *rpoS* inducing culture conditions, these differences are less surprising. My data support a critical reevaluation of hypotheses surrounding vertebrate adaption in of *B. burgdorferi*. While RpoS certainly plays a significant role in host adaptation of the spirochete, it is apparent that additional factors also control this adaptation. BadR and CsrA have both been previously postulated to act through activity on *rpoS*, and this work provides substantial support that they drive vertebrate adaptive programs independently of the RpoS protein. What is still lacking is

an understanding of what gene regulatory effects are mediated directly versus those that are mediated indirectly. Both ChIP and RIP approaches were pioneered in the Stevenson lab for use in *B. burgdorferi*, and their application to these two proteins would provide substantial insight in to their place within the wider gene regulatory network. These and past studies highlight a significant limitation of such studies and most experiments in the life sciences, namely that a single snap shot of a single condition may not extrapolate to all processes. While my data provide substantial insight into the interactions between these four regulatory factors, time-series or multi-conditional comparisons would significant additional insight in to the dynamics between these and other factors.

Biochemical evidence from multiple groups demonstrated that BadR binds *rpoS* promoter DNA and regulates its transcription, yet *rpoS* transcript was not impacted by deletion of *badR* in my study. This is almost certainly due to the use of non-*rpoS* inducing conditions, which would obscure any role for a negative regulator but does highlight tht BadR is not the only repressor of *rpoS* transcription. RpoN is a sigma-54 type factor and these typically require an enhancer binding protein (EBP) for their activity [44]. The proposed EBP in *B. burgdorferi* is the response regulator Rrp2, whose activity is phosphorylation dependent and thought to be activated the sensor histidine kinase HK2 [118]. The histidine sensor-response regulator relay, HK2 nor Rrp2, are not thought to be strongly activated during the culture conditions utilized in these studies and offer a potential explanation for the lack of effect by the deletion of *rpoN*.

The obvious next step for further discerning critical *B. burgdorferi* gene regulatory networks is to perform transcriptome analysis on significantly larger numbers of mutants and culture conditions. Experiments such as these have provided substantial insight in a variety of prokaryotic organisms, including *E. coli* [201] and *Halobacterium salinarum* [78, 79], which benefit from rapid doubling times and high-throughput culture methods. If high-throughput methods could be combined with low input transcriptomics to account for the

comparably low bacterial densities achieved during *B. burgdorferi in vitro* cultivation, a more comprehensive view of important GRNs could be ascertained.

Finally, the last, and likely most significant limitation of these studies is that they solely focus on regulation at the level of transcript abundance. While it is clear that RNA-Seq does not measure transcription alone, but also transcript stability and structural dynamics, it still does not inform about protein levels or protein activity. This limitation is not newly recognized, but it should be reiterated: transcript abundance is only one fraction of the story. Combinations of genomic, transcriptomic, proteomic, and metabolomic tools will provide substantially more insight when combined than any single approach. In summary, the work described in Chapters 5 and 6, along with the recent work of Popitsch *et al.* and Adams *et al*., provide a firm foundation for -omics experiments to build data sets beyond the genomic sequence of this important human pathogen.

Closing thoughts

More than a handful of dissertations worth of work remain to be done before the growth-virulence connection in *B. burgdorferi* or the regulatory networks underlying it, let alone other pathogens, begins to be even partially elucidated. The work I have described here only begins to open that door and pose the earliest series of questions. This work, and that of innumerable others has also begun to provide opportunity for future study aimed at intervention in *B. burgdorferi* infections. If the signals that *B. burgdorferi* senses during the tick's blood meal, and the mechanisms by which they convey that information are understood, they can be potentially targeted.

Appendix

The following chapter contains the differential expression testing tables generated in Chapter 5 and Chapter 6, and the coordinates of predicted terminators and non-coding RNAs from Chapter 5. These data have also been deposited as a static, citable repository of tables at Figshare (10.6084/m9.figshare.67390)

Table 8-1 Differentially abundant transcripts when comparing early- to mid-exponential phase

Genetic Element	Gene ID	Early Expression	Mid Expression	Fold Change	P-Value	Adjusted P-Value
cp32-8	BB_L25_-_hypothetical_protein	198.58615	88.07865	0.44353	3.5299E-04	1.3563E-02
cp32-8	BB_L26_-_hypothetical_protein	386.97847	122.60457	0.31683	8.7400E-08	3.0300E-05
cp32-6	BB_M26_-_hypothetical_protein	282.77018	104.78590	0.37057	2.8300E-06	6.5298E-04
cp32-4	BB_R26_-_hypothetical_protein	213.96985	81.55307	0.38114	2.9000E-05	2.6784E-03
cp32-3	BB_S26_-_hypothetical_protein	186.38953	81.84602	0.43911	2.8986E-04	1.3482E-02

A) Decreased in abundance

B) Increased in abundance

Genetic Element	Gene ID	Early Expression	Mid Expression	Fold Change	P-Value	Adjusted P-Value
Chromosome	BB_0331_-_hypothetical_protein	6.74490	31.45814	4.66399	3.3494E-04	1.3563E-02
lp28-4	BB_I19_-_hypothetical_protein	1335.20134	2769.22118	2.07401	7.4000E-09	4.7600E-06
lp36	BB_K54_-_hypothetical_protein	25.51892	64.34795	2.52158	1.8231E-03	4.7642E-02
cp32-7	BB_O38_bppC_protein_BppC	0.23055	8.00251	34.71043	1.4046E-03	3.9701E-02

Those in (A) lower and (B) higher abundance in stationary phase compared to mid-exponential. Genes are listed which were identified by DEseq [9] as differentially expressed by meeting the criteria of >2X greater abundance and an adjusted P-value of <.05. In order from left to right columns list genetic element on which a given gene resides, the gene ID, the early-exponential expression, mid-exponential expression, fold change, P-value, adjusted P-value.

Table 8-2 Differentially abundant transcripts when comparing mid-exponential to stationary phase

A) Decreased in abundance

Genetic Element	Gene ID	Mid Expression	Stat Expression	Fold Change	P-Value	Adjusted P-Value
Chromosome	BB_0450_rpoN_RNA_polymerase_sigma-54_factor	950.80453	296.76798	0.31212	3.5832E-04	1.0796E-02
Chromosome	BB_0641_-_spermidine/putrescine_transport_system_permease	847.29382	283.93297	0.33511	1.5453E-03	3.1041E-02
Chromosome	BB_0739_-_hypothetical_protein	1036.35817	338.83289	0.32695	7.3679E-04	1.8236E-02
cp32-8	BB_L40_erpO_ErpB1_protein	8165.10277	3001.91488	0.36765	1.0128E-03	2.2845E-02
cp32-9	BB_N39_erpQ_protein_ErpQ	2559.43425	988.26692	0.38613	2.7013E-03	4.3536E-02
cp32-1	BB_P39_erpB_protein_ErpB	7775.79525	2923.42189	0.37596	1.1482E-03	2.4865E-02
lp28-2	BB_G0036_-_hypothetical_protein	2.64349	0.00000	Inf	1.3894E-03	2.8320E-02

A) Increased in abundance

Genetic Element	Gene ID	Mid Expression	Stat Expression	Fold Change	P-Value	Adjusted P-Value
Chromosome	BB_0007_-_hypothetical_protein	1656.65227	4198.01475	2.53403	1.2000E-05	1.2335E-03
Chromosome	BB_0026_-_bifunctional_methylenetetrahydrofolate_dehydrogenase/methenyltetrahydrofolate_cyclohydrolase	1504.90269	3311.62556	2.20056	1.1184E-03	2.4605E-02
Chromosome	BB_0083_-_hypothetical_protein	986.21189	2256.34684	2.28789	4.3459E-04	1.2549E-02
Chromosome	BB_0133_-_hypothetical_protein	7487.80456	15694.90171	2.09606	1.2562E-03	2.6381E-02
Chromosome	BB_0153_-_superoxide_dismutase	1519.02890	3672.56311	2.41770	4.3500E-05	2.6213E-03
Chromosome	BB_0179_trmE_tRNA_modification_GTPase	3573.53902	8667.22088	2.42539	1.8574E-04	6.7746E-03
Chromosome	BB_0226_serS_serine--tRNA_ligase	2548.90331	5703.54381	2.23765	1.9275E-04	6.8501E-03
Chromosome	BB_0253_lon_ATP-dependent_protease_La	5332.42441	12739.31042	2.38903	8.7000E-05	4.3082E-03
Chromosome	BB_0269_-_ATP-binding_protein	5550.75274	15646.76500	2.81885	7.7600E-07	1.6501E-04
Chromosome	BB_0299_ftsZ_cell_division_protein_FtsZ	4093.50271	8514.43293	2.07999	1.2589E-04	5.4524E-03
Chromosome	BB_0300_ftsA_cell_division_protein_FtsA	7296.63800	17205.45614	2.35800	8.0800E-05	4.1467E-03
Chromosome	BB_0386_rpsG_30S_ribosomal_protein_S7	7173.63418	20533.28355	2.86233	8.3300E-07	1.6501E-04
Chromosome	BB_0394_nusG_transcription_termination/antitermination_factor	6957.34021	14665.18601	2.10787	5.0794E-04	1.3804E-02
Chromosome	BB_0402_proS_proline--tRNA_ligase	1399.15943	2826.33862	2.02003	6.3111E-04	1.6254E-02
Chromosome	BB_0478_rplC_50S_ribosomal_protein_L3	8474.90371	18778.14094	2.21574	3.0595E-04	9.4844E-03
Chromosome	BB_0485_rplP_50S_ribosomal_protein_L16	2423.20662	4864.16283	2.00732	9.5917E-04	2.2157E-02
Chromosome	BB_0488_rplN_50S_ribosomal_protein_L14	1226.44546	2766.39204	2.25562	2.1200E-05	1.3981E-03
Chromosome	BB_0493_-_50S_ribosomal_protein_L6	4471.77473	9773.26761	2.18555	1.0860E-04	5.0175E-03
Chromosome	BB_0495_rpsE_30S_ribosomal_protein_S5	1726.28274	5105.39817	2.95745	9.5700E-07	1.6587E-04
Chromosome	BB_0534_xth_exodeoxyribonuclease_III	583.24606	1266.35188	2.17121	2.2797E-04	7.7063E-03
Chromosome	BB_0536_-_zinc_protease	1124.25517	2645.00403	2.35267	7.0200E-05	3.7419E-03
Chromosome	BB_0599_cysS_cysteine--tRNA_ligase	2175.51971	5350.43395	2.45938	1.2500E-05	1.2335E-03

Chromosome	BB_0621_-_4-methyl-5(b-hydroxyethyl)-thiazole_monophosphate_biosynthesis_protein	875.74098	2340.74643	2.67288	1.3936E-04	5.8531E-03
Chromosome	BB_0691_fusA_elongation_factor_G	10486.16082	21911.76904	2.08959	8.4073E-04	2.0091E-02
Chromosome	BB_0698_trmD_tRNA_(guanine-N(1)-)-methyltransferase	5066.43739	12046.84776	2.37777	4.4392E-04	1.2557E-02
Chromosome	BB_0704_acpP_acyl_carrier_protein	2485.23582	5748.97822	2.31325	1.5000E-05	1.3379E-03
Chromosome	BB_0705_rnc_ribonuclease_III	3558.39177	8195.16894	2.30305	6.1000E-05	3.3823E-03
Chromosome	BB_0738_valS_valine--tRNA_ligase	5016.83042	12754.13258	2.54227	2.0700E-05	1.3981E-03
Chromosome	BB_0749_-_hypothetical_protein	9901.65472	27334.62798	2.76061	2.5700E-05	1.6202E-03
Chromosome	BB_0804_rpsO_30S_ribosomal_protein_S15	1647.99931	3699.24376	2.24469	1.2291E-04	5.4524E-03
Chromosome	BB_0805_-_polyribonucleotide_nucleotidyltransferase	17634.94619	42138.86720	2.38951	3.0794E-04	9.4844E-03
Chromosome	BB_0816_-_hypothetical_protein	2653.08014	6860.36064	2.58581	1.5400E-05	1.3379E-03
lp54	BB_A43_-_hypothetical_protein	528.52591	1201.42123	2.27315	7.7552E-04	1.8857E-02
lp54	BB_A52_-_outer_membrane_protein	1308.79641	3123.81337	2.38678	1.3600E-06	1.9710E-04
lp54	BB_A74_osm28_outer_membrane_porin_OMS28	10584.11040	23714.89375	2.24061	1.3019E-03	2.6931E-02
lp17	BB_D21_-_hypothetical_protein	870.29195	2505.10897	2.87847	7.4400E-06	8.5965E-04
lp28-1	BB_F06_-_hypothetical_protein	14.13518	68.14145	4.82070	9.4357E-04	2.2157E-02
lp28-3	BB_H13_-_protein_RepU	784.17597	1824.34624	2.32645	1.8060E-03	3.3009E-02
lp28-3	BB_H32_-_antigen_P35	147.63987	521.57508	3.53275	1.7200E-06	2.1710E-04
lp28-3	BB_H37_-_lipoprotein	874.07528	2343.18493	2.68076	1.7300E-05	1.3981E-03
lp28-3	BB_H40_-_transposase-like_protein	14.01908	57.17008	4.07802	2.6100E-03	4.2559E-02
lp28-4	BB_I19_-_hypothetical_protein	2015.82056	6386.78179	3.16833	1.4200E-06	1.9710E-04
lp28-4	BB_I20_-_hypothetical_protein	401.04241	1635.60630	4.07839	2.2200E-08	6.1400E-06
lp28-4	BB_I21_-_PF-32_protein	622.28578	4496.09463	7.22513	9.5600E-20	6.6200E-17
lp28-4	BB_I22_-_PF-49_protein	331.29853	949.26210	2.86528	2.5947E-04	8.3634E-03
lp38	BB_J48_-_hypothetical_protein	161.21439	434.92115	2.69778	1.6912E-03	3.3009E-02
lp36	BB_K13_-_hypothetical_protein	3248.70637	7429.79420	2.28700	6.3326E-04	1.6254E-02
lp36	BB_K40_-_hypothetical_protein	1922.08954	4013.33616	2.08801	1.5098E-04	6.0535E-03
lp36	BB_K45_-_immunogenic_protein_P37	3927.66165	9863.14469	2.51120	2.0100E-05	1.3981E-03
cp32-8	BB_L31_-_hypothetical_protein	236.51806	634.63648	2.68325	9.2300E-05	4.4105E-03
cp32-9	BB_N28_mlpI_lipoprotein	136.39036	432.80008	3.17325	1.9300E-05	1.3981E-03
cp32-9	BB_N30_-_hypothetical_protein	1117.38096	2464.88361	2.20595	4.6832E-04	1.2982E-02
cp32-9	BB_N31_-_hypothetical_protein	124.10864	316.78842	2.55251	2.3428E-04	7.7313E-03
lp56	BB_Q07_-_plasmid_partition_protein	181.98173	482.59448	2.65188	1.0219E-03	2.2845E-02
lp56	BB_Q34_bdrW_protein_BdrW_protein	326.69158	982.69060	3.00801	5.6800E-05	3.2792E-03
lp56	BB_Q38_-_hypothetical_protein	2587.77422	6218.11924	2.40288	5.5639E-04	1.4830E-02
lp56	BB_Q39_-_hypothetical_protein	163.86638	758.91934	4.63133	1.1400E-08	3.9400E-06
lp56	BB_Q40_-_PF-32_protein	416.10624	1202.49810	2.88988	1.5287E-04	6.0535E-03
cp32-4	BB_R31_-_hypothetical_protein	916.15127	1943.84927	2.12176	6.8008E-04	1.7138E-02
cp32-4	BB_R32_-_hypothetical_protein	149.36200	772.42758	5.17151	1.6000E-11	7.3900E-09
cp32-4	BB_R33_-_plasmid_partition_protein,_putative	182.31441	508.89515	2.79131	1.8537E-04	6.7746E-03
cp32-4	BB_R34_-_hypothetical_protein	107.29289	285.91129	2.66477	1.7869E-03	3.3009E-02
cp32-4	BB_R44_-_hypothetical_protein	49.78824	144.35307	2.89934	2.2068E-04	7.6465E-03
cp32-3	BB_S34_-_hypothetical_protein	173.16988	436.01624	2.51785	1.5775E-04	6.0735E-03
Chromosome	Rfam_ncRNA1_NC_001318_SRP_bact_Rfam_annotation	2827.60605	40168.05042	14.20567	4.6500E-28	6.4500E-25

Those in (A) lower and (B) higher abundance in stationary phase compared to mid-exponential. Genes are listed which were identified by DEseq [9] as differentially expressed by meeting the criteria of >2X greater abundance and an adjusted P-value of <.05. In order from left to right columns list genetic element on which a given gene resides, the gene ID, the mid-log expression, stationary expression, fold change, P-value, adjusted P-value.

Table 8-3 Transcripts that were differentially abundant between early-exponential and stationary phase

A) Decreased in abundance

Genetic Element	Gene ID	Early Expression	Stat Expression	Fold Change	P-Value	Adjusted P-Value
Chromosome	BB_0009_-_hypothetical_protein	337.08924	150.88217	0.44760	6.8815E-04	3.1830E-03
Chromosome	BB_0012_truA_tRNA_pseudouridine_synthase_A	625.60812	299.79831	0.47921	1.1600E-04	6.9752E-04
Chromosome	BB_0013_-_hypothetical_protein	406.49089	155.23899	0.38190	5.5400E-06	5.3500E-05
Chromosome	BB_0014_priA_primosomal_protein_N	723.03223	294.68038	0.40756	6.6500E-07	8.5900E-06
Chromosome	BB_0040_cheR_chemotaxis_protein_methyltransferase	125.79145	51.41407	0.40872	2.3285E-03	8.6106E-03
Chromosome	BB_0077_-_hypothetical_protein	561.48651	259.26760	0.46175	2.6900E-05	2.0129E-04
Chromosome	BB_0196_prfA_peptide_chain_release_factor_1	717.68996	325.95274	0.45417	5.5400E-05	3.6993E-04
Chromosome	BB_0199_-_hypothetical_protein	871.84979	313.57160	0.35966	2.5600E-08	4.7800E-07
Chromosome	BB_0208_-_hypothetical_protein	622.47938	242.64847	0.38981	3.1200E-07	4.3600E-06
Chromosome	BB_0211_-_DNA_mismatch_repair_protein	1858.15944	909.06258	0.48923	6.5400E-06	6.0300E-05
Chromosome	BB_0218_pstB_phosphate_ABC_transporter_ATP-binding_protein	585.13237	240.94437	0.41178	1.9200E-05	1.4941E-04
Chromosome	BB_0237_lnt_apolipoprotein_N-acyltransferase	491.11309	228.08342	0.46442	4.2133E-04	2.0987E-03
Chromosome	BB_0251_leuS_leucine--tRNA_ligase	5802.43846	2344.75863	0.40410	3.3700E-08	6.0500E-07
Chromosome	BB_0252_-_hypothetical_protein	2401.84986	742.90570	0.30931	1.7100E-11	6.2300E-10
Chromosome	BB_0255_-_M23_peptidase_domain-containing_protein	815.06549	382.52021	0.46931	7.8000E-06	6.9700E-05
Chromosome	BB_0317_-_integral_membrane_protein	1815.65389	836.57266	0.46076	1.5900E-06	1.8300E-05
Chromosome	BB_0363_-_hypothetical_protein	1609.28100	548.46694	0.34081	1.4800E-09	4.0800E-08
Chromosome	BB_0375_pfs_nucleosidase	1772.01181	821.36958	0.46352	1.8600E-06	2.1000E-05
Chromosome	BB_0376_metK_S-adenosylmethionine_synthetase	2811.93420	1091.18557	0.38806	1.1300E-07	1.7400E-06
Chromosome	BB_0399_-_hypothetical_protein	71.32611	28.95200	0.40591	9.7023E-03	2.8540E-02
Chromosome	BB_0404_-_hypothetical_protein	131.72712	54.01437	0.41005	9.6688E-03	2.8512E-02
Chromosome	BB_0406_-_hypothetical_protein	421.82995	200.49637	0.47530	5.1824E-04	2.4973E-03
Chromosome	BB_0409_-_hypothetical_protein	207.57895	96.18330	0.46336	1.1848E-03	4.9655E-03
Chromosome	BB_0437_dnaA_chromosomal_replication_initiation_protein	1373.78280	523.57494	0.38112	7.2300E-08	1.1500E-06
Chromosome	BB_0450_rpoN_RNA_polymerase_sigma-54_factor	1145.83220	276.95471	0.24171	1.9600E-13	9.0400E-12
Chromosome	BB_0507_-_hypothetical_protein	804.03291	322.03239	0.40052	5.7700E-06	5.4900E-05
Chromosome	BB_0547_coaE_dephospho-CoA_kinase	378.51301	167.43961	0.44236	5.1520E-04	2.4913E-03
Chromosome	BB_0548_polA_DNA_polymerase_I	3157.34653	1120.83088	0.35499	1.1300E-09	3.1800E-08
Chromosome	BB_0554_-_hypothetical_protein	2883.92539	1345.07556	0.46640	1.5300E-05	1.2340E-04
Chromosome	BB_0555_-_hypothetical_protein	791.74640	292.90027	0.36994	2.0200E-06	2.2300E-05
Chromosome	BB_0586_-_FemA_protein	792.61480	251.61185	0.31745	4.8500E-09	1.1800E-07
Chromosome	BB_0603_p66_integral_outer_membrane_protein_p66	7477.75660	3576.49441	0.47828	4.2900E-06	4.2700E-05
Chromosome	BB_0620_-_beta-glucosidase	324.31878	131.55377	0.40563	3.9600E-05	2.7680E-04
Chromosome	BB_0632_recD_exodeoxyribonuclease_V_subunit_alpha	373.48624	99.96354	0.26765	4.4200E-08	7.4600E-07
Chromosome	BB_0633_recB_exodeoxyribonuclease_V_subunit_beta	932.89827	323.50216	0.34677	1.6500E-08	3.2300E-07
Chromosome	BB_0639_-_spermidine/putrescine_ABC_transporter_substrate-binding_protein	1106.98110	309.87719	0.27993	1.1700E-10	3.8500E-09
Chromosome	BB_0640_-_spermidine/putrescine_ABC_transporter_permease	562.98794	154.44527	0.27433	1.7000E-09	4.5800E-08
Chromosome	BB_0641_-_spermidine/putrescine_transport_system_permease	934.56747	264.56098	0.28308	1.1600E-10	3.8500E-09

Chromosome	BB_0642_-_spermidine/putrescine_ABC_transporter_ATP-binding_protein	2194.65581	881.46085	0.40164	8.8500E-08	1.3900E-06
Chromosome	BB_0713_-_hypothetical_protein	3165.93427	1301.43863	0.41108	4.6600E-07	6.3800E-06
Chromosome	BB_0739_-_hypothetical_protein	936.79632	315.79479	0.33710	1.3200E-07	1.9800E-06
Chromosome	BB_0751_-_hypothetical_protein	683.51486	322.81327	0.47228	9.4400E-06	8.0600E-05
Chromosome	BB_0752_-_hypothetical_protein	2228.79764	792.16348	0.35542	4.4200E-10	1.3300E-08
Chromosome	BB_0753_-_hypothetical_protein	1744.07574	657.51209	0.37700	2.6300E-08	4.8400E-07
Chromosome	BB_0754_-_ABC_transporter_ATP-binding_protein	1427.96204	568.14917	0.39787	3.8800E-08	6.8700E-07
Chromosome	BB_0755_rnz_ribonuclease_Z	865.14974	420.87390	0.48648	2.0000E-05	1.5453E-04
Chromosome	BB_0764_-_sensory_transduction_histidine_kinase	485.66170	217.35069	0.44754	6.8600E-05	4.4542E-04
Chromosome	BB_0765_-_hypothetical_protein	403.90329	130.60350	0.32335	5.1000E-07	6.8500E-06
Chromosome	BB_0766_cvpA_colicin_V_production_protein	394.90518	181.60382	0.45987	2.8107E-04	1.4837E-03
Chromosome	BB_0769_-_tRNA_N6-adenosine_threonylcarbamoyltransferase	1190.91121	567.50638	0.47653	1.5300E-05	1.2340E-04
Chromosome	BB_0771a_-_hypothetical_protein	270.00690	129.40850	0.47928	2.3545E-03	8.6835E-03
Chromosome	BB_0773_-_hypothetical_protein	322.97503	94.00100	0.29105	1.4800E-07	2.1800E-06
Chromosome	BB_0782_nadD_nicotinate-nucleotide_adenylyltransferase	620.89236	274.14473	0.44153	1.3500E-05	1.1157E-04
Chromosome	BB_0834_-_ATP-dependent_Clp_protease_subunit_C	5166.90380	2467.97020	0.47765	4.0800E-06	4.1000E-05
Chromosome	BB_0835_-_phosphomannomutase	411.99700	164.89674	0.40024	8.3300E-06	7.2900E-05
Chromosome	BB_0838_-_hypothetical_protein	2676.73652	1189.67028	0.44445	2.5300E-06	2.7400E-05
lp54	BB_A10_-_hypothetical_protein	115.20935	56.97838	0.49456	9.1240E-03	2.7137E-02
lp54	BB_A11_-_hypothetical_protein	79.85892	37.67239	0.47174	1.0732E-02	3.0985E-02
lp54	BB_A13_-_hypothetical_protein	111.97512	45.39231	0.40538	2.6730E-03	9.5524E-03
lp54	BB_A20_-_PF-32_protein	973.18094	436.40522	0.44843	9.6900E-07	1.2200E-05
lp54	BB_A31_-_pbsx_family_phage_terminase	590.88121	265.67377	0.44962	5.2400E-05	3.5211E-04
lp54	BB_A32_-_hypothetical_protein	64.73942	27.81277	0.42961	1.1554E-02	3.3016E-02
lp54	BB_A41_-_hypothetical_protein	366.14853	142.24488	0.38849	1.2100E-05	1.0067E-04
lp54	BB_A46_-_hypothetical_protein	446.41579	219.88100	0.49255	1.1452E-04	6.9163E-04
lp54	BB_A64_-_P35_antigen	26.41418	6.92210	0.26206	1.6519E-02	4.4447E-02
cp26	BB_B06_-_chitibiose_transporter_protein_ChbB	137.21042	52.32826	0.38137	5.6765E-04	2.7165E-03
cp26	BB_B07_-_alpha3-beta1_integrin-binding_protein	533.88248	187.91672	0.35198	1.3400E-06	1.6300E-05
cp26	BB_B12_-_PF-32_protein	735.94124	321.50005	0.43686	4.0900E-06	4.1000E-05
cp26	BB_B13_-_plasmid_partition_protein	293.15407	116.73775	0.39821	3.1500E-05	2.2688E-04
lp28-1	BB_F25_-_hypothetical_protein	183.24629	77.11307	0.42082	2.0269E-04	1.1258E-03
cp32-8	BB_L08_-_hypothetical_protein	14.67914	2.80349	0.19098	5.1263E-03	1.7002E-02
cp32-8	BB_L21_-_hypothetical_protein	48.57141	17.94922	0.36954	7.7824E-03	2.3759E-02
cp32-8	BB_L24_blyB_holin_protein	94.71962	42.78236	0.45167	5.5227E-03	1.8029E-02
cp32-8	BB_L25_-_hypothetical_protein	134.20654	60.66260	0.45201	2.6842E-03	9.5676E-03
cp32-8	BB_L26_-_hypothetical_protein	262.15074	97.92359	0.37354	9.8600E-05	6.0904E-04
cp32-8	BB_L40_erpO_ErpB1_protein	6458.99004	2796.61255	0.43298	9.1500E-06	7.8700E-05
cp32-6	BB_M25_-_hypothetical_protein	97.15662	27.32484	0.28125	1.0210E-04	6.2756E-04
cp32-6	BB_M26_-_hypothetical_protein	191.11242	48.68464	0.25474	2.8300E-06	3.0100E-05
cp32-6	BB_M33_-_PF-49_protein	244.75884	106.61657	0.43560	2.9445E-04	1.5425E-03
cp32-6	BB_M34_bdrK_BdrK	368.20418	148.20456	0.40251	1.3600E-06	1.6300E-05
cp32-9	BB_N25_-_hypothetical_protein	71.33098	29.53064	0.41399	7.2777E-03	2.2618E-02
cp32-9	BB_N39_erpQ_protein_ErpQ	1863.00605	920.29945	0.49399	1.4365E-04	8.4180E-04
cp32-7	BB_O02_-_hypothetical_protein	34.07245	13.97117	0.41004	1.4961E-02	4.1134E-02

cp32-7	BB_O21_-_hypothetical_protein	38.03625	15.17437	0.39894	1.4999E-02	4.1158E-02
cp32-7	BB_O33_-_plasmid_partition_protein	287.78902	117.83565	0.40945	1.4318E-04	8.4180E-04
cp32-7	BB_O34_bdrM_protein_BdrM	313.77346	149.13921	0.47531	1.9612E-04	1.0981E-03
cp32-1	BB_P21_-_hypothetical_protein	46.56013	16.61645	0.35688	2.5186E-03	9.1183E-03
cp32-1	BB_P25_-_hypothetical_protein	95.28585	34.88293	0.36609	1.2487E-03	5.2015E-03
cp32-1	BB_P26_-_hypothetical_protein	237.12128	90.52797	0.38178	1.0256E-04	6.2761E-04
cp32-1	BB_P33_-_PF-49_protein	1040.44099	408.85645	0.39296	1.7700E-07	2.5500E-06
cp32-1	BB_P34_bdrA_protein_BdrA	1164.18747	542.00474	0.46556	7.8200E-06	6.9700E-05
cp32-1	BB_P39_erpB_protein_ErpB	6107.20153	2723.34364	0.44592	1.5800E-05	1.2540E-04
cp32-4	BB_R25_-_hypothetical_protein	94.59779	29.99717	0.31710	6.2595E-04	2.9246E-03
cp32-3	BB_R26_-_hypothetical_protein	144.79968	66.60394	0.45997	5.0913E-03	1.6926E-02
cp32-3	BB_S21_-_hypothetical_protein	38.14528	14.69844	0.38533	1.4420E-02	4.0369E-02
cp32-3	BB_S25_-_hypothetical_protein	94.84991	33.11997	0.34918	8.1493E-04	3.6952E-03
lp21	BB_U07_-_protein_BBC01	140.86599	45.65445	0.32410	6.5700E-05	4.2866E-04
lp21	BB_U08_-_SUA5_subfamily_protein	24.96945	5.60438	0.22445	4.9047E-03	1.6464E-02

B) Increased in abundance

Genetic Element	Gene ID	Early Expression	Stat Expression	Fold Change	P-Value	Adjusted P-Value
Chromosome	BB_0007_-_hypothetical_protein	1381.46976	3892.47953	2.81764	3.1600E-15	2.1900E-13
Chromosome	BB_0016_-_GlpE_protein	1962.61099	4064.61718	2.07103	1.1100E-07	1.7200E-06
Chromosome	BB_0026_-_bifunctional_methylenetetrahydrofolate_dehydrogenase/methenyltetrahydrofolate_cyclohydrolase	1377.07854	3067.06873	2.22723	1.5600E-10	5.0000E-09
Chromosome	BB_0061_trx_thioredoxin	2008.18083	5336.51539	2.65739	4.9000E-13	2.1900E-11
Chromosome	BB_0083_-_hypothetical_protein	741.14672	2090.29269	2.82035	7.0400E-14	3.8900E-12
Chromosome	BB_0135_hisS_histidine--tRNA_ligase	2064.72124	4490.32409	2.17478	7.9900E-09	1.7500E-07
Chromosome	BB_0137_-_long-chain-fatty-acid_CoA_ligase	7632.80029	16615.00048	2.17679	1.2800E-08	2.6000E-07
Chromosome	BB_0138_-_hypothetical_protein	423.53765	1082.79183	2.55654	4.1300E-12	1.6300E-10
Chromosome	BB_0153_-_superoxide_dismutase	1511.59366	3402.07571	2.25065	5.1900E-09	1.2400E-07
Chromosome	BB_0166_malQ_4-alpha-glucanotransferase	229.39227	485.04807	2.11449	7.4000E-07	9.3800E-06
Chromosome	BB_0179_trmE_tRNA_modification_GTPase	2857.19576	8041.07702	2.81432	8.7200E-15	5.2400E-13
Chromosome	BB_0253_lon_ATP-dependent_protease_La	5516.55150	11797.16013	2.13850	1.3100E-08	2.6200E-07
Chromosome	BB_0269_-_ATP-binding_protein	5744.33527	14478.56719	2.52049	1.8500E-12	7.5300E-11
Chromosome	BB_0300_ftsA_cell_division_protein_FtsA	7237.88877	15937.18515	2.20191	6.0800E-09	1.4000E-07
Chromosome	BB_0331_-_hypothetical_protein	4.54742	18.30338	4.02500	1.6564E-03	6.6016E-03
Chromosome	BB_0386_rpsG_30S_ribosomal_protein_S7	7631.36854	19017.66197	2.49204	1.0400E-10	3.6000E-09
Chromosome	BB_0394_nusG_transcription_termination/antitermination_factor	6477.82807	13583.17028	2.09687	2.0200E-08	3.8800E-07
Chromosome	BB_0395_secE_protein_translocase_subunit_SecE	3199.82428	6400.93660	2.00040	7.2000E-08	1.1500E-06
Chromosome	BB_0488_rplN_50S_ribosomal_protein_L14	1247.84666	2563.43842	2.05429	4.3900E-08	7.4600E-07
Chromosome	BB_0495_rpsE_30S_ribosomal_protein_S5	1597.59368	4734.25824	2.96337	5.4100E-17	4.9900E-15
Chromosome	BB_0508_engA_GTPase_Der	5651.57997	11779.82218	2.08434	2.2400E-08	4.2400E-07
Chromosome	BB_0534_xth_exodeoxyribonuclease_III	552.89536	1174.57073	2.12440	4.4100E-08	7.4600E-07

Chromosome	BB_0536_-_zinc_protease	1227.42056	2456.03130	2.00097	6.5000E-07	8.4800E-06
Chromosome	BB_0578_-_methyl-accepting_chemotaxis_protein	2190.56338	4647.03461	2.12139	1.6600E-08	3.2300E-07
Chromosome	BB_0599_cysS_cysteine--tRNA_ligase	2135.90410	4959.49925	2.32197	5.4500E-10	1.6000E-08
Chromosome	BB_0621_-_4-methyl-5(b-hydroxyethyl)-thiazole_monophosphate_biosynthesis_protein	802.37582	2165.33960	2.69866	1.7700E-13	8.4400E-12
Chromosome	BB_0628_-_lipoprotein	2088.85745	5614.38058	2.68778	8.1900E-14	4.2000E-12
Chromosome	BB_0656_-_oxygen-independent_coproporphyrinogen_III_oxidase	600.55210	1361.98616	2.26789	3.0900E-09	7.9200E-08
Chromosome	BB_0698_trmD_tRNA_(guanine-N(1)-)-methyltransferase	3795.95530	11188.36815	2.94744	9.6700E-16	7.8700E-14
Chromosome	BB_0705_rnc_ribonuclease_III	3742.85235	7592.74748	2.02860	4.6400E-08	7.7300E-07
Chromosome	BB_0714_-_hypothetical_protein	2568.07292	5458.77495	2.12563	4.8100E-09	1.1800E-07
Chromosome	BB_0715_-_cell_division_protein_FtsA	5216.03512	11700.12540	2.24311	1.7200E-09	4.5800E-08
Chromosome	BB_0723_-_adenylyl_cyclase	36.85845	79.91207	2.16808	2.6209E-03	9.4149E-03
Chromosome	BB_0738_valS_valine--tRNA_ligase	4467.52613	11822.67135	2.64636	6.3500E-13	2.7400E-11
Chromosome	BB_0745_-_endonuclease_III	95.61633	263.42921	2.75506	4.7000E-09	1.1800E-07
Chromosome	BB_0749_-_hypothetical_protein	7742.32859	25299.29858	3.26766	1.5400E-19	2.1200E-17
Chromosome	BB_0760_-_protein_Gp37	291.22766	598.01648	2.05343	9.8400E-06	8.3500E-05
Chromosome	BB_0761_-_peptidoglycan-binding_protein	330.79366	770.80486	2.33017	1.8600E-09	4.8500E-08
Chromosome	BB_0804_rpsO_30S_ribosomal_protein_S15	1497.35030	3426.07706	2.28809	2.7200E-10	8.3500E-09
Chromosome	BB_0805_-_polyribonucleotide_nucleotidyltransferase	15942.12190	39010.65242	2.44702	3.3100E-11	1.1700E-09
Chromosome	BB_0816_-_hypothetical_protein	2894.45759	6358.50548	2.19679	7.4100E-09	1.6500E-07
Chromosome	BB_0824_-_hypothetical_protein	2919.25038	6057.87705	2.07515	1.3500E-07	2.0100E-06
lp54	BB_A24_dbpA_decorin-binding_protein_A	34.93355	84.50144	2.41892	4.4707E-04	2.2004E-03
lp54	BB_A25_dbpB_decorin-binding_protein_B	6.89777	31.30814	4.53888	3.0600E-05	2.2191E-04
lp54	BB_A36_-_lipoprotein	12.88527	36.93724	2.86663	4.1827E-04	2.0959E-03
lp54	BB_A43_-_hypothetical_protein	439.52643	1112.01975	2.53004	9.7800E-14	4.8300E-12
lp54	BB_A52_-_outer_membrane_protein	1295.37613	2897.55834	2.23685	7.8500E-10	2.2600E-08
lp54	BB_A54_-_hypothetical_protein	477.31298	954.64336	2.00004	1.0800E-06	1.3300E-05
lp54	BB_A57_-_P45-13	332.67601	698.66503	2.10014	6.4800E-08	1.0500E-06
lp17	BB_D10_-_lipoprotein	272.05032	739.97786	2.72000	8.4800E-12	3.2600E-10
lp17	BB_D21_-_hypothetical_protein	611.29346	2321.63739	3.79791	8.0200E-25	1.8500E-22
lp17	BB_D22_-_hypothetical_protein	146.99470	333.54339	2.26908	4.5100E-06	4.4600E-05
lp28-1	BB_F0034_-_hypothetical_protein	27.73222	57.76731	2.08304	7.9137E-03	2.4002E-02
lp28-1	BB_F06_-_hypothetical_protein	13.53798	63.25921	4.67272	1.6600E-07	2.4100E-06
lp28-1	BB_F17_-_putative_transmembrane_protein	17.69075	50.06402	2.82995	1.0180E-03	4.3762E-03
lp28-1	BB_F20_-_BBF20	77.05580	205.57919	2.66793	5.9800E-06	5.5800E-05
lp28-2	BB_G07_-_hypothetical_protein	416.25459	893.57216	2.14670	1.4500E-06	1.6900E-05
lp28-3	BB_H13_-_protein_RepU	540.60961	1702.16932	3.14861	1.0900E-15	8.3700E-14
lp28-3	BB_H25_-_hypothetical_protein	6.42698	17.48243	2.72016	2.5555E-03	9.2039E-03
lp28-3	BB_H26_-_hypothetical_protein	155.23930	527.97732	3.40105	4.5900E-15	3.0300E-13
lp28-3	BB_H28_-_PF-32_protein	110.03583	234.47743	2.13092	4.0947E-04	2.0668E-03
lp28-3	BB_H32_-_antigen_P35	111.14145	483.05343	4.34629	2.9400E-20	4.5200E-18
lp28-3	BB_H33_-_adenine_deaminase	32.94565	86.52038	2.62615	1.6818E-04	9.6112E-04
lp28-3	BB_H37_-_lipoprotein	750.52454	2173.11902	2.89547	4.2800E-16	3.7000E-14
lp28-3	BB_H40_-_transposase-like_protein	7.95332	53.29080	6.70045	6.0100E-09	1.4000E-07
lp28-4	BB_I19_-_hypothetical_protein	903.89487	5957.28429	6.59068	8.0200E-45	2.7700E-42
lp28-4	BB_I20_-_hypothetical_protein	222.99870	1523.06568	6.82993	1.2200E-45	5.6200E-43

lp28-4	BB_I21_-_PF-32_protein	380.95382	4168.23442	10.94157	1.7100E-72	1.1800E-69
lp28-4	BB_I22_-_PF-49_protein	222.11828	883.32536	3.97682	2.1900E-21	4.3300E-19
lp28-4	BB_I42_-_outer_membrane_protein	217.53874	442.80318	2.03551	4.5500E-07	6.2900E-06
lp38	BB_J11_-_hypothetical_protein	6.43141	23.32932	3.62741	9.4475E-04	4.1348E-03
lp38	BB_J46_-_hypothetical_protein	28.86918	60.42085	2.09292	2.2230E-03	8.3773E-03
lp38	BB_J47_-_hypothetical_protein	72.88274	183.65030	2.51981	9.2400E-05	5.7545E-04
lp38	BB_J48_-_hypothetical_protein	80.62931	403.35617	5.00260	5.2800E-21	9.1300E-19
lp36	BB_K07_-_lipoprotein	48.50724	118.73249	2.44773	3.7100E-06	3.8000E-05
lp36	BB_K13_-_hypothetical_protein	2291.81895	6905.16629	3.01296	1.1500E-15	8.3700E-14
lp36	BB_K24_-_PF-49_protein	153.98267	348.32647	2.26211	1.4500E-06	1.6900E-05
lp36	BB_K32_-_fibronectin-binding_protein	68.00955	193.15493	2.84011	5.5400E-07	7.3700E-06
lp36	BB_K34_-_hypothetical_protein	70.28427	141.55291	2.01401	2.1375E-03	8.1213E-03
lp36	BB_K35_-_hypothetical_protein	136.74791	447.24776	3.27060	7.9900E-14	4.2000E-12
lp36	BB_K40_-_hypothetical_protein	1747.02318	3720.91095	2.12986	1.0900E-08	2.3500E-07
lp36	BB_K45_-_immunogenic_protein_P37	3440.66137	9172.16224	2.66581	1.5100E-12	6.3200E-11
lp36	BB_K49_-_hypothetical_protein	710.38768	1428.96830	2.01153	1.2700E-07	1.9400E-06
lp36	BB_K54_-_hypothetical_protein	17.33747	58.54895	3.37702	4.7400E-05	3.2148E-04
lp36	BB_L27_bdrP_protein_BdrP	505.53991	1035.08303	2.04748	4.0500E-08	7.0900E-07
cp32-8	BB_L30_-_hypothetical_protein	1070.05088	2578.75476	2.40994	1.2700E-11	4.7300E-10
cp32-6	BB_M35_bppA_BppA	20.68947	55.37801	2.67663	1.9263E-04	1.0830E-03
cp32-6	BB_M36_bppB_BppB	5.56634	17.32319	3.11213	5.2847E-03	1.7360E-02
cp32-6	BB_M41_-_hypothetical_protein	20.71621	57.66656	2.78364	4.7400E-05	3.2148E-04
cp32-9	BB_N03_-_hypothetical_protein	14.23059	28.89235	2.03030	1.0977E-02	3.1628E-02
cp32-9	BB_N27_bdrR_BdrR_protein	246.86230	596.04810	2.41450	1.1200E-08	2.3800E-07
cp32-9	BB_N28_mlpI_lipoprotein	170.03849	403.07595	2.37050	6.7100E-09	1.5200E-07
cp32-9	BB_N30_-_hypothetical_protein	709.22242	2301.03966	3.24445	5.5800E-19	6.4400E-17
cp32-9	BB_N31_-_hypothetical_protein	133.97155	294.35934	2.19718	8.8500E-05	5.5622E-04
cp32-9	BB_N36_bppB_protein_BppB	7.95341	21.45583	2.69769	1.0862E-03	4.6078E-03
cp32-9	BB_N42_-_hypothetical_protein	7.79016	34.26490	4.39848	7.8600E-06	6.9700E-05
cp32-7	BB_O30_-_hypothetical_protein	765.29336	1564.16760	2.04388	3.3400E-08	6.0500E-07
cp32-7	BB_O36_bppA_protein_BppA	15.49878	48.36667	3.12068	1.6431E-04	9.4289E-04
cp32-1	BB_P29_-_hypothetical_protein	18.14399	37.75820	2.08103	5.1460E-03	1.7026E-02
cp32-1	BB_P35_bppA_protein_BppA	21.08284	43.82085	2.07851	1.1526E-02	3.3004E-02
lp56	BB_Q03_-_outer_membrane_protein	47.78358	114.04540	2.38671	6.7989E-04	3.1553E-03
lp56	BB_Q05_-_antigen,_P35	16.94388	39.07172	2.30595	8.0483E-03	2.4303E-02
lp56	BB_Q06_-_membrane_protein	661.17979	1333.83297	2.01735	2.1300E-06	2.3200E-05
lp56	BB_Q07_-_plasmid_partition_protein	100.54913	449.64366	4.47188	3.9900E-19	5.0200E-17
lp56	BB_Q22_-_hypothetical_protein	13.10315	39.07406	2.98204	3.2044E-03	1.1135E-02
lp56	BB_Q34_bdrW_protein_BdrW_protein	288.84376	911.49132	3.15566	5.5000E-15	3.4600E-13
lp56	BB_Q37_-_hypothetical_protein	13.89577	42.82579	3.08193	2.9993E-04	1.5653E-03
lp56	BB_Q38_-_hypothetical_protein	1248.46277	5800.00611	4.64572	9.0700E-32	2.5100E-29
lp56	BB_Q39_-_hypothetical_protein	183.88882	702.51359	3.82032	7.4400E-19	7.9200E-17
lp56	BB_Q40_-_PF-32_protein	492.53750	1117.06114	2.26797	5.5000E-08	9.0500E-07
lp56	BB_Q43_bppA_protein_BppA	10.20867	39.99468	3.91772	1.3400E-04	7.9882E-04
lp56	BB_Q45_bppC_protein_BppC	1.15948	10.99358	9.48150	1.0567E-04	6.4378E-04
lp56	BB_Q54_-_hypothetical_protein	4.66050	18.94375	4.06474	1.5590E-03	6.2677E-03

cp32-4	BB_R27_bdrH_BdrH	180.60636	463.01786	2.56369	1.2300E-08	2.5300E-07
cp32-4	BB_R31_-_hypothetical_protein	646.72266	1811.64243	2.80127	1.4000E-14	8.0500E-13
cp32-4	BB_R32_-_hypothetical_protein	195.31099	714.08627	3.65615	1.2400E-18	1.2300E-16
cp32-4	BB_R33_-_plasmid_partition_protein,_putative	224.08252	472.30089	2.10771	4.9800E-06	4.8600E-05
cp32-4	BB_R36_bppA_BppA	14.47084	43.04487	2.97459	2.0997E-03	8.0218E-03
cp32-4	BB_R44_-_hypothetical_protein	30.57151	133.75231	4.37506	1.5900E-10	5.0000E-09
cp32-4	BB_R45_-_phage_terminase_large_subunit	21.03824	52.22975	2.48261	9.4196E-04	4.1348E-03
cp32-3	BB_S31_-_hypothetical_protein	12.49136	34.58624	2.76881	4.9315E-03	1.6514E-02
cp32-3	BB_S33_-_hypothetical_protein	1198.02898	2602.04408	2.17194	1.1500E-08	2.4000E-07
cp32-3	BB_S34_-_hypothetical_protein	195.50969	404.33451	2.06810	4.7100E-05	3.2148E-04
cp32-3	BB_S38_bppA_protein_BppA	13.51524	36.66507	2.71287	5.5863E-04	2.6826E-03
cp32-3	BB_S44_-_hypothetical_protein	46.26957	93.94267	2.03033	2.2390E-03	8.4146E-03
lp5	BB_T04_-_hypothetical_protein	17.80917	58.02374	3.25808	4.6000E-05	3.1627E-04
lp21	BB_U05_-_PF-32_protein	144.17353	327.57493	2.27209	1.8700E-06	2.1000E-05
lp28-2	frameshift_BB_G03_BB_G03	30.61363	67.35336	2.20011	6.3023E-03	2.0242E-02
Chromosome	Rfam_ncRNA1_NC_001318_SRP_bact_Rfam_annotation	3242.23709	37127.73015	11.45127	3.9000E-73	5.4000E-70

Those in (A) lower and (B) higher abundance in early-exponential compared to stationary phase. Genes are listed which were identified by DEseq [9] as differentially expressed by meeting the criteria of >2X greater abundance and an adjusted P-value of <.05. In order from left to right columns list genetic element on which a given gene resides, the gene ID, the early-log expression, stationary expression, fold change, P-value, adjusted P-value.

Table 8-4 Identified Intrinsic Terminators

Genetic Element	Start Location	Strand	Length	Program Predicted	Score	Relative Location
Chromosome	18193	-	40	T	|T90	5'
Chromosome	60406	-	36	R	|R-10.80	5'
Chromosome	80830	+	34	T	|T100	3'
Chromosome	82961	+	22	T	|T90	3'
Chromosome	82961	-	22	T	|T93	3'
Chromosome	101510	-	28	B	|T100|R-10.20	3'
Chromosome	147616	-	31	T	|T100	3'
Chromosome	174407	-	19	T	|T91	Internal
Chromosome	250131	+	24	B	|T93|R-9.40	3'
Chromosome	318984	-	25	T	|T100	5'
Chromosome	329204	+	27	B	|T100|R-9.50	Intergenic
Chromosome	346385	+	20	T	|T90	3'
Chromosome	373548	-	31	T	|T100	3'
Chromosome	374673	+	33	X	|F-14.1|F-14.1|R-12.30	Internal
Chromosome	375954	+	19	T	|T91	3'
Chromosome	375958	-	27	T	|T100	3'
Chromosome	395347	-	28	T	|T89	Intergenic
Chromosome	396600	-	24	T	|T100	3'
Chromosome	401007	+	31	R	|R-9.20	Intergenic
Chromosome	418385	-	29	T	|T100	3'
Chromosome	438133	-	22	T	|T90	5'
Chromosome	441378	-	22	T	|T90	5'
Chromosome	442676	-	39	T	|T95	3'
Chromosome	443427	-	30	T	|T95	Intergenic
Chromosome	443570	-	38	T	|T100	Intergenic
Chromosome	450538	-	39	R	|R-10.30	Internal AS
Chromosome	450929	+	30	T	|T95	3'
Chromosome	452017	-	27	T	|T100	3'
Chromosome	465177	+	22	T	|T90	3'
Chromosome	467880	+	35	R	|R-10.30	Internal AS
Chromosome	474740	+	38	R	|R-9.50	5'
Chromosome	492515	+	45	T	|T95	5'
Chromosome	526296	+	44	T	|T93	5'
Chromosome	526427	+	34	R	|R-11.40	5'
Chromosome	547443	+	42	T	|T100	3'
Chromosome	552277	+	37	R	|R-9.10	Intergenic
Chromosome	552301	+	32	T	|T100	Intergenic
Chromosome	571876	-	26	B	|T100|R-11.00	3'
Chromosome	571876	+	26	T	|T95	3'
Chromosome	571889	+	52	T	|T100	3'
Chromosome	614014	+	35	T	|T100	3'
Chromosome	614014	-	35	T	|T100	3'
Chromosome	627083	+	23	B	|T100|R-10.80	3'
Chromosome	627085	-	26	Z	|F-13.2|T100|R-11.60|T100|R-11.60|F-13.2	3'

Chromosome	636072	+	31	T	|T100	Intergenic
Chromosome	642464	-	23	T	|T95	3'
Chromosome	642464	+	23	T	|T100	3'
Chromosome	656159	+	34	T	|T100	Internal
Chromosome	659662	+	37	T	|T100	3'
Chromosome	662592	+	31	T	|T100	3'
Chromosome	676381	+	32	T	|T93	3'
Chromosome	677871	+	37	T	|T100	3'
Chromosome	677871	-	37	T	|T100	3'
Chromosome	685007	+	40	T	|T100	3'
Chromosome	690167	+	37	T	|T100	5'
Chromosome	698379	+	27	T	|T100	3'
Chromosome	699222	+	29	F	|F-13.5	Internal AS
Chromosome	717948	+	33	R	|R-9.40	Internal AS
Chromosome	726570	+	16	T	|T91	5'
Chromosome	726722	+	26	T	|T100	Internal
Chromosome	745262	+	44	T	|T91	5'
Chromosome	789031	+	27	T	|T100	3'
Chromosome	829116	+	29	T	|T95	3'
Chromosome	855659	+	30	T	|T100	Internal
Chromosome	856869	+	40	T	|T100	Internal
Chromosome	868783	-	33	R	|R-10.90	3'
Chromosome	897051	-	45	T	|T100	5'
cp26	2425	-	25	T	|T100	3'
cp26	10071	+	44	T	|T100	3'
cp26	10078	+	58	T	|T100	3'
cp26	10808	+	23	T	|T93	Intergenic
cp26	13689	+	28	T	|T95	Intergenic
cp26	13693	-	36	T	|T100	Intergenic
cp26	17625	+	35	T	|T95	3'
cp32-1	11976	-	37	R	|R-10.40	3'
cp32-1	16546	-	41	T	|T91	3'
cp32-1	16546	+	41	T	|T89	5'
cp32-1	17704	-	22	T	|T100	3'
cp32-1	17704	+	22	B	|T100|R-9.10	3' Antisense
cp32-1	23141	+	47	T	|T100	5'
cp32-1	27996	+	36	T	|T100	Intergenic
cp32-3	11976	-	37	R	|R-10.40	5' Antisense
cp32-3	18276	+	22	B	|T91|R-9.60	3'
cp32-3	23322	+	47	T	|T93	Intergenic
cp32-3	23600	+	57	T	|T89	5'
cp32-3	28045	+	32	T	|T100	Intergenic
cp32-4	11920	-	37	R	|R-10.40	5' Antisense
cp32-4	22452	+	47	T	|T90	3'
cp32-4	22747	+	59	T	|T95	5'
cp32-6	11986	-	37	R	|R-10.40	5' Antisense
cp32-6	16561	-	41	T	|T100	3'
cp32-6	17722	+	22	B	|T95|R-9.60	3'
cp32-6	23154	+	53	T	|T93	5'
cp32-6	27051	+	33	R	|R-10.10	3' Antisense

cp32-6	27076	-	36	B	|T100|T100|T100|R-9.70	3'
cp32-6	27076	+	36	T	|T100	3'
cp32-7	17691	+	22	T	|T100	3'
cp32-7	21524	-	35	R	|R-11.10	3' Antisense
cp32-8	11976	-	37	R	|R-10.40	5' Antisense
cp32-8	17677	+	22	B	|T95|R-9.60	3'
cp32-8	22703	+	34	T	|T93	3'
cp32-8	22973	+	43	T	|T100	Intergenic
cp32-8	23120	+	47	T	|T100	Intergenic
cp32-8	28131	+	36	T	|T100	3'
cp32-9	12065	-	37	R	|R-10.40	5' Antisense
cp32-9	18918	+	47	T	|T93	Intergenic
cp32-9	22815	+	47	T	|T95	3'
cp32-9	27906	+	37	T	|T100	3'
lp17	1820	+	30	T	|T93	3'
lp17	1828	+	46	T	|T88	3'
lp17	2893	+	46	T	|T89	5'
lp17	4289	-	23	T	|T89	Intergenic
lp17	15920	+	60	T	|T100	Internal AS
lp21	1296	-	50	T	|T100	Intergenic
lp21	16221	+	26	T	|T91	3' Antisense
lp21	16230	+	44	T	|T100	3' Antisense
lp21	16231	-	46	T	|T100	3'
lp25	2308	+	28	R	|R-9.20	Internal
lp25	4262	-	29	T	|T100	3' Antisense
lp25	8042	-	42	T	|T100	Intergenic
lp25	14992	-	22	T	|T90	3'
lp25	18583	+	36	T	|T100	Intergenic
lp25	21876	+	41	B	|T95|T100|R-10.30	3' Antisense
lp25	21912	-	29	T	|T100	3'
lp25	21912	+	29	T	|T100	3' Antisense
lp28-1	5051	+	50	T	|T95	3'
lp28-1	5863	-	17	T	|T100	3'
lp28-1	12235	-	60	T	|T100	3'
lp28-2	2127	-	36	T	|T88	5' Antisense
lp28-2	2130	+	42	T	|T93	5'
lp28-2	6713	+	20	T	|T100	3'
lp28-2	7374	-	29	T	|T100	3'
lp28-2	7374	+	29	T	|T90	3'
lp28-2	27059	+	33	R	|R-9.90	3'
lp28-3	7820	-	49	T	|T100	5'
lp28-3	8250	-	26	T	|T100	Internal AS
lp28-3	9507	-	26	R	|R-9.50	Intergenic
lp28-3	11471	-	34	F	|F-14.2	Intergenic
lp28-3	19697	+	36	T	|T100	Intergenic
lp28-3	24459	-	37	T	|T100	Intergenic
lp28-3	25391	-	28	B	|T100|T95|R-10.30	3'
lp28-4	1414	-	51	T	|T100	Intergenic
lp28-4	1573	+	35	T	|T100	5'
lp28-4	1573	-	35	T	|T88	5' Antisense

lp28-4	1579	+	47	T	|T100	5'
lp28-4	3361	+	34	T	|T100	3'
lp28-4	3361	-	34	T	|T100	3' Antisense
lp28-4	6892	-	37	R	|R-10.60	3' Antisense
lp28-4	7122	+	48	T	|T100	5'
lp28-4	10568	-	55	T	|T100	3'
lp28-4	13241	+	21	T	|T88	3'
lp28-4	16687	+	39	T	|T100	3'
lp28-4	20741	+	32	T	|T100	3' Antisense
lp28-4	24085	-	39	T	|T100	3'
lp28-4	24180	-	23	T	|T93	5'
lp36	11104	+	34	F	|F-13.1	Internal
lp36	13271	+	30	R	|R-11.40	3' Antisense
lp36	13288	-	30	R	|R-12.20	3'
lp36	17353	+	26	T	|T100	5'
lp36	17815	+	57	T	|T100	5'
lp36	23749	-	31	T	|T91	5'
lp36	24698	+	24	T	|T93	3'
lp36	24785	+	26	T	|T90	3'
lp36	25791	-	50	T	|T91	3'
lp36	34370	+	26	T	|T91	3' Antisense
lp54	1167	+	47	T	|T100	3'
lp54	1943	+	35	R	|R-9.20	3'
lp54	1973	+	44	T	|T100	3'
lp54	9211	+	21	T	|T100	3'
lp54	11238	+	31	T	|T95	3'
lp54	14964	+	57	T	|T100	3'
lp54	15880	+	35	R	|R-9.40	3'
lp54	15897	-	38	R	|R-9.60	3'
lp54	15902	+	29	T	|T100	3'
lp54	21595	+	27	T	|T100	3'
lp54	21605	-	47	T	|T100	3'
lp54	21606	+	49	T	|T100	3'
lp54	24397	+	29	T	|T100	3'
lp54	25094	-	34	R	|R-10.20	3'
lp54	25094	+	27	B	|T89|R-10.90	3' Antisense
lp54	42536	-	34	X	|F-15.2|R-9.70	3'
lp54	43598	-	21	T	|T100	3'
lp54	44590	-	24	T	|T89	3'
lp54	46365	-	23	T	|T91	3'
lp54	48375	-	23	T	|T100	5'
lp54	49326	-	23	T	|T91	Intergenic
lp56	658	+	41	T	|T100	Intergenic
lp56	15466	-	37	R	|R-10.40	5'
lp56	21521	+	22	B	|T95|R-9.10	3'
lp56	25293	-	31	R	|R-9.70	3' Antisense
lp56	25294	+	25	T	|T91	3'
lp56	26565	+	47	T	|T100	Intergenic
lp56	31052	+	37	T	|T100	3'
lp56	37706	+	29	T	|T100	3'

lp56	37706	-	29	T	|T100	3' Antisense
lp56	44259	-	31	T	|T100	Internal
lp56	45722	+	33	T	|T100	3' Antisense
lp56	45748	+	33	T	|T100	3' Antisense
lp56	47723	+	37	R	|R-10.40	3' Antisense
lp56	47747	+	31	T	|T100	3' Antisense
lp56	51144	-	30	T	|T100	3'

The full list of predicted intrinsic terminators predicted by the SIPHT pipeline [190]. Included is are the genetic element, start location, strand, length, program predicted (T: TransTerm, R: RNAMotif, F: FindTerm, B: RNAMotif and TransTerm, X: RNAMotif and FindTerm, Z: RNAMotif, FindTerm, and TransTerm), score as described in materials and methods, and relative location compared to nearby genes.

Table 8-5 Putative non-coding RNAs

Genetic Element	Start	End	Strand	Relative Location	Length	Flanking Genes
Chromosome	3138	3343	-	PI	205	(BB_0003,BB_0003/BB_0004)
Chromosome	4958	5220	-	AI	262	(BB_0004,BB_0004/BB_0005)
Chromosome	10770	11082	-	A	312	(BB_0011)
Chromosome	12221	12447	-	A	226	(BB_0013)
Chromosome	13593	13767	-	A	174	(BB_0014)
Chromosome	45459	45739	-	A	280	(BB_0046)
Chromosome	46621	46688	-	I	67	(BB_t25/BB_0050)
Chromosome	46721	47049	-	I	328	(BB_t25/BB_0050)
Chromosome	65600	65790	-	AIA	190	(BB_0070,BB_0070/BB_0071,BB_0071)
Chromosome	68049	68243	-	A	194	(BB_0072)
Chromosome	73802	74090	-	A	288	(BB_0077)
Chromosome	80390	80539	-	A	149	(BB_0084)
Chromosome	151461	151753	-	A	292	(BB_0151)
Chromosome	170239	170515	-	A	276	(BB_0167)
Chromosome	182989	183252	-	A	263	(BB_0180)
Chromosome	184976	185175	-	A	199	(BB_0181)
Chromosome	185214	185535	-	AA	321	(BB_0181,BB_0182)
Chromosome	188516	188703	-	I	187	(BB_0187/BB_0188)
Chromosome	194536	194807	-	A	271	(BB_0196)
Chromosome	196949	197248	-	A	299	(BB_0198)
Chromosome	197645	197876	-	AA	231	(BB_0198,BB_0199)
Chromosome	204521	204670	-	A	149	(BB_0203)
Chromosome	204756	205105	-	AI	349	(BB_0203,BB_0203/BB_0204)
Chromosome	207622	207750	-	A	128	(BB_0205)
Chromosome	209719	209942	-	A	223	(BB_0208)
Chromosome	214966	215257	-	A	291	(BB_0210)
Chromosome	216412	216605	-	A	193	(BB_0211)
Chromosome	221798	222147	-	A	349	(BB_0217)
Chromosome	233386	233669	-	A	283	(BB_0228)
Chromosome	245893	246071	-	A	178	(BB_0240)
Chromosome	253173	253408	-	A	235	(BB_0248)
Chromosome	255770	255850	-	A	80	(BB_0250)
Chromosome	255889	256097	-	A	208	(BB_0250)
Chromosome	256196	256297	-	AI	101	(BB_0250,BB_0250/BB_0251)
Chromosome	340422	340650	-	A	228	(BB_0332)
Chromosome	343370	343557	-	A	187	(BB_0335)
Chromosome	355816	356079	-	A	263	(BB_0347)

Chromosome	356096	356234	-	A	138	(BB_0347)
Chromosome	369356	369471	-	A	115	(BB_0361)
Chromosome	369531	369724	-	A	193	(BB_0361)
Chromosome	384357	384598	-	A	241	(BB_0374)
Chromosome	416715	416960	-	A	245	(BB_0404)
Chromosome	422883	423198	-	pA	315	(BB_0411,BB_0412)
Chromosome	457756	458089	-	AI	333	(BB_0437,BB_0437/BB_0438)
Chromosome	458090	458187	-	I	97	(BB_0437/BB_0438)
Chromosome	483157	483283	-	A	126	(BB_0461)
Chromosome	486699	486997	-	AA	298	(BB_0465,BB_0466)
Chromosome	505982	506228	-	A	246	(BB_0498)
Chromosome	507282	507483	-	AIA	201	(BB_0500,BB_0500/BB_0501,BB_0501)
Chromosome	514725	514976	-	A	251	(BB_0509)
Chromosome	532104	532282	-	p	178	(BB_0522)
Chromosome	568895	569212	-	AI	317	(BB_0556,BB_0556/BB_0557)
Chromosome	596657	596815	-	A	158	(BB_0581)
Chromosome	600533	600717	-	A	184	(BB_0583)
Chromosome	607274	607419	-	A	145	(BB_0588)
Chromosome	607443	607706	-	A	263	(BB_0588)
Chromosome	631847	631985	-	A	138	(BB_0605)
Chromosome	633675	633894	-	A	219	(BB_0607)
Chromosome	634228	634508	-	AI	280	(BB_0607,BB_0607/BB_0608)
Chromosome	638554	638848	-	AIA	294	(BB_0611,BB_0611/BB_0612,BB_0612)
Chromosome	639730	640018	-	AA	288	(BB_0612,BB_0613)
Chromosome	640045	640384	-	A	339	(BB_0613)
Chromosome	642343	642433	-	A	90	(BB_0614)
Chromosome	644836	644890	-	A	54	(BB_0617)
Chromosome	662384	662550	-	AI	166	(BB_0630,BB_0630/BB_0631)
Chromosome	688561	688679	-	A	118	(BB_0649)
Chromosome	688729	688888	-	A	159	(BB_0649)
Chromosome	690193	690481	-	A	288	(BB_0650)
Chromosome	696333	696589	-	A	256	(BB_0656)
Chromosome	702007	702116	-	A	109	(BB_0663)
Chromosome	719746	719903	-	A	157	(BB_0680)
Chromosome	730109	730199	-	A	90	(BB_0688)
Chromosome	737294	737634	-	A	340	(BB_0697)
Chromosome	745726	745823	-	A	97	(BB_0709)
Chromosome	751060	751257	-	IA	197	(BB_0713/BB_0714,BB_0714)
Chromosome	758380	758598	-	A	218	(BB_0720)
Chromosome	819269	819400	-	A	131	(BB_0780)
Chromosome	831811	831882	-	A	71	(BB_0794)
Chromosome	831883	832089	-	A	206	(BB_0794)

Chromosome	836043	836345	-	AIA	302	(BB_0794,BB_0794/BB_0795,BB_0795)
Chromosome	839756	840096	-	A	340	(BB_0797)
Chromosome	841129	841360	-	A	231	(BB_0797)
Chromosome	844393	844581	-	AA	188	(BB_0800,BB_0801)
Chromosome	855692	855935	-	A	243	(BB_0809)
cp26	7474	7782	-	AI	308	(BB_B09,BB_B09/BB_B10)
cp32-1	49	327	-	IA	278	(ORIG/BB_P01,BB_P01)
cp32-1	1250	1340	-	AIA	90	(BB_P01,BB_P01/BB_P02,BB_P02)
cp32-1	1341	1590	-	A	249	(BB_P02)
cp32-1	11284	11597	-	A	313	(BB_P17)
cp32-1	13522	13823	-	AIA	301	(BB_P20,BB_P20/BB_P21,BB_P21)
cp32-1	14010	14287	-	A	277	(BB_P21)
cp32-1	18857	18932	-	I	75	(BB_P29/BB_P30)
cp32-1	19138	19264	-	A	126	(BB_P30)
cp32-1	21537	21716	-	IA	179	(BB_P32/BB_P33,BB_P33)
cp32-1	24537	24688	-	AIA	151	(BB_P35,BB_P35/BB_P36,BB_P36)
cp32-3	7415	7729	-	A	314	(BB_S11)
cp32-3	19351	19491	-	I	140	(BB_S31/BB_S33)
cp32-3	19564	19879	-	IA	315	(BB_S31/BB_S33,BB_S33)
cp32-3	24999	25148	-	AIA	149	(BB_S38,BB_S38/BB_S39,BB_S39)
cp32-5	30	266	-	IA	236	(ORIG/BB_R01,BB_R01)
cp32-5	1275	1590	-	AIp	315	(BB_R01,BB_R01/BB_R02,BB_R02)
cp32-5	3569	3690	-	A	121	(BB_R05)
cp32-5	11273	11539	-	A	266	(BB_R17)
cp32-5	13475	13776	-	AIA	301	(BB_R20,BB_R20/BB_R21,BB_R21)
cp32-5	13989	14240	-	A	251	(BB_R21)
cp32-5	18707	18773	-	I	66	(BB_R29/BB_R31)
cp32-5	22102	22331	-	p	229	(BB_R35)
cp32-5	24136	24289	-	AIA	153	(BB_R36,BB_R36/BB_R37,BB_R37)
cp32-5	25969	26191	-	IA	222	(BB_R38/BB_R41,BB_R41)
cp32-5	27950	28167	-	A	217	(BB_R43)
cp32-5	28990	29272	-	A	282	(BB_R45)
cp32-6	41	266	-	IA	225	(ORIG/BB_M01,BB_M01)
cp32-6	1221	1283	-	A	62	(BB_M01)
cp32-6	1284	1587	-	AIA	303	(BB_M01,BB_M01/BB_M02,BB_M02)
cp32-6	6854	7140	-	A	286	(BB_M11)
cp32-6	15927	16126	-	AA	199	(BB_M25,BB_M26)
cp32-6	18799	18884	-	I	85	(BB_M29/BB_M30)
cp32-6	19051	19341	-	IA	290	(BB_M29/BB_M30,BB_M30)
cp32-6	24567	24698	-	IA	131	(BB_M35/BB_M36,BB_M36)
cp32-7	34	265	-	IA	231	(ORIG/BB_O01,BB_O01)
cp32-7	1247	1586	-	AIA	339	(BB_O01,BB_O01/BB_O02,BB_O02)

cp32-7	10840	11094	-	AA	254	(BB_O16,BB_O17)
cp32-7	12523	12723	-	A	200	(BB_O19)
cp32-7	16855	17185	-	AI	330	(BB_O27,BB_O27/BB_O28)
cp32-7	18851	18934	-	I	83	(BB_O29/BB_O30)
cp32-7	21498	21704	-	AIA	206	(BB_O32,BB_O32/BB_O33,BB_O33)
cp32-7	23214	23460	-	A	246	(BB_O36)
cp32-7	23461	23718	-	A	257	(BB_O36)
cp32-7	24440	24664	-	AIA	224	(BB_O36,BB_O36/BB_O37,BB_O37)
cp32-7	26199	26459	-	A	260	(BB_O39)
cp32-7	29877	30102	-	A	225	(BB_O44)
cp32-8	34	266	-	IA	232	(ORIG/BB_L01,BB_L01)
cp32-8	822	1071	-	A	249	(BB_L01)
cp32-8	1275	1595	-	AIA	320	(BB_L01,BB_L01/BB_L02,BB_L02)
cp32-8	7106	7351	-	A	245	(BB_L11)
cp32-8	7384	7729	-	A	345	(BB_L11)
cp32-8	8850	9091	-	AIA	241	(BB_L14,BB_L14/BB_L15,BB_L15)
cp32-8	13521	13805	-	AIA	284	(BB_L20,BB_L20/BB_L21,BB_L21)
cp32-8	18832	18915	-	I	83	(BB_L29/BB_L30)
cp32-8	18916	19180	-	IA	264	(BB_L29/BB_L30,BB_L30)
cp32-8	19437	19601	-	A	164	(BB_L30)
cp32-8	22038	22356	-	pIA	318	(BB_L34,BB_L34/BB_L35,BB_L35)
cp32-8	22390	22605	-	A	215	(BB_L35)
cp32-8	22607	22659	-	A	52	(BB_L35)
cp32-8	23515	23714	-	A	199	(BB_L36)
cp32-8	24709	24823	-	IA	114	(BB_L36/BB_L37,BB_L37)
cp32-8	29614	29826	-	A	212	(BB_L43)
cp32-9	36	383	-	IA	347	(ORIG/BB_N01,BB_N01)
cp32-9	910	1155	-	A	245	(BB_N01)
cp32-9	2841	3089	-	A	248	(BB_N04)
cp32-9	3090	3146	-	A	56	(BB_N04)
cp32-9	3556	3695	-	p	139	(BB_N05)
cp32-9	11418	11684	-	A	266	(BB_N17)
cp32-9	13620	13919	-	AI	299	(BB_N20,BB_N20/BB_N23)
cp32-9	14509	14771	-	I	262	(BB_N20/BB_N23)
cp32-9	18910	18980	-	I	70	(BB_N29/BB_N30)
cp32-9	20362	20577	-	A	215	(BB_N31)
cp32-9	21585	21762	-	IA	177	(BB_N32/BB_N33,BB_N33)
cp32-9	22491	22727	-	AI	236	(BB_N34,BB_N34/BB_N35)
cp32-9	24150	24494	-	A	344	(BB_N35)
cp32-9	24501	24651	-	AIA	150	(BB_N35,BB_N35/BB_N36,BB_N36)
cp32-9	25613	25814	-	PI	201	(BB_N37,BB_N37/BB_N38)
cp32-9	27124	27222	-	A	98	(BB_N39)

cp32-9	27250	27434	-	A	184	(BB_N39)
lp17	3621	3926	-	IAI	305	(BB_D05a/BB_D0027,BB_D0027,BB_D0027/BB_D09)
lp17	7977	8261	-	AI	284	(BB_D13,BB_D13/BB_D14)
lp17	11859	12179	-	I	320	(BB_D18/BB_D20)
lp17	12393	12594	-	p	201	(BB_D20)
lp17	14378	14580	-	I	202	(BB_D22/BB_D23)
lp17	15329	15576	-	p	247	(BB_D23)
lp21	1281	1340	-	I	59	(BB_U02/BB_U04)
lp21	3250	3464	-	A	214	(BB_U05)
lp25	4719	4998	-	I	279	(BB_E02/BB_E05)
lp25	6929	7014	-	A	85	(BB_E09)
lp25	7048	7300	-	A	252	(BB_E09)
lp25	7339	7559	-	A	220	(BB_E09)
lp25	18592	18830	-	I	238	(BB_E23b/BB_E29a)
lp28-1	2896	3098	-	pI	202	(BB_F05,BB_F05/BB_F06)
lp28-1	5538	5644	-	PI	106	(BB_F11a,BB_F11a/BB_F12)
lp28-1	5717	5904	-	I	187	(BB_F11a/BB_F12)
lp28-1	7968	8218	-	Ip	250	(BB_F14/BB_F14a,BB_F14a)
lp28-1	8230	8462	-	pIp	232	(BB_F14a,BB_F14a/BB_F16,BB_F16)
lp28-2	2703	2761	-	I	58	(BB_G02/BB_G05)
lp28-2	3997	4057	-	PI	60	(BB_G05,BB_G05/BB_G06)
lp28-2	4836	5053	-	p	217	(BB_G06)
lp28-2	5846	6131	-	AA	285	(BB_G07,BB_G08)
lp28-2	7147	7360	-	AI	213	(BB_G09,BB_G09/BB_G10)
lp28-2	24365	24490	-	IA	125	(BB_G28/BB_G29,BB_G29)
lp28-2	26781	26974	-	A	193	(BB_G31)
lp28-3	567	865	-	AI	298	(BB_H02,BB_H02/BB_H04)
lp28-3	12492	12734	-	p	242	(BB_H18)
lp28-3	17744	18093	-	AA	349	(BB_H27,BB_H28)
lp28-3	20533	20795	-	P	262	(BB_H30)
lp28-4	2676	2939	-	A	263	(BB_I06)
lp28-4	9653	9828	-	I	175	(BB_I16/BB_I18)
lp28-4	16650	16806	-	I	156	(BB_I26/BB_I28)
lp36	4408	4509	-	I	101	(BB_K02a/BB_K07)
lp36	11123	11338	-	A	215	(BB_K17)
lp36	13006	13099	-	A	93	(BB_K19)
lp36	13100	13235	-	A	135	(BB_K19)
lp36	18451	18615	-	I	164	(BB_K55/BB_K56)
lp36	20890	21158	-	A	268	(BB_K32)
lp36	21748	21985	-	AIA	237	(BB_K33,BB_K33/BB_K34,BB_K34)
lp38	4651	4887	-	A	236	(BB_J08)
lp38	7242	7498	-	IpI	256	(BB_J09/BB_J10,BB_J10,BB_J10/BB_J11)

lp38	24304	24559	-	I	255	(BB_J31/BB_J34)
lp54	5792	5997	-	A	205	(BB_A09)
lp54	5998	6196	-	A	198	(BB_A09)
lp54	6826	7065	-	A	239	(BB_A10)
lp54	8332	8588	-	AA	256	(BB_A12,BB_A13)
lp54	11291	11411	-	I	120	(BB_A16/BB_A18)
lp54	11429	11584	-	I	155	(BB_A16/BB_A18)
lp54	17615	17934	-	I	319	(BB_A25/BB_A30)
lp54	18551	18781	-	AA	230	(BB_A30,BB_A31)
lp54	25129	25436	-	I	307	(BB_A37/BB_A38)
lp54	41157	41315	-	I	158	(BB_A60/BB_A61)
lp54	46069	46402	-	I	333	(BB_A66/BB_A68)
lp56	209	462	-	Ip	253	(ORIG/BB_Q01,BB_Q01)
lp56	1555	1808	-	p	253	(BB_Q04)
lp56	1809	2066	-	p	257	(BB_Q04)
lp56	10965	11199	-	A	234	(BB_Q18)
lp56	17021	17322	-	AIA	301	(BB_Q27,BB_Q27/BB_Q28,BB_Q28)
lp56	22607	22685	-	I	78	(BB_Q37/BB_Q38)
lp56	23213	23378	-	A	165	(BB_Q38)
lp56	26125	26421	-	A	296	(BB_Q42)
lp56	28226	28487	-	AIA	261	(BB_Q43,BB_Q43/BB_Q44,BB_Q44)
lp56	30445	30657	-	A	212	(BB_Q47)
lp56	33856	34073	-	Ip	217	(BB_Q50/BB_Q51,BB_Q51)
lp56	35061	35151	-	pIA	90	(BB_Q51,BB_Q51/BB_Q52,BB_Q52)
lp56	35152	35396	-	A	244	(BB_Q52)
lp56	46941	47073	-	I	132	(BB_Q74/BB_Q79)
lp56	47245	47448	-	Ip	203	(BB_Q74/BB_Q79,BB_Q79)
Chromosome	6195	6515	+	AA	320	(BB_0005,BB_0006)
Chromosome	7248	7531	+	AIA	283	(BB_0006,BB_0006/BB_0007,BB_0007)
Chromosome	120029	120216	+	A	187	(BB_0123)
Chromosome	120217	120446	+	A	229	(BB_0123)
Chromosome	124199	124455	+	A	256	(BB_0128)
Chromosome	141334	141680	+	p	346	(BB_0140)
Chromosome	141689	141950	+	p	261	(BB_0140)
Chromosome	177495	177787	+	A	292	(BB_0175)
Chromosome	188410	188590	+	AI	180	(BB_0187,BB_0187/BB_0188)
Chromosome	191997	192165	+	A	168	(BB_0194)
Chromosome	227226	227555	+	A	329	(BB_0221)
Chromosome	230783	231006	+	A	223	(BB_0226)
Chromosome	250385	250588	+	A	203	(BB_0244)
Chromosome	267323	267566	+	A	243	(BB_0257)
Chromosome	270114	270374	+	A	260	(BB_0258)

Chromosome	282439	282700	+	AIA	261	(BB_0269,BB_0269/BB_0270,BB_0270)
Chromosome	297224	297529	+	AA	305	(BB_0287,BB_0288)
Chromosome	299202	299426	+	A	224	(BB_0289)
Chromosome	324866	325152	+	A	286	(BB_0318)
Chromosome	367322	367588	+	A	266	(BB_0359)
Chromosome	388221	388453	+	A	232	(BB_0378)
Chromosome	390486	390673	+	A	187	(BB_0381)
Chromosome	406812	407029	+	AA	217	(BB_0392,BB_0393)
Chromosome	410470	410691	+	I	221	(BB_0398/BB_0399)
Chromosome	466326	466588	+	A	262	(BB_0446)
Chromosome	470513	470715	+	A	202	(BB_0450)
Chromosome	473513	473700	+	A	187	(BB_0454)
Chromosome	482310	482471	+	I	161	(BB_t06/BB_0461)
Chromosome	564460	564719	+	A	259	(BB_0553)
Chromosome	650007	650319	+	A	312	(BB_0622)
Chromosome	650660	650847	+	A	187	(BB_0623)
Chromosome	666067	666279	+	A	212	(BB_0633)
Chromosome	668772	669065	+	p	293	(BB_0634)
Chromosome	700413	700621	+	A	208	(BB_0660)
Chromosome	700661	700847	+	A	186	(BB_0660)
Chromosome	750817	751164	+	I	347	(BB_0713/BB_0714)
Chromosome	768395	768595	+	A	200	(BB_0729)
Chromosome	791352	791701	+	A	349	(BB_0747)
Chromosome	807263	807441	+	A	178	(BB_0765)
Chromosome	810040	810389	+	A	349	(BB_0768)
Chromosome	812086	812343	+	A	257	(BB_0770)
Chromosome	814113	814435	+	A	322	(BB_0772)
Chromosome	881440	881713	+	A	273	(BB_0833)
Chromosome	885663	885968	+	A	305	(BB_0834)
Chromosome	905118	905387	+	pI	269	(BB_0845a,BB_0845a/BB_0845b)
cp26	856	1050	+	A	194	(BB_B03)
cp26	1972	2272	+	AI	300	(BB_B03,BB_B03/BB_B04)
cp26	2273	2436	+	I	163	(BB_B03/BB_B04)
cp26	10733	10815	+	I	82	(BB_B13/BB_B14)
cp26	19419	19748	+	IA	329	(BB_B22/BB_B23,BB_B23)
cp26	19749	19819	+	A	70	(BB_B23)
cp26	19820	20014	+	A	194	(BB_B23)
cp26	20689	20829	+	AI	140	(BB_B23,BB_B23/BB_B24)
cp26	22625	22781	+	A	156	(BB_B27)
cp32-1	18165	18333	+	A	168	(BB_P29)
cp32-6	17753	18101	+	A	348	(BB_M29)
cp32-6	18102	18259	+	A	157	(BB_M29)

lp17	2639	2711	+	I	72	(BB_D04/BB_D05a)
lp17	3121	3189	+	P	68	(BB_D05a)
lp17	11705	11846	+	I	141	(BB_D18/BB_D20)
lp17	16230	16515	+		285	)
lp25	3803	4067	+	p	264	(BB_E02)
lp25	12558	12885	+	AA	327	(BB_E19,BB_E20)
lp25	21073	21319	+	IP	246	(BB_E23b/BB_E29a,BB_E29a)
lp25	22726	23036	+	I	310	(BB_E31/BB_E33)
lp25	23037	23334	+	I	297	(BB_E31/BB_E33)
lp25	23583	23822	+	I	239	(BB_E31/BB_E33)
lp28-1	2136	2438	+	A	302	(BB_F03)
lp28-1	2439	2785	+	AIP	346	(BB_F03,BB_F03/BB_F05,BB_F05)
lp28-1	14609	14698	+	A	89	(BB_F26)
lp28-1	18004	18331	+	I	327	(BB_F0040/BB_F32)
lp28-2	11054	11212	+	IA	158	(BB_G10/BB_G12,BB_G12)
lp28-2	11213	11354	+	A	141	(BB_G12)
lp28-3	4412	4719	+	A	307	(BB_H09)
lp28-3	6970	7176	+	A	206	(BB_H09)
lp28-3	19454	19725	+	I	271	(BB_H29/BB_H30)
lp28-3	23441	23694	+	I	253	(BB_H34/BB_H36a)
lp28-3	24884	25057	+	P	173	(BB_H36b)
lp28-4	18054	18315	+	I	261	(BB_I28/BB_I29)
lp28-4	19230	19481	+	I	251	(BB_I29/BB_I31)
lp36	1150	1277	+	Ip	127	(BB_K01/BB_K02a,BB_K02a)
lp36	6780	7117	+	IpI	337	(BB_K09/BB_K10,BB_K10,BB_K10/BB_K12)
lp36	7720	7873	+	P	153	(BB_K12)
lp36	7874	8061	+	PI	187	(BB_K12,BB_K12/BB_K13)
lp36	27908	28155	+	A	247	(BB_K45)
lp36	33622	33878	+	A	256	(BB_K50)
lp36	35055	35386	+	A	331	(BB_K52)
lp38	4161	4359	+	I	198	(BB_J05/BB_J08)
lp38	10644	10962	+	A	318	(BB_J16)
lp38	11938	12150	+	A	212	(BB_J18)
lp38	12781	12939	+	A	158	(BB_J19)
lp38	14022	14267	+	I	245	(BB_J20/BB_J0058)
lp38	14272	14543	+	I	271	(BB_J20/BB_J0058)
lp38	26142	26384	+	A	242	(BB_J34)
lp38	27792	27981	+	A	189	(BB_J36)
lp38	29116	29322	+	I	206	(BB_J37/BB_J41)
lp38	29323	29534	+	I	211	(BB_J37/BB_J41)
lp38	29535	29878	+	I	343	(BB_J37/BB_J41)
lp38	29879	30085	+	IA	206	(BB_J37/BB_J41,BB_J41)

lp38	37006	37165	+	I	159	(BB_J50/BB_J51)
lp38	37166	37383	+	I	217	(BB_J50/BB_J51)
lp38	37396	37695	+	Ip	299	(BB_J50/BB_J51,BB_J51)
lp54	2051	2257	+	A	206	(BB_A04)
lp54	11715	12027	+	IP	312	(BB_A16/BB_A18,BB_A18)
lp54	17337	17660	+	I	323	(BB_A25/BB_A30)
lp54	40761	41022	+	A	261	(BB_A60)
lp54	45194	45511	+	A	317	(BB_A66)
lp54	47286	47440	+	I	154	(BB_A68/BB_A69)
lp54	51333	51603	+	I	270	(BB_A73/BB_A74)
lp56	4121	4249	+	IA	128	(BB_Q06/BB_Q07,BB_Q07)
lp56	4250	4513	+	A	263	(BB_Q07)
lp56	5921	6144	+	A	223	(BB_Q09)
lp56	41696	41932	+	A	236	(BB_Q67)
lp56	43244	43500	+	A	256	(BB_Q67)
lp56	46949	47179	+	I	230	(BB_Q74/BB_Q79)
lp56	48312	48571	+	p	259	(BB_Q80)
lp56	49562	49860	+	I	298	(BB_Q82/BB_Q0091)
lp56	49861	50108	+	I	247	(BB_Q82/BB_Q0091)
lp56	52127	52401	+	IA	274	(BB_Q85/BB_Q88,BB_Q88)

Non-coding RNAs were identified as described in the materials and methods. Included are the genetic element, start position, end position, strand, relative location (I: Intergenic, A: Antisense, P: Pseudogene), length, associated genes, and those genes functions. Orders of numeric position and annotations are given according to order of the (+) strand. Note that Position 1 and Position 2 reflect start and stop sites differently depending on strand. For ncRNAs located on the (+) strand position 1 is the start and position 2 is the stop. For entries located on the (-) strand, position 1 is the end site and position 2 is the start site. Commas between associated genes and functional annotations indicate that the ncRNA overlaps both contiguously and "/" between them indicate that it is located intergenically between the two genes.

Table 8-6 Differentially abundant transcripts comparing WT to Δ*rpoN*

Gene Name	RefSeq CDS/Custom Transcript ID	baseMean	Log2 FC	lfcSE	stat	pvalue	padj
A-(BB_0450)	ncRNA0071	65.28090	-6.05115	0.70254	-8.61330	7.1000E-18	1.9400E-15
A-(BB_F03)	ncRNA0247	1699.00234	-1.50590	0.29570	-5.09261	3.5300E-07	4.8200E-05
I-(BB_F11a/BB_F12)	ncRNA0251	727.74533	-1.18687	0.18681	-6.35324	2.1100E-10	3.4600E-08
BB_0449	lcl|NC_001318.1_cds_NP_212583.1_424	973.87220	1.05379	0.26434	3.98648	6.7100E-05	6.8695E-03
rpoN	lcl|NC_001318.1_cds_NP_212584.1_425	1371.15279	-3.84743	0.13386	-28.74303	1.1100E-181	1.8100E-178
BB_F03	lcl|NC_001851.2_cds_NP_045439.1_1144	189.08402	-1.38167	0.37769	-3.65827	2.5393E-04	2.2687E-02
BB_F20	lcl|NC_001851.2_cds_NP_045453.2_1150	136.22755	-1.21603	0.24468	-4.96992	6.7000E-07	8.4400E-05
BB_F23	lcl|NC_001851.2_cds_NP_045456.1_1151	367.92274	-1.21157	0.24784	-4.88849	1.0200E-06	1.1896E-04

The included transcripts met the criteria of >1 log2 fold-change and an adjusted P-value (padj) when comparing the Δ*rpoN* mutant to wild-type. A total of 6 transcripts were differentially regulated, not including the mutated gene, by the mutation. The first column contains the CDS/custom transcript ID which is the transcript ID for all coding sequences obtained from the NCBI Gene file format file or the transcript ID given to ncRNAs. RefSeq entries are further separated by the character "_". The first portion gives the genetic element from which it is derived, the second describes the type of element (CDS), the third provides RefSeq ID, and the fourth provides a number indicating the particular entries ordered number in the RefSeq entry. The second column is the gene information, for the ncRNAs it contains the location relative to other genes and for predicted or known genes it contains gene name. The remaining columns describe the various metrics of expression of each impacted transcript including, base mean (average library size normalized counts across all samples), log2FC (Fold change estimate), lfcSE (uncertainty of the log fold change estimate), stat (Wald statistic), pvalue, padj (pvalue following Benjamini-Hochberg adjustment). ORFs and ncRNAs are identified according to the names or numbers assigned

to genes and transcripts by the initial genome sequencing of *B. burgdorferi* strain B31 [56, 101] or from our previous analyses of that strain's ncRNA transcriptome [14].

Table 8-7 Differentially abundant transcripts comparing WT to Δ*rpoS*

Gene Name	RefSeq CDS/Custom Transcript ID	baseMean	Log2 FC	lfcSE	stat	pvalue	padj
I-(BB_A16/BB_A18)	ncRNA0317	934.04967	1.30342	0.27937	4.66565	3.0800E-06	2.6196E-03
rpoS	lcl|NC_001318.1_cds_NP_212905.1_724	827.49827	3.86936	0.26638	14.52547	8.3600E-48	1.4200E-44

The included transcript met the criteria of >1 log2 fold-change and an adjusted P-value (padj) when comparing the Δ*rpoS* mutant to wild-type. One transcript was impacted, not including the mutated gene, by the mutation. The first column contains the CDS/custom transcript ID which is the transcript ID for all coding sequences obtained from the NCBI Gene file format file or the transcript ID given to ncRNAs. RefSeq entries are further separated by the character "_". The first portion gives the genetic element from which it is derived, the second describes the type of element (CDS), the third provides RefSeq ID, and the fourth provides a number indicating the particular entries ordered number in the RefSeq entry. The second column is the gene information, for the ncRNAs it contains the location relative to other genes and for predicted or known genes it contains gene name. The remaining columns describe the various metrics of expression of each impacted transcript including, base mean (average library size normalized counts across all samples), log2FC (Fold change estimate), lfcSE (uncertainty of the log fold change estimate), stat (Wald statistic), pvalue, padj (pvalue following Benjamini-Hochberg adjustment). The ncRNA is listed according to the nomenclature the previous analyses of the strain B31 ncRNA transcriptome [14].

Table 8-8 Differentially abundant transcripts comparing WT to Δ*badR*

Gene Name	RefSeq CDS/Custom Transcript ID	baseMean	Log2 FC	lfcSE	stat	pvalue	padj
PI-(BB_0003,BB_0003/BB_0004)	ncRNA0001	968.82087	-1.09112	0.28077	-3.88617	1.0184E-04	6.9651E-04
AI-(BB_0004,BB_0004/BB_0005)	ncRNA0002	3041.85842	-1.46663	0.24896	-5.89114	3.8400E-09	6.8700E-08
AA-(BB_0005,BB_0006)	ncRNA0003	1243.57656	-1.40263	0.31154	-4.50219	6.7300E-06	5.7800E-05
A-(BB_0013)	ncRNA0006	3033.89498	-1.65126	0.33972	-4.86068	1.1700E-06	1.1800E-05
A-(BB_0014)	ncRNA0007	214.85270	-1.49644	0.48279	-3.09953	1.9382E-03	9.0932E-03
A-(BB_0084)	ncRNA0014	380.54610	-1.16896	0.38865	-3.00773	2.6321E-03	1.1626E-02
AA-(BB_0198,BB_0199)	ncRNA0031	400.71340	-1.25450	0.37399	-3.35434	7.9554E-04	4.3845E-03
A-(BB_0208)	ncRNA0035	510.91058	-1.36787	0.29213	-4.68233	2.8400E-06	2.6400E-05
A-(BB_0211)	ncRNA0037	1238.76926	-1.49984	0.31476	-4.76505	1.8900E-06	1.8100E-05
A-(BB_0240)	ncRNA0042	2021.45874	-1.86846	0.34914	-5.35166	8.7200E-08	1.1000E-06
A-(BB_0244)	ncRNA0043	577.79571	-2.19383	0.40474	-5.42038	5.9500E-08	7.7300E-07
AIA-(BB_0269,BB_0269/BB_0270,BB_0270)	ncRNA0050	1285.29820	-1.97098	0.55621	-3.54357	3.9474E-04	2.3923E-03
A-(BB_0347)	ncRNA0057	34.51260	-1.77185	0.54862	-3.22963	1.2395E-03	6.2637E-03
A-(BB_0374)	ncRNA0061	321.08071	-1.22151	0.29276	-4.17242	3.0100E-05	2.2610E-04
A-(BB_0381)	ncRNA0063	391.05521	-1.49965	0.43302	-3.46324	5.3371E-04	3.1234E-03
A-(BB_0446)	ncRNA0070	529.31721	-2.03125	0.31340	-6.48129	9.0900E-11	2.1200E-09
A-(BB_0450)	ncRNA0071	65.28090	-4.49737	0.70339	-6.39389	1.6200E-10	3.6700E-09
A-(BB_0454)	ncRNA0072	396.65108	2.95589	0.65949	4.48209	7.3900E-06	6.2900E-05
I-(BB_t06/BB_0461)	ncRNA0073	2784.93399	1.60501	0.22993	6.98039	2.9400E-12	8.0900E-11
AA-(BB_0465,BB_0466)	ncRNA0076	1466.20007	-1.17375	0.25862	-4.53847	5.6700E-06	5.0000E-05
p-(BB_0522)	ncRNA0080	879.81309	-1.91147	0.23693	-8.06754	7.1700E-16	2.8100E-14
AI-(BB_0556,BB_0556/BB_0557)	ncRNA0083	349.18194	-1.07180	0.26873	-3.98835	6.6500E-05	4.7015E-04
A-(BB_0581)	ncRNA0084	87.52936	-2.55403	0.47013	-5.43263	5.5500E-08	7.3300E-07
A-(BB_0588)	ncRNA0087	1536.15642	-2.23217	0.70922	-3.14736	1.6475E-03	7.9482E-03
A-(BB_0633)	ncRNA0099	150.86401	-4.91216	0.64018	-7.67313	1.6800E-14	6.0800E-13
A-(BB_0660)	ncRNA0105	99.27360	-2.45137	0.75704	-3.23811	1.2032E-03	6.1168E-03
A-(BB_0697)	ncRNA0110	1608.78180	-1.36302	0.25646	-5.31467	1.0700E-07	1.3000E-06
A-(BB_0747)	ncRNA0117	270.28006	-1.17753	0.47325	-2.48819	1.2840E-02	4.3806E-02
AIA-(BB_0794,BB_0794/BB_0795,BB_0795)	ncRNA0125	2242.03629	-1.57326	0.26039	-6.04184	1.5200E-09	2.9800E-08
pI-(BB_0845a,BB_0845a/BB_0845b)	ncRNA0132	211.25465	-2.25855	0.53598	-4.21390	2.5100E-05	1.9255E-04
A-(BB_B03)	ncRNA0133	471.62837	-1.62632	0.24686	-6.58789	4.4600E-11	1.1000E-09
AI-(BB_B03,BB_B03/BB_B04)	ncRNA0134	130.50382	2.10478	0.37642	5.59151	2.2500E-08	3.2400E-07
I-(BB_B03/BB_B04)	ncRNA0135	1218.80954	3.52274	0.29625	11.89113	1.3200E-32	1.4900E-30
AI-(BB_B09,BB_B09/BB_B10)	ncRNA0136	476.36984	-2.09054	0.35434	-5.89983	3.6400E-09	6.5900E-08
A-(BB_P21)	ncRNA0148	93.09626	-1.90633	0.42832	-4.45076	8.5600E-06	7.2500E-05

I-(BB_P29/BB_P30)	ncRNA0150	412.49914	1.15130	0.44834	2.56788	1.0232E-02	3.6685E-02
IA-(BB_P32/BB_P33,BB_P33)	ncRNA0152	276.35152	2.11738	0.36507	5.79987	6.6400E-09	1.1300E-07
A-(BB_S11)	ncRNA0154	104.52579	-1.47724	0.47704	-3.09671	1.9568E-03	9.1301E-03
I-(BB_O29/BB_O30)	ncRNA0185	1573.01516	1.54572	0.47774	3.23551	1.2143E-03	6.1544E-03
AIA-(BB_O32,BB_O32/BB_O33,BB_O33)	ncRNA0186	90.75800	1.65807	0.32571	5.09068	3.5700E-07	3.9200E-06
A-(BB_O36)	ncRNA0188	23.57876	-1.93466	0.73137	-2.64525	8.1631E-03	3.0756E-02
A-(BB_O44)	ncRNA0191	8.70865	-1.95208	0.79305	-2.46149	1.3836E-02	4.6405E-02
IA-(BB_L29/BB_L30,BB_L30)	ncRNA0200	867.04480	-2.25465	0.35334	-6.38104	1.7600E-10	3.8900E-09
A-(BB_L36)	ncRNA0205	27.97465	-1.84728	0.73841	-2.50168	1.2360E-02	4.2697E-02
IA-(BB_N32/BB_N33,BB_N33)	ncRNA0218	29.86142	2.01267	0.51769	3.88782	1.0115E-04	6.9577E-04
I-(BB_D04/BB_D05a)	ncRNA0225	86.57889	-2.20574	0.54226	-4.06769	4.7500E-05	3.4119E-04
P-(BB_D05a)	ncRNA0226	56.82862	-4.17247	0.63131	-6.60919	3.8600E-11	9.6800E-10
I-(BB_D18/BB_D20)	ncRNA0229	117.85300	-1.35183	0.34541	-3.91370	9.0900E-05	6.3180E-04
p-(BB_D23)	ncRNA0233	46.44976	-2.51966	0.75095	-3.35527	7.9286E-04	4.3839E-03
A-(BB_E09)	ncRNA0239	1464.22355	-2.30974	0.42823	-5.39371	6.9000E-08	8.8400E-07
A-(BB_E09)	ncRNA0240	74.83749	-2.66273	0.85330	-3.12052	1.8053E-03	8.6120E-03
I-(BB_E23b/BB_E29a)	ncRNA0242	107.05005	-1.63438	0.59175	-2.76193	5.7461E-03	2.2704E-02
I-(BB_E31/BB_E33)	ncRNA0245	314.76149	-1.44551	0.48476	-2.98193	2.8644E-03	1.2381E-02
PI-(BB_G05,BB_G05/BB_G06)	ncRNA0257	56.23394	-3.93529	0.79525	-4.94850	7.4800E-07	8.0100E-06
AA-(BB_G07,BB_G08)	ncRNA0259	88.14975	1.10443	0.26314	4.19712	2.7000E-05	2.0553E-04
IpI-(BB_K09/BB_K10,BB_K10,BB_K10/BB_K12)	ncRNA0281	166.24839	-1.37454	0.50527	-2.72043	6.5197E-03	2.5292E-02
A-(BB_K17)	ncRNA0284	123.82711	-2.10430	0.29631	-7.10179	1.2300E-12	3.6200E-11
A-(BB_K19)	ncRNA0286	219.94179	-1.26203	0.49759	-2.53627	1.1204E-02	3.9528E-02
A-(BB_J18)	ncRNA0297	206.52360	-4.03412	0.71716	-5.62515	1.8500E-08	2.7400E-07
I-(BB_J20/BB_J0058)	ncRNA0299	119.12666	-1.62021	0.32287	-5.01815	5.2200E-07	5.6200E-06
I-(BB_J37/BB_J41)	ncRNA0304	103.27966	-1.37834	0.48298	-2.85383	4.3195E-03	1.7515E-02
I-(BB_J50/BB_J51)	ncRNA0308	893.05821	-5.20270	0.49451	-10.52094	6.9200E-26	4.9100E-24
A-(BB_A04)	ncRNA0311	361.98141	2.13591	0.41127	5.19340	2.0600E-07	2.3800E-06
IP-(BB_A16/BB_A18,BB_A18)	ncRNA0318	1800.37672	-1.63311	0.56659	-2.88233	3.9474E-03	1.6317E-02
I-(BB_A37/BB_A38)	ncRNA0322	2507.45399	-1.82706	0.46457	-3.93284	8.3900E-05	5.8833E-04
I-(BB_A66/BB_A68)	ncRNA0326	456.29968	1.58132	0.36726	4.30573	1.6600E-05	1.3370E-04
I-(BB_A68/BB_A69)	ncRNA0327	288.56940	1.26427	0.41152	3.07217	2.1251E-03	9.7548E-03
p-(BB_Q04)	ncRNA0330	720.36163	-1.02436	0.39854	-2.57027	1.0162E-02	3.6573E-02
I-(BB_Q37/BB_Q38)	ncRNA0337	248.20404	1.38205	0.42404	3.25922	1.1172E-03	5.6963E-03
tRNA-Ile-1	rna11	3677.25129	-1.07076	0.43186	-2.47941	1.3160E-02	4.4644E-02
BB_0004	lcl|NC_001318.1_cds_NP_212138.2_3	3213.61271	-1.16128	0.35025	-3.31560	9.1445E-04	4.8065E-03
BB_0008	lcl|NC_001318.1_cds_NP_212142.2_7	904.70176	-1.11034	0.15143	-7.33258	2.2600E-13	6.9900E-12
BB_0010	lcl|NC_001318.1_cds_NP_212144.1_9	909.55235	-1.05158	0.24540	-4.28510	1.8300E-05	1.4536E-04
ruvB	lcl|NC_001318.1_cds_NP_212156.1_20	2074.85845	-1.61520	0.20259	-7.97292	1.5500E-15	5.8600E-14
ruvA	lcl|NC_001318.1_cds_NP_212157.1_21	1097.97296	-1.27309	0.15188	-8.38203	5.2000E-17	2.3900E-15

BB_0026	lcl|NC_001318.1_cds_NP_212160.1_24	1860.31604	-1.01008	0.18200	-5.54999	2.8600E-08	4.0200E-07
BB_0027	lcl|NC_001318.1_cds_NP_212161.1_25	9710.08595	-2.08218	0.33747	-6.17004	6.8300E-10	1.4500E-08
BB_0035	lcl|NC_001318.1_cds_NP_212169.1_33	2717.90772	1.16654	0.21471	5.43305	5.5400E-08	7.3300E-07
cheR	lcl|NC_001318.1_cds_NP_212174.1_38	2192.91826	-1.27180	0.18779	-6.77229	1.2700E-11	3.3200E-10
malQ	lcl|NC_001318.1_cds_NP_212300.1_155	848.92993	1.25223	0.32051	3.90697	9.3500E-05	6.4700E-04
BB_0172	lcl|NC_001318.1_cds_NP_212306.2_161	2887.76489	-1.26105	0.12397	-10.17219	2.6400E-24	1.6100E-22
BB_0240	lcl|NC_001318.1_cds_NP_212374.1_225	2634.82078	1.09613	0.21449	5.11029	3.2200E-07	3.5800E-06
glpK	lcl|NC_001318.1_cds_NP_212375.1_226	5175.05698	2.39201	0.33787	7.07965	1.4500E-12	4.1700E-11
BB_0242	lcl|NC_001318.1_cds_NP_212376.1_227	990.14647	2.16828	0.41966	5.16676	2.3800E-07	2.7000E-06
BB_0243	lcl|NC_001318.1_cds_NP_212377.1_228	6087.03774	2.00725	0.23639	8.49112	2.0500E-17	9.6800E-16
BB_0285	lcl|NC_001318.1_cds_NP_212419.2_270	4139.07947	-1.00597	0.31761	-3.16732	1.5385E-03	7.5507E-03
BB_0330	lcl|NC_001318.1_cds_NP_212464.1_313	9233.47510	1.24683	0.21901	5.69309	1.2500E-08	1.9500E-07
BB_0331	lcl|NC_001318.1_cds_NP_212465.1_314	360.85379	1.05649	0.34945	3.02334	2.5000E-03	1.1234E-02
gatC	lcl|NC_001318.1_cds_NP_212477.1_326	285.30099	-1.21150	0.21671	-5.59038	2.2700E-08	3.2400E-07
mgsA	lcl|NC_001318.1_cds_NP_212498.1_345	3019.34634	1.88485	0.16473	11.44229	2.5700E-30	2.5700E-28
la7	lcl|NC_001318.1_cds_NP_212499.1_346	8401.74564	1.98028	0.28233	7.01415	2.3100E-12	6.4600E-11
metK	lcl|NC_001318.1_cds_NP_212510.1_357	3414.26722	1.00717	0.30325	3.32125	8.9615E-04	4.7968E-03
rpmG	lcl|NC_001318.1_cds_NP_212530.1_377	7700.52393	-1.01428	0.22521	-4.50383	6.6700E-06	5.7800E-05
BB_0408	lcl|NC_001318.1_cds_NP_212542.1_389	6219.62582	1.35986	0.22211	6.12252	9.2100E-10	1.8400E-08
BB_0415	lcl|NC_001318.1_cds_NP_212549.1_394	1448.60433	-1.27909	0.22206	-5.76023	8.4000E-09	1.3900E-07
BB_0427	lcl|NC_001318.1_cds_NP_212561.2_403	376.59155	-1.24518	0.39844	-3.12510	1.7774E-03	8.5027E-03
BB_0428	lcl|NC_001318.1_cds_NP_212562.1_404	2667.65490	-1.13848	0.21358	-5.33050	9.7900E-08	1.2100E-06
BB_0429	lcl|NC_001318.1_cds_NP_212563.1_405	2866.18584	-1.04523	0.20512	-5.09567	3.4800E-07	3.8400E-06
BB_0430	lcl|NC_001318.1_cds_NP_212564.2_406	199.01921	-1.02289	0.32470	-3.15030	1.6310E-03	7.8911E-03
BB_0434	lcl|NC_001318.1_cds_NP_212568.1_409	410.65472	-1.04234	0.30603	-3.40599	6.5924E-04	3.7175E-03
rpmH	lcl|NC_001318.1_cds_NP_212574.1_415	1315.25246	-1.11789	0.18134	-6.16445	7.0700E-10	1.4900E-08
BB_0451	lcl|NC_001318.1_cds_NP_212585.1_426	435.99128	1.00758	0.20928	4.81442	1.4800E-06	1.4400E-05
BB_0454	lcl|NC_001318.1_cds_NP_212588.1_429	2730.88885	-1.03160	0.18436	-5.59544	2.2000E-08	3.2100E-07
BB_0465	lcl|NC_001318.1_cds_NP_212599.1_440	2885.54585	-1.00750	0.23048	-4.37136	1.2300E-05	1.0013E-04
BB_0509	lcl|NC_001318.1_cds_NP_212643.1_482	8232.92191	-2.70977	0.36572	-7.40945	1.2700E-13	4.1500E-12
BB_0533	lcl|NC_001318.1_cds_NP_212667.1_496	5644.77797	-1.06287	0.10687	-9.94531	2.6400E-23	1.5500E-21
BB_0537	lcl|NC_001318.1_cds_NP_212671.1_500	1848.25226	1.05591	0.23840	4.42912	9.4600E-06	7.9000E-05
BB_0543	lcl|NC_001318.1_cds_NP_212677.2_505	8778.76132	-1.01909	0.16382	-6.22080	4.9500E-10	1.0700E-08
BB_0562	lcl|NC_001318.1_cds_NP_212696.1_524	1222.60891	1.05371	0.14723	7.15694	8.2500E-13	2.4600E-11
BB_0577	lcl|NC_001318.1_cds_NP_212711.1_539	1867.11586	-1.51685	0.22326	-6.79418	1.0900E-11	2.9000E-10
BB_0588	lcl|NC_001318.1_cds_NP_212722.1_550	1645.23671	-2.28085	0.13243	-17.22261	1.8000E-66	5.1000E-64
murB	lcl|NC_001318.1_cds_NP_212732.1_560	2605.56083	-1.09345	0.25655	-4.26217	2.0200E-05	1.6036E-04
p66	lcl|NC_001318.1_cds_NP_212737.1_565	18788.96545	1.19152	0.37085	3.21297	1.3137E-03	6.6190E-03
rnmV	lcl|NC_001318.1_cds_NP_212760.1_587	17091.35904	-1.62228	0.41009	-3.95594	7.6200E-05	5.3647E-04
BB_0627	lcl|NC_001318.1_cds_YP_008686584.1_588	1365.69883	-1.13722	0.23568	-4.82529	1.4000E-06	1.3800E-05
BB_0637	lcl|NC_001318.1_cds_NP_212771.2_597	8048.19773	1.24731	0.26134	4.77279	1.8200E-06	1.7500E-05
BB_0638	lcl|NC_001318.1_cds_NP_212772.1_598	3886.71871	1.37448	0.20993	6.54741	5.8500E-11	1.3800E-09
BB_0639	lcl|NC_001318.1_cds_NP_212773.1_599	1482.68946	1.11139	0.28704	3.87185	1.0801E-04	7.3284E-04
ylqF	lcl|NC_001318.1_cds_NP_212777.1_603	699.04670	-1.01227	0.22468	-4.50538	6.6300E-06	5.7800E-05

BB_0644	lcl|NC_001318.1_cds_NP_212778.1_604	697.38844	1.09191	0.19929	5.47909	4.2800E-08	5.8200E-07
BB_0678	lcl|NC_001318.1_cds_NP_212812.1_638	5061.70052	1.13088	0.18467	6.12376	9.1400E-10	1.8400E-08
BB_0679	lcl|NC_001318.1_cds_NP_212813.2_639	4281.29084	1.09289	0.19250	5.67736	1.3700E-08	2.1200E-07
BB_0681	lcl|NC_001318.1_cds_NP_212815.2_641	1841.56416	1.13210	0.19872	5.69708	1.2200E-08	1.9200E-07
BB_0683	lcl|NC_001318.1_cds_NP_212817.1_643	9215.74716	-1.34261	0.20023	-6.70547	2.0100E-11	5.1800E-10
fni	lcl|NC_001318.1_cds_NP_212818.2_644	5419.35053	-1.36046	0.31096	-4.37507	1.2100E-05	9.8900E-05
BB_0693	lcl|NC_001318.1_cds_NP_212827.1_652	1586.51137	-7.78866	0.50598	-15.39320	1.8200E-53	3.8700E-51
ffh	lcl|NC_001318.1_cds_NP_212828.2_653	14060.76269	-3.01855	0.37424	-8.06591	7.2700E-16	2.8100E-14
rpsP	lcl|NC_001318.1_cds_NP_212829.1_654	1323.09899	-1.03940	0.25376	-4.09602	4.2000E-05	3.0720E-04
BB_0696	lcl|NC_001318.1_cds_NP_212830.1_655	1648.93321	-1.06417	0.33229	-3.20256	1.3621E-03	6.8226E-03
BB_0724	lcl|NC_001318.1_cds_YP_008686588.1_680	3690.87567	-1.21343	0.26757	-4.53493	5.7600E-06	5.0600E-05
BB_0739	lcl|NC_001318.1_cds_YP_008686589.1_694	1873.95784	-1.41965	0.17302	-8.20498	2.3100E-16	1.0100E-14
BB_0765	lcl|NC_001318.1_cds_NP_212899.1_718	561.76005	1.07980	0.17529	6.16015	7.2700E-10	1.5100E-08
cvpA	lcl|NC_001318.1_cds_NP_212900.1_719	420.51092	1.35652	0.23960	5.66172	1.5000E-08	2.3000E-07
murG	lcl|NC_001318.1_cds_NP_212901.1_720	901.26760	1.56083	0.28107	5.55315	2.8100E-08	3.9800E-07
BB_0768	lcl|NC_001318.1_cds_NP_212902.1_721	1156.42566	1.03455	0.23465	4.40882	1.0400E-05	8.5900E-05
BB_0769	lcl|NC_001318.1_cds_NP_212903.1_722	1653.77636	1.26192	0.24096	5.23707	1.6300E-07	1.9300E-06
BB_0770	lcl|NC_001318.1_cds_NP_212904.1_723	1364.05445	1.29725	0.24460	5.30344	1.1400E-07	1.3700E-06
BB_0773	lcl|NC_001318.1_cds_NP_212907.1_727	467.79866	1.23579	0.17932	6.89159	5.5200E-12	1.4900E-10
BB_0785	lcl|NC_001318.1_cds_NP_212919.1_739	2664.70377	1.60156	0.21191	7.55769	4.1000E-14	1.4600E-12
BB_0794	lcl|NC_001318.1_cds_YP_008686594.1_748	8844.21241	-1.00439	0.17426	-5.76361	8.2300E-09	1.3700E-07
BB_0798	lcl|NC_001318.1_cds_NP_212932.1_752	412.74295	-1.27472	0.23076	-5.52411	3.3100E-08	4.6200E-07
arcA	lcl|NC_001318.1_cds_NP_212975.1_793	2690.75653	3.20828	0.15655	20.49298	2.4900E-93	1.0600E-90
argF	lcl|NC_001318.1_cds_NP_212976.2_794	2452.38136	2.75300	0.24753	11.12176	9.8300E-29	8.3700E-27
BB_0843	lcl|NC_001318.1_cds_NP_212977.2_795	9954.80128	2.00513	0.22501	8.91146	5.0400E-19	2.6800E-17
BB_0852	lcl|NC_001318.1_cds_NP_212985.1_797	258.47242	-1.10879	0.36278	-3.05636	2.2405E-03	1.0175E-02
BB_B04	lcl|NC_001903.1_cds_NP_046990.2_801	11469.16755	5.57723	0.22386	24.91438	5.2000E-137	4.4300E-134
BB_B05	lcl|NC_001903.1_cds_NP_046991.1_802	2551.06647	5.13641	0.27541	18.64996	1.2600E-77	4.3000E-75
BB_B06	lcl|NC_001903.1_cds_NP_046992.2_803	1687.19872	6.04192	0.26257	23.01027	3.6800E-117	2.0900E-114
BB_B07	lcl|NC_001903.1_cds_NP_046993.1_804	8409.80978	4.82405	0.16267	29.65532	2.9000E-193	4.9300E-190
BB_B10	lcl|NC_001903.1_cds_NP_046996.1_806	3773.69113	-1.28185	0.38183	-3.35713	7.8755E-04	4.3687E-03
BB_B29	lcl|NC_001903.1_cds_NP_047015.1_821	24118.64600	-2.30295	0.21295	-10.81453	2.9400E-27	2.1800E-25
BB_P10	lcl|NC_000948.1_cds_NP_051171.1_830	89.29313	-1.80857	0.56895	-3.17880	1.4788E-03	7.3211E-03
BB_P15	lcl|NC_000948.1_cds_NP_051176.1_835	57.75190	-1.51185	0.53321	-2.83538	4.5771E-03	1.8471E-02
BB_P26	lcl|NC_000948.1_cds_NP_051187.2_846	172.83719	1.04426	0.26881	3.88475	1.0244E-04	6.9779E-04
BB_P31	lcl|NC_000948.1_cds_NP_051192.1_851	319.42777	1.34368	0.33180	4.04963	5.1300E-05	3.6706E-04
BB_P32	lcl|NC_000948.1_cds_NP_051193.1_852	812.84291	1.85498	0.23580	7.86670	3.6400E-15	1.3500E-13
BB_P33	lcl|NC_000948.1_cds_NP_051194.2_853	507.55300	2.04110	0.24574	8.30588	9.9100E-17	4.4400E-15
bdrA	lcl|NC_000948.1_cds_NP_051195.1_854	840.20823	1.45969	0.30269	4.82243	1.4200E-06	1.4000E-05
erpB	lcl|NC_000948.1_cds_NP_051200.1_859	7072.92180	1.01694	0.34463	2.95083	3.1692E-03	1.3359E-02
BB_S15	lcl|NC_000949.1_cds_NP_051218.1_876	10.07083	2.31542	0.80661	2.87056	4.0974E-03	1.6734E-02

BB_S26	lcl|NC_000949.1_cds_NP_051229.2_886	135.85820	1.00586	0.34907	2.88153	3.9575E-03	1.6319E-02
BB_S31	lcl|NC_000949.1_cds_NP_051234.2_890	105.76745	-1.26827	0.50405	-2.51613	1.1865E-02	4.1491E-02
BB_S35	lcl|NC_000949.1_cds_NP_051238.1_893	265.73103	1.02294	0.24110	4.24281	2.2100E-05	1.7166E-04
bdrE	lcl|NC_000949.1_cds_NP_051240.1_894	326.73654	1.38462	0.24237	5.71294	1.1100E-08	1.7800E-07
BB_R25	lcl|NC_000950.1_cds_NP_051272.1_925	73.69031	1.56785	0.47258	3.31765	9.0777E-04	4.8065E-03
bdrH	lcl|NC_000950.1_cds_NP_051274.2_927	752.05999	-1.40743	0.23927	-5.88221	4.0500E-09	7.1100E-08
BB_R34	lcl|NC_000950.1_cds_NP_051281.1_933	206.01635	1.06212	0.21925	4.84427	1.2700E-06	1.2700E-05
BB_M25	lcl|NC_000951.1_cds_NP_051316.1_965	73.66911	1.56778	0.47277	3.31614	9.1270E-04	4.8065E-03
BB_O32	lcl|NC_000952.1_cds_NP_051365.1_1013	381.81421	1.01708	0.24524	4.14728	3.3600E-05	2.5131E-04
BB_O35	lcl|NC_000952.1_cds_NP_051368.1_1016	19.61632	1.53154	0.61461	2.49190	1.2706E-02	4.3593E-02
erpM	lcl|NC_000952.1_cds_NP_051373.1_1021	506.31238	1.17864	0.24099	4.89077	1.0000E-06	1.0300E-05
BB_L10	lcl|NC_000953.1_cds_NP_051387.1_1034	89.29313	-1.80857	0.56895	-3.17880	1.4788E-03	7.3211E-03
BB_L15	lcl|NC_000953.1_cds_NP_051392.1_1039	57.75190	-1.51185	0.53321	-2.83538	4.5771E-03	1.8471E-02
erpO	lcl|NC_000953.1_cds_NP_051417.1_1062	7072.82966	1.01694	0.34462	2.95088	3.1687E-03	1.3359E-02
BB_N31	lcl|NC_000954.1_cds_NP_051443.1_1087	161.08556	1.59706	0.34921	4.57338	4.8000E-06	4.3000E-05
BB_N32	lcl|NC_000954.1_cds_NP_051444.1_1088	241.99693	1.72863	0.30894	5.59530	2.2000E-08	3.2100E-07
BB_N33	lcl|NC_000954.1_cds_NP_051445.1_1089	157.32165	1.90141	0.28879	6.58398	4.5800E-11	1.1100E-09
bdrQ	lcl|NC_000954.1_cds_NP_051446.1_1090	227.79632	1.58497	0.26408	6.00177	1.9500E-09	3.6900E-08
erpQ	lcl|NC_000954.1_cds_NP_051450.1_1094	1968.30569	1.24087	0.36008	3.44612	5.6870E-04	3.2609E-03
BB_D13	lcl|NC_001849.2_cds_NP_045397.1_1115	908.20998	-1.44679	0.30477	-4.74717	2.0600E-06	1.9400E-05
BB_D14	lcl|NC_001849.2_cds_NP_045398.1_1116	3487.08319	-1.95219	0.32696	-5.97068	2.3600E-09	4.3900E-08
BB_D15	lcl|NC_001849.2_cds_NP_045399.2_1117	1008.77152	-1.19758	0.19885	-6.02263	1.7200E-09	3.3200E-08
BB_D21	lcl|NC_001849.2_cds_NP_045404.1_1119	967.68593	-1.85289	0.44007	-4.21045	2.5500E-05	1.9463E-04
BB_D22	lcl|NC_001849.2_cds_NP_045405.1_1120	128.56257	-1.39609	0.31811	-4.38872	1.1400E-05	9.3800E-05
BB_D0031	lcl|NC_001849.2_cds_YP_004940417.1_1121	25.13307	-2.33283	0.70063	-3.32961	8.6968E-04	4.7318E-03
BB_F03	lcl|NC_001851.2_cds_NP_045439.1_1144	189.08402	1.75394	0.35531	4.93638	7.9600E-07	8.4700E-06
BB_F23	lcl|NC_001851.2_cds_NP_045456.1_1151	367.92274	2.20505	0.25695	8.58173	9.3500E-18	4.5500E-16
BB_F25	lcl|NC_001851.2_cds_NP_045458.1_1153	156.06800	1.05922	0.43576	2.43078	1.5066E-02	4.9437E-02
BB_G12	lcl|NC_001852.1_cds_NP_045472.1_1163	81.95387	-2.20532	0.67061	-3.28855	1.0070E-03	5.1969E-03
BB_G22	lcl|NC_001852.1_cds_NP_045482.1_1174	64.42227	-3.12561	0.64182	-4.86995	1.1200E-06	1.1300E-05
BB_G24	lcl|NC_001852.1_cds_NP_045484.2_1176	50.67292	-1.45041	0.56138	-2.58363	9.7765E-03	3.5652E-02
BB_G25	lcl|NC_001852.1_cds_NP_045485.1_1177	3.96162	-2.09091	0.85482	-2.44603	1.4444E-02	4.7594E-02
BB_G29	lcl|NC_001852.1_cds_NP_045489.1_1181	357.36922	-1.00911	0.37730	-2.67457	7.4825E-03	2.8443E-02
BB_G31	lcl|NC_001852.1_cds_NP_045491.2_1183	41.00950	-1.49032	0.46959	-3.17367	1.5053E-03	7.4303E-03
BB_H17	lcl|NC_001853.1_cds_NP_045510.1_1195	10.29556	-2.14867	0.80072	-2.68342	7.2872E-03	2.7825E-02
BB_H26	lcl|NC_001853.1_cds_NP_045517.1_1197	1195.44669	-1.14494	0.46106	-2.48330	1.3017E-02	4.4248E-02
BB_K01	lcl|NC_001855.1_cds_NP_045575.1_1225	1354.45058	1.45603	0.33410	4.35803	1.3100E-05	1.0593E-04
BB_K23	lcl|NC_001855.1_cds_NP_045597.1_1234	2453.83614	-1.42525	0.38678	-3.68488	2.2881E-04	1.4816E-03
BB_K24	lcl|NC_001855.1_cds_NP_045598.1_1235	377.57698	-1.45242	0.43696	-3.32396	8.8750E-04	4.7927E-03
BB_K33	lcl|NC_001855.1_cds_NP_045606.1_1238	37.62541	-1.38194	0.44482	-3.10676	1.8915E-03	8.8986E-03
BB_K40	lcl|NC_001855.1_cds_NP_045612.1_1242	3811.74482	-1.25835	0.23171	-5.43069	5.6100E-08	7.3500E-07
BB_K47	lcl|NC_001855.1_cds_NP_045618.1_1246	2505.67165	1.67722	0.31704	5.29021	1.2200E-07	1.4700E-06
BB_K49	lcl|NC_001855.1_cds_NP_045620.1_1248	1392.93963	1.63203	0.35449	4.60395	4.1500E-06	3.7600E-05
BB_K53	lcl|NC_001855.1_cds_NP_045624.1_1252	359.83957	-1.24036	0.48431	-2.56107	1.0435E-02	3.7334E-02

BB_J09	lcl|NC_001856.1_cds_NP_045633.1_1254	24951.96368	1.39691	0.37730	3.70236	2.1361E-04	1.3884E-03
BB_J18	lcl|NC_001856.1_cds_NP_045642.1_1259	652.40141	-1.21354	0.49348	-2.45913	1.3927E-02	4.6598E-02
BB_J19	lcl|NC_001856.1_cds_NP_045643.1_1260	8721.99449	-1.17852	0.35743	-3.29718	9.7661E-04	5.0552E-03
BB_J24	lcl|NC_001856.1_cds_NP_045648.1_1264	96.33456	-1.44666	0.37916	-3.81544	1.3594E-04	9.1144E-04
BB_J36	lcl|NC_001856.1_cds_NP_045660.1_1272	1399.44454	-1.03854	0.23544	-4.41111	1.0300E-05	8.5400E-05
BB_J37	lcl|NC_001856.1_cds_NP_045661.2_1273	15.94581	-1.80958	0.69423	-2.60661	9.1443E-03	3.3490E-02
BB_J43	lcl|NC_001856.1_cds_NP_045667.1_1276	43.39694	-1.68354	0.66952	-2.51453	1.1919E-02	4.1513E-02
BB_J45	lcl|NC_001856.1_cds_NP_045669.1_1277	396.44271	-1.38960	0.38796	-3.58180	3.4124E-04	2.1209E-03
BB_A03	lcl|NC_001857.2_cds_NP_045676.1_1287	12443.29488	2.36516	0.33649	7.02897	2.0800E-12	5.9100E-11
BB_A04	lcl|NC_001857.2_cds_NP_045677.1_1288	322.05765	1.18668	0.43938	2.70082	6.9170E-03	2.6711E-02
BB_A23	lcl|NC_001857.2_cds_NP_045696.2_1302	697.32621	-1.50946	0.58734	-2.57002	1.0169E-02	3.6573E-02
dbpA	lcl|NC_001857.2_cds_NP_045697.1_1303	424.40618	-1.29417	0.53236	-2.43101	1.5057E-02	4.9437E-02
BB_A30	lcl|NC_001857.2_cds_NP_045703.1_1305	869.61499	1.58222	0.21686	7.29613	2.9600E-13	9.0100E-12
BB_A31	lcl|NC_001857.2_cds_NP_045704.1_1306	693.65642	1.99326	0.26890	7.41253	1.2400E-13	4.1400E-12
BB_A32	lcl|NC_001857.2_cds_NP_045705.1_1307	110.74219	1.11056	0.32443	3.42311	6.1910E-04	3.5144E-03
BB_A34	lcl|NC_001857.2_cds_NP_045707.1_1309	190.08384	-1.75906	0.57717	-3.04771	2.3059E-03	1.0416E-02
BB_A37	lcl|NC_001857.2_cds_NP_045710.1_1311	93.94412	-1.86769	0.65266	-2.86168	4.2140E-03	1.7127E-02
BB_A52	lcl|NC_001857.2_cds_NP_045725.1_1323	1613.06144	1.07870	0.31276	3.44902	5.6262E-04	3.2590E-03
BB_A53	lcl|NC_001857.2_cds_NP_045726.1_1324	375.69121	1.38055	0.37584	3.67323	2.3950E-04	1.5334E-03
BB_A54	lcl|NC_001857.2_cds_NP_045727.1_1325	599.96245	1.95210	0.36710	5.31758	1.0500E-07	1.2900E-06
BB_A58	lcl|NC_001857.2_cds_NP_045731.1_1327	8350.06409	1.31910	0.29668	4.44625	8.7400E-06	7.3700E-05
BB_A60	lcl|NC_001857.2_cds_NP_045733.1_1329	1031.73146	1.63033	0.22173	7.35286	1.9400E-13	6.1200E-12
BB_A66	lcl|NC_001857.2_cds_NP_045739.1_1334	625.48633	1.00938	0.33861	2.98095	2.8735E-03	1.2389E-02
osm28	lcl|NC_001857.2_cds_NP_045747.1_1339	12273.60539	2.10264	0.39422	5.33374	9.6200E-08	1.2000E-06
BB_Q05	lcl|NC_000956.1_cds_NP_051469.1_1342	100.93680	1.79670	0.59584	3.01542	2.5662E-03	1.1411E-02
BB_Q27	lcl|NC_000956.1_cds_NP_051489.1_1361	184.69201	2.14346	0.44678	4.79760	1.6100E-06	1.5600E-05
BB_Q29	lcl|NC_000956.1_cds_NP_051491.1_1363	93.20451	1.48726	0.36228	4.10530	4.0400E-05	2.9640E-04
BB_Q32	lcl|NC_000956.1_cds_NP_051494.1_1366	73.68259	1.56809	0.47196	3.32251	8.9213E-04	4.7927E-03
BB_Q40	lcl|NC_000956.1_cds_NP_051502.1_1373	481.17033	1.26206	0.36821	3.42753	6.0909E-04	3.4692E-03
bdrV	lcl|NC_000956.1_cds_NP_051504.1_1374	634.19622	2.37238	0.31762	7.46914	8.0700E-14	2.8100E-12
BB_Q62	lcl|NC_000956.1_cds_NP_051521.1_1385	20.48709	3.14255	0.53526	5.87107	4.3300E-09	7.5200E-08

The included transcripts met the criteria of >1 log2 fold-change and an adjusted P-value (padj) when comparing the Δ*badR* mutant to wild-type sorted by fold change. A total of 239 transcripts were differentially regulated, not including the mutated gene, by the mutation. The first column contains the CDS/custom transcript ID which is the transcript ID for all coding sequences obtained from the NCBI Gene file format file or the transcript ID given to ncRNAs. RefSeq entries are further separated by the character "_". The first portion gives the genetic element from which it is derived, the second describes the type of element (CDS), the third provides RefSeq ID, and

the fourth provides a number indicating the particular entries ordered number in the RefSeq entry. The second column is the gene information, for the ncRNAs it contains the location relative to other genes and for predicted or known genes it contains gene name. The remaining columns describe the various metrics of expression of each impacted transcript including, base mean (average library size normalized counts across all samples), log2FC (Fold change estimate), lfcSE (uncertainty of the log fold change estimate), stat (Wald statistic), pvalue, padj (pvalue following Benjamini-Hochberg adjustment). ORFs and ncRNAs are identified according to the names or numbers assigned to genes and transcripts by the initial genome sequencing of *B. burgdorferi* strain B31 [56, 101] or from our previous analyses of that strain's ncRNA transcriptome [14].

Table 8-9 Differentially abundant transcripts comparing WT to Δ*csrA*

Gene Name	RefSeq CDS/Custom Transcript ID	baseMean	Log2 FC	lfcSE	stat	pvalue	padj
AI-(BB_0004,BB_0004/BB_0005)	ncRNA0002	3041.85842	-1.36714	0.24879	-5.49508	3.9100E-08	7.5600E-07
AA-(BB_0005,BB_0006)	ncRNA0003	1243.57656	-1.54533	0.31157	-4.95977	7.0600E-07	1.0300E-05
A-(BB_0013)	ncRNA0006	3033.89498	-1.60870	0.33963	-4.73659	2.1700E-06	2.7400E-05
A-(BB_0014)	ncRNA0007	214.85270	-1.21565	0.48187	-2.52277	1.1643E-02	4.0193E-02
A-(BB_0084)	ncRNA0014	380.54610	-1.35790	0.38875	-3.49295	4.7771E-04	2.8849E-03
AA-(BB_0198,BB_0199)	ncRNA0031	400.71340	-1.33223	0.37396	-3.56255	3.6727E-04	2.3603E-03
A-(BB_0208)	ncRNA0035	510.91058	-1.07338	0.29111	-3.68721	2.2673E-04	1.5262E-03
A-(BB_0211)	ncRNA0037	1238.76926	-1.36930	0.31459	-4.35262	1.3500E-05	1.3476E-04
A-(BB_0240)	ncRNA0042	2021.45874	-1.87999	0.34911	-5.38509	7.2400E-08	1.3300E-06
A-(BB_0244)	ncRNA0043	577.79571	-1.25665	0.40387	-3.11154	1.8611E-03	9.0300E-03
AIA-(BB_0269,BB_0269/BB_0270,BB_0270)	ncRNA0050	1285.29820	-1.69651	0.55613	-3.05059	2.2839E-03	1.0686E-02
A-(BB_0347)	ncRNA0057	34.51260	-1.88774	0.54860	-3.44101	5.7954E-04	3.3685E-03
A-(BB_0381)	ncRNA0063	391.05521	-1.63583	0.43307	-3.77733	1.5852E-04	1.1202E-03
A-(BB_0446)	ncRNA0070	529.31721	-1.78518	0.31267	-5.70938	1.1300E-08	2.5400E-07
A-(BB_0450)	ncRNA0071	65.28090	-4.68307	0.69731	-6.71589	1.8700E-11	7.7600E-10
A-(BB_0454)	ncRNA0072	396.65108	2.95600	0.65946	4.48249	7.3800E-06	8.1600E-05
I-(BB_t06/BB_0461)	ncRNA0073	2784.93399	1.30508	0.23004	5.67324	1.4000E-08	3.1000E-07
p-(BB_0522)	ncRNA0080	879.81309	-1.66871	0.23588	-7.07443	1.5000E-12	6.7300E-11
A-(BB_0581)	ncRNA0084	87.52936	-1.86383	0.46531	-4.00556	6.1900E-05	4.9008E-04
A-(BB_0588)	ncRNA0087	1536.15642	-1.98302	0.70918	-2.79621	5.1706E-03	2.0916E-02
A-(BB_0633)	ncRNA0099	150.86401	-2.11214	0.59679	-3.53920	4.0135E-04	2.5315E-03
AIA-(BB_0794,BB_0794/BB_0795,BB_0795)	ncRNA0125	2242.03629	-1.51380	0.26026	-5.81640	6.0100E-09	1.4200E-07
pI-(BB_0845a,BB_0845a/BB_0845b)	ncRNA0132	211.25465	-1.88231	0.53454	-3.52136	4.2935E-04	2.6492E-03
A-(BB_B03)	ncRNA0133	471.62837	-1.01768	0.24563	-4.14310	3.4300E-05	2.9925E-04
AI-(BB_B09,BB_B09/BB_B10)	ncRNA0136	476.36984	-1.31493	0.35221	-3.73333	1.8897E-04	1.3029E-03
AIA-(BB_P01,BB_P01/BB_P02,BB_P02)	ncRNA0144	5.38658	-2.40525	0.85509	-2.81287	4.9102E-03	2.0150E-02
A-(BB_P21)	ncRNA0148	93.09626	-1.05797	0.42004	-2.51875	1.1777E-02	4.0193E-02

IA-(BB_P32/BB_P33,BB_P33)	ncRNA0152	276.35152	2.16730	0.36494	5.93882	2.8700E-09	7.6400E-08
AIA-(BB_P35,BB_P35/BB_P36,BB_P36)	ncRNA0153	34.01766	-1.98207	0.79874	-2.48151	1.3083E-02	4.3686E-02
A-(BB_R43)	ncRNA0168	73.05907	-1.33932	0.46258	-2.89530	3.7879E-03	1.6127E-02
I-(BB_O29/BB_O30)	ncRNA0185	1573.01516	1.54399	0.47773	3.23193	1.2296E-03	6.4036E-03
AIA-(BB_O32,BB_O32/BB_O33,BB_O33)	ncRNA0186	90.75800	1.56315	0.32570	4.79931	1.5900E-06	2.0600E-05
A-(BB_O36)	ncRNA0187	30.42656	-1.80347	0.72033	-2.50366	1.2291E-02	4.1403E-02
A-(BB_O44)	ncRNA0191	8.70865	-2.53078	0.79762	-3.17293	1.5091E-03	7.5146E-03
IA-(BB_L29/BB_L30,BB_L30)	ncRNA0200	867.04480	-1.76368	0.35213	-5.00855	5.4800E-07	8.1200E-06
IA-(BB_N32/BB_N33,BB_N33)	ncRNA0218	29.86142	2.06059	0.51686	3.98676	6.7000E-05	5.2566E-04
P-(BB_D05a)	ncRNA0226	56.82862	-5.38102	0.67964	-7.91751	2.4200E-15	1.2900E-13
I-(BB_D18/BB_D20)	ncRNA0229	117.85300	-1.45064	0.34542	-4.19961	2.6700E-05	2.4882E-04
p-(BB_D20)	ncRNA0231	3348.60358	-1.31010	0.38751	-3.38080	7.2276E-04	4.0892E-03
I-(BB_D22/BB_D23)	ncRNA0232	141.50067	-1.09254	0.25214	-4.33312	1.4700E-05	1.4641E-04
p-(BB_D23)	ncRNA0233	46.44976	-2.61541	0.75070	-3.48395	4.9407E-04	2.9732E-03
A-(BB_E09)	ncRNA0239	1464.22355	-2.36320	0.42819	-5.51901	3.4100E-08	6.9100E-07
A-(BB_E09)	ncRNA0240	74.83749	-2.99150	0.85344	-3.50523	4.5621E-04	2.7648E-03
I-(BB_E23b/BB_E29a)	ncRNA0242	107.05005	-1.83201	0.59248	-3.09208	1.9876E-03	9.5347E-03
I-(BB_E31/BB_E33)	ncRNA0245	314.76149	-1.87552	0.48535	-3.86424	1.1144E-04	8.2511E-04
I-(BB_E31/BB_E33)	ncRNA0246	124.51613	-1.36783	0.43230	-3.16405	1.5559E-03	7.7252E-03
A-(BB_F03)	ncRNA0247	1699.00234	-3.04305	0.29398	-10.35133	4.1300E-25	5.4100E-23
AIP-(BB_F03,BB_F03/BB_F05,BB_F05)	ncRNA0248	239.22758	-1.69134	0.55610	-3.04145	2.3545E-03	1.0985E-02
pI-(BB_F05,BB_F05/BB_F06)	ncRNA0249	9.67900	-2.37442	0.74116	-3.20366	1.3569E-03	6.9319E-03
PI-(BB_F11a,BB_F11a/BB_F12)	ncRNA0250	15.60877	-2.95591	0.73380	-4.02824	5.6200E-05	4.5389E-04
I-(BB_F11a/BB_F12)	ncRNA0251	727.74533	-3.62895	0.25387	-14.29478	2.3600E-46	1.0000E-43
Ip-(BB_F14/BB_F14a,BB_F14a)	ncRNA0252	58.86305	-1.38969	0.45918	-3.02643	2.4746E-03	1.1514E-02

pIp-(BB_F14a,BB_F14a/BB_F16,BB_F16)	ncRNA0253	16.14596	-1.98672	0.79362	-2.50337	1.2302E-02	4.1403E-02
I-(BB_F0040/BB_F32)	ncRNA0255	49.42843	-2.20005	0.63767	-3.45014	5.6030E-04	3.2790E-03
PI-(BB_G05,BB_G05/BB_G06)	ncRNA0257	56.23394	-3.08570	0.78871	-3.91233	9.1400E-05	6.9495E-04
AA-(BB_G07,BB_G08)	ncRNA0259	88.14975	1.50710	0.26069	5.78118	7.4200E-09	1.7100E-07
IA-(BB_G28/BB_G29,BB_G29)	ncRNA0263	24.07894	-1.66874	0.65024	-2.56633	1.0278E-02	3.6239E-02
P-(BB_H30)	ncRNA0271	22.38916	-1.76720	0.65562	-2.69548	7.0288E-03	2.6366E-02
IpI-(BB_K09/BB_K10,BB_K10,BB_K10/BB_K12)	ncRNA0281	166.24839	-1.67274	0.50558	-3.30857	9.3773E-04	5.0536E-03
A-(BB_K17)	ncRNA0284	123.82711	-2.27394	0.29672	-7.66354	1.8100E-14	8.8000E-13
A-(BB_K19)	ncRNA0285	59.46916	-1.71066	0.51499	-3.32174	8.9459E-04	4.8829E-03
A-(BB_K19)	ncRNA0286	219.94179	-1.50018	0.49802	-3.01233	2.5925E-03	1.1877E-02
I-(BB_K55/BB_K56)	ncRNA0287	86.56071	-2.02386	0.57269	-3.53396	4.0939E-04	2.5632E-03
AIA-(BB_K33,BB_K33/BB_K34,BB_K34)	ncRNA0289	54.01824	-1.71061	0.41699	-4.10228	4.0900E-05	3.4835E-04
A-(BB_J18)	ncRNA0297	206.52360	-2.30714	0.68815	-3.35269	8.0030E-04	4.4394E-03
I-(BB_J20/BB_J0058)	ncRNA0299	119.12666	-1.71310	0.32271	-5.30853	1.1100E-07	1.9000E-06
I-(BB_J20/BB_J0058)	ncRNA0300	169.44276	-1.62217	0.54796	-2.96038	3.0726E-03	1.3687E-02
I-(BB_J37/BB_J41)	ncRNA0304	103.27966	-1.32101	0.48244	-2.73820	6.1776E-03	2.3910E-02
I-(BB_J37/BB_J41)	ncRNA0306	3515.78937	1.03960	0.35567	2.92291	3.4678E-03	1.4951E-02
IA-(BB_J37/BB_J41,BB_J41)	ncRNA0307	1187.10572	1.02844	0.37532	2.74014	6.1413E-03	2.3824E-02
I-(BB_J50/BB_J51)	ncRNA0308	893.05821	-5.42145	0.49484	-10.95597	6.2200E-28	1.0600E-25
Ip-(BB_J50/BB_J51,BB_J51)	ncRNA0310	106.49195	-1.60068	0.60746	-2.63505	8.4125E-03	3.0810E-02
A-(BB_A04)	ncRNA0311	361.98141	1.92915	0.41140	4.68926	2.7400E-06	3.3600E-05
IP-(BB_A16/BB_A18,BB_A18)	ncRNA0318	1800.37672	-2.04790	0.56668	-3.61387	3.0166E-04	1.9835E-03
I-(BB_A37/BB_A38)	ncRNA0322	2507.45399	-1.93472	0.46456	-4.16467	3.1200E-05	2.7656E-04
A-(BB_A66)	ncRNA0325	457.92944	-1.54003	0.33922	-4.53991	5.6300E-06	6.3500E-05
I-(BB_A66/BB_A68)	ncRNA0326	456.29968	1.39790	0.36727	3.80618	1.4113E-04	1.0141E-03
I-(BB_A68/BB_A69)	ncRNA0327	288.56940	1.13475	0.41155	2.75730	5.8281E-03	2.2764E-02
I-(BB_A73/BB_A74)	ncRNA0328	55.68358	-1.57915	0.64646	-2.44275	1.4576E-02	4.7921E-02
A-(BB_Q52)	ncRNA0344	10.93289	-2.49207	0.85894	-2.90133	3.7158E-03	1.5860E-02

IA-(BB_Q85/BB_Q88,BB_Q88)	ncRNA0353	66.89125	-1.49930	0.61692	-2.43030	1.5087E-02	4.9219E-02
BB_0004	lcl|NC_001318.1_cds_NP_212138.2_3	3213.61271	-1.01184	0.35019	-2.88940	3.8597E-03	1.6311E-02
ruvB	lcl|NC_001318.1_cds_NP_212156.1_20	2074.85845	-1.07657	0.20208	-5.32751	9.9600E-08	1.7500E-06
BB_0027	lcl|NC_001318.1_cds_NP_212161.1_25	9710.08595	-1.78806	0.33744	-5.29896	1.1600E-07	1.9600E-06
BB_0035	lcl|NC_001318.1_cds_NP_212169.1_33	2717.90772	1.11041	0.21469	5.17204	2.3200E-07	3.6500E-06
BB_0172	lcl|NC_001318.1_cds_NP_212306.2_161	2887.76489	-1.21732	0.12374	-9.83751	7.7600E-23	8.8100E-21
csrA	lcl|NC_001318.1_cds_NP_212318.1_173	568.07262	-7.89432	0.51931	-15.20141	3.4600E-52	1.9600E-49
BB_0185	lcl|NC_001318.1_cds_NP_212319.1_174	1345.32378	1.34977	0.21874	6.17069	6.8000E-10	1.9300E-08
BB_0285	lcl|NC_001318.1_cds_NP_212419.2_270	4139.07947	-1.15495	0.31761	-3.63636	2.7651E-04	1.8395E-03
BB_0330	lcl|NC_001318.1_cds_NP_212464.1_313	9233.47510	1.14909	0.21901	5.24680	1.5500E-07	2.5600E-06
BB_0334	lcl|NC_001318.1_cds_NP_212468.1_317	3335.87046	1.04932	0.15772	6.65313	2.8700E-11	1.1400E-09
mgsA	lcl|NC_001318.1_cds_NP_212498.1_345	3019.34634	1.74256	0.16475	10.57677	3.8200E-26	5.4200E-24
la7	lcl|NC_001318.1_cds_NP_212499.1_346	8401.74564	1.81349	0.28233	6.42324	1.3300E-10	4.0900E-09
manA	lcl|NC_001318.1_cds_NP_212541.1_388	2887.10319	1.17975	0.14930	7.90190	2.7500E-15	1.4200E-13
BB_0408	lcl|NC_001318.1_cds_NP_212542.1_389	6219.62582	1.50125	0.22207	6.76041	1.3800E-11	5.8600E-10
BB_0415	lcl|NC_001318.1_cds_NP_212549.1_394	1448.60433	-1.23145	0.22193	-5.54874	2.8800E-08	5.9800E-07
BB_0434	lcl|NC_001318.1_cds_NP_212568.1_409	410.65472	-1.02624	0.30576	-3.35635	7.8977E-04	4.4098E-03
BB_0451	lcl|NC_001318.1_cds_NP_212585.1_426	435.99128	1.06529	0.20899	5.09729	3.4500E-07	5.3300E-06
rpmC	lcl|NC_001318.1_cds_NP_212620.2_459	492.18291	1.00774	0.20234	4.98052	6.3400E-07	9.3100E-06
BB_0509	lcl|NC_001318.1_cds_NP_212643.1_482	8232.92191	-2.92550	0.36573	-7.99904	1.2500E-15	6.8900E-14
dnaK	lcl|NC_001318.1_cds_NP_212652.1_488	5264.98352	1.17822	0.19904	5.91943	3.2300E-09	8.2100E-08
BB_0537	lcl|NC_001318.1_cds_NP_212671.1_500	1848.25226	1.23238	0.23828	5.17209	2.3100E-07	3.6500E-06
BB_0538	lcl|NC_001318.1_cds_NP_212672.1_501	967.74510	1.12146	0.23907	4.69092	2.7200E-06	3.3600E-05
BB_0562	lcl|NC_001318.1_cds_NP_212696.1_524	1222.60891	1.19559	0.14703	8.13164	4.2400E-16	2.4900E-14
BB_0577	lcl|NC_001318.1_cds_NP_212711.1_539	1867.11586	-1.43804	0.22294	-6.45042	1.1200E-10	3.5900E-09
BB_0588	lcl|NC_001318.1_cds_NP_212722.1_550	1645.23671	-1.76961	0.13087	-13.52170	1.1600E-41	3.3100E-39
BB_0617	lcl|NC_001318.1_cds_NP_212751.1_578	777.72142	1.01563	0.22639	4.48609	7.2500E-06	8.0700E-05
rnmV	lcl|NC_001318.1_cds_NP_212760.1_587	17091.35904	-1.23733	0.41006	-3.01746	2.5491E-03	1.1824E-02
BB_0637	lcl|NC_001318.1_cds_NP_212771.2_597	8048.19773	1.09516	0.26134	4.19047	2.7800E-05	2.5591E-04
BB_0638	lcl|NC_001318.1_cds_NP_212772.1_598	3886.71871	1.10557	0.20998	5.26502	1.4000E-07	2.3400E-06
BB_0639	lcl|NC_001318.1_cds_NP_212773.1_599	1482.68946	1.25421	0.28693	4.37118	1.2400E-05	1.2527E-04
BB_0644	lcl|NC_001318.1_cds_NP_212778.1_604	697.38844	1.07361	0.19917	5.39034	7.0300E-08	1.3200E-06
BB_0678	lcl|NC_001318.1_cds_NP_212812.1_638	5061.70052	1.19085	0.18463	6.45005	1.1200E-10	3.5900E-09
BB_0679	lcl|NC_001318.1_cds_NP_212813.2_639	4281.29084	1.08726	0.19246	5.64926	1.6100E-08	3.4700E-07
ffh	lcl|NC_001318.1_cds_NP_212828.2_653	14060.76269	-2.51168	0.37419	-6.71235	1.9200E-11	7.7700E-10
BB_0724	lcl|NC_001318.1_cds_YP_008686588.1_680	3690.87567	-1.14649	0.26750	-4.28595	1.8200E-05	1.7607E-04
cvpA	lcl|NC_001318.1_cds_NP_212900.1_719	420.51092	1.15754	0.23978	4.82754	1.3800E-06	1.8600E-05
murG	lcl|NC_001318.1_cds_NP_212901.1_720	901.26760	1.36619	0.28113	4.85964	1.1800E-06	1.6200E-05
BB_0768	lcl|NC_001318.1_cds_NP_212902.1_721	1156.42566	1.01241	0.23459	4.31566	1.5900E-05	1.5664E-04
BB_0769	lcl|NC_001318.1_cds_NP_212903.1_722	1653.77636	1.25352	0.24092	5.20315	1.9600E-07	3.1800E-06
BB_0770	lcl|NC_001318.1_cds_NP_212904.1_723	1364.05445	1.31817	0.24452	5.39077	7.0200E-08	1.3200E-06
BB_0773	lcl|NC_001318.1_cds_NP_212907.1_727	467.79866	1.27392	0.17883	7.12344	1.0500E-12	4.8400E-11

BB_0785	lcl|NC_001318.1_cds_NP_212919.1_739	2664.70377	1.26140	0.21198	5.95051	2.6700E-09	7.2300E-08
BB_0794	lcl|NC_001318.1_cds_YP_008686594.1_748	8844.21241	-1.02084	0.17424	-5.85885	4.6600E-09	1.1500E-07
BB_0798	lcl|NC_001318.1_cds_NP_212932.1_752	412.74295	-1.36726	0.23061	-5.92898	3.0500E-09	7.9400E-08
arcA	lcl|NC_001318.1_cds_NP_212975.1_793	2690.75653	1.01162	0.15753	6.42193	1.3500E-10	4.0900E-09
argF	lcl|NC_001318.1_cds_NP_212976.2_794	2452.38136	1.16126	0.24793	4.68373	2.8200E-06	3.4300E-05
BB_B01	lcl|NC_001903.1_cds_NP_046987.2_798	877.53814	1.38832	0.21556	6.44047	1.1900E-10	3.7600E-09
BB_B02	lcl|NC_001903.1_cds_NP_046988.1_799	2128.09907	1.09381	0.19651	5.56617	2.6000E-08	5.4700E-07
BB_B04	lcl|NC_001903.1_cds_NP_046990.2_801	11469.16755	1.51829	0.22423	6.77099	1.2800E-11	5.5800E-10
BB_B05	lcl|NC_001903.1_cds_NP_046991.1_802	2551.06647	1.80247	0.27613	6.52767	6.6800E-11	2.4200E-09
BB_B06	lcl|NC_001903.1_cds_NP_046992.2_803	1687.19872	2.39923	0.26394	9.08997	9.9100E-20	8.8800E-18
BB_B07	lcl|NC_001903.1_cds_NP_046993.1_804	8409.80978	1.37986	0.16316	8.45724	2.7400E-17	1.7900E-15
guaA	lcl|NC_001903.1_cds_NP_047004.2_812	11235.00282	1.12297	0.13674	8.21263	2.1600E-16	1.3200E-14
BB_B19	lcl|NC_001903.1_cds_NP_047005.1_813	292.24252	-1.44479	0.48707	-2.96630	3.0140E-03	1.3508E-02
BB_B23	lcl|NC_001903.1_cds_NP_047009.2_815	2583.01398	1.19428	0.15392	7.75903	8.5600E-15	4.2900E-13
BB_B27	lcl|NC_001903.1_cds_NP_047013.1_819	1716.86092	1.09086	0.18403	5.92752	3.0800E-09	7.9400E-08
BB_B28	lcl|NC_001903.1_cds_NP_047014.1_820	4249.14215	1.26673	0.14368	8.81609	1.1900E-18	9.1800E-17
BB_B29	lcl|NC_001903.1_cds_NP_047015.1_821	24118.64600	1.40725	0.21269	6.61638	3.6800E-11	1.4200E-09
BB_P10	lcl|NC_000948.1_cds_NP_051171.1_830	89.29313	-1.66558	0.56815	-2.93158	3.3724E-03	1.4651E-02
BB_P29	lcl|NC_000948.1_cds_NP_051190.1_849	117.59027	-1.92535	0.65110	-2.95706	3.1059E-03	1.3738E-02
BB_P31	lcl|NC_000948.1_cds_NP_051192.1_851	319.42777	1.45061	0.33148	4.37613	1.2100E-05	1.2328E-04
BB_P32	lcl|NC_000948.1_cds_NP_051193.1_852	812.84291	1.90916	0.23564	8.10216	5.4000E-16	3.0600E-14
BB_P33	lcl|NC_000948.1_cds_NP_051194.2_853	507.55300	2.13541	0.24544	8.70025	3.3100E-18	2.4500E-16
bdrA	lcl|NC_000948.1_cds_NP_051195.1_854	840.20823	1.32762	0.30269	4.38603	1.1500E-05	1.1915E-04
bppA	lcl|NC_000948.1_cds_NP_051196.1_855	59.03590	-1.40683	0.55848	-2.51902	1.1768E-02	4.0193E-02
bppB	lcl|NC_000948.1_cds_NP_051197.1_856	16.41223	-1.50057	0.59553	-2.51971	1.1745E-02	4.0193E-02
BB_S31	lcl|NC_000949.1_cds_NP_051234.2_890	105.76745	-1.61577	0.50478	-3.20094	1.3698E-03	6.9634E-03
BB_S34	lcl|NC_000949.1_cds_NP_051237.1_892	208.77819	1.12270	0.37216	3.01674	2.5551E-03	1.1824E-02
BB_S35	lcl|NC_000949.1_cds_NP_051238.1_893	265.73103	1.32530	0.23976	5.52756	3.2500E-08	6.6600E-07
bdrE	lcl|NC_000949.1_cds_NP_051240.1_894	326.73654	1.35838	0.24208	5.61123	2.0100E-08	4.2800E-07
bppA	lcl|NC_000949.1_cds_NP_051241.2_895	41.41867	-2.50757	0.64449	-3.89080	9.9900E-05	7.5289E-04
bdrH	lcl|NC_000950.1_cds_NP_051274.2_927	752.05999	-1.01933	0.23870	-4.27032	1.9500E-05	1.8675E-04
BB_R31	lcl|NC_000950.1_cds_NP_051278.1_930	1579.32556	-1.11301	0.44312	-2.51176	1.2013E-02	4.0672E-02
BB_R33	lcl|NC_000950.1_cds_NP_051280.1_932	295.78915	1.07063	0.25471	4.20341	2.6300E-05	2.4602E-04
BB_R34	lcl|NC_000950.1_cds_NP_051281.1_933	206.01635	1.16113	0.21843	5.31579	1.0600E-07	1.8500E-06
bppA	lcl|NC_000950.1_cds_NP_051282.1_934	20.65803	-2.41916	0.67216	-3.59907	3.1935E-04	2.0758E-03
BB_M10	lcl|NC_000951.1_cds_NP_051301.1_951	26.57919	-1.78380	0.55298	-3.22580	1.2562E-03	6.5025E-03
erpK	lcl|NC_000951.1_cds_NP_051329.2_978	89.22936	-1.23805	0.47123	-2.62728	8.6071E-03	3.1253E-02
BB_M39	lcl|NC_000951.1_cds_NP_051330.1_979	174.83403	-1.36451	0.51840	-2.63215	8.4846E-03	3.1007E-02
BB_O05	lcl|NC_000952.1_cds_NP_051338.1_986	56.56386	-1.29221	0.46550	-2.77593	5.5044E-03	2.1851E-02
BB_O29	lcl|NC_000952.1_cds_NP_051362.1_1010	207.63259	-1.10670	0.44193	-2.50423	1.2272E-02	4.1403E-02
BB_O32	lcl|NC_000952.1_cds_NP_051365.1_1013	381.81421	1.02602	0.24502	4.18743	2.8200E-05	2.5591E-04
BB_O33	lcl|NC_000952.1_cds_NP_051366.1_1014	262.11731	1.01035	0.21034	4.80344	1.5600E-06	2.0400E-05
erpL	lcl|NC_000952.1_cds_NP_051372.1_1020	12.95800	-1.94971	0.71378	-2.73153	6.3041E-03	2.4180E-02
BB_L10	lcl|NC_000953.1_cds_NP_051387.1_1034	89.29313	-1.66558	0.56815	-2.93158	3.3724E-03	1.4651E-02

BB_N31	lcl|NC_000954.1_cds_NP_051443.1_1087	161.08556	1.62741	0.34882	4.66543	3.0800E-06	3.6900E-05
BB_N32	lcl|NC_000954.1_cds_NP_051444.1_1088	241.99693	1.58643	0.30895	5.13489	2.8200E-07	4.4100E-06
BB_N33	lcl|NC_000954.1_cds_NP_051445.1_1089	157.32165	1.88871	0.28826	6.55200	5.6800E-11	2.1000E-09
bdrQ	lcl|NC_000954.1_cds_NP_051446.1_1090	227.79632	1.70185	0.26326	6.46453	1.0200E-10	3.4600E-09
erpQ	lcl|NC_000954.1_cds_NP_051450.1_1094	1968.30569	1.45829	0.35989	4.05207	5.0800E-05	4.1566E-04
BB_D04	lcl|NC_001849.2_cds_NP_045388.1_1111	31.08243	-1.09455	0.42826	-2.55581	1.0594E-02	3.7123E-02
BB_D13	lcl|NC_001849.2_cds_NP_045397.1_1115	908.20998	-1.39490	0.30458	-4.57973	4.6600E-06	5.3600E-05
BB_D14	lcl|NC_001849.2_cds_NP_045398.1_1116	3487.08319	-1.74493	0.32686	-5.33844	9.3700E-08	1.6600E-06
BB_D21	lcl|NC_001849.2_cds_NP_045404.1_1119	967.68593	-1.89590	0.44002	-4.30864	1.6400E-05	1.5985E-04
BB_D22	lcl|NC_001849.2_cds_NP_045405.1_1120	128.56257	-1.23419	0.31627	-3.90230	9.5300E-05	7.2118E-04
BB_D0031	lcl|NC_001849.2_cds_YP_004940417.1_1121	25.13307	-2.77368	0.70351	-3.94261	8.0600E-05	6.2677E-04
BB_E09	lcl|NC_001850.1_cds_NP_045416.1_1133	524.59592	-1.11888	0.39643	-2.82240	4.7666E-03	1.9799E-02
BB_E21	lcl|NC_001850.1_cds_NP_045428.1_1139	8358.69302	-1.13151	0.25337	-4.46583	7.9800E-06	8.7600E-05
BB_E31	lcl|NC_001850.1_cds_NP_045436.1_1141	93.10927	-1.87910	0.38170	-4.92292	8.5300E-07	1.2100E-05
BB_F01	lcl|NC_001851.2_cds_YP_004940409.1_1142	9.14003	-1.99841	0.81867	-2.44104	1.4645E-02	4.7972E-02
BB_F03	lcl|NC_001851.2_cds_NP_045439.1_1144	189.08402	-2.28693	0.37858	-6.04085	1.5300E-09	4.2100E-08
BB_F06	lcl|NC_001851.2_cds_NP_045442.1_1145	11.18133	-2.26114	0.82738	-2.73287	6.2785E-03	2.4136E-02
BB_F08	lcl|NC_001851.2_cds_NP_045444.1_1146	152.54532	-1.25312	0.41564	-3.01495	2.5702E-03	1.1848E-02
BB_F0034	lcl|NC_001851.2_cds_YP_004940410.1_1147	131.68027	-1.22031	0.49845	-2.44823	1.4356E-02	4.7565E-02
BB_F14	lcl|NC_001851.2_cds_NP_045449.2_1148	47.65069	-3.14409	0.73615	-4.27096	1.9500E-05	1.8675E-04
BB_F17	lcl|NC_001851.2_cds_YP_004940411.1_1149	21.28081	-2.38055	0.75923	-3.13549	1.7157E-03	8.4444E-03
BB_F20	lcl|NC_001851.2_cds_NP_045453.2_1150	136.22755	-2.84907	0.29514	-9.65321	4.7600E-22	4.7700E-20
BB_F24	lcl|NC_001851.2_cds_NP_045457.1_1152	283.27478	-2.12742	0.36857	-5.77202	7.8300E-09	1.7800E-07
BB_F25	lcl|NC_001851.2_cds_NP_045458.1_1153	156.06800	-1.98978	0.45128	-4.40918	1.0400E-05	1.0976E-04
BB_F26	lcl|NC_001851.2_cds_NP_045459.1_1154	1080.03777	-2.75640	0.44494	-6.19502	5.8300E-10	1.6800E-08
BB_F0041	lcl|NC_001851.2_cds_YP_004940414.1_1157	431.59447	-2.39330	0.51679	-4.63111	3.6400E-06	4.2700E-05
BB_G02	lcl|NC_001852.1_cds_NP_045464.1_1159	182.65163	1.36790	0.39719	3.44397	5.7325E-04	3.3433E-03
BB_G12	lcl|NC_001852.1_cds_NP_045472.1_1163	81.95387	-2.35931	0.67080	-3.51717	4.3617E-04	2.6720E-03
BB_G21	lcl|NC_001852.1_cds_NP_045481.1_1172	257.53631	-1.92019	0.71077	-2.70154	6.9019E-03	2.6120E-02
BB_G22	lcl|NC_001852.1_cds_NP_045482.1_1174	64.42227	-2.66476	0.63847	-4.17370	3.0000E-05	2.6863E-04
BB_H04	lcl|NC_001853.1_cds_NP_045498.1_1188	146.02448	-1.76483	0.51766	-3.40925	6.5141E-04	3.7605E-03
BB_H17	lcl|NC_001853.1_cds_NP_045510.1_1195	10.29556	-2.23494	0.80032	-2.79255	5.2294E-03	2.0966E-02
BB_H25	lcl|NC_001853.1_cds_NP_045516.1_1196	30.47678	-1.56105	0.51826	-3.01211	2.5943E-03	1.1877E-02
BB_H26	lcl|NC_001853.1_cds_NP_045517.1_1197	1195.44669	-1.59160	0.46118	-3.45118	5.5814E-04	3.2776E-03
BB_K22	lcl|NC_001855.1_cds_NP_045596.1_1233	260.18235	-1.08282	0.34636	-3.12624	1.7706E-03	8.6399E-03
BB_K23	lcl|NC_001855.1_cds_NP_045597.1_1234	2453.83614	-1.76011	0.38683	-4.55008	5.3600E-06	6.0900E-05
BB_K24	lcl|NC_001855.1_cds_NP_045598.1_1235	377.57698	-1.77495	0.43727	-4.05913	4.9300E-05	4.0524E-04
BB_K54	lcl|NC_001855.1_cds_YP_004940636.1_1236	131.60135	-1.95752	0.65270	-2.99911	2.7077E-03	1.2362E-02
BB_K32	lcl|NC_001855.1_cds_NP_045605.1_1237	213.65101	-1.87343	0.48966	-3.82601	1.3024E-04	9.4379E-04
BB_K33	lcl|NC_001855.1_cds_NP_045606.1_1238	37.62541	-1.37927	0.44404	-3.10618	1.8952E-03	9.1690E-03
BB_K34	lcl|NC_001855.1_cds_NP_045607.1_1239	221.99723	-1.17304	0.21314	-5.50367	3.7200E-08	7.4500E-07
BB_K0058	lcl|NC_001855.1_cds_YP_004940637.1_1241	51.97230	-1.39907	0.54440	-2.56994	1.0172E-02	3.5978E-02
BB_K40	lcl|NC_001855.1_cds_NP_045612.1_1242	3811.74482	-1.35989	0.23172	-5.86859	4.4000E-09	1.1000E-07
BB_K47	lcl|NC_001855.1_cds_NP_045618.1_1246	2505.67165	1.24932	0.31710	3.93979	8.1600E-05	6.3129E-04

BB_K49	lcl|NC_001855.1_cds_NP_045620.1_1248	1392.93963	1.08561	0.35461	3.06146	2.2026E-03	1.0333E-02
BB_K52	lcl|NC_001855.1_cds_NP_045623.1_1251	62.12418	-1.65067	0.58619	-2.81594	4.8634E-03	2.0054E-02
BB_K53	lcl|NC_001855.1_cds_NP_045624.1_1252	359.83957	-1.31984	0.48424	-2.72560	6.4185E-03	2.4508E-02
BB_J09	lcl|NC_001856.1_cds_NP_045633.1_1254	24951.96368	1.80964	0.37729	4.79639	1.6200E-06	2.0700E-05
BB_J19	lcl|NC_001856.1_cds_NP_045643.1_1260	8721.99449	-1.22674	0.35743	-3.43214	5.9884E-04	3.4688E-03
BB_J23	lcl|NC_001856.1_cds_NP_045647.2_1263	37.83775	-2.45297	0.48759	-5.03081	4.8800E-07	7.3100E-06
BB_J24	lcl|NC_001856.1_cds_NP_045648.1_1264	96.33456	-1.30741	0.37642	-3.47326	5.1418E-04	3.0455E-03
BB_J26	lcl|NC_001856.1_cds_NP_045650.1_1266	38.55969	-1.05461	0.37975	-2.77712	5.4843E-03	2.1851E-02
BB_J43	lcl|NC_001856.1_cds_NP_045667.1_1276	43.39694	-1.94798	0.67037	-2.90582	3.6629E-03	1.5713E-02
BB_A03	lcl|NC_001857.2_cds_NP_045676.1_1287	12443.29488	2.13654	0.33649	6.34946	2.1600E-10	6.4600E-09
dbpB	lcl|NC_001857.2_cds_NP_045698.1_1304	89.46809	-2.64700	0.55833	-4.74096	2.1300E-06	2.7000E-05
BB_A30	lcl|NC_001857.2_cds_NP_045703.1_1305	869.61499	1.35254	0.21700	6.23299	4.5800E-10	1.3400E-08
BB_A31	lcl|NC_001857.2_cds_NP_045704.1_1306	693.65642	1.56591	0.26915	5.81799	5.9600E-09	1.4200E-07
BB_A34	lcl|NC_001857.2_cds_NP_045707.1_1309	190.08384	-2.16419	0.57789	-3.74501	1.8039E-04	1.2533E-03
BB_A36	lcl|NC_001857.2_cds_NP_045709.2_1310	46.52933	-2.13048	0.58213	-3.65982	2.5239E-04	1.6856E-03
BB_A37	lcl|NC_001857.2_cds_NP_045710.1_1311	93.94412	-1.91041	0.65253	-2.92769	3.4149E-03	1.4777E-02
BB_A52	lcl|NC_001857.2_cds_NP_045725.1_1323	1613.06144	1.01788	0.31273	3.25479	1.1348E-03	5.9646E-03
BB_A53	lcl|NC_001857.2_cds_NP_045726.1_1324	375.69121	1.34683	0.37570	3.58488	3.3724E-04	2.1837E-03
BB_A54	lcl|NC_001857.2_cds_NP_045727.1_1325	599.96245	1.90054	0.36702	5.17833	2.2400E-07	3.6000E-06
BB_A58	lcl|NC_001857.2_cds_NP_045731.1_1327	8350.06409	1.29824	0.29668	4.37597	1.2100E-05	1.2328E-04
BB_A60	lcl|NC_001857.2_cds_NP_045733.1_1329	1031.73146	1.00642	0.22212	4.53102	5.8700E-06	6.5800E-05
BB_A65	lcl|NC_001857.2_cds_NP_045738.1_1333	185.75096	-1.57120	0.49676	-3.16287	1.5622E-03	7.7338E-03
BB_A0078	lcl|NC_001857.2_cds_YP_004940408.1_1337	99.05634	-1.78179	0.58155	-3.06389	2.1848E-03	1.0300E-02
BB_A73	lcl|NC_001857.2_cds_NP_045746.1_1338	233.22334	-1.82910	0.42445	-4.30931	1.6400E-05	1.5985E-04
osm28	lcl|NC_001857.2_cds_NP_045747.1_1339	12273.60539	2.23417	0.39421	5.66748	1.4500E-08	3.1600E-07
BB_Q27	lcl|NC_000956.1_cds_NP_051489.1_1361	184.69201	1.47825	0.44760	3.30263	9.5783E-04	5.1425E-03
BB_Q40	lcl|NC_000956.1_cds_NP_051502.1_1373	481.17033	1.46362	0.36788	3.97853	6.9300E-05	5.4169E-04
bdrV	lcl|NC_000956.1_cds_NP_051504.1_1374	634.19622	2.69953	0.31722	8.51007	1.7400E-17	1.1800E-15
BB_Q62	lcl|NC_000956.1_cds_NP_051521.1_1385	20.48709	2.09146	0.54478	3.83906	1.2351E-04	9.0270E-04
BB_Q85	lcl|NC_000956.1_cds_NP_051533.1_1388	31.08243	-1.09455	0.42826	-2.55581	1.0594E-02	3.7123E-02

The included transcripts met the criteria of >1 log2 fold-change and an adjusted P-value (padj) when comparing the Δ*csrA* mutant to wild-type. A total of 239 transcripts were differentially regulated, not including the mutated gene, by the mutation. The first column contains the CDS/custom transcript ID which is the transcript ID for all coding sequences obtained from the NCBI Gene file format file or the transcript ID given to ncRNAs. RefSeq entries are further separated by the character "_". The first portion gives the genetic element from which it is derived, the second describes the type of element (CDS), the third provides RefSeq ID, and the fourth provides

a number indicating the particular entries ordered number in the RefSeq entry. The second column is the gene information, for the ncRNAs it contains the location relative to other genes and for predicted or known genes it contains gene name. The remaining columns describe the various metrics of expression of each impacted transcript including, base mean (average library size normalized counts across all samples), log2FC (Fold change estimate), lfcSE (uncertainty of the log fold change estimate), stat (Wald statistic), pvalue, padj (pvalue following Benjamini-Hochberg adjustment). ORFs and ncRNAs are identified according to the names or numbers assigned to genes and transcripts by the initial genome sequencing of *B. burgdorferi* strain B31 [56, 101] or from our previous analyses of that strain's ncRNA transcriptome [14].

References

1. R: A Language and Environment for Statistical Computing. [http://www.R-project.org].

2. AbdelRahman YM, Belland RJ. The chlamydial developmental cycle. FEMS Microbiology Reviews. 2005;29(5):949-59. doi: 10.1016/j.femsre.2005.03.002.

3. Adams PP, Flores Avile C, Popitsch N, Bilusic I, Schroeder R, Lybecker M, et al. *In vivo* expression technology and 5' end mapping of the *Borrelia burgdorferi* transcriptome identify novel RNAs expressed during mammalian infection. Nucl Acids Res. 2017;45:775-92.

4. Adams PP, Flores Avile C, Popitsch N, Bilusic I, Schroeder R, Lybecker M, et al. *In vivo* expression technology and 5´ end mapping of the *Borrelia burgdorferi* transcriptome identify novel RNAs expressed during mammalian infection. Nucleic Acids Research. 2017;45(2):775-92. doi: 10.1093/nar/gkw1180.

5. Aguero-Rosenfeld ME, Wang G, Schwartz I, Wormser GP. Diagnosis of lyme borreliosis. Clinical microbiology reviews. 2005;18(3):484-509. Epub 2005/07/16. doi: 10.1128/cmr.18.3.484-509.2005.

6. Ahmer BM, van Reeuwijk J, Watson PR, Wallis TS, Heffron F. Salmonella SirA is a global regulator of genes mediating enteropathogenesis. Mol Microbiol. 1999;31(3):971-82. Epub 1999/02/27.

7. Akins DR, Bourell KW, Caimano MJ, Norgard MV, Radolf JD. A new animal model for studying Lyme disease spirochetes in a mammalian host-adapted state. The Journal of Clinical Investigation. 1998;101(10):2240-50. doi: 10.1172/JCI2325.

8. Akopian D, Shen K, Zhang X, Shan S-o. Signal Recognition Particle: An essential protein targeting machine. Annual review of biochemistry. 2013;82:693-721. doi: 10.1146/annurev-biochem-072711-164732.

9. Anders S, Huber W. Differential expression analysis for sequence count data. Genome Biology. 2010;11(10):R106. doi: 10.1186/gb-2010-11-10-r106.

10. Andrew S. FastQC: a quality control tool for high throughput sequence data. 2010.

11. Archambault L, Linscott J, Swerdlow N, Boyland K, Riley E, Schlax P. Translational efficiency of *rpoS* mRNA from *Borrelia burgdorferi*: effects of the length and sequence of the mRNA leader region. Biochem Biophys Res Commun. 2013;433(1):73-8. doi: 10.1016/j.bbrc.2013.02.063.

12. Armbruster CE, Pang B, Murrah K, Juneau RA, Perez AC, Weimer KED, et al. RbsB (NTHI_0632) mediates quorum signal uptake in nontypeable *Haemophilus influenzae* strain 86-028NP. Molecular microbiology. 2011;82(4):836-50. doi: 10.1111/j.1365-2958.2011.07831.x.

13. Arnold WK, Savage CR, Antonicello AD, Stevenson B. Apparent role for *Borrelia burgdorferi* LuxS during mammalian infection. Infection and immunity. 2015;83(4):1347-53. Epub 2015/01/22. doi: 10.1128/iai.00032-15.

14. Arnold WK, Savage CR, Brissette CA, Seshu J, Livny J, Stevenson B. RNA-Seq of *Borrelia burgdorferi* in multiple phases of growth reveals insights into the dynamics of gene expression, transcriptome architecture, and noncoding RNAs. PloS One. 2016;11(10):e0164165. doi: 10.1371/journal.pone.0164165.

15. Auerbuch V, Lenz LL, Portnoy DA. Development of a competitive index assay to evaluate the virulence of *Listeria monocytogenes actA* mutants during primary and secondary infection of mice. Infection and immunity. 2001;69(9):5953-7. Epub 2001/08/14.

16. Babb K, Bykowski T, Riley SP, Miller MC, Demoll E, Stevenson B. *Borrelia burgdorferi* EbfC, a novel, chromosomally encoded protein, binds specific DNA sequences adjacent to erp loci on the spirochete's resident cp32 prophages. Journal of bacteriology. 2006;188(12):4331-9. Epub 2006/06/03. doi: 10.1128/jb.00005-06.

17. Babb K, von Lackum K, Wattier RL, Riley SP, Stevenson B. Synthesis of Autoinducer 2 by the Lyme Disease Spirochete, *Borrelia burgdorferi*. J Bacteriol. 2005;187(9):3079-87. doi: 10.1128/JB.187.9.3079-3087.2005.

18. Babu MM, Luscombe NM, Aravind L, Gerstein M, Teichmann SA. Structure and evolution of transcriptional regulatory networks. Curr Opin Struct Biol. 2004;14(3):283-91. doi: 10.1016/j.sbi.2004.05.004.

19. Baker CS, Eöry LA, Yakhnin H, Mercante J, Romeo T, Babitzke P. CsrA inhibits translation initiation of *Escherichia coli hfq* by binding to a single site overlapping the Shine-Dalgarno sequence. J Bacteriol. 2007;189(15):5472-81. doi: 10.1128/JB.00529-07.

20. Barbour AG. Fall and rise of Lyme disease and other Ixodes tick-borne infections in North America and Europe. British medical bulletin. 1998;54(3):647-58. Epub 1999/05/18.

21. Barbour AG, Bunikis J, Travinsky B, Hoen AG, Diuk-Wasser MA, Fish D, et al. Niche partitioning of *Borrelia burgdorferi* and *Borrelia miyamotoi* in the same tick vector and mammalian reservoir species. Am J Trop Med Hyg. 2009;81(6):1120-31. doi: 10.4269/ajtmh.2009.09-0208.

22. Barrick JE, Breaker RR. The distributions, mechanisms, and structures of metabolite-binding riboswitches. Genome Biol. 2007;8(11):R239. doi: 10.1186/gb-2007-8-11-r239.

23. Belcastro V, Siciliano V, Gregoretti F, Mithbaokar P, Dharmalingam G, Berlingieri S, et al. Transcriptional gene network inference from a massive dataset elucidates transcriptome organization and gene function. Nucleic Acids Res. 2011;39(20):8677-88. doi: 10.1093/nar/gkr593.

24. Bensing BA, Dunny GM. Pheromone-inducible expression of an aggregation protein in *Enterococcus faecalis* requires interaction of a plasmid-encoded RNA with components of the ribosome. Mol Microbiol. 1997;24(2):295-308.

25. Berende A, ter Hofstede HJM, Vos FJ, van Middendorp H, Vogelaar ML, Tromp M, et al. Randomized Trial of Longer-Term Therapy for Symptoms Attributed to Lyme Disease. New England Journal of Medicine. 2016;374(13):1209-20. doi: 10.1056/NEJMoa1505425.

26. Beuzon CR, Holden DW. Use of mixed infections with Salmonella strains to study virulence genes and their interactions *in vivo*. Microbes Infect. 2001;3(14-15):1345-52. Epub 2002/01/05.

27. Blevins JS, Revel AT, Caimano MJ, Yang XF, Richardson JA, Hagman KE, et al. The *luxS* gene is not required for *Borrelia burgdorferi* tick colonization, transmission to a mammalian host, or induction of disease. Infect Immun. 2004;72(8):4864-7. doi: 10.1128/IAI.72.8.4864-4867.2004.

28. Blevins JS, Xu H, He M, Norgard MV, Reitzer L, Yang XF. Rrp2, a σ(54)-Dependent Transcriptional Activator of *Borrelia burgdorferi,* Activates *rpoS* in an Enhancer-Independent Manner. **J Bacteriol**. 2009;191(8):2902-5. doi: 10.1128/jb.01721-08.

29. Blow MJ, Clark TA, Daum CG, Deutschbauer AM, Fomenkov A, Fries R, et al. The Epigenomic Landscape of Prokaryotes. PLOS Genetics. 2016;12(2):e1005854. doi: 10.1371/journal.pgen.1005854.

30. Bolger AM, Lohse M, Usadel B. Trimmomatic: a flexible trimmer for Illumina sequence data. Bioinformatics. 2014;30(15):2114-20. doi: 10.1093/bioinformatics/btu170.

31. Bolz DD, Weis JJ. Molecular mimicry to *Borrelia burgdorferi*: pathway to autoimmunity? Autoimmunity. 2004;37(5):387-92. Epub 2004/12/29. doi: 10.1080/08916930410001713098.

32. Bono JL, Tilly K, Stevenson B, Hogan D, Rosa P. Oligopeptide permease in *Borrelia burgdorferi*: putative peptide-binding components encoded by both chromosomal and plasmid loci. Microbiology. 1998;144:1033-44.

33. Bontemps-Gallo S, Lawrence K, Gherardini FC. Two Different Virulence-Related Regulatory Pathways in *Borrelia burgdorferi* Are Directly Affected by Osmotic Fluxes in the Blood Meal of Feeding Ixodes Ticks. PLoS pathogens. 2016;12(8):e1005791. doi: 10.1371/journal.ppat.1005791.

34. Boylan JA, Posey JE, Gherardini FC. Borrelia oxidative stress response regulator, BosR: a distinct Zn-dependent transcriptional activator. Proceedings of the National Academy of Sciences USA. 2003;100:11684-9.

35. Brissette CA, Bykowski T, Cooley AE, Bowman A, Stevenson B. *Borrelia burgdorferi* RevA antigen binds host fibronectin. Infect Immun. 2009;77(7):2802-12. doi: 10.1128/IAI.00227-09.

36. Brissette CA, Gaultney RA. That's my story, and I'm sticking to it--an update on *B. burgdorferi* adhesins. Front Cell Infect Microbiol. 2014;4:41. doi: 10.3389/fcimb.2014.00041.

37. Brissette CA, Haupt K, Barthel D, Cooley AE, Bowman A, Skerka C, et al. *Borrelia burgdorferi* infection-associated surface proteins ErpP, ErpA, and ErpC bind human plasminogen. Infect Immun. 2009;77(1):300-6. doi: 10.1128/IAI.01133-08.

38. Bugrysheva JV, Pappas CJ, Terekhova DA, Iyer R, Godfrey HP, Schwartz I, et al. Characterization of the RelBbu Regulon in *Borrelia burgdorferi* Reveals Modulation of Glycerol Metabolism by (p)ppGpp. PLoS One. 2015;10(2):e0118063. doi: 10.1371/journal.pone.0118063.

39. Bunikis I, Kutschan-Bunikis S, Bonde M, Bergström S. Multiplex PCR as a tool for validating plasmid content of *Borrelia burgdorferi*. J Microbiol Methods. 2011;86:243-7.

40. Burgdorfer W, Barbour AG, Hayes SF, Benach JL, Grunwaldt E, Davis JP. Lyme disease-a tick-borne spirochetosis? Science. 1982;216(4552):1317-9.

41. Burke TP, Portnoy DA. SpoVG Is a sonserved RNA-binding protein that regulates *Listeria monocytogenes* bysozyme resistance, virulence, and swarming motility. MBio. 2016;7(2):e00240. Epub 2016/04/07. doi: 10.1128/mBio.00240-16.

42. Burns LH, Adams CA, Riley SP, Jutras BL, Bowman A, Chenail AM, et al. BpaB, a novel protein encoded by the Lyme disease spirochete's cp32 prophages, binds to *erp* Operator 2 DNA. Nucleic Acids Res. 2010;38(16):5443-55. Epub 2010/04/28. doi: 10.1093/nar/gkq284.

43. Burtnick MN, Downey JS, Brett PJ, Boylan JA, Frye JG, Hoover TR, et al. Insights into the complex regulation of *rpoS* in *Borrelia burgdorferi*. Molecular Microbiology. 2007;65(2):277-93. doi: 10.1111/j.1365-2958.2007.05813.x.

44. Bush M, Dixon R. The Role of Bacterial Enhancer Binding Proteins as Specialized Activators of σ(54)-Dependent Transcription. Microbiology and molecular biology reviews : MMBR. 2012;76(3):497-529. doi: 10.1128/MMBR.00006-12.

45. Caimano MJ. Cultivation of *Borrelia burgdorferi* in dialysis membrane chambers in rat peritonea. In: Coico RT, Kowalik TF, Quarles J, Stevenson B, Taylor R, editors. Current protocols in microbiology. Hoboken, N.J.: J. Wiley and Sons; 2005.

46. Caimano MJ, Dunham-Ems S, Allard AM, Cassera MB, Kenedy M, Radolf JD. Cyclic di-GMP modulates gene expression in Lyme disease spirochetes at the tick-mammal interface to promote spirochete survival during the blood meal and tick-to-mammal transmission. Infection and immunity. 2015;83(8):3043-60. Epub 2015/05/20. doi: 10.1128/iai.00315-15.

47. Caimano MJ, Eggers CH, Gonzalez CA, Radolf JD. Alternate sigma factor RpoS is required for the in vivo-specific repression of *Borrelia burgdorferi* plasmid lp54-borne *ospA* and *lp6.6* genes. Journal of bacteriology. 2005;187:7845-52.

48. Caimano MJ, Eggers CH, Hazlett KR, Radolf JD. RpoS is not central to the general stress response in *Borrelia burgdorferi* but does control expression of one or more essential virulence determinants. Infection and immunity. 2004;72(11):6433-45. Epub 2004/10/27. doi: 10.1128/iai.72.11.6433-6445.2004.

49. Caimano MJ, Iyer R, Eggers CH, Gonzalez C, Morton EA, Gilbert MA, et al. Analysis of the RpoS regulon in *Borrelia burgdorfer*i in response to mammalian host signals provides insight into RpoS function during the enzootic cycle. Molecular Microbiology. 2007;65(5):1193-217. doi: 10.1111/j.1365-2958.2007.05860.x.

50. Caimano MJ, Sivasankaran SK, Allard A, Hurley D, Hokamp K, Grassmann AA, et al. A model system for studying the transcriptomic and physiological changes associated with mammalian host-adaptation by *Leptospira interrogans* serovar Copenhageni. PLoS Pathog. 2014;10(3):e1004004. doi: 10.1371/journal.ppat.1004004.

51. Caine JA, Coburn J. Multifunctional and Redundant Roles of *Borrelia burgdorferi* Outer Surface Proteins in Tissue Adhesion, Colonization, and Complement Evasion. Front Immunol. 2016;7:442. doi: 10.3389/fimmu.2016.00442.

52. Carabetta VJ, Cristea IM. Regulation, Function, and Detection of Protein Acetylation in Bacteria. Journal of bacteriology. 2017;199(16). Epub 2017/04/26. doi: 10.1128/jb.00107-17.

53. Carroll JA, El-Hage N, Miller JC, Babb K, Stevenson B. *Borrelia burgdorferi* RevA antigen is a surface-exposed outer membrane protein whose expression is regulated in response to environmental temperature and pH. Infect Immun. 2001;69(9):5286-93. doi: 10.1128/IAI.69.9.5286-5293.2001.

54. Carroll JA, Garon CF, Schwan TG. Effects of environmental pH on membrane proteins in *Borrelia burgdorferi*. Infect Immun. 1999;67:3181-7.

55. Casadevall A, Pirofski L-a. The damage-response framework of microbial pathogenesis. Nature Reviews Microbiology. 2003;1:17. doi: 10.1038/nrmicro732.

56. Casjens S, Palmer N, van Vugt R, Huang WM, Stevenson B, Rosa P, et al. A bacterial genome in flux: the twelve linear and nine circular extrachromosomal DNAs of an infectious isolate of the Lyme disease spirochete *Borrelia burgdorferi*. Mol Microbiol. 2000;35:490-516.

57. Casjens S, Palmer N, van Vugt R, Huang WM, Stevenson B, Rosa P, et al. A bacterial genome in flux: the twelve linear and nine circular extrachromosomal DNAs of an infectious isolate of the Lyme disease spirochete *Borrelia burgdorferi*. Molecular Microbiology. 2000;35:490-516.

58. Casjens S, Palmer N, van Vugt R, Huang WM, Stevenson B, Rosa P, et al. A bacterial genome in Flux: the twelve linear and nine circular extrachromosomal DNAs in an infectious isolate of the Lyme disease spirochete *Borrelia burgdorferi*. Mol Microbiol. 2000;35(3):490-516.

59. Casselli T, Tourand Y, Scheidegger A, Arnold W, Proulx A, Stevenson B, et al. DNA Methylation by Restriction Modification Systems Affects the Global Transcriptome Profile in Borrelia burgdorferi. bioRxiv. 2018. doi: 10.1101/375352.

60. Cerqueira GM, Kostoulias X, Khoo C, Aibinu I, Qu Y, Traven A, et al. A global virulence regulator in *Acinetobacter baumannii* and its control of the phenylacetic acid catabolic pathway. The Journal of infectious diseases. 2014;210(1):46-55. Epub 2014/01/17. doi: 10.1093/infdis/jiu024.

61. Chatterji D, Ojha AK. Revisiting the stringent response, ppGpp and starvation signaling. Curr Opin Microbiol. 2001;4(2):160-5.

62. Chenail AM, Jutras BL, Adams CA, Burns LH, Bowman A, Verma A, et al. *Borrelia burgdorferi* cp32 BpaB Modulates Expression of the Prophage NucP Nuclease and SsbP Single-Stranded DNA-Binding Protein. J Bacteriol. 2012;194(17):4570-8. doi: 10.1128/JB.00661-12.

63. Chenail AM, Jutras BL, Adams CA, Burns LH, Bowman A, Verma A, et al. *Borrelia burgdorferi* cp32 BpaB modulates expression of the prophage NucP nuclease and SsbP single-stranded DNA-binding protein. J Bacteriol. 2012;194:4570-8.

64. Cheng L, Keiler KC. Correct timing of *dnaA* transcription and initiation of DNA replication requires trans translation. J Bacteriol. 2009;191(13):4268-75. doi: 10.1128/JB.00362-09.

65. Chien A-C, Hill NS, Levin PA. Cell size control in bacteria. Curr Biol. 2012;22(9):R340-9. doi: 10.1016/j.cub.2012.02.032.

66. Chien A-C, Zareh SKG, Wang YM, Levin PA. Changes in the oligomerization potential of the division inhibitor UgtP co-ordinate *Bacillus subtilis* cell size with nutrient availability. Mol Microbiol. 2012;86(3):594-610. doi: 10.1111/mmi.12007.

67. Cloud JL, Marconi RT, Eggers CH, Garon CF, Tilly K, Samuels DS. Cloning and expression of the *Borrelia burgdorferi* lon gene. Gene. 1997;194(1):137-41. doi: 10.1016/S0378-1119(97)00196-0.

68. Coleman JL, Katona LI, Kuhlow C, Toledo A, Okan NA, Tokarz R, et al. Evidence That Two ATP-Dependent (Lon) Proteases in *Borrelia burgdorferi* Serve Different Functions. PLoS Pathog. 2009;5(11):e1000676. doi: 10.1371/journal.ppat.1000676.

69. Coli E. Replication cycle-coordinated change of the adenine nucleotide-bound forms of DnaA protein in. Plan Perspect. 1999;6642:6652.

70. Collier J, Murray SR, Shapiro L. DnaA couples DNA replication and the expression of two cell cycle master regulators. EMBO J. 2006;25(2):346-56. doi: 10.1038/sj.emboj.7600927.

71. Collier J, Shapiro L. Feedback Control of DnaA-Mediated Replication Initiation by Replisome-Associated HdaA Protein in *Caulobacter crescentus*. J Bacteriol. 2009;191(18):5706-16. doi: 10.1128/JB.00525-09.

72. Concepcion MB, Nelson DR. Expression of spoT in Borrelia burgdorferi during serum starvation. J Bacteriol. 2003;185(2):444-52. doi: 10.1128/JB.185.2.444-452.2003.

73. Conway JR, Lex A, Gehlenborg N. UpSetR: an R package for the visualization of intersecting sets and their properties. Bioinformatics. 2017;33(18):2938-40. doi: 10.1093/bioinformatics/btx364.

74. Cook LC, Federle MJ. Peptide pheromone signaling in Streptococcus and Enterococcus. FEMS microbiology reviews. 2014;38(3):473-92. doi: 10.1111/1574-6976.12046.

75. Cooley AE, Riley SP, Kral K, Miller MC, DeMoll E, Fried MG, et al. DNA-binding by Haemophilus influenzae and *Escherichia coli* YbaB, members of a widely-distributed bacterial protein family. BMC Microbiol. 2009;9:137. doi: 10.1186/1471-2180-9-137.

76. Corona A, Schwartz I. *Borrelia burgdorferi*: Carbon Metabolism and the Tick-Mammal Enzootic Cycle. Microbiology spectrum. 2015;3(3). Epub 2015/07/18. doi: 10.1128/microbiolspec.MBP-0011-2014.

77. Crick F. Central Dogma of Molecular Biology. Nature. 1970;227:561. doi: 10.1038/227561a0.

78. Darnell CL, Schmid AK. Systems biology approaches to defining transcription regulatory networks in halophilic archaea. Methods. 2015;86:102-14. doi: 10.1016/j.ymeth.2015.04.034.

79. Darnell CL, Tonner PD, Gulli JG, Schmidler SC, Schmid AK. Systematic Discovery of Archaeal Transcription Factor Functions in Regulatory Networks through Quantitative Phenotyping Analysis. mSystems. 2017;2(5). doi: 10.1128/mSystems.00032-17.

80. Davidson E, Levin M. Gene regulatory networks. Proceedings of the National Academy of Sciences of the United States of America. 2005;102(14):4935. doi: 10.1073/pnas.0502024102.

81. Diaz Z, Xavier KB, Miller ST. The Crystal Structure of the Escherichia coli Autoinducer-2 Processing Protein LsrF. PLOS ONE. 2009;4(8):e6820. doi: 10.1371/journal.pone.0006820.

82. Dobrikova EY, Bugrysheva J, Cabello FC. Two independent transcriptional units control the complex and simultaneous expression of the *bmp* paralogous chromosomal gene family in *Borrelia burgdorferi*. Molecular Microbiology. 2001;39(2):370-9. doi: 10.1046/j.1365-2958.2001.02220.x.

83. Dowdell AS, Murphy MD, Azodi C, Swanson SK, Florens L, Chen S, et al. Comprehensive Spatial Analysis of the *Borrelia burgdorferi* Lipoproteome Reveals a Compartmentalization Bias toward the Bacterial Surface. J Bacteriol. 2017;199(6). doi: 10.1128/JB.00658-16.

84. Drecktrah D, Lybecker M, Popitsch N, Rescheneder P, Hall LS, Samuels DS. The *Borrelia burgdorferi* RelA/SpoT Homolog and Stringent Response Regulate Survival in the

Tick Vector and Global Gene Expression during Starvation. PLoS Pathog. 2015;11(9):e1005160. doi: 10.1371/journal.ppat.1005160.

85. Dugar G, Svensson SL, Bischler T, Wäldchen S, Reinhardt R, Sauer M, et al. The CsrA-FliW network controls polar localization of the dual-function flagellin mRNA in *Campylobacter jejuni*. Nat Commun. 2016;7:11667. doi: 10.1038/ncomms11667.

86. Dulebohn DP, Hayes BM, Rosa PA. Global repression of host-associated genes of the Lyme disease spirochete through post-transcriptional modulation of the alternative sigma factor RpoS. PLoS One. 2014;9(3):e93141. doi: 10.1371/journal.pone.0093141.

87. Dulmage KA, Todor H, Schmid AK. Growth-Phase-Specific Modulation of Cell Morphology and Gene Expression by an Archaeal Histone Protein. MBio. 2015;6(5):e00649-15. doi: 10.1128/mBio.00649-15.

88. Dunham-Ems SM, Caimano MJ, Pal U, Wolgemuth CW, Eggers CH, Balic A, et al. Live imaging reveals a biphasic mode of dissemination of *Borrelia burgdorferi* within ticks. J Clin Invest. 2009;119(12):3652-65. doi: 10.1172/JCI39401.

89. Durfee T, Hansen AM, Zhi H, Blattner FR, Jin DJ. Transcription profiling of the stringent response in Escherichia coli. Journal of bacteriology. 2008;190(3):1084-96. Epub 2007/11/28. doi: 10.1128/jb.01092-07.

90. Ebright RH. RNA Polymerase: Structural Similarities Between Bacterial RNA Polymerase and Eukaryotic RNA Polymerase II. Journal of Molecular Biology. 2000;304(5):687-98. doi: https://doi.org/10.1006/jmbi.2000.4309.

91. Eggers CH, Caimano MJ, Malizia RA, Kariu T, Cusack B, Desrosiers DC, et al. The coenzyme A disulphide reductase of *Borrelia burgdorferi* is important for rapid growth throughout the enzootic cycle and essential for infection of the mammalian host. Mol Microbiol. 2011;82(3):679-97. Epub 2011/09/20. doi: 10.1111/j.1365-2958.2011.07845.x.

92. Eggers CH, Caimano MJ, Radolf JD. Analysis of promoter elements involved in the transcriptional initiation of RpoS-dependent *Borrelia burgdorferi* genes. Journal of bacteriology. 2004;186(21):7390-402. Epub 2004/10/19. doi: 10.1128/jb.186.21.7390-7402.2004.

93. Elias AF, Stewart PE, Grimm D, Caimano MJ, Eggers CH, Tilly K, et al. Clonal Polymorphism of *Borrelia burgdorferi* Strain B31 MI: Implications for Mutagenesis in an Infectious Strain Background. Infection and immunity. 2002;70(4):2139-50. doi: 10.1128/iai.70.4.2139-2150.2002.

94. Embers ME, Barthold SW, Borda JT, Bowers L, Doyle L, Hodzic E, et al. Persistence of *Borrelia burgdorferi* in rhesus macaques following antibiotic treatment of disseminated infection. PLoS One. 2012;7(1):e29914. doi: 10.1371/journal.pone.0029914.

95. Esquerré T, Bouvier M, Turlan C, Carpousis AJ, Girbal L, Cocaign-Bousquet M. The Csr system regulates genome-wide mRNA stability and transcription and thus gene expression in *Escherichia coli*. Sci Rep. 2016;6:25057. doi: 10.1038/srep25057.

96. Esteve-Gassent MD, Elliott NL, Seshu J. *sodA* is essential for virulence of *Borrelia burgdorferi* in the murine model of Lyme disease. Molecular Microbiology. 2009;71(3):594-612. Epub 2008/12/02. doi: 10.1111/j.1365-2958.2008.06549.x.

97. Faherty SL, Campbell CR, Larsen PA, Yoder AD. Evaluating whole transcriptome amplification for gene profiling experiments using RNA-Seq. BMC Biotechnology. 2015;15(1):65. doi: 10.1186/s12896-015-0155-7.

98. Fisher MA, Grimm D, Henion AK, Elias AF, Stewart PE, Rosa PA, et al. *Borrelia burgdorferi* sigma54 is required for mammalian infection and vector transmission but not for tick colonization. Proc Natl Acad Sci U S A. 2005;102(14):5162-7. doi: 10.1073/pnas.0408536102.

99. Fisher MA, Grimm D, Henion AK, Elias AF, Stewart PE, Rosa PA, et al. *Borrelia burgdorferi* σ(54) is required for mammalian infection and vector transmission but not for tick colonization. Proceedings of the National Academy of Sciences of the United States of America. 2005;102(14):5162-7. doi: 10.1073/pnas.0408536102.

100. Fraser CM, Casjens S, Huang WM, Sutton GG, Clayton R, Lathigra R, et al. Genomic sequence of a Lyme disease spirochaete, *Borrelia burgdorferi*. Nature. 1997;390. doi: 10.1038/37551.

101. Fraser CM, Casjens S, Huang WM, Sutton GG, Clayton R, Lathigra R, et al. Genomic sequence of a Lyme disease spirochaete, *Borrelia burgdorferi*. Nature. 1997;390:580-6.

102. Frazee AC, Pertea G, Jaffe AE, Langmead B, Salzberg SL, Leek JT. Flexible analysis of transcriptome assemblies with Ballgown. bioRxiv. 2014. doi: 10.1101/003665.

103. Frederick JR, Rogers EA, Marconi RT. Analysis of a growth-phase-regulated two-component regulatory system in the periodontal pathogen *Treponema denticola*. J Bacteriol. 2008;190(18):6162-9. doi: 10.1128/JB.00046-08.

104. Freedman JC, Rogers EA, Kostick JL, Zhang H, Iyer R, Schwartz I, et al. Identification and molecular characterization of a cyclic-di-GMP effector protein, PlzA (BB0733): additional evidence for the existence of a functional cyclic-di-GMP regulatory network in the Lyme disease spirochete, *Borrelia burgdorferi*. FEMS immunology and medical microbiology. 2010;58(2):285-94. Epub 2009/12/25. doi: 10.1111/j.1574-695X.2009.00635.x.

105. Frenzel E, Kranzler M, Stark TD, Hofmann T, Ehling-Schulz M. The Endospore-Forming Pathogen Bacillus cereus Exploits a Small Colony Variant-Based Diversification Strategy in Response to Aminoglycoside Exposure. MBio. 2015;6(6):e01172-15. doi: 10.1128/mBio.01172-15.

106. Frimodt-Møller J, Charbon G, Krogfelt KA, Løbner-Olesen A. DNA Replication Control Is Linked to Genomic Positioning of Control Regions in *Escherichia coli*. PLoS Genet. 2016;12(9):e1006286. doi: 10.1371/journal.pgen.1006286.

107. Fujikawa N, Kurumizaka H, Nureki O, Terada T, Shirouzu M, Katayama T, et al. Structural basis of replication origin recognition by the DnaA protein. Nucleic Acids Research. 2003;31(8):2077-86.

108. Garcia EC, Perault AI, Marlatt SA, Cotter PA. Interbacterial signaling via Burkholderia contact-dependent growth inhibition system proteins. Proceedings of the National Academy of Sciences. 2016;113(29):8296-301. doi: 10.1073/pnas.1606323113.

109. García-del Portillo F, Núñez-Hernández C, Eisman B, Ramos-Vivas J. Growth control in the Salmonella-containing vacuole. Current Opinion in Microbiology. 2008;11(1):46-52. doi: https://doi.org/10.1016/j.mib.2008.01.001.

110. Gengenbacher M, Kaufmann SHE. *Mycobacterium tuberculosis*: success through dormancy. FEMS Microbiology Reviews. 2012;36(3):514-32. doi: 10.1111/j.1574-6976.2012.00331.x.

111. Gherardini SB-GaFC. *Borrelia burgdorferi* Transport and Metabolism map. ResearchGate2017.

112. Gimpel M, Brantl S. Dual-function small regulatory RNAs in bacteria. Mol Microbiol. 2017;103(3):387-97. doi: 10.1111/mmi.13558.

113. Goranov AI, Breier AM, Merrikh H, Grossman AD. YabA of *Bacillus subtilis* controls DnaA-mediated replication initiation but not the transcriptional response to replication stress. Mol Microbiol. 2009;74(2):454-66. doi: 10.1111/j.1365-2958.2009.06876.x.

114. Gorbatyuk B, Marczynski GT. Regulated degradation of chromosome replication proteins DnaA and CtrA in *Caulobacter crescentus*. Mol Microbiol. 2005;55(4):1233-45. doi: 10.1111/j.1365-2958.2004.04459.x.

115. Grabherr MG, Haas BJ, Yassour M, Levin JZ, Thompson Da, Amit I, et al. Full-length transcriptome assembly from RNA-Seq data without a reference genome. Nature Biotechnology. 2011;29. doi: 10.1038/nbt.1883.

116. Graebsch A, Roche S, Kostrewa D, Söding J, Niessing D. Of Bits and Bugs — On the Use of Bioinformatics and a Bacterial Crystal Structure to Solve a Eukaryotic Repeat-Protein Structure. PLoS ONE. 2010;5(10):e13402. doi: 10.1371/journal.pone.0013402.

117. Grant MAA, Saggioro C, Ferrari U, Bassetti B, Sclavi B, Cosentino Lagomarsino M. DnaA and the timing of chromosome replication in *Escherichia coli* as a function of growth rate. BMC Syst Biol. 2011;5:201. doi: 10.1186/1752-0509-5-201.

118. Groshong AM, Gibbons NE, Yang XF, Blevins JS. Rrp2, a prokaryotic enhancer-like binding protein, is essential for viability of *Borrelia burgdorferi*. J Bacteriol. 2012;194(13):3336-42. doi: 10.1128/JB.00253-12.

119. Grosso-Becera MV, Servín-González L, Soberón-Chávez G. RNA structures are involved in the thermoregulation of bacterial virulence-associated traits. Trends Microbiol. 2015;23(8):509-18. doi: 10.1016/j.tim.2015.04.004.

120. Grove AP, Liveris D, Iyer R, Petzke M, Rudman J, Caimano MJ, et al. Two distinct mechanisms govern RpoS-mediated repression of tick-phase genes during mammalian host adaptation by *Borrelia burgdorferi*, the Lyme Disease Spirochete. MBio. 2017;8(4): e01204-17. Epub 2017/08/24. doi: 10.1128/mBio.01204-17.

121. Gusarov I, Nudler E. The Mechanism of Intrinsic Transcription Termination. Molecular Cell. 1999;3(4):495-504. doi: https://doi.org/10.1016/S1097-2765(00)80477-3.

122. Haas BJ, Chin M, Nusbaum C, Birren BW, Livny J. How deep is deep enough for RNA-Seq profiling of bacterial transcriptomes? BMC Genomics. 2012;13(1):1-11. doi: 10.1186/1471-2164-13-734.

123. Hagman KE, Lahdenne P, Popova TG, Porcella SF, Akins DR, Radolf JD, et al. Decorin-binding protein of *Borrelia burgdorferi* is encoded within a two-gene operon and is protective in the murine model of Lyme borreliosis. Infect Immun. 1998;66(6):2674-83.

124. Hagman KE, Porcella SF, Popova TG, Norgard MV. Evidence for a methyl-accepting chemotaxis protein gene (*mcp1*) that encodes a putative sensory transducer in virulent *Treponema pallidum*. Infect Immun. 1997;65(5):1701-9.

125. Hauryliuk V, Atkinson GC, Murakami KS, Tenson T, Gerdes K. Recent functional insights into the role of (p)ppGpp in bacterial physiology. Nature reviews Microbiology. 2015;13(5):298-309. doi: 10.1038/nrmicro3448.

126. He M, Ouyang Z, Troxell B, Xu H, Moh A, Piesman J, et al. Cyclic di-GMP is essential for the survival of the lyme disease spirochete in ticks. PLoS Pathog. 2011;7(6):e1002133. Epub 2011/07/09. doi: 10.1371/journal.ppat.1002133.

127. He M, Zhang JJ, Ye M, Lou Y, Yang XF. Cyclic Di-GMP receptor PlzA controls virulence gene expression through RpoS in *Borrelia burgdorferi*. Infection and immunity. 2014;82(1):445-52. Epub 2013/11/13. doi: 10.1128/iai.01238-13.

128. Henke JM, Bassler BL. Three parallel quorum-sensing systems regulate gene expression in *Vibrio harveyi*. Journal of bacteriology. 2004;186(20):6902-14. Epub 2004/10/07. doi: 10.1128/jb.186.20.6902-6914.2004.

129. Henkin TM. Riboswitch RNAs: using RNA to sense cellular metabolism. Genes Dev. 2008;22(24):3383-90. doi: 10.1101/gad.1747308.

130. Higgins D, Dworkin J. Recent progress in *Bacillus subtilis* sporulation. FEMS Microbiol Rev. 2012;36(1):131-48. Epub 2011/11/19. doi: 10.1111/j.1574-6976.2011.00310.x.

131. Hill NS, Buske PJ, Shi Y, Levin PA. A moonlighting enzyme links *Escherichia coli* cell size with central metabolism. PLoS Genet. 2013;9(7):e1003663. doi: 10.1371/journal.pgen.1003663.

132. Hokkanen S, Feldmann HM, Ding H, Jung CK, Bojarski L, Renner-Muller I, et al. Lack of Pur-alpha alters postnatal brain development and causes megalencephaly. Human molecular genetics. 2012;21(3):473-84. Epub 2011/10/20. doi: 10.1093/hmg/ddr476.

133. Hoover SE, Xu W, Xiao W, Burkholder WF. Changes in DnaA-dependent gene expression contribute to the transcriptional and developmental response of *Bacillus subtilis* to manganese limitation in Luria-Bertani medium. J Bacteriol. 2010;192(15):3915-24. doi: 10.1128/JB.00210-10.

134. Hottes AK, Shapiro L, McAdams HH. DnaA coordinates replication initiation and cell cycle transcription in *Caulobacter crescentus*. Mol Microbiol. 2005;58(5):1340-53. doi: 10.1111/j.1365-2958.2005.04912.x.

135. Hu LI, Lima BP, Wolfe AJ. Bacterial Protein Acetylation: the Dawning of a New Age. Molecular microbiology. 2010;77(1):15-21. doi: 10.1111/j.1365-2958.2010.07204.x.

136. Huang J, Lih CJ, Pan KH, Cohen SN. Global analysis of growth phase responsive gene expression and regulation of antibiotic biosynthetic pathways in *Streptomyces coelicolor* using DNA microarrays. Genes Dev. 2001;15(23):3183-92. Epub 2001/12/04. doi: 10.1101/gad.943401.

137. Hubner A, Revel AT, Nolen DM, Hagman KE, Norgard MV. Expression of a *luxS* gene is not required for *Borrelia burgdorferi* infection of mice via needle inoculation. Infection and immunity. 2003;71(5):2892-6. Epub 2003/04/22.

138. Hübner A, Yang X, Nolen DM, Popova TG, Cabello FC, Norgard MV. Expression of *Borrelia burgdorferi* OspC and DbpA is controlled by a RpoN-RpoS regulatory pathway. Proceedings of the National Academy of Sciences. 2001;98(22):12724-9. doi: 10.1073/pnas.231442498.

139. Hübner A, Yang X, Nolen DM, Popova TG, Cabello FC, Norgard MV. Expression of *Borrelia burgdorferi* OspC and DbpA is controlled by a RpoN–RpoS regulatory pathway. Proceedings of the National Academy of Sciences of the United States of America. 2001;98(22):12724-9. doi: 10.1073/pnas.231442498.

140. Hyde JA, Shaw DK, Smith R, Trzeciakowski JP, Skare JT. The BosR regulatory protein of *Borrelia burgdorferi* interfaces with the RpoS regulatory pathway and modulates both the oxidative stress response and pathogenic properties of the Lyme disease spirochete. Molecular Microbiology. 2009;74:1344-55.

141. Hyde JA, Shaw DK, Smith RI, Trzeciakowski JP, Skare JT. The BosR regulatory protein of *Borrelia burgdorferi* interfaces with the RpoS regulatory pathway and modulates both the oxidative stress response and pathogenic properties of the Lyme disease spirochete. Mol Microbiol. 2009;74(6):1344-55. doi: 10.1111/j.1365-2958.2009.06951.x.

142. Imai D, Holden K, Velazquez EM, Feng S, Hodzic E, Barthold SW. Influence of arthritis-related protein (BBF01) on infectivity of *Borrelia burgdorferi* B31. BMC Microbiology. 2013;13(1):100. doi: 10.1186/1471-2180-13-100.

143. Indest KJ, Ramamoorthy R, Sole M, Gilmore RD, Johnson BJ, Philipp MT. Cell-density-dependent expression of *Borrelia burgdorferi* lipoproteins *in vitro*. Infection and immunity. 1997;65(4):1165-71. Epub 1997/04/01.

144. Iqbal H, Kenedy MR, Lybecker M, Akins DR. The TamB ortholog of *Borrelia burgdorferi* interacts with the β-barrel assembly machine (BAM) complex protein BamA. Molecular Microbiology. 2016:n/a-n/a. doi: 10.1111/mmi.13492.

145. Ishihama A. Functional Modulation of *Escherichia coli* RNA Polymerase. Annual review of microbiology. 2000;54(1):499-518. doi: 10.1146/annurev.micro.54.1.499.

146. Iyer R, Caimano MJ, Luthra A, Axline D, Jr., Corona A, Iacobas DA, et al. Stage-specific global alterations in the transcriptomes of Lyme disease spirochetes during tick feeding and following mammalian host adaptation. Mol Microbiol. 2015;95(3):509-38. Epub 2014/11/27. doi: 10.1111/mmi.12882.

147. Iyer R, Schwartz I. Microarray-based comparative genomic and transcriptome analysis of *Borrelia burgdorferi*. Microarrays. 2016;5(2):9. doi: 10.3390/microarrays5020009.

148. Jacob F, Monod J. On the Regulation of Gene Activity. Cold Spring Harbor Symposia on Quantitative Biology. 1961;26:193-211. doi: 10.1101/sqb.1961.026.01.024.

149. James D, Shao H, Lamont RJ, Demuth DR. The *Actinobacillus actinomycetemcomitans* ribose binding protein RbsB interacts with cognate and heterologous autoinducer 2 signals. Infection and immunity. 2006;74(7):4021-9. Epub 2006/06/23. doi: 10.1128/iai.01741-05.

150. Jenior ML, Leslie JL, Young VB, Schloss PD. Clostridium difficile colonizes alternative nutrient niches during infection across distinct murine gut microbiomes. bioRxiv. 2017. doi: 10.1101/092304.

151. Johnson TL, Graham CB, Hojgaard A, Breuner NE, Maes SE, Boegler KA, et al. Isolation of the Lyme Disease Spirochete *Borrelia mayonii* From Naturally Infected Rodents in Minnesota. Journal of medical entomology. 2017;54(4):1088-92. Epub 2017/04/27. doi: 10.1093/jme/tjx062.

152. Jonas K, Liu J, Chien P, Laub MT. Proteotoxic stress induces a cell-cycle arrest by stimulating Lon to degrade the replication initiator DnaA. Cell. 2013;154(3):623-36. doi: 10.1016/j.cell.2013.06.034.

153. Jutras BL, Bowman A, Brissette CA, Adams CA, Verma A, Chenail AM, et al. EbfC (YbaB) is a new type of bacterial nucleoid-associated protein and a global regulator of gene expression in the Lyme disease spirochete. Journal of bacteriology. 2012;194(13):3395-406. Epub 2012/05/01. doi: 10.1128/jb.00252-12.

154. Jutras BL, Chenail AM, Carroll DW, Miller MC, Zhu H, Bowman A, et al. Bpur, the Lyme disease spirochete's PUR domain protein: identification as a transcriptional modulator and characterization of nucleic acid interactions. The Journal of biological chemistry. 2013;288(36):26220-34. Epub 2013/07/13. doi: 10.1074/jbc.M113.491357.

155. Jutras BL, Chenail AM, Carroll DW, Miller MC, Zhu H, Bowman A, et al. Bpur, the Lyme disease spirochete's PUR-domain protein: identification as a transcriptional modulator and characterization of nucleic acid interactions. J Biol Chem. 2013;288:26220-34.

156. Jutras BL, Chenail AM, Rowland CL, Carroll D, Miller MC, Bykowski T, et al. Eubacterial SpoVG homologs constitute a new family of site-specific DNA-binding proteins. PLoS One. 2013;8(6):e66683. Epub 2013/07/03. doi: 10.1371/journal.pone.0066683.

157. Jutras BL, Chenail AM, Stevenson B. Changes in bacterial growth rate govern expression of the *Borrelia burgdorferi* OspC and Erp infection-associated surface proteins. Journal of bacteriology. 2013;195(4):757-64. Epub 2012/12/12. doi: 10.1128/jb.01956-12.

158. Jutras BL, Jones G, Verma A, Brown NA, Antonicello AD, Chenail AM, et al. Post-transcriptional autoregulation of the Lyme disease bacterium's BpuR DNA/RNA-binding protein. J Bacteriol. 2013;195:4915-23.

159. Jutras BL, Scott M, Parry B, Biboy J, Gray J, Vollmer W, et al. Lyme disease and relapsing fever Borrelia elongate through zones of peptidoglycan synthesis that mark division sites of daughter cells. Proceedings of the National Academy of Sciences of the United States of America. 2016;113(33):9162-70. doi: 10.1073/pnas.1610805113.

160. Jutras BL, Verma A, Adams CA, Brissette CA, Burns LH, Whetstine CR, et al. BpaB and EbfC DNA-binding proteins regulate production of the Lyme disease spirochete's infection-associated Erp surface proteins. Journal of bacteriology. 2012;194(4):778-86. Epub 2011/12/14. doi: 10.1128/jb.06394-11.

161. Jutras BL, Verma A, Stevenson B. Identification of novel DNA-binding proteins using DNA-affinity chromatography/pull down. Current protocols in microbiology. 2012;Chapter 1:Unit1F Epub 2012/02/07. doi: 10.1002/9780471729259.mc01f01s24.

162. Kaguni JM. DnaA: controlling the initiation of bacterial DNA replication and more. Annu Rev Microbiol. 2006;60:351-75. doi: 10.1146/annurev.micro.60.080805.142111.

163. Karna SL, Sanjuan E, Esteve-Gassent MD, Miller CL, Maruskova M, Seshu J. CsrA modulates levels of lipoproteins and key regulators of gene expression critical for pathogenic mechanisms of *Borrelia burgdorferi*. Infection and immunity. 2011;79(2):732-44. Epub 2010/11/17. doi: 10.1128/iai.00882-10.

164. Karna SLR, Prabhu RG, Lin YH, Miller CL, Seshu J. Contributions of Environmental Signals and Conserved Residues to the Functions of Carbon Storage Regulator A of *Borrelia burgdorferi*. Infect Immun. 2013;81(8):2972-85. doi: 10.1128/IAI.00494-13.

165. Karna SLR, Sanjuan E, Esteve-Gassent MD, Miller CL, Maruskova M, Seshu J. CsrA Modulates Levels of Lipoproteins and Key Regulators of Gene Expression Critical for Pathogenic Mechanisms of *Borrelia burgdorferi*. Infect Immun. 2011;79(2):732-44. doi: 10.1128/IAI.00882-10.

166. Kasho K, Katayama T. DnaA binding locus *datA* promotes DnaA-ATP hydrolysis to enable cell cycle-coordinated replication initiation. Proc Natl Acad Sci U S A. 2013;110(3):936-41. doi: 10.1073/pnas.1212070110.

167. Keiler KC. Biology of trans-translation. Annu Rev Microbiol. 2008;62:133-51. doi: 10.1146/annurev.micro.62.081307.162948.

168. Keyamura K, Fujikawa N, Ishida T, Ozaki S, Su'etsugu M, Fujimitsu K, et al. The interaction of DiaA and DnaA regulates the replication cycle in *E. coli* by directly promoting ATP DnaA-specific initiation complexes. Genes Dev. 2007;21(16):2083-99. doi: 10.1101/gad.1561207.

169. Khajanchi BK, Odeh E, Gao L, Jacobs MB, Philipp MT, Lin T, et al. Phosphoenolpyruvate Phosphotransferase System Components Modulate Gene Transcription and Virulence of *Borrelia burgdorferi*. Infection and immunity. 2015;84(3):754-64. Epub 2015/12/30. doi: 10.1128/iai.00917-15.

170. Kitagawa R, Ozaki T, Moriya S, Ogawa T. Negative control of replication initiation by a novel chromosomal locus exhibiting exceptional affinity for *Escherichia coli* DnaA protein. Genes Dev. 1998;12(19):3032-43.

171. Klemm BP, Wu N, Chen Y, Liu X, Kaitany KJ, Howard MJ, et al. The Diversity of Ribonuclease P: Protein and RNA Catalysts with Analogous Biological Functions. Biomolecules. 2016;6(2):27. doi: 10.3390/biom6020027.

172. Knight SW, Kimmel BJ, Eggers CH, Samuels DS. Disruption of the *Borrelia burgdorferi gac* gene, encoding the naturally synthesized GyrA C-terminal domain. Journal of bacteriology. 2000;182(7):2048-51. Epub 2000/03/14.

173. Kobryn K, Naigamwalla DZ, Chaconas G. Site-specific DNA binding and bending by the *Borrelia burgdorferi* Hbb protein. Mol Microbiol. 2000;37(1):145-55.

174. Kolter R, Siegele DA, Tormo A. The stationary phase of the bacterial life cycle. Annual review of microbiology. 1993;47:855-74. Epub 1993/01/01. doi: 10.1146/annurev.mi.47.100193.004231.

175. Labandeira-Rey M, Skare JT. Decreased infectivity in *Borrelia burgdorferi* strain B31 is associated with loss of linear plasmid 25 or 28-1. Infection and immunity. 2001;69(1):446-55. Epub 2000/12/19. doi: 10.1128/iai.69.1.446-455.2001.

176. Landt SG, Abeliuk E, McGrath PT, Lesley JA, McAdams HH, Shapiro L. Small non-coding RNAs in *Caulobacter crescentus*. Mol Microbiol. 2008;68(3):600-14. doi: 10.1111/j.1365-2958.2008.06172.x.

177. Lane RS, Piesman J, Burgdorfer W. Lyme borreliosis: relation of its causative agent to its vectors and hosts in North America and Europe. Annu Rev Entomol. 1991;36. doi: 10.1146/annurev.en.36.010191.003103.

178. Lanouette S, Mongeon V, Figeys D, Couture JF. The functional diversity of protein lysine methylation. Molecular systems biology. 2014;10(4):724. doi: 10.1002/msb.134974.

179. Leonard AC, Grimwade JE. Regulating DnaA complex assembly: it is time to fill the gaps. Curr Opin Microbiol. 2010;13(6):766-72. doi: 10.1016/j.mib.2010.10.001.

180. Lesley JA, Shapiro L. SpoT regulates DnaA stability and initiation of DNA replication in carbon-starved *Caulobacter crescentus*. J Bacteriol. 2008;190(20):6867-80. doi: 10.1128/JB.00700-08.

181. Leslie DJ, Heinen C, Schramm FD, Thüring M, Aakre CD, Murray SM, et al. Nutritional Control of DNA Replication Initiation through the Proteolysis and Regulated Translation of DnaA. PLOS Genetics. 2015;11(7):e1005342. doi: 10.1371/journal.pgen.1005342.

182. Lewis K. Multidrug tolerance of biofilms and persister cells. Current topics in microbiology and immunology. 2008;322:107-31. Epub 2008/05/06.

183. Li X, Pal U, Ramamoorthi N, Liu X, Desrosiers DC, Eggers CH, et al. The Lyme disease agent *Borrelia burgdorferi* requires BB0690, a Dps homologue, to persist within ticks. Mol Microbiol. 2007;63(3):694-710. Epub 2006/12/22. doi: 10.1111/j.1365-2958.2006.05550.x.

184. Lim JG, Choi SH. IscR is a global regulator essential for pathogenesis of *Vibrio vulnificus* and induced by host cells. Infection and immunity. 2014;82(2):569-78. Epub 2014/01/31. doi: 10.1128/iai.01141-13.

185. Lin T, Gao L, Zhang C, Odeh E, Jacobs MB, Coutte L, et al. Analysis of an ordered, comprehensive STM mutant library in infectious *Borrelia burgdorferi*: insights into the genes required for mouse infectivity. PLoS One. 2012;7(10):e47532. doi: 10.1371/journal.pone.0047532.

186. Lin T, Troy EB, Hu LT, Gao L, Norris SJ. Transposon mutagenesis as an approach to improved understanding of Borrelia pathogenesis and biology. Front Cell Infect Microbiol. 2014;4:63. doi: 10.3389/fcimb.2014.00063.

187. Lin YH, Romo JA, Smith TC, 2nd, Reyes AN, Karna SL, Miller CL, et al. Spermine and Spermidine alter gene expression and antigenic profile of *Borrelia burgdorferi*. Infection and immunity. 2017;85(3):e00684-16. Epub 2017/01/06. doi: 10.1128/iai.00684-16.

188. Liu J, Francis L, Chien P. Lon recognition of the replication initiator DnaA is not confined to a single degron. bioRxiv. 2018. doi: 10.1101/301655.

189. Liu MY, Romeo T. The global regulator CsrA of *Escherichia coli* is a specific mRNA-binding protein. Journal of bacteriology. 1997;179(14):4639-42.

190. Livny J. Bioinformatic discovery of bacterial regulatory RNAs using SIPHT. Methods Mol Biol. 2012;905:3-14.

191. Livny J, Zhou X, Mandlik A, Hubbard T, Davis BM, Waldor MK. Comparative RNA-Seq based dissection of the regulatory networks and environmental stimuli underlying *Vibrio parahaemolyticus* gene expression during infection. Nucl Acids Res. 2014;42:12212-23.

192. Lobel L, Herskovits AA. Systems Level Analyses Reveal Multiple Regulatory Activities of CodY Controlling Metabolism, Motility and Virulence in *Listeria monocytogenes*. PLoS Genet. 2016;12(2):e1005870. doi: 10.1371/journal.pgen.1005870.

193. Lourdault K, Matsunaga J, Haake DA. High-Throughput Parallel Sequencing to Measure Fitness of *Leptospira interrogans* Transposon Insertion Mutants during Acute

Infection. PLoS Negl Trop Dis. 2016;10(11):e0005117. doi: 10.1371/journal.pntd.0005117.

194. Love MI, Huber W, Anders S. Moderated estimation of fold change and dispersion for RNA-seq data with DESeq2. Genome Biology. 2014;15(12):550. doi: 10.1186/s13059-014-0550-8.

195. Lybecker MC, Abel CA, Feig AL, Samuels DS. Identification and function of the RNA chaperone Hfq in the Lyme disease spirochete *Borrelia burgdorferi*. Molecular Microbiology. 2010;78:622-35.

196. Lybecker MC, Samuels DS. Temperature-induced regulation of RpoS by a small RNA in *Borrelia burgdorferi*. Mol Microbiol. 2007;64:1075-89.

197. Lybecker MC, Samuels DS. Temperature-induced regulation of RpoS by a small RNA in *Borrelia burgdorferi*. Molecular Microbiology. 2007;64(4):1075-89. doi: 10.1111/j.1365-2958.2007.05716.x.

198. Ma H-W, Kumar B, Ditges U, Gunzer F, Buer J, Zeng A-P. An extended transcriptional regulatory network of *Escherichia coli* and analysis of its hierarchical structure and network motifs. Nucleic Acids Res. 2004;32(22):6643-9. doi: 10.1093/nar/gkh1009.

199. Maas WK, Clark AJ. Studies on the mechanism of repression of arginine biosynthesis in Escherichia coli: II. Dominance of repressibility in diploids. Journal of Molecular Biology. 1964;8(3):365-70. doi: https://doi.org/10.1016/S0022-2836(64)80200-X.

200. Madan Babu M, Teichmann SA. Evolution of transcription factors and the gene regulatory network in *Escherichia coli*. Nucleic Acids Res. 2003;31(4):1234-44. doi: 10.1093/nar/gkg210.

201. Martínez-Antonio A, Collado-Vides J. Identifying global regulators in transcriptional regulatory networks in bacteria. Curr Opin Microbiol. 2003;6(5):482-9. doi: 10.1016/j.mib.2003.09.002.

202. Masuzawa T, Kurita T, Kawabata H, Yanagihara Y. Relationship between infectivity and OspC expression in Lyme disease Borrelia. FEMS Microbiology Letters. 1994;123(3):319-24. doi: 10.1111/j.1574-6968.1994.tb07242.x.

203. Matsunaga J, Schlax PJ, Haake DA. Role for cis-acting RNA sequences in the temperature-dependent expression of the multiadhesive lig proteins in *Leptospira interrogans*. J Bacteriol. 2013;195(22):5092-101. doi: 10.1128/JB.00663-13.

204. McClintock B. The Origin and Behavior of Mutable Loci in Maize. Proceedings of the National Academy of Sciences of the United States of America. 1950;36(6):344-55.

205. Mead PS. Epidemiology of Lyme disease. Infect Dis Clin N Am. 2015;29. doi: 10.1016/j.idc.2015.02.010.

206. Mead PS. Epidemiology of Lyme disease. Infectious disease clinics of North America. 2015;29(2):187-210. Epub 2015/05/23. doi: 10.1016/j.idc.2015.02.010.

207. Merlo LM, Pepper JW, Reid BJ, Maley CC. Cancer as an evolutionary and ecological process. Nature reviews Cancer. 2006;6(12):924-35. Epub 2006/11/17. doi: 10.1038/nrc2013.

208. Merrikh H, Grossman AD. Control of the replication initiator DnaA by an anti-cooperativity factor. Mol Microbiol. 2011;82(2):434-46. doi: 10.1111/j.1365-2958.2011.07821.x.

209. Messer W, Weigel C. DnaA initiator—also a transcription factor. Mol Microbiol. 1997;24(1):1-6.

210. Miller CL, Karna SL, Seshu J. Borrelia host adaptation regulator (BadR) regulates *rpoS* to modulate host adaptation and virulence factors in *Borrelia burgdorferi*. Molecular Microbiology. 2013;88:105-24.

211. Miller CL, Karna SLR, Seshu J. Borrelia host adaptation Regulator (BadR) regulates *rpoS* to modulate host adaptation and virulence factors in *Borrelia burgdorferi*. Mol Microbiol. 2013;88(1):105-24. doi: 10.1111/mmi.12171.

212. Miller JC. Example of real-time quantitative reverse transcription-PCR (Q-RT-PCR) analysis of bacterial gene expression during mammalian infection: *Borrelia burgdorferi* in mouse tissues. Current protocols in microbiology. 2005;1D:3. Epub 2008/09/05. doi: 10.1002/9780471729259.mc01d03s00.

213. Miller MB, Bassler BL. Quorum sensing in bacteria. Annu Rev Microbiol. 2001;55:165-99. doi: 10.1146/annurev.micro.55.1.165.

214. Miller MB, Skorupski K, Lenz DH, Taylor RK, Bassler BL. Parallel quorum sensing systems converge to regulate virulence in *Vibrio cholerae*. Cell. 2002;110(3):303-14. Epub 2002/08/15.

215. Milohanic E, Glaser P, Coppée J-Y, Frangeul L, Vega Y, Vázquez-Boland JA, et al. Transcriptome analysis of *Listeria monocytogenes* identifies three groups of genes differently regulated by PrfA. Molecular Microbiology. 2003;47(6):1613-25. doi: 10.1046/j.1365-2958.2003.03413.x.

216. Mittenhuber G. Comparative genomics and evolution of genes encoding bacterial (p)ppGpp synthetases/hydrolases (the Rel, RelA and SpoT proteins). J Mol Microbiol Biotechnol. 2001;3(4):585-600.

217. Moat AG, Foster JW, Spector MP. Regulation of Prokaryotic Gene Expression. Microbial Physiology: John Wiley & Sons, Inc.; 2002. p. 194-238.

218. Molloy PJ, Telford SR, 3rd, Chowdri HR, Lepore TJ, Gugliotta JL, Weeks KE, et al. *Borrelia miyamotoi* Disease in the Northeastern United States: A Case Series. Ann Intern Med. 2015;163(2):91-8. Epub 2015/06/09. doi: 10.7326/m15-0333.

219. Monack D. Stanley Falkow (1934-2018). Cell Host & Microbe. 2018;23(6):687-8. doi: 10.1016/j.chom.2018.05.014.

220. Montgomery RR, Malawista SE, Feen KJ, Bockenstedt LK. Direct demonstration of antigenic substitution of *Borrelia burgdorferi* ex vivo: exploration of the paradox of the early immune response to outer surface proteins A and C in Lyme disease. The Journal of experimental medicine. 1996;183(1):261-9. doi: 10.1084/jem.183.1.261.

221. Morgan JK, Carroll RK, Harro CM, Vendura KW, Shaw LN, Riordan JT. Global Regulator of Virulence A (GrvA) Coordinates Expression of Discrete Pathogenic Mechanisms in Enterohemorrhagic *Escherichia coli* through Interactions with GadW-GadE. Journal of bacteriology. 2015;198(3):394-409. Epub 2015/11/04. doi: 10.1128/jb.00556-15.

222. Murray H, Koh A. Multiple regulatory systems coordinate DNA replication with cell growth in *Bacillus subtilis*. PLoS Genet. 2014;10(10):e1004731. doi: 10.1371/journal.pgen.1004731.

223. Narasimhan S, Santiago F, Koski RA, Brei B, Anderson JF, Fish D, et al. Examination of the *Borrelia burgdorferi* transcriptome in Ixodes scapularis during feeding. Journal of bacteriology. 2002;184(11):3122-5. Epub 2002/05/11.

224. Nogueira SV, Smith AA, Qin J-H, Pal U. A surface enolase participates in *Borrelia burgdorferi*-plasminogen interaction and contributes to pathogen survival within feeding ticks. Infect Immun. 2012;80(1):82-90. doi: 10.1128/IAI.05671-11.

225. Nonaka G, Blankschien M, Herman C, Gross CA, Rhodius VA. Regulon and promoter analysis of the *E. coli* heat-shock factor, σ32, reveals a multifaceted cellular response to heat stress. Genes Dev. 2006;20.

226. Noppa L, Burman N, Sadziene A, Barbour AG, Bergström S. Expression of the flagellin gene in Borrelia is controlled by an alternative sigma factor. Microbiology. 1995;141 (Pt 1):85-93. doi: 10.1099/00221287-141-1-85.

227. Novak EA, Sultan SZ, Motaleb MA. The cyclic-di-GMP signaling pathway in the Lyme disease spirochete, *Borrelia burgdorferi*. Front Cell Infect Microbiol. 2014;4:56. doi: 10.3389/fcimb.2014.00056.

228. Oliva G, Sahr T, Buchrieser C. Small RNAs, 5' UTR elements and RNA-binding proteins in intracellular bacteria: impact on metabolism and virulence. FEMS Microbiol Rev. 2015;39:331-49.

229. Ostberg Y, Bunikis I, Bergstrom S, Johansson J. The etiological agent of Lyme disease, *Borrelia burgdorferi*, appears to contain only a few small RNA molecules. Journal of bacteriology. 2004;186(24):8472-7. Epub 2004/12/04. doi: 10.1128/jb.186.24.8472-8477.2004.

230. Ouyang Z, Blevins JS, Norgard MV. Transcriptional interplay among the regulators Rrp2, RpoN and RpoS in *Borrelia burgdorferi*. Microbiology. 2008;154(Pt 9):2641-58. Epub 2008/09/02. doi: 10.1099/mic.0.2008/019992-0.

231. Ouyang Z, Deka RK, Norgard MV. BosR (BB0647) controls the RpoN-RpoS regulatory pathway and virulence expression in *Borrelia burgdorferi* by a novel DNA-binding mechanism. PLoS Pathog. 2011;7(2):e1001272. doi: 10.1371/journal.ppat.1001272.

232. Ouyang Z, Haq S, Norgard MV. Analysis of the *dbpBA* upstream regulatory region controlled by RpoS in *Borrelia burgdorferi*. J Bacteriol. 2010;192(7):1965-74. doi: 10.1128/JB.01616-09.

233. Ouyang Z, Zhou J. BadR (BB0693) controls growth phase-dependent induction of *rpoS* and *bosR* in *Borrelia burgdorferi* via recognizing TAAAATAT motifs. Molecular Microbiology. 2015;98(6):1147-67. doi: 10.1111/mmi.13206.

234. Ouyang Z, Zhou J, Brautigam CA, Deka R, Norgard MV. Identification of a core sequence for the binding of BosR to the *rpoS* promoter region in *Borrelia burgdorferi*. Microbiology. 2014;160(Pt 5):851-62. doi: 10.1099/mic.0.075655-0.

235. Ouyang Z, Zhou J, Norgard MV. CsrA (BB0184) is not involved in activation of the RpoN-RpoS regulatory pathway in *Borrelia burgdorferi*. Infection and immunity. 2014;82(4):1511-22. Epub 2014/01/24. doi: 10.1128/iai.01555-13.

236. Papenfort K, Vogel J. Small RNA functions in carbon metabolism and virulence of enteric pathogens. Front Cell Infect Microbiol. 2014;4:91. doi: 10.3389/fcimb.2014.00091.

237. Pappas CJ, Iyer R, Petzke MM, Caimano MJ, Radolf JD, Schwartz I. *Borrelia burgdorferi* requires glycerol for maximum fitness during the tick phase of the enzootic cycle. PLoS Pathog. 2011;7(7):e1002102. Epub 2011/07/14. doi: 10.1371/journal.ppat.1002102.

238. Patro R, Duggal G, Love MI, Irizarry RA, Kingsford C. Salmon provides fast and bias-aware quantification of transcript expression. Nat Methods. 2017;14(4):417-9. doi: 10.1038/nmeth.4197.

239. Picardeau M, Lobry JR, Hinnebusch BJ. Analyzing DNA strand compositional asymmetry to identify candidate replication origins of *Borrelia burgdorferi* linear and circular plasmids. Genome Res. 2000;10(10):1594-604. Epub 2000/10/24.

240. Picardeau M, Lobry JR, Hinnebusch BJ. Physical mapping of an origin of bidirectional replication at the centre of the *Borrelia burgdorferi* linear chromosome. Mol Microbiol. 1999;32(2):437-45.

241. Piesman J. Dynamics of *Borrelia burgdorferi* transmission by nymphal Ixodes dammini ticks. The Journal of infectious diseases. 1993;167(5):1082-5. Epub 1993/05/01.

242. Piesman J, Oliver JR, Sinsky RJ. Growth kinetics of the Lyme disease spirochete (*Borrelia burgdorferi*) in vector ticks (*Ixodes dammini*). Am J Trop Med Hyg. 1990;42(4):352-7. Epub 1990/04/01.

243. Popitsch N, Bilusic I, Rescheneder P, Schroeder R, Lybecker M. Temperature-dependent sRNA transcriptome of the Lyme disease spirochete. BMC Genomics. 2017;18(1):28. doi: 10.1186/s12864-016-3398-3.

244. Potrykus K, Cashel M. (p)ppGpp: still magical? Annu Rev Microbiol. 2008;62:35-51. doi: 10.1146/annurev.micro.62.081307.162903.

245. Pritt BS, Respicio-Kingry LB, Sloan LM, Schriefer ME, Replogle AJ, Bjork J, et al. *Borrelia mayonii* sp. nov., a member of the *Borrelia burgdorferi* sensu lato complex, detected in patients and ticks in the upper midwestern United States. International journal of systematic and evolutionary microbiology. 2016;66(11):4878-80. Epub 2016/08/26. doi: 10.1099/ijsem.0.001445.

246. Purser JE, Norris SJ. Correlation between plasmid content and infectivity in *Borrelia burgdorferi*. Proceedings of the National Academy of Sciences. 2000;97:13865-70.

247. Radolf JD, Caimano MJ, Stevenson B, Hu LT. Of ticks, mice and men: understanding the dual-host lifestyle of Lyme disease spirochaetes. Nature reviews Microbiology. 2012;10(2):87-99. Epub 2012/01/11. doi: 10.1038/nrmicro2714.

248. Rahn-Lee L, Merrikh H, Grossman AD, Losick R. The sporulation protein SirA inhibits the binding of DnaA to the origin of replication by contacting a patch of clustered amino acids. J Bacteriol. 2011;193(6):1302-7. doi: 10.1128/JB.01390-10.

249. Ramamoorthy R, McClain NA, Gautam A, Scholl-Meeker D. Expression of the *bmpB* gene of *Borrelia burgdorferi* is modulated by two distinct transcription termination events. Journal of bacteriology. 2005;187(8):2592-600. Epub 2005/04/05. doi: 10.1128/jb.187.8.2592-2600.2005.

250. Ramamoorthy R, Philipp MT. Differential Expression of *Borrelia burgdorferi* Proteins during Growth *In Vitro*. Infection and immunity. 1998;66(11):5119-24.

251. Revel AT, Talaat AM, Norgard MV. DNA microarray analysis of differential gene expression in *Borrelia burgdorferi*, the Lyme disease spirochete. Proceedings of the National Academy of Sciences of the United States of America. 2002;99(3):1562-7. doi: 10.1073/pnas.032667699.

252. Rhodes RG, Coy W, Nelson DR. Chitobiose utilization in *Borrelia burgdorferi* is dually regulated by RpoD and RpoS. BMC Microbiology. 2009;9(1):1-15. doi: 10.1186/1471-2180-9-108.

253. Riley SP, Bykowski T, Babb K, von Lackum K, Stevenson B. Genetic and physiological characterization of the *Borrelia burgdorferi ORF-BB0374-pfs-metK-luxS* operon. Microbiology. 2007;153(Pt 7):2304-11. Epub 2007/06/30. doi: 10.1099/mic.0.2006/004424-0.

254. Riley SP, Bykowski T, Cooley AE, Burns LH, Babb K, Brissette CA, et al. *Borrelia burgdorfer*i EbfC defines a newly-identified, widespread family of bacterial DNA-binding proteins. Nucleic Acids Res. 2009;37(6):1973-83. doi: 10.1093/nar/gkp027.

255. Rogers EA, Terekhova D, Zhang H-M, Hovis KM, Schwartz I, Marconi RT. Rrp1, a cyclic-di-GMP-producing response regulator, is an important regulator of *Borrelia burgdorferi* core cellular functions. Mol Microbiol. 2009;71(6):1551-73. doi: 10.1111/j.1365-2958.2009.06621.x.

256. Rogers EA, Terekhova D, Zhang HM, Hovis KM, Schwartz I, Marconi RT. Rrp1, a cyclic-di-GMP-producing response regulator, is an important regulator of *Borrelia burgdorferi* core cellular functions. Molecular Microbiology. 2009;71(6):1551-73. Epub 2009/02/13. doi: 10.1111/j.1365-2958.2009.06621.x.

257. Rogovskyy AS, Casselli T, Tourand Y, Jones CR, Owen JP, Mason KL, et al. Evaluation of the Importance of VlsE Antigenic Variation for the Enzootic Cycle of *Borrelia burgdorferi*. PLoS ONE. 2015;10(4):e0124268. doi: 10.1371/journal.pone.0124268.

258. Rollend L, Fish D, Childs JE. Transovarial transmission of Borrelia spirochetes by *Ixodes scapularis*: a summary of the literature and recent observations. Ticks and tick-borne diseases. 2013;4(1-2):46-51. Epub 2012/12/15. doi: 10.1016/j.ttbdis.2012.06.008.

259. Rutherford ST, Bassler BL. Bacterial quorum sensing: its role in virulence and possibilities for its control. Cold Spring Harb Perspect Med. 2012;2(11). doi: 10.1101/cshperspect.a012427.

260. Ryan VT, Grimwade JE, Camara JE, Crooke E, Leonard AC. *Escherichia coli* prereplication complex assembly is regulated by dynamic interplay among Fis, IHF and DnaA. Mol Microbiol. 2004;51(5):1347-59. doi: 10.1046/j.1365-2958.2003.03906.x.

261. Saggioro C, Olliver A, Sclavi B. Temperature-dependence of the DnaA-DNA interaction and its effect on the autoregulation of *dnaA* expression. Biochem J. 2013;449(2):333-41. doi: 10.1042/BJ20120876.

262. Salman-Dilgimen A, Hardy P-O, Radolf JD, Caimano MJ, Chaconas G. HrpA, an RNA Helicase Involved in RNA Processing, Is Required for Mouse Infectivity and Tick Transmission of the Lyme Disease Spirochete. PLoS pathogens. 2013;9(12):e1003841. doi: 10.1371/journal.ppat.1003841.

263. Salman-Dilgimen A, Hardy PO, Dresser AR, Chaconas G. HrpA, a DEAH-box RNA helicase, is involved in global gene regulation in the Lyme disease spirochete. PLoS One. 2011;6. doi: 10.1371/journal.pone.0022168.

264. Samuels DS. Gene regulation in *Borrelia burgdorferi*. Annual review of microbiology. 2011;65:479-99. Epub 2011/08/02. doi: 10.1146/annurev.micro.112408.134040.

265. Samuels DS. Gene regulation in *Borrelia burgdorferi*. Annu Rev Microbiol. 2011;65:479-99.

266. Sanjuan E, Esteve-Gassent MD, Maruskova M, Seshu J. Overexpression of CsrA (BB0184) alters the morphology and antigen profiles of *Borrelia burgdorferi*. Infection and immunity. 2009;77(11):5149-62. Epub 2009/09/10. doi: 10.1128/iai.00673-09.

267. Santangelo TJ, Artsimovitch I. Termination and antitermination: RNA polymerase runs a stop sign. Nature reviews Microbiology. 2011;9(5):319-29. doi: 10.1038/nrmicro2560.

268. Savage CR, Arnold WK, Gjevre-Nail A, Koestler BJ, Bruger EL, Barker JR, et al. Intracellular concentrations of *Borrelia burgdorferi* Cyclic Di-AMP are not changed by

altered expression of the CdaA synthase. PLoS One. 2015;10(4):e0125440. Epub 2015/04/24. doi: 10.1371/journal.pone.0125440.

269. Savage CR, Jutras BL, Bestor A, Tilly K, Rosa PA, Tourand Y, et al. *Borrelia burgdorferi* SpoVG DNA- and RNA-binding protein modulates physiology of the Lyme disease spirochete. Journal of bacteriology. 2018. Epub 2018/04/11. doi: 10.1128/jb.00033-18.

270. Schaechter M, Maaloe O, Kjeldgaard NO. Dependency on medium and temperature of cell size and chemical composition during balanced grown of *Salmonella typhimurium*. J Gen Microbiol. 1958;19(3):592-606. Epub 1958/12/01. doi: 10.1099/00221287-19-3-592.

271. Schmittgen TD, Livak KJ. Analyzing real-time PCR data by the comparative CT method. Nat Protocols. 2008;3(6):1101-8.

272. Schwan TG, Piesman J, Golde WT, Dolan MC, Rosa PA. Induction of an outer surface protein on *Borrelia burgdorferi* during tick feeding. Proceedings of the National Academy of Sciences USA. 1995;92:2909-13.

273. Seshu J, Boylan JA, Gherardini FC, Skare JT. Dissolved oxygen levels alter gene expression and antigen profiles in *Borrelia burgdorferi*. Infect Immun. 2004;72(3):1580-6. doi: 10.1128/IAI.72.3.1580-1586.2004.

274. Sevostyanova A, Groisman EA. An RNA motif advances transcription by preventing Rho-dependent termination. Proc Natl Acad Sci U S A. 2015;112(50):E6835-43. doi: 10.1073/pnas.1515383112.

275. Shah P, Swiatlo E. A multifaceted role for polyamines in bacterial pathogens. Mol Microbiol. 2008;68(1):4-16. doi: 10.1111/j.1365-2958.2008.06126.x.

276. Sharma B, Brown AV, Matluck NE, Hu LT, Lewis K. *Borrelia burgdorferi*, the Causative Agent of Lyme Disease, Forms Drug-Tolerant Persister Cells. Antimicrob Agents Chemother. 2015;59(8):4616-24. doi: 10.1128/AAC.00864-15.

277. Sharma CM, Hoffmann S, Darfeuille F, Reignier J, Findeisz S, Sittka A, et al. The primary transcriptome of the major human pathogen *Helicobacter pylori*. Nature. 2010;464(7286):250-5. doi: http://www.nature.com/nature/journal/v464/n7286/suppinfo/nature08756_S1.html.

278. Sherlock ME, Sudarsan N, Breaker RR. Riboswitches for the alarmone ppGpp expand the collection of RNA-based signaling systems. Proceedings of the National Academy of Sciences. 2018;115(23):6052-7. doi: 10.1073/pnas.1720406115.

279. Shi Y, Xu Q, McShan K, Liang FT. Both decorin-binding proteins A and B are critical for the overall virulence of *Borrelia burgdorferi*. Infect Immun. 2008;76(3):1239-46. doi: 10.1128/IAI.00897-07.

280. Shin JJ, Glickstein LJ, Steere AC. High levels of inflammatory chemokines and cytokines in joint fluid and synovial tissue throughout the course of antibiotic-refractory

lyme arthritis. Arthritis and rheumatism. 2007;56(4):1325-35. Epub 2007/03/30. doi: 10.1002/art.22441.

281. Shishkin AA, Giannoukos G, Kucukural A, Ciulla D, Busby M, Surka C, et al. Simultaneous generation of many RNA-seq libraries in a single reaction. Nat Methods. 2015;12(4):323-5. Epub 2015/03/03. doi: 10.1038/nmeth.3313.

282. Skarstad K, Katayama T. Regulating DNA replication in bacteria. Cold Spring Harb Perspect Biol. 2013;5(4):a012922. doi: 10.1101/cshperspect.a012922.

283. Smith AH, Blevins JS, Bachlani GN, Yang XF, Norgard MV. Evidence that RpoS (σS) in *Borrelia burgdorferi* is controlled directly by RpoN (σ54/σN). Journal of bacteriology. 2007;189(5):2139-44. Epub 2006/12/13. doi: 10.1128/jb.01653-06.

284. Smith AH, Blevins JS, Bachlani GN, Yang XF, Norgard MV. Evidence that RpoS (σS) in *Borrelia burgdorferi* is controlled directly by RpoN (σ54/σN). J Bacteriol. 2007;189(5):2139-44. doi: 10.1128/JB.01653-06.

285. Smith JL, Grossman AD. *In Vitro* Whole Genome DNA Binding Analysis of the Bacterial Replication Initiator and Transcription Factor DnaA. PLoS Genet. 2015;11(5):e1005258. doi: 10.1371/journal.pgen.1005258.

286. Smith TC, 2nd, Helm SM, Chen Y, Lin YH, Karna SLR, Seshu J. Borrelia host adaptation Protein (BadP) is required for the colonization of a mammalian host by the agent of Lyme disease. Infection and immunity. 2018. Epub 2018/04/25. doi: 10.1128/iai.00057-18.

287. Solomon SP, Hilton E, Weinschel BS, Pollack S, Grolnick E. Psychological factors in the prediction of Lyme disease course. Arthritis care and research : the official journal of the Arthritis Health Professions Association. 1998;11(5):419-26. Epub 1998/11/27.

288. Somerville GA, Proctor RA. At the crossroads of bacterial metabolism and virulence factor synthesis in Staphylococci. Microbiology and molecular biology reviews : MMBR. 2009;73(2):233-48. Epub 2009/06/03. doi: 10.1128/mmbr.00005-09.

289. Speck C, Weigel C, Messer W. ATP- and ADP-dnaA protein, a molecular switch in gene regulation. The EMBO journal. 1999;18(21):6169-76. Epub 1999/11/02. doi: 10.1093/emboj/18.21.6169.

290. Speck C, Weigel C, Messer W. ATP– and ADP–DnaA protein, a molecular switch in gene regulation. Plan Perspect. 1999;6169:6176.

291. Steere AC. Lyme Disease. New England Journal of Medicine. 2001;345(2):115-25. doi: doi:10.1056/NEJM200107123450207.

292. Steere AC, Angelis SM. Therapy for Lyme arthritis: Strategies for the treatment of antibiotic-refractory arthritis. Arthritis & Rheumatism. 2006;54(10):3079-86. doi: 10.1002/art.22131.

293. Steere AC, Coburn J, Glickstein L. The emergence of Lyme disease. J Clin Invest. 2004;113:1093-101.

294. Steere AC, Drouin EE, Glickstein LJ. Relationship between immunity to Borrelia burgdorferi outer-surface protein A (OspA) and Lyme arthritis. Clinical infectious diseases : an official publication of the Infectious Diseases Society of America. 2011;52 Suppl 3:s259-65. Epub 2011/01/19. doi: 10.1093/cid/ciq117.

295. Steere AC, Malawista SE, Snydman DR, Shope RE, Andiman WA, Ross MR, et al. Lyme arthritis: an epidemic of oligoarticular arthritis in children and adults in three connecticut communities. Arthritis and rheumatism. 1977;20(1):7-17. Epub 1977/01/01.

296. Steere AC, Strle F, Wormser GP, Hu LT, Branda JA, Hovius JW, et al. Lyme borreliosis. Nature reviews Disease primers. 2016;2:16090. Epub 2016/12/16. doi: 10.1038/nrdp.2016.90.

297. Stevenson B, Babb K. LuxS-mediated quorum sensing in *Borrelia burgdorferi*, the lyme disease spirochete. Infect Immun. 2002;70(8):4099-105. doi: 10.1128/IAI.70.8.4099-4105.2002.

298. Stevenson B, Schwan TG, Rosa PA. Temperature-related differential expression of antigens in the Lyme disease spirochete, *Borrelia burgdorferi*. Infection and immunity. 1995;63(11):4535-9. Epub 1995/11/01.

299. Stevenson B, von Lackum K, Riley SP, Cooley AE, Woodman ME, Bykowski T. Evolving models of Lyme disease spirochete gene regulation. Wien Klin Wochenschr. 2006;118:643-52.

300. Stevenson B, von Lackum K, Wattier RL, McAlister JD, Miller JC, Babb K. Quorum sensing by the Lyme disease spirochete. Microbes Infect. 2003;5(11):991-7. doi: 10.1016/S1286-4579(03)00184-9.

301. Stone BL, Tourand Y, Brissette CA. Brave New Worlds: The Expanding Universe of Lyme Disease. Vector Borne Zoonotic Dis. 2017;17(9):619-29. Epub 2017/07/21. doi: 10.1089/vbz.2017.2127.

302. Storz G, Opdyke JA, Wassarman KM. Regulating bacterial transcription with small RNAs. Cold Spring Harb Symp Quant Biol. 2006;71:269-73. doi: 10.1101/sqb.2006.71.033.

303. Storz G, Vogel J, Wassarman Karen M. Regulation by Small RNAs in Bacteria: Expanding Frontiers. Molecular Cell. 43(6):880-91. doi: 10.1016/j.molcel.2011.08.022.

304. Sudarsan N, Lee ER, Weinberg Z, Moy RH, Kim JN, Link KH, et al. Riboswitches in eubacteria sense the second messenger cyclic di-GMP. Science. 2008;321(5887):411-3. doi: 10.1126/science.1159519.

305. Surette MG, Miller MB, Bassler BL. Quorum sensing in *Escherichia coli*, *Salmonella typhimurium*, and *Vibrio harveyi*: a new family of genes responsible for autoinducer production. Proceedings of the National Academy of Sciences of the United States of America. 1999;96(4):1639-44. Epub 1999/02/17.

306. Szalewska-Palasz A, Wegrzyn A, Blaszczak A, Taylor K, Wegrzyn G. DnaA-stimulated transcriptional activation of oriλ: *Escherichia coli* RNA polymerase β subunit as

a transcriptional activator contact site. Proceedings of the National Academy of Sciences of the United States of America. 1998;95(8):4241-6.

307. Sze CW, Li C. Inactivation of *bb0184*, which encodes carbon storage regulator A, represses the infectivity of *Borrelia burgdorferi*. Infection and immunity. 2011;79(3):1270-9. Epub 2010/12/22. doi: 10.1128/iai.00871-10.

308. Sze CW, Morado DR, Liu J, Charon NW, Xu H, Li C. Carbon storage regulator A (CsrA(Bb)) is a repressor of *Borrelia burgdorferi* flagellin protein FlaB. Molecular Microbiology. 2011;82(4):851-64. Epub 2011/10/18. doi: 10.1111/j.1365-2958.2011.07853.x.

309. Sze CW, Smith A, Choi YH, Yang X, Pal U, Yu A, et al. Study of the response regulator Rrp1 reveals its regulatory role in chitobiose utilization and virulence of *Borrelia burgdorferi*. Infect Immun. 2013;81(5):1775-87. doi: 10.1128/IAI.00050-13.

310. Taga ME, Semmelhack JL, Bassler BL. The LuxS-dependent autoinducer AI-2 controls the expression of an ABC transporter that functions in AI-2 uptake in *Salmonella typhimurium*. Mol Microbiol. 2001;42(3):777-93. Epub 2001/11/28.

311. Taheri-Araghi S, Bradde S, Sauls JT, Hill NS, Levin PA, Paulsson J, et al. Cell-size control and homeostasis in bacteria. Curr Biol. 2015;25(3):385-91. doi: 10.1016/j.cub.2014.12.009.

312. Tilly K, Elias AF, Errett J, Fischer E, Iyer R, Schwartz I, et al. Genetics and regulation of chitobiose utilization in *Borrelia burgdorferi*. Journal of bacteriology. 2001;183(19):5544-53. doi: 10.1128/JB.183.19.5544-5553.2001.

313. Tilly K, Grimm D, Bueschel DM, Krum JG, Rosa P. Infectious cycle analysis of a *Borrelia burgdorferi* mutant defective in transport of chitobiose, a tick cuticle component. Vector Borne Zoonotic Dis. 2004;4(2):159-68. doi: 10.1089/1530366041210738.

314. Tilly K, Krum JG, Bestor A, Jewett MW, Grimm D, Bueschel D, et al. *Borrelia burgdorferi* OspC protein required exclusively in a crucial early stage of mammalian infection. Infection and immunity. 2006;74(6):3554-64. Epub 2006/05/23. doi: 10.1128/iai.01950-05.

315. Tobi Limke JGM, Jon S. Blevins and Alan Doty. A Readily Available Source of BSA Consistently Supports Cultivation and Differential Gene Expression. Bioprocess International [Internet]. 2009.

316. Tokarz R, Anderton JM, Katona LI, Benach JL. Combined effects of blood and temperature shift on *Borrelia burgdorferi* gene expression as determined by whole genome DNA array. Infection and immunity. 2004;72(9):5419-32. doi: 10.1128/IAI.72.9.5419-5432.2004.

317. Troy EB, Lin T, Gao L, Lazinski DW, Camilli A, Norris SJ, et al. Understanding barriers to *Borrelia burgdorferi* dissemination during infection using massively parallel sequencing. Infect Immun. 2013;81(7):2347-57. doi: 10.1128/IAI.00266-13.

318. Troy EB, Lin T, Gao L, Lazinski DW, Lundt M, Camilli A, et al. Global Tn-seq analysis of carbohydrate utilization and vertebrate infectivity of *Borrelia burgdorferi*. Molecular Microbiology. 2016;101(6):1003-23. doi: 10.1111/mmi.13437.

319. Vadia S, Levin PA. Growth rate and cell size: a re-examination of the growth law. Curr Opin Microbiol. 2015;24:96-103. doi: 10.1016/j.mib.2015.01.011.

320. Vadia S, Tse JL, Lucena R, Yang Z, Kellogg DR, Wang JD, et al. Fatty Acid Availability Sets Cell Envelope Capacity and Dictates Microbial Cell Size. Curr Biol. 2017;27(12):1757-67.e5. doi: 10.1016/j.cub.2017.05.076.

321. Vakulskas CA, Potts AH, Babitzke P, Ahmer BM, Romeo T. Regulation of bacterial virulence by Csr (Rsm) systems. Microbiology and molecular biology reviews : MMBR. 2015;79(2):193-224. Epub 2015/04/03. doi: 10.1128/mmbr.00052-14.

322. van Opijnen T, Camilli A. Transposon insertion sequencing: a new tool for systems-level analysis of microorganisms. Nat Rev Microbiol. 2013;11(7):435-42. doi: 10.1038/nrmicro3033.

323. Verma A, Brissette CA, Bowman A, Stevenson B. *Borrelia burgdorferi* BmpA is a laminin-binding protein. Infect Immun. 2009;77(11):4940-6. doi: 10.1128/IAI.01420-08.

324. Verma A, Kumar P, Babb K, Timoney JF, Stevenson B. Cross-reactivity of antibodies against leptospiral recurrent uveitis-associated proteins A and B (LruA and LruB) with eye proteins. PLoS neglected tropical diseases. 2010;4(8):e778-e. doi: 10.1371/journal.pntd.0000778.

325. von Lackum K, Babb K, Riley SP, Wattier RL, Bykowski T, Stevenson B. Functionality of *Borrelia burgdorferi* LuxS: the Lyme disease spirochete produces and responds to the pheromone autoinducer-2 and lacks a complete activated-methyl cycle. Int J Med Microbiol. 2006;296 Suppl 40:92-102. Epub 2006/03/15. doi: 10.1016/j.ijmm.2005.12.011.

326. von Lackum K, Stevenson B. Carbohydrate utilization by the Lyme borreliosis spirochete, *Borrelia burgdorferi*. FEMS Microbiol Lett. 2005;243:173-9.

327. Wang G, Iyer R, Bittker S, Cooper D, Small J, Wormser GP, et al. Variations in Barbour-Stoenner-Kelly Culture Medium Modulate Infectivity and Pathogenicity of *Borrelia burgdorferi* Clinical Isolates. Infection and immunity. 2004;72(11):6702-6. doi: 10.1128/IAI.72.11.6702-6706.2004.

328. Wang JD, Levin PA. Metabolism, cell growth and the bacterial cell cycle. Nat Rev Microbiol. 2009;7(11):822-7. doi: 10.1038/nrmicro2202.

329. Wang P, Dadhwal P, Cheng Z, Zianni MR, Rikihisa Y, Liang FT, et al. *Borrelia burgdorferi* oxidative stress regulator BosR directly represses lipoproteins primarily expressed in the tick during mammalian infection. Mol Microbiol. 2013;89(6):1140-53. doi: 10.1111/mmi.12337.

330. Wang Y, MacKenzie KD, White AP. An empirical strategy to detect bacterial transcript structure from directional RNA-seq transcriptome data. BMC Genomics. 2015;16(1):1-15. doi: 10.1186/s12864-015-1555-8.

331. Wang Z, Gerstein M, Snyder M. RNA-Seq: a revolutionary tool for transcriptomics. Nat Rev Genet. 2009;10. doi: 10.1038/nrg2484.

332. Washington TA, Smith JL, Grossman AD. Genetic networks controlled by the bacterial replication initiator and transcription factor DnaA in *Bacillus subtilis*. Molecular Microbiology. 2017;106(1):109-28. doi: 10.1111/mmi.13755.

333. Wassarman KM. 6S RNA: a regulator of transcription. Mol Microbiol. 2007;65(6):1425-31. doi: 10.1111/j.1365-2958.2007.05894.x.

334. Watve SS, Thomas J, Hammer BK. CytR Is a Global Positive Regulator of Competence, Type VI Secretion, and Chitinases in Vibrio cholerae. PLoS One. 2015;10(9):e0138834. Epub 2015/09/25. doi: 10.1371/journal.pone.0138834.

335. Weart RB, Lee AH, Chien A-C, Haeusser DP, Hill NS, Levin PA. A metabolic sensor governing cell size in bacteria. Cell. 2007;130(2):335-47. doi: 10.1016/j.cell.2007.05.043.

336. Weinstock GM, Hardham JM, McLeod MP, Sodergren EJ, Norris SJ. The genome of *Treponema pallidum*: new light on the agent of syphilis. FEMS Microbiol Rev. 1998;22(4):323-32.

337. Westfall CS, Levin PA. Bacterial Cell Size: Multifactorial and Multifaceted. Annu Rev Microbiol. 2017;71:499-517. doi: 10.1146/annurev-micro-090816-093803.

338. Wilson GG, Murray NE. Restriction and modification systems. Annu Rev Genet. 1991;25:585-627. Epub 1991/01/01. doi: 10.1146/annurev.ge.25.120191.003101.

339. Woodman ME, Savage, C.R., Arnold, W.K., and Stevenson, B. . Direct PCR of intact bacteria (colony PCR). Curr Protoc Microbiol 2016;42:A.3D.1-A.3D.7. doi: doi: 10.1002/cpmc.14.

340. Wu Q, Guan G, Liu Z, Li Y, Luo J, Yin H. RNA-Seq-based analysis of changes in *Borrelia burgdorferi* gene expression linked to pathogenicity. Parasites & Vectors. 2015;8:155. doi: 10.1186/s13071-014-0623-2.

341. Xavier KB, Bassler BL. Regulation of uptake and processing of the quorum-sensing autoinducer AI-2 in *Escherichia co*li. Journal of bacteriology. 2005;187(1):238-48. Epub 2004/12/17. doi: 10.1128/jb.187.1.238-248.2005.

342. Xiang X, Yang Y, Du J, Lin T, Chen T, Yang XF, et al. Investigation of *ospC* Expression Variation among *Borrelia burgdorferi* Strains. Frontiers in Cellular and Infection Microbiology. 2017;7:131. doi: 10.3389/fcimb.2017.00131.

343. Xu Q, Shi Y, Dadhwal P, Liang FT. RpoS regulates essential virulence factors remaining to be identified in Borrelia burgdorferi. PLoS One. 2012;7(12):e53212. doi: 10.1371/journal.pone.0053212.

344. Yang L, Gal J, Chen J, Zhu H. Self-assembled FUS binds active chromatin and regulates gene transcription. Proceedings of the National Academy of Sciences of the United States of America. 2014;111(50):17809-14. Epub 2014/12/03. doi: 10.1073/pnas.1414004111.

345. Yang X, Popova TG, Goldberg MS, Norgard MV. Influence of Cultivation Media on Genetic Regulatory Patterns in *Borrelia burgdorferi*. Infection and immunity. 2001;69(6):4159-63. doi: 10.1128/iai.69.6.4159-4163.2001.

346. Yang XF, Alani SM, Norgard MV. The response regulator Rrp2 is essential for the expression of major membrane lipoproteins in *Borrelia burgdorferi*. Proceedings of the National Academy of Sciences. 2003;100(19):11001-6. doi: 10.1073/pnas.1834315100.

347. Yarnell WS, Roberts JW. Mechanism of intrinsic transcription termination and antitermination. Science. 1999;284(5414):611-5.

348. Ye M, Zhang J-J, Fang X, Lawlis GB, Troxell B, Zhou Y, et al. DhhP, a cyclic di-AMP phosphodiesterase of *Borrelia burgdorferi*, is essential for cell growth and virulence. Infect Immun. 2014;82(5):1840-9. doi: 10.1128/IAI.00030-14.

349. Zückert WR. A call to order at the spirochaetal host-pathogen interface. Mol Microbiol. 2013;89(2):207-11. doi: 10.1111/mmi.12286.

350. Zückert WR. Laboratory maintenance of *Borrelia burgdorferi*. Current protocols in microbiology. 2007;12C:1-10.

VITA

William K. Arnold

Education

Ph.D. – Microbiology, University of Kentucky - Lexington, KY
2012 – 2018

B.S. – Biology, University of Kentucky - Lexington, KY 2007 – 2011

Professional Experience

Graduate Research Assistant May 2013 – April 2018
Advisor: Dr. Brian Stevenson – Department of Microbiology, Immunology, and Molecular Genetics, University of Kentucky – Lexington, KY

Research Technician February 2012 – July 2012
Advisor: Dr. Jeramiah Smith – Department of Biology, University of Kentucky – Lexington, KY

Research Technician May 2011 - February 2012
Advisor: Dr. Marcielle DeBeer – Department of Physiology, University of Kentucky – Lexington, KY

Research Assistant May 2009 – May 2011
Advisor: Dr. Nancy Webb – Department of Nutritional Sciences, University of Kentucky – Lexington, KY

Peer Reviewed Publications

Arnold, W. K.*, Savage, C. R.*, Lethbridge, K. G., Smith, T. C., 2nd, Brissette, C. A., Seshu, J., & Stevenson, B. (2018). Transcriptomic insights on the virulence-controlling CsrA, BadR, RpoN, and RpoS regulatory networks in the Lyme disease spirochete. PLOS ONE, 13(8), e0203286. doi:10.1371/journal.pone.0203286
*Contributed equally to this work

Bobrov, AG, Kirillina, O, Fosso, MY, Fetherston, JD, Miller, MC, VanCleave, TT, Burlison, JA, **Arnold, WK**, Lawrenz, MB, Garneau-Tsodikova, S, Perry, R. D. (2017). "Zinc transporters YbtX and ZnuABC are required for the virulence of Yersinia pestis in bubonic and pneumonic plague in mice." Metallomics 9(6): 757-772.

Arnold, WK, Savage, CR, Brissette, C. A., Seshu, J., Livny, J., Stevenson, B. (2016). "RNA-Seq of *Borrelia burgdorferi* in Multiple Phases of Growth Reveals Insights into the Dynamics of Gene Expression, Transcriptome Architecture, and Noncoding RNAs." PLoS ONE 11(10): e0164165.

Savage CR, **Arnold WK**, Gjevre-Nail A, Koestler, B. J. Bruger, E. L. Barker, J. R. Waters, C. M. Stevenson, B. (2015). “Intracellular Concentrations of *Borrelia*

burgdorferi Cyclic Di-AMP Are Not Changed by Altered Expression of the CdaA Synthase." PLoS ONE 10(4): e0125440.

Arnold WK, Savage CR, Antonicello AD, Stevenson B. (2015). "Apparent Role for *Borrelia burgdorferi* LuxS during Mammalian Infection." Infection and Immunity 83(4): 1347-1353.

Published Works

Casselli, T., Tourand, Y., Scheidegger, A., **Arnold, WK**, Proulx, A., Stevenson, B., Brissette, C.A. DNA Methylation by Restriction Modification Systems Affects the Global Transcriptome Profile in *Borrelia burgdorferi*. BioRxiv.

Woodman, M. E., Savage, C.R., Arnold, W.K., and Stevenson, B. (2016). "Direct PCR of intact bacteria (colony PCR)." Curr. Protoc. Microbiol. 42:A.3D.1-A.3D.7.

Honors and Awards

Domestic Travel Award - University of Kentucky - 2014.
International Travel Award - University of Kentucky - 2015.
Dissertation Enhancement Award – University of Kentucky - 2016.
Sponsored AAAS Membership Award – University of Kentucky - 2016, 2017
Outstanding Poster Award – Departmental Retreat – 2017